

PL-TR-95-2042(I)

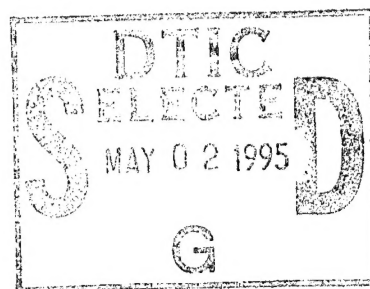
Environmental Research Papers, No. 1168

**PROCEEDINGS OF THE 16TH ANNUAL
CONFERENCE ON ATMOSPHERIC
TRANSMISSION MODELS,
8-9 JUNE 1993**

Editors:

Gail P. Anderson

James H. Chetwynd



7 April 1995

APPROVED FOR PUBLIC RELEASE; DISTRIBUTION UNLIMITED



PHILLIPS LABORATORY

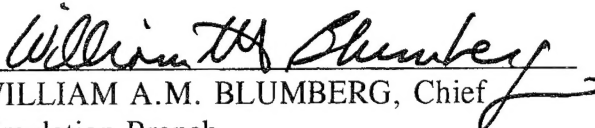
Directorate of Geophysics

AIR FORCE MATERIEL COMMAND

HANSCOM AIR FORCE BASE, MA 01731-3010

19950501 025

"This technical report has been reviewed and is approved for publication"


WILLIAM A.M. BLUMBERG, Chief
Simulation Branch
Optical Environment Division


ROGER A. VAN TASSEL, Director
Optical Environment Division

This report has been reviewed by the ESC Public Affairs Office (PA) and is releasable to the National Technical Information Service (NTIS).

Qualified requestors may obtain additional copies from the Defense Technical Information Center (DTIC). All others should apply to the National Technical Information Service (NTIS).

If your address has changed, or if you wish to be removed from the mailing list, or if the addressee is no longer employed by your organization, please notify PL/IM, 29 Randolph Road, Hanscom AFB, MA 01731-3010. This will assist us in maintaining a current mailing list.

Do not return copies of this report unless contractual obligations or notices on a specific document requires that it be returned.

DISCLAIMER NOTICE



THIS DOCUMENT IS BEST QUALITY AVAILABLE. THE COPY FURNISHED TO DTIC CONTAINED A SIGNIFICANT NUMBER OF PAGES WHICH DO NOT REPRODUCE LEGIBLY.

REPORT DOCUMENTATION PAGEForm Approved
OMB No. 0704-0188

Public reporting burden for this collection of information is estimated to average 1 hour per response, including the time for reviewing instructions, searching existing data sources, gathering and maintaining the data needed, and completing and reviewing the collection of information. Send comments regarding this burden estimate or any other aspect of this collection of information, including suggestions for reducing this burden, to Washington Headquarters Services, Directorate for Information Operations and Reports, 1215 Jefferson Davis Highway, Suite 1204, Arlington, VA 22202-4302, and to the Office of Management and Budget, Paperwork Reduction Project (0704-0188), Washington, DC 20503.

1. AGENCY USE ONLY (Leave blank)		2. REPORT DATE 7 April 1995	3. REPORT TYPE AND DATES COVERED Scientific	
4. TITLE AND SUBTITLE Proceedings of the 16th Annual Conference on Atmospheric Transmission Models, 8-9 June 1993			5. FUNDING NUMBERS PE: 62101F PR 3054 TA GD WU 01	
6. AUTHOR(S) Editors: Gail P. Anderson James H. Chetwynd				
7. PERFORMING ORGANIZATION NAME(S) AND ADDRESS(ES) Phillips Laboratory/GPOS 29 Randolph Road Hanscom AFB, MA 01731-3010			8. PERFORMING ORGANIZATION REPORT NUMBER PL-TR-95-2042 (I) ERP, No. 1168	
9. SPONSORING / MONITORING AGENCY NAME(S) AND ADDRESS(ES)			10. SPONSORING / MONITORING AGENCY REPORT NUMBER	
11. SUPPLEMENTARY NOTES Volume I consists of pages 1 - 379; Volume II consists of pages 380 - 778				
12a. DISTRIBUTION / AVAILABILITY STATEMENT Approved for public release; distribution unlimited			12b. DISTRIBUTION CODE	
13. ABSTRACT (Maximum 200 words) This report contains the viewgraphs and other materials for the 37 papers presented at the 16th Annual Review Conference on Atmospheric Transmission Models held at the Geophysics Directorate, Phillips Laboratory (AFMC), Hanscom AFB, MA On 8-9 June 1993.				
14. SUBJECT TERMS Atmospheric transmittance Radiance Propagation			15. NUMBER OF PAGES 392	
			16. PRICE CODE	
17. SECURITY CLASSIFICATION OF REPORT Unclassified		18. SECURITY CLASSIFICATION OF THIS PAGE Unclassified	19. SECURITY CLASSIFICATION OF ABSTRACT Unclassified	20. LIMITATION OF ABSTRACT SAR

CONTENTS

SESSION A: REMOTE SENSING AND APPLICATIONS

Chairs: Gail Anderson, PL/GPOS; David Robertson, SSI

(Invited) Jean I.F. King	3
PL/Geophysics Directorate	
<i>Dependence of Remote Temperature Retrieval on Atmospheric Transmittance Accuracy</i>	
(Invited) Robert O. Green, James E. Conel and Thomas G. Chrien	5
Jet Propulsion Lab	
<i>Mapping Atmospheric Water Vapor and the Inversion of Spectral Radiance to Apparent Reflectance with MODTRAN2 and Data Measured by the Airborne Visible-Infrared Imaging Spectrometer (AVIRIS)</i>	
Bo-Cai Gao	37
NASA/GSFC	
<i>The Presence of Earth Atmospheric Bands in the LOWTRAN 7 Solar Irradiance Curve</i>	
William M. Cornette and Joseph G. Shanks	48
Photon Research Associates	
<i>The Impact of Thin Cirrus Clouds on Terrain Remote Sensing</i>	
T. Schmugge, P. Bougarel, M. Sugita, W. Brutsaert	69
USDA Hydrology Lab	
<i>Application of LOWTRAN 7 to AVHRR Thermal Data in FIFE</i>	
Zhengming Wan and Jeff Dozier	86
UC Santa Barbara	
<i>An Urgent Need of Validating Water Vapor Absorption Coefficients for the Development of EOS's Earth Surface Temperature Algorithms</i>	
Kelly V Chance and Akihiko Kuze	102
Smithsonian Astrophysical Observatory	
<i>Analysis of Cloud-Top Height and Related Cloud Parameters from Satellites Using the O₂ A and B Bands</i>	
Peter Ashcroft	116
Carnegie Mellon Univ.	
<i>The Use of Space Based Remote Sensing for Estimation of the Methane Mixing Ratio in the Mixing Layer</i>	
A.S. Grossman, K.E. Grant	132
Lawrence Livermore National Laboratory	
<i>A Correlated K-Distribution Model of the Atmospheric Heating Rates for Overlapping Spectra of CO₂/H₂O and CH₄/N₂O</i>	

By _____	
Distribution / _____	
Availability Codes	
Dist	Avail and/or Special
A-1	

CONTENTS

SESSION B: RADIATIVE TRANSFER CODE DEVELOPMENT

Chair: William A.M. Blumberg, PL/GPOS	156
G. Anderson, J. Chetwynd, F. Kneizys, A. Berk, L. Bernstein, D. Robertson, P. Acharya, J.-M. Theriault, L. Abreu, S.A. Clough, J.-L. Moncet	157
PL/Geophysics Directorate, SSI, DREV, ONTAR, AER <i>FASCODE/MODTRAN: Validation and Applications</i>	
J.-M. Theriault, G.P. Anderson, J.H. Chetwynd, E. Murphy, V. Turner, M. Cloutier, A. Smith, J.-L. Moncet	192
DREV (Valcartier), PL/Geophysics Directorate, ONTAR, Univ. of Wisc., AER <i>Retrieval of Tropospheric Profiles from IR Emission Spectra: Preliminary Results With DBIS</i>	
L.W. Abreu, J. Schroeder, A. McCann, J. Kristl, S. Harvey, and M. Voltaire	199
ONTAR Corp <i>PcModTRAN 2: ONTAR'S PC Compatible MODTRAN 2 Software</i>	
A. Berk, D.C. Robertson, L.S. Bernstein, R.L. Sundberg, R.J. Healey R.D. Sharma, G.P. Anderson, J.H. Chetwynd, M.L. Hoke	214
Spectral Sciences, Inc., Yap Analytics, PL/Geophysics Directorate <i>SAMM: SHARC and MODTRAN Merged</i>	
William M. Cornette and David C. Robertson	234
Photon Research Assoc., and Spectral Sciences Inc. <i>The Moderate Spectral Atmospheric Radiance and Transmittance (MOSART) Program</i>	
K. Stamnes, S. Tsay, and M. Yeh	291
Univ. of Alaska and Calem Research Corp <i>Inclusion of Accurate Multiple Scattering in MODTRAN</i>	
Donald E. Anderson, Robert De Majistre and Scott Evans	305
John Hopkins/APL and Computational Physics Inc. <i>Rayleigh and Aerosol Scattering in the Troposphere and Stratosphere in the Spectral Range 175-850nm: An Interactive Model</i>	
P.C. Ip, S.B. Downer, M. Noah, K. Radermacher, J.P. Kennealy and D. Einstein, F.O. Clark	318
Mission Research and PL/Geophysics Directorate <i>PLEXUS: Expert System and Expert-Assisted User Software</i>	
Susan McKenzie	340
Mission Research Corp. <i>Earthlimb Backgrounds in the Strategic Scene Generator Model</i>	
Larrene K. Harada & Daniel H. Leslie	353/391
W.J. Schafer Associates <i>Atmospheric Extinction Analysis for the Air Force Airborne Laser Program</i>	

SESSION C: SPECTROSCOPY APPLICATIONS

Chair: Laila Jeong, PL/GPOS	354
Shinji Kadokura and Akiro Shimota	355
Komae Research Lab, Japan <i>A Fast Scheme for Line-by-Line Forward Model</i>	
Nobuo Takeuchi	357
Chiba University, Japan <i>Application of FASCODE Program to a High Temperature Gas Monitoring</i>	
K. Yoshino, J.R. Esmond, J.E. Murray, Y. Sun, A. Dalgarno, W.H. Parkinson, A.P. Thorne	380
Smithsonian Center for Astrophysics and Blackett Laboratory <i>VUV Fourier Transform Spectroscopy of the $\delta(0,0)$ Band of NO</i>	

SESSION D: Non-LTE SPECTROSCOPY APPLICATIONS

Chair: Richard H. Picard, PL/GPOS	440
David Robertson, Robert Sundberg, James Duff, John Gruninger, Steve Adler-Golden, and Ramesh Sharma	441
Spectral Sciences Inc. and PL/Geophysics Directorate <i>SHARC: A Model for Calculating Atmospheric Radiation Under Non-Equilibrium Conditions</i>	
David P. Edwards, Manuel Lopez-Puertas, Miguel Lopez-Valverde	462
National Center for Atmospheric Research and Institute for Astrophysics, Andalucia <i>Non-LTE Studies of the 15 μm Bands of CO₂ for Atmospheric Remote Sensing</i>	
R.H. Picard, J.R. Winick, U. Makhlof, A. J. Paboojian, A. J. Ratkowski, K.U. Grossmann, D. Homann, and J.C. Ulwick	464
PL/Geophysics Directorate, Stewart Radiance Lab, ARCON, and Univ. of Wuppertal <i>Critical Tests of Non-LTE Radiative Models Against High Latitude Rocket Data</i>	

SESSION E: STRUCTURE ALGORITHMS

Chair: Edmond M. Dewan, PL/GPOS	490
James H. Brown	491
PL/Geophysics Directorate <i>Atmospheric Structure Simulation: An Autoregressive Model for Smooth Geophysical Power Spectra with Known Autocorrelation Function</i>	
Edmond M. Dewan	512
PL/Geophysics Directorate <i>An Update on the AFGL Optical Turbulence Radiosonde Model</i>	
James H. Brown	530
PL/Geophysics Directorate <i>A Nighttime Structure Model of Atmospheric Optical Turbulence, C_n^2, Derived from Thermosonde and High Resolution Rawinsonde Measurements</i>	

SESSION F: CLIMATOLOGIES

Chair: James H. Chetwynd, PL/GPOS 557

William M. Cornette 558

Photon Research Assoc.

The MOSART Global Climatological and Terrain Data Bases

S. Adler-Golden, J. Gruninger and M. Matthew 662

Spectral Science Inc.

SHARC/SAMM/MODTRAN Calculations Using a Climatology Model Atmosphere Generator

SESSION G: LIDAR APPLICATIONS

Chair: E.P. Shettle, Naval Research Lab 643

M.G. Cheifetz, D.R. Longtin, and J.R. Hummel 644

SPARTA

Development of a Signal-to-Noise Performance Model with Backscat Version 4.0

Neal H. Kilmer and Henry Rachele 659

Physcial Science Laboratory and Army Research Laboratory

An Optical Profile Function for Modeling Extinction and Backscatter Coefficients in Very Low Stratus Clouds and Subcloud Regions

Richard Garner 677

PhotoMetrics Inc.

Time and Polarization Dependent Double Scattering Calculations of Lidar Returns from Water Clouds

Gertrude Kornfeld 711

Army Research Laboratory

Sky Radiance and Ray Bending Calculation

S.A. Wood and G.D. Emmit 725

Simpson Weather Associates, Inc

Integration of LOWTRAN into Global Circulation Models for Observing System Simulation Experiments

Mireille Tanguy, Michel Autric, Bernard Salles 743

DGA FRANCE

Aerosol Distribution and IR Broadband Transmittance in the Marine Boundary Layer in the Mediterranean Environment

Carl R. Zeisse 756

Naval Command Control and Ocean Surveillance Center

Maritime Modifications to LOWTRAN Radiance

ATMOSPHERIC TRANSMISSION MODELS MEETING

8-9 JUNE 1993

ATTENDANCE LIST

NAME	AFFILIATION	PHONE NUMBER
ROBERT O. GREEN	JPL	818-354-9136
PAUL E. LEWIS	NPIC	202-863-3422
DANIEL E. CRAUN	NRAA	619-553-4598
BROOKE KOFFEND	AEROSPACE	319-336-7412
KURT STAMMES	UNIV OF ALASKA	907-474-7368
STACY L. ANGLE	LORAL	617-863-3918
ISABELLE LE NAOUR	ENSSAT BPHH7	33 96465030
WILLIAM M. CORNETTE	PRA	619-455-9741
LARRY BERNSTEIN	SSI	617-273-4770
TATSUYA YOKOTA	NIFS	81 298-51-6111
SHINUI KADOTURA	CRIEPE	81-3-3480-2111
ROBERT L. HAWKINS	PL/GPOS	617-377-8664
DOUGLAS YOUMANS	W J SCHAFER	508-256-2070
ROBERT WATERLAND	DUPONT	302-695-1511
JEAN RENE JEVAIS	CEA	33 56685083
YONG HAN	WPL	303-497-7109
ALLEN S. GROSSMAN	LLNL	510-423-6371
KEN PATTEN	LLNL	510-423-9418
RICHARD SHIRKEY	ARL/BE	505-678-5470
TOM SCHMUGGE	USDA/HYDROLOGY	301-504-8554
DAN LESLIE	W J SCHAFER	703-558-7900
JOHN SCHROEDER	ONTAR	617-739-6607
JEAN-MARIE FLAUD	LPMA, CNRS	33 144273161
NOBUO TAKEUCHI	RSIRC, CHIBA UNIV	81 43-251-1111
STEVE MAZUK	AEROSPACE	310-336-5614
MELANIE GOUVEIA	HUGHES STX	617-862-0715
STEVEN J. LIPSON	PL/GPOS	617-377-3626
JON MURRAY	SMITHSONIAN OBSER	617-496-7614
SAM MAKHLOUF	STEWART RADIANCE LAB	617-377-4203
VINCE DILEONE	MIT-LINCOLN LAB	617-981-2333
STEVEN ADLER-GOLDEN	SSI	617-273-4770
SEAN P. McGOWAN	MISSION RESEARCH	603-891-0070
LAILA S. JEONG	PL/GPOS	617-377-3671
RUTH LIEBOWITZ	PL/HO	617-377-3643
K. DIERER KLAES	EUMETSAT	49 6151 950 211
RICHARD TIPPING	UNIV OF ALABAMA	205-348-3799

JAMES H. CHETWYND	PL/GPOS	617-377-2613
LEONARD W. ABREU	ONTAR	508-689-9622
GERTRUDE KORNFELD	ARL/MSB	703-704-3201
RICHARD E. DAVIS	NASA-LANGLEY RES CTR	804-864-1647
KEN JUCKS	SMITHSONIAN AST OBSV	617-496-7580
RON RODNEY	WL/DOWA WPAFB	513-255-1978
OLGA LADO-BORDOWSKY	ENSSAT	33 96466613
JOHN BALLARD	RUTHERFORD LAB, UK	44 235 44 5132
LEX BERK	SSI	617-273-4770
AKIHIKO KUZE	SMITHSONIAN AST OBSV	617-496-7614
PETER ASHCROFT	CARNEGIE MELLON UNIV	412-268-2670
ANGELA PHILLIPS	HUGHES AIRCRAFT	310-616-0124
DAVID ROBERTSON	SSI	617-273-4770
C. MULDER	BELG INST SPACE AER	32 2 3730372
J MESGENTHCLER	LOCKHEED	415-424-2483
ERIC SHETTLE	NRL	202-404-8604
TESS HOFFMAN	PL/EDWARDS	805-275-5419
ALAN WETMORE	ARL-BED, WSMR, NM	505-678-5563
C R ZEISSE	NCWSC RDT&E	619-553-3602
ZHENGMING WAN	UNIV OF CA	805-893-4541
SHERMAN NESTE	MARTIN MARIETTA	215-531-6360
RICHARD GARNER	PHOTOMETRICS	617-935-6500
GEORG ECHLE	METEOROLOGIE INSTITUT	49 7247822847
JOHN KEREKES	MIT LINCOLN LAB	617-981-0805
ROLANDO RIZZI	ECMWF, UK	44 734 499080
CHARLES HUMPHREY	VISIDYNE	617-273-2820
REBECCA HEALEY	YAP ANALYTICS	617-863-1599
KOUICHI YOSHINU	CTR FOR ASTROPHYSICS	617-495-2796
GIL DAVIDSON	PHOTO METRICS	617-935-6500
EARL CURTIS	ROCKETDYNE	818-586-3121
MIREILLE TANGUY	DGA/PCN	33 94162190
ROBERT DEMAJISTRE	CPI/APL	301-953-6000
NEAL KILMER	PS LAB, NMSU	505-522-9495
ED NIPLE	ARI	508-663-9500
PIERRE SIMONEAU	ONERA, FRANCE	33 46936850
PAUL EITNER	MARTIN MARIETTA	215-531-1195
ELEANOR WALTHER	SANDIA NATIONAL LABS	505-844-4728
MARK CANN	YORK UNIV	416-736-2100
IAN S. ROBINSON	AEROSPACE	310-336-6142
MARC R. HAMMOND	MISSION RESEARCH CORP	603-891-0070
RONALD E. ALLEY	JET PROPULSION LAB	818-354-0751
AL ZACHOR	ARC	508-263-1931
ROBERT R. O'NEIL	PL/GPOS	617-377-4775
MARIE-ANNIDE GIRAUD	DGA/DCN	33 94162140
SHEPARD A. CLOUGH	AER	617-349-2282
WILLIAM A.M. BLUMBERG	PL/GPOS	617-377-3688

QUANCHENG MA	GISS, NASA	212-678-5574
GINAS VALDAR	HUGHES HTX	212-678-5528
RICHARD H. PICARD	PL/GPOS	617-377-2222
SUSAN MCKENZIE	MRC	603-891-0070
CHAN TOUART	HSTX	617-863-0677
STUART GATHMAN	NCCOSC-NKAD	619-554-1417
DAVID EDWARDS	NCAR, BOULDER, CO	303-497-1857
HARRY FINKLE	MIT/LL	617-981-4905
HANK REVERCOMB	UNIV OF WISCONSIN	608-263-6758
BERNARD SALLES	DGA/DCN	33 94162281
TERRY E. BATTALINO	NAWC	805-989-8383
ROBERT WILSON	BOSTON COLLEGE	617-552-8765
MARGARET GARDNER	VISIDYNE	617-273-2820
JAMES H. BROWN	PL/GPOS	617-377-4412
LARRY S. ROTHMAN	PL/GPOS	617-377-2336
JOHN EOLL	GRC	508-777-6323
JAMES WALLACE	FAR FIELD, INC	508-443-9214
JOHN O. WISE	PL/GPOB	617-377-5993
NICOLE HUSSON	LMD/CNRS	33 69334802
AGNES BAUER	LSH-UNIV LILLE	33 20434789
SUSAN DOWNER	MRC	603-891-0070
ROGER A. VAN TASSEL	PL/GPO	617-377-2951
WILLIAM GALLERY	AER	617-349-2284
RAFAEL QUIROGA	ITT-FED SERV	805-734-8232
MEG NOAH	MRC	613-891-0070
JAMES J. GIBSON	PL/GPOS	617-377-4171
JAMES J. KLEESPIES	PL/GPAS	617-377-3136
KELLY CHANCE	SMITHSONIAN/HARVARD	617-495-7389
ALBERT BOEHM	HUGHES STX	617-377-2971
DON GRANTHAM	PL/GPA	617-377-2982
DAVE LONGTIN	SPARTA	617-863-1060
RICHARD ENG	MIT/LINCOLN LAB	617-981-3695
JEREMY R. WINICK	PL/GPOS	617-377-3619
JULIA VAIL	YAP ANALYTICS	617-377-3654
G. DAVID EMMITT	SWA	804-979-3571
ROBERT A. JOSEPH	ARCON	617-890-3330
VINCENT FALCONE	PL/GPAS	617-377-4029
PRECILA IP	MRC	603-891-0070
PETER P. WINTERSTEINER	ARCON	617-890-3330
PAUL HILTON	HUGHES STX	617-863-0388
ROBERT SUNDBERG	SPECTRAL SCIENCES	617-377-4770
PHAN DAO	PL/GPIM	617-377-4944
EDMOND M. DEWAN	PL/GPOS	617-377-4401
ROBERT HUFFMAN	PL/GPIM	617-377-3311
ARMAND PABOOJIAN	ARCON	617-377-2262
PIALI DE	SPECTRAL SCIENCES	617-273-4770

GABRIEL VAZQUEZ
MICHAEL CHEIFETZ
JAN HERRMANN
JOHN HUMMEL
ROY WALTERS
DAVID EDWARDS

NCAR
SPARTA
MIT/LINCOLN LAB
SPARTA
GENERAL RESEARCH
NCAR

303-497-1605
617-863-1060
617-981-3780
617-863-1060
508-777-6323
303-497-1857

AUTHOR INDEX

L.W. Abreu	199	J.I.F. King	3
P. Acharya	157	F.X. Kneizys	157
S. Adler-Golden	441,662	G. Kornfeld	711
G. P. Anderson	157,192,214	J. Kristl	199
D.E. Anderson	305	A. Kuze	102
P. Ashcroft	116	D.H. Leslie	353/391
M. Autric	743	D.R. Longtin	644
A. Berk	157,214	M. Lopez-Puertas	462
L.S. Bernstein	157,214	M. Lopez-Valverde	462
P. Bougarel	69	U. Makhlof	464
J.H. Brown	491,530	M. Matthew	662
W. Brutsaert	69	A. McCann	199
Kelly V Chance	102	S. McKenzie	340
M.G. Cheifetz	644	J.-L. Moncet	157,192
J.H. Chetwynd	157,192,214	E. Murphy	192
T. G. Chrien	5	J.E. Murray	380
F.O. Clark	318	M. Noah	318
S.A. Clough	157	A. J. Paboojian	464
M. Cloutier	192	W.H. Parkinson	380
J.E. Conel	5	R.H. Picard	464
W.M. Cornette	48,234,558	Henry Rachele	659
A. Dalgarno	380	K. Radermacher	318
R. DeMajistre	305	A. J. Ratkowski	464
E.M. Dewan	512	D. Robertson	157,214,234,441
S.B. Downer	318	B. Salles	743
J. Dozier	86	T. Schmugge	69
J. Duff	441	J. Schroeder	199
D.P. Edwards	462	J. G. Shanks	48
D. Einstein	318	R.D. Sharma	214,441
G.D. Ermit	725	A. Shimota	355
J.R. Esmond	380	A. Smith	192
S. Evans	305	K. Stamnes	291
B.-C. Gao	37	M. Sugita	69
R. Garner	677	Y. Sun	380
K.E. Grant	132	R.L. Sundberg	214,441
R.O. Green	5	N. Takeuchi	357
A.S. Grossman	132	M. Tanguy	743
K.U. Grossmann	464	J.-M. Theriault	157,192
J. Gruninger	441,662	A.P. Thorne	380
L.K. Harada	353/391	S. Tsay	291
S. Harvey	199	V. Turner	192
R.J. Healey	214	J.C. Ulwick	464
M.L. Hoke	214	M. Voltaire	199
D. Homann	464	Z. Wan	86
J.R. Hummel	644	J.R. Winick	464
P.C. Ip	318	S.A. Wood	725
S. Kadokura	355	M. Yeh	291
J.P. Kennealy	318	K. Yoshino	380
N.H. Kilmer	659	Carl R. Zeisse	756

ANNUAL REVIEW CONFERENCE ON:
ATMOSPHERIC TRANSMISSION MODELS

Tuesday 8 June 1993 a.m.

SESSION A: REMOTE SENSING AND APPLICATIONS

Chairs: Gail Anderson, PL/GPOS; David Robertson, SSI

BLANK PAGE

DEPENDENCE OF REMOTE TEMPERATURE RETRIEVAL ON ATMOSPHERIC TRANSMITTANCE ACCURACY

J.I.F. King

Geophysics Directorate
Phillips Laboratory
Hanscom AFB, MA 01731-3010

In the remote temperature sensing problem the earth-atmospheric system is scanned across the far-infrared emission bands of CO_2 and H_2O . The Planck radiation profile is degraded in its upward passage by scattering, absorption, and re-emission interactions with the transmitting medium. The effects of inaccurate atmospheric transmittances on the temperature inferences from the satellite data will be demonstrated and discussed.

VIEWGRAPHS UNAVAILABLE

MAPPING ATMOSPHERIC WATER VAPOR AND THE INVERSION OF SPECTRAL RADIANCE TO APPARENT REFLECTANCE WITH MODTRAN2 AND DATA MEASURED BY THE AIRBORNE VISIBLE-INFRARED IMAGING SPECTROMETER (AVIRIS)

R.O. Green, J.E. Conel, T.G. Chrien

Jet Propulsion Laboratory
California Institute of Technology

The Airborne Visible-Infrared Imaging Spectrometer (AVIRIS) is a NASA-sponsored Earth-looking imaging spectrometer designed, built and operated by the Jet Propulsion Laboratory. AVIRIS acquires flight data from the Q-bay of a NASA ER-2 at 20 km altitude that is operated from the Ames Research Center. This imaging spectrometer measures the total upwelling spectral radiance from 400 to 2500 nm in the electromagnetic spectrum through 224 channels at 10 nm spectral intervals. Data are acquired as 11 km by up to 100 km images with 20 m by 20 m spatial resolution. The spectral, radiometric and geometric characteristics of AVIRIS are calibrated in the laboratory. These characteristics are validated through inflight calibration experiments that are carried out each year. MODTRAN2 is used for mapping atmospheric water vapor and for the inversion of spectral radiance to apparent surface reflectance with data measured by AVIRIS.

**Work with MODTRAN2 and the
Airborne Visible-Infrared Imaging Spectrometer (AVIRIS)**

Robert O. Green

NASA

JET PROPULSION LABORATORY

OVERVIEW

AVIRIS Characteristics and Objectives

Inflight Calibration Experiment

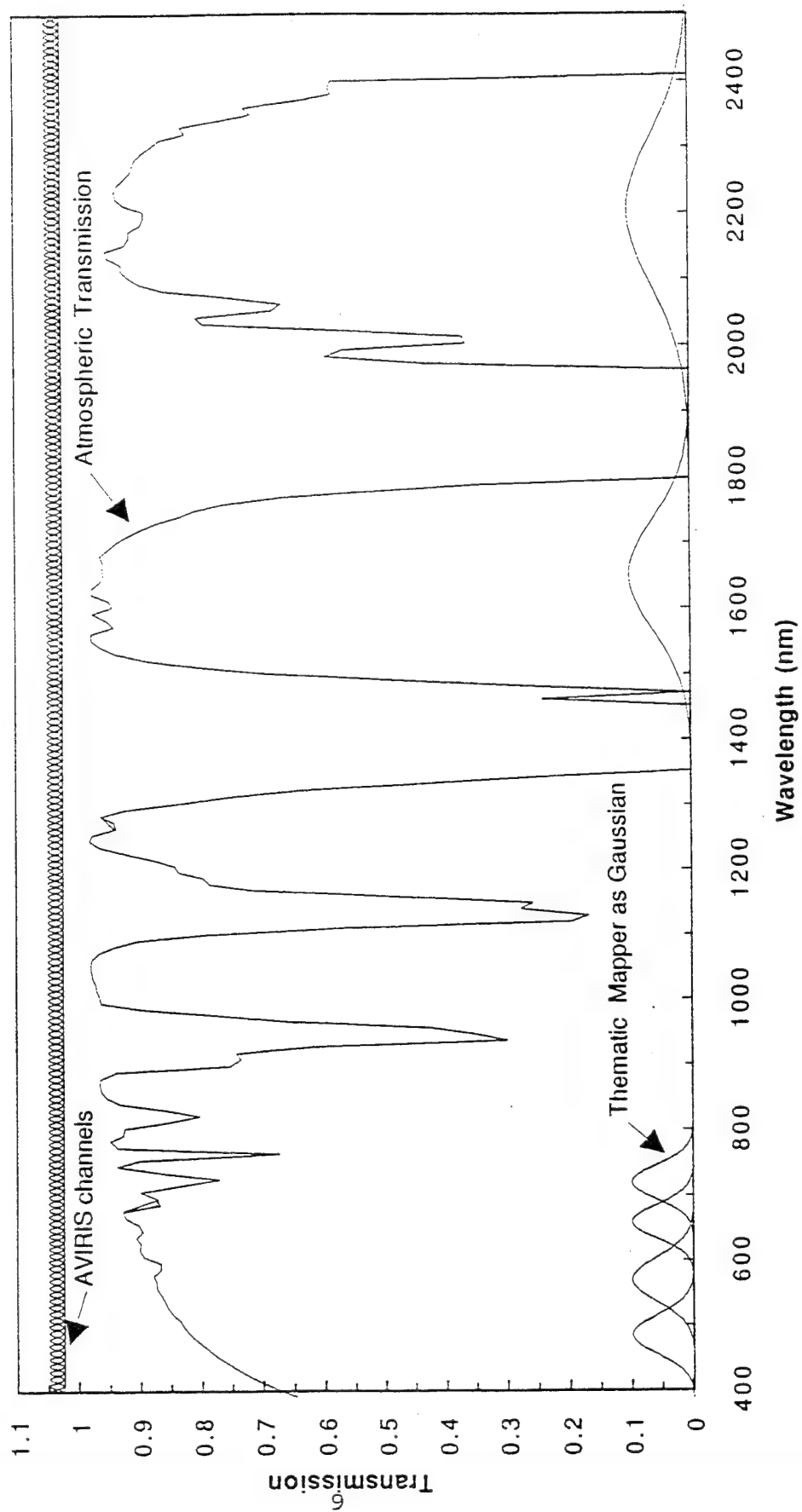
Water Vapor

Reflectance Calculation

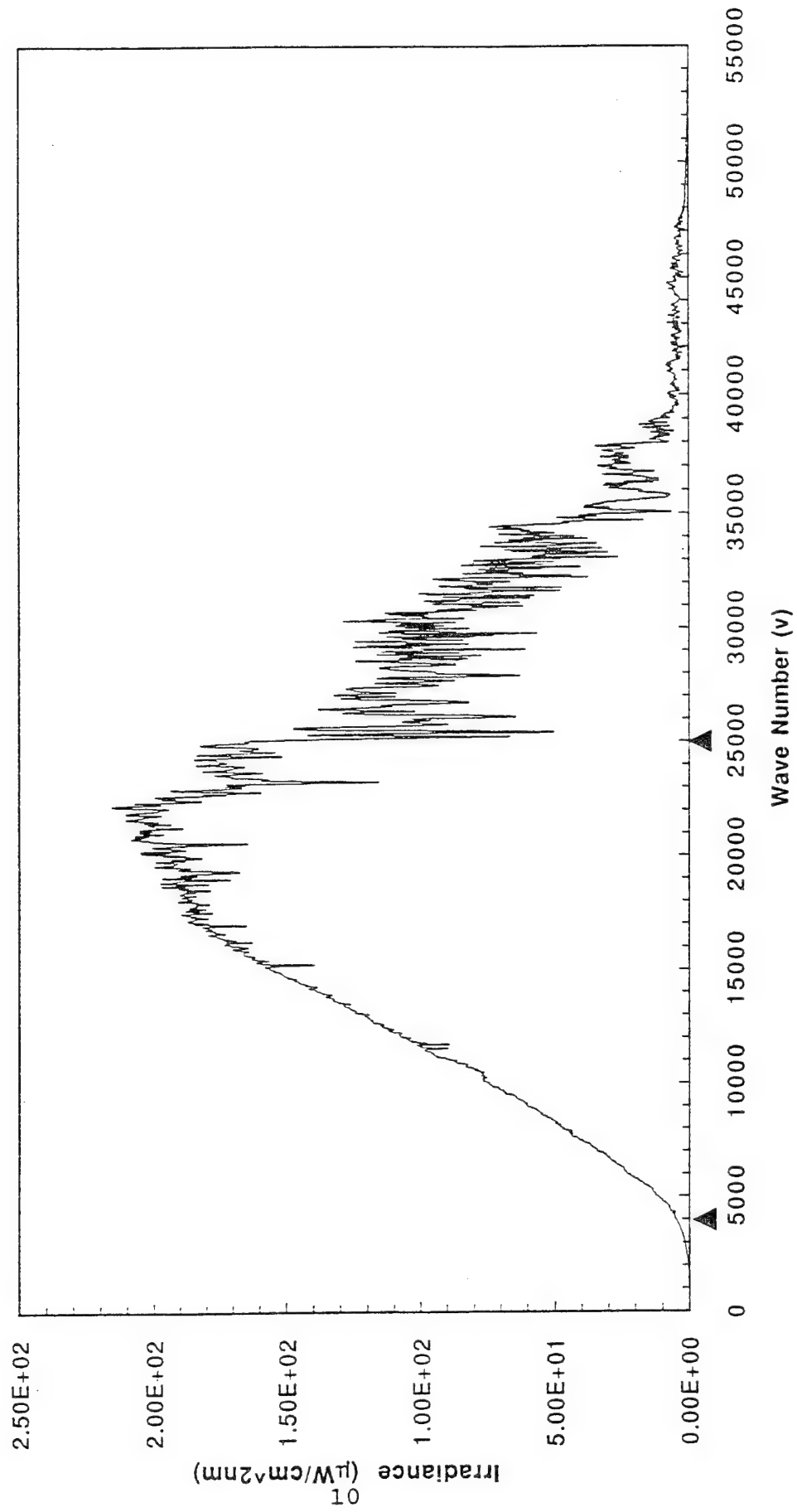
Possible Improvements to MODTRAN

AVIRIS Characteristics and Objectives

AVIRIS SPECTRAL RANGE AND RESOLUTION



AVIRIS Spectral Coverage in the MODTRAN Range



SCIENCE OBJECTIVE

Quantitative characterization of the Earth's terrestrial surface and atmosphere from geometrically coherent spectroradiometric measurements.

APPROACH

Measure the contiguous spectral signature of the upwelling radiance from 400 to 2500 nm

11 Use the resolved molecular spectral absorptions and partical scattering signatures to:

- Detect and identify the surface and atmospheric constituents present
- Assess and measure the expressed constituent concentrations
- Assign proportions to constituents in mixed spatial elements
- Delineate spatial distribution of the constituents
- Monitor changes in constituents through periodic data acquisitions

SCIENCE/APPLICATION DISCIPLINES

Terrestrial ecology: ecosystem type, constituents, chemistry, delineation, change...

Oceanography/inland waters: constituents, sediments, productivity, bathymetry ...

Geology & soils: mineralogy, rock & soil type, degradation, regional analysis..

Atmosphere: water vapor, gas constitutes, aerosols...

Clouds: type, extent, radiative properties...

Snow and ice hydrology: extent, grain size, impurities, runoff...

Environmental: resource monitoring, land use planing, evaluation...

Agriculture: crop type, state of growth, yield, stress...

Volcanology: gases, lava temperatures, lava type, lava age relationships...

Calibration: atmosphere, satellites, aircraft systems

DATA CHARACTERISTICS

SPECTRAL

Wavelength range 400 to 2500 nm
 Sampling <10 nm
 Spectral response (fwhm) 10 nm nominal
 Calibration 1nm

RADIOMETRIC

Radiometric range 0 to maximum lambertion radiance
 Sampling ~ 1 dn noise rms
 Absolute calibration <= 7 %
 Intra flight calibration <= 2 %
 Noise Exceeding nedl/snr requirement

GEOMETRIC

Field of view 30 degrees (11 km)
 Instantaneous FOV 1.0 mrad (20 m)
 Calibration <=0.1 mrad
 Flight line length Ten 100 km

OPERATIONAL CHARACTERISTICS

SENSOR

Imager type	Whiskbroom scanner (12 hz)
Dispersion	Four grating spectrometers (a,b,c,d)
Detection	224 detectors (32,64,64,64) Si and InSb
Digitization	10 bits (12 in 94)
Data rate	17 mbits/second (20.4 in 94)
Spectrum rate	7300 spectra/second
Data capacity	>10 gigabytes (>10,000 km ²)
Launches	~30 per year

PLATFORM

Aircraft	NASA ER-2
Altitude	20 km
Velocity	734 km/h
Range	<= 2100km
Flight duration	<=6.5 hours
Launch sites	Domestic & foreign

DATA ACQUISITION AND DISTRIBUTION

AVIRIS DATA ACQUISITION

- NASA investigators with flight request and sponsor support
- Non-NASA reimbursable acquisition with flight request

DATA DISTRIBUTION

- One week for quicklook distribution
- Two weeks for calibration and distribution upon request
- Possible special processing for same day distribution

HISTORIC DATA FROM THE ARCHIVE

- For marginal costs of reproduction \$250.00 per scene (10*11km)

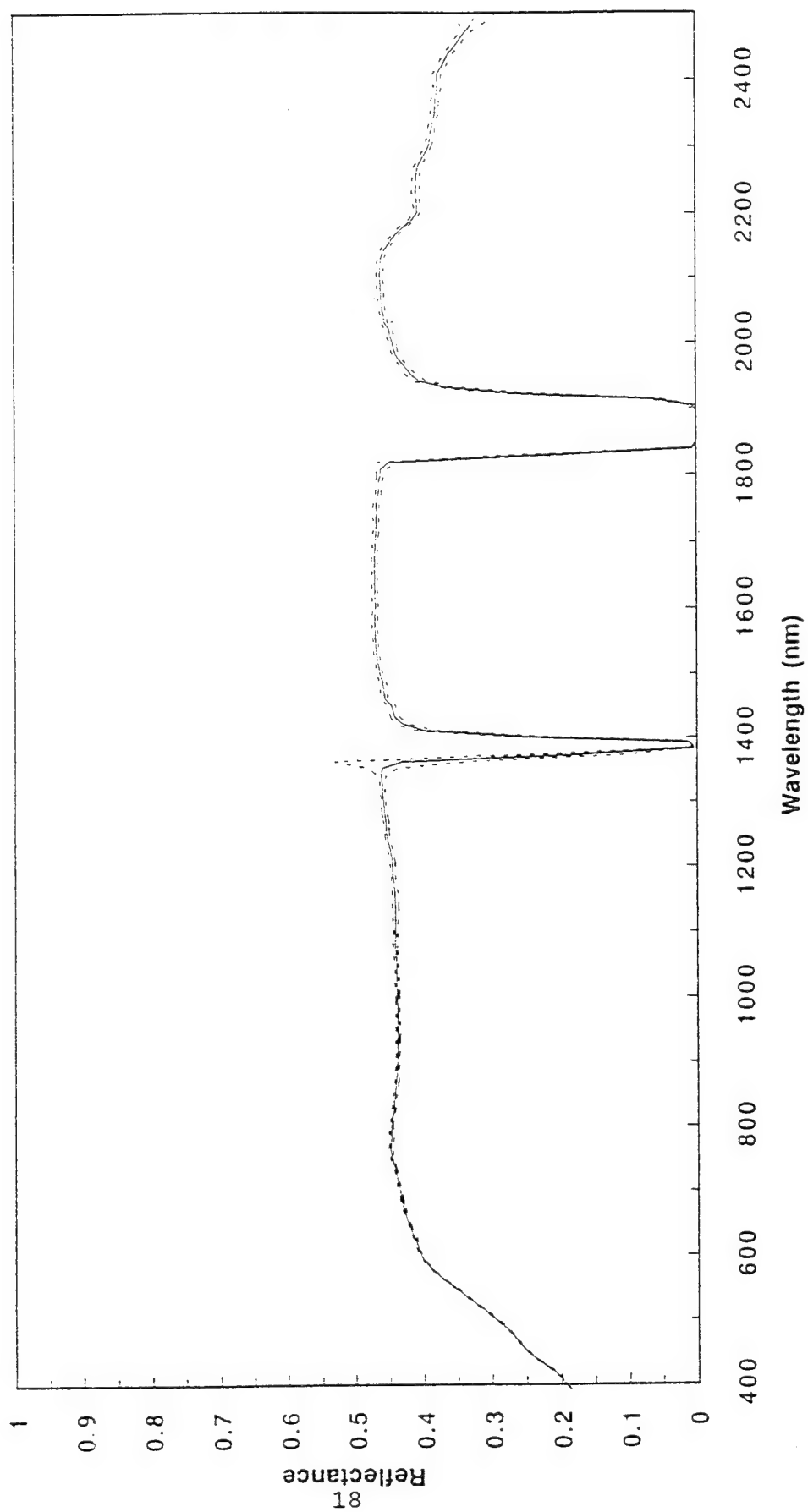
Inflight Calibration Experiment

CALIBRATION REQUIREMENT

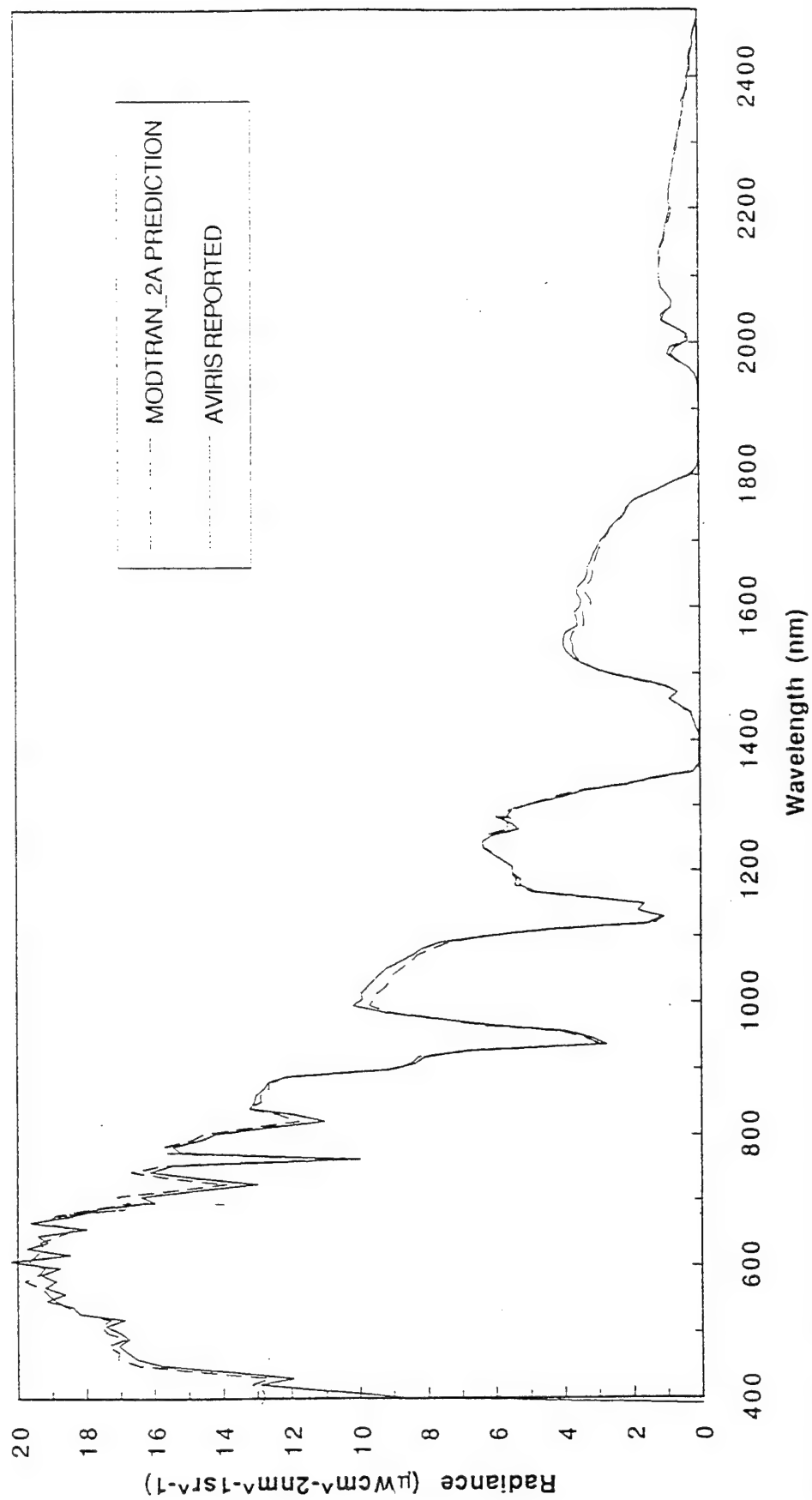
Imaging spectrometry data must be spectrally, radiometrically and geometrically calibrated in order to:

- Derive physical parameters from measured radiance
- Compare data acquired from different regions and from different times
- Compare and analyze imaging spectrometry data with data acquired by other instruments or generated by system models

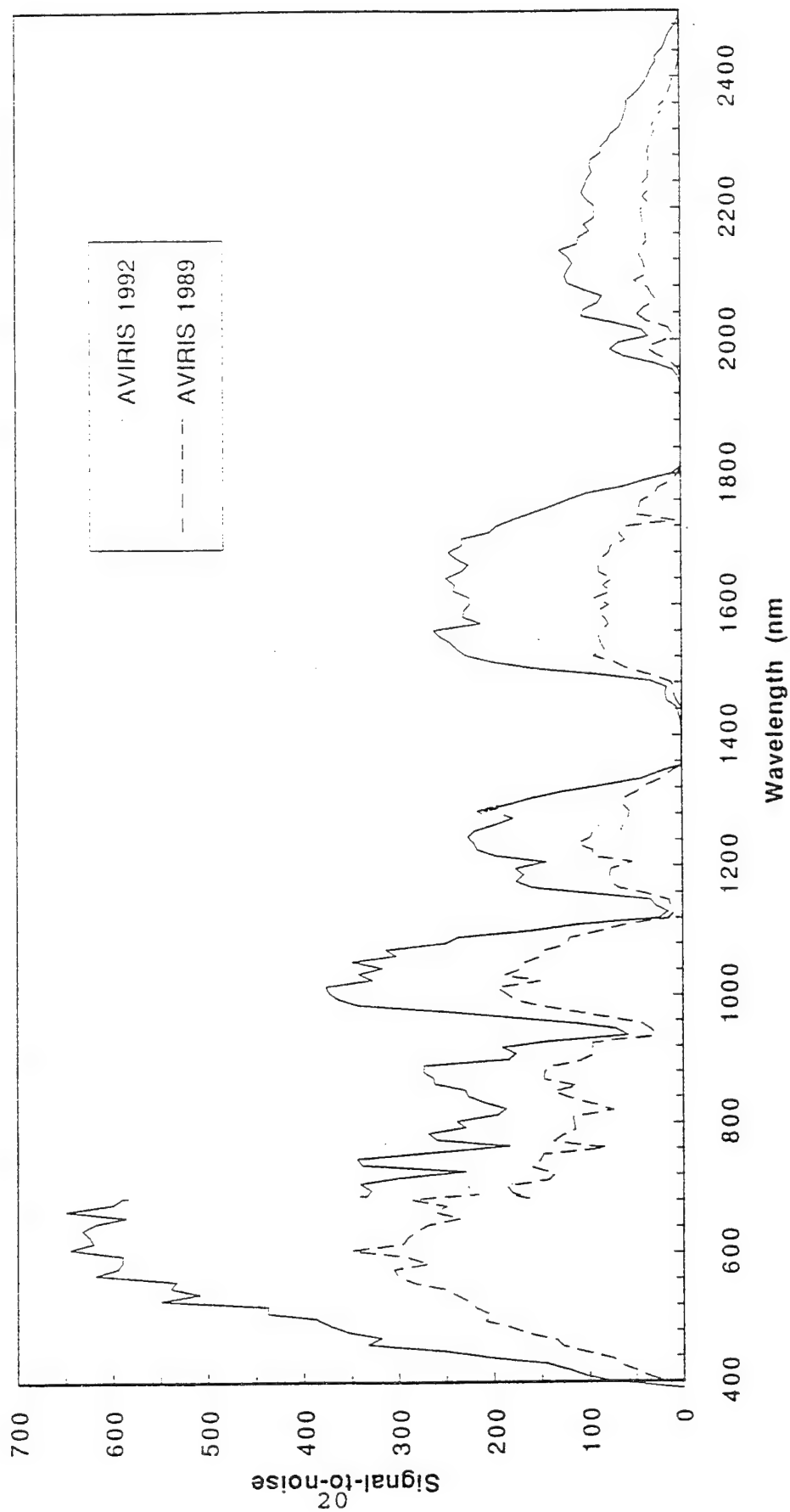
Inflight Calibration Experiment Rogers Dry Lake, 30 May 92



AVIRIS INFLIGHT CALIBRATION EXPERIMENT 30 MAY 1992

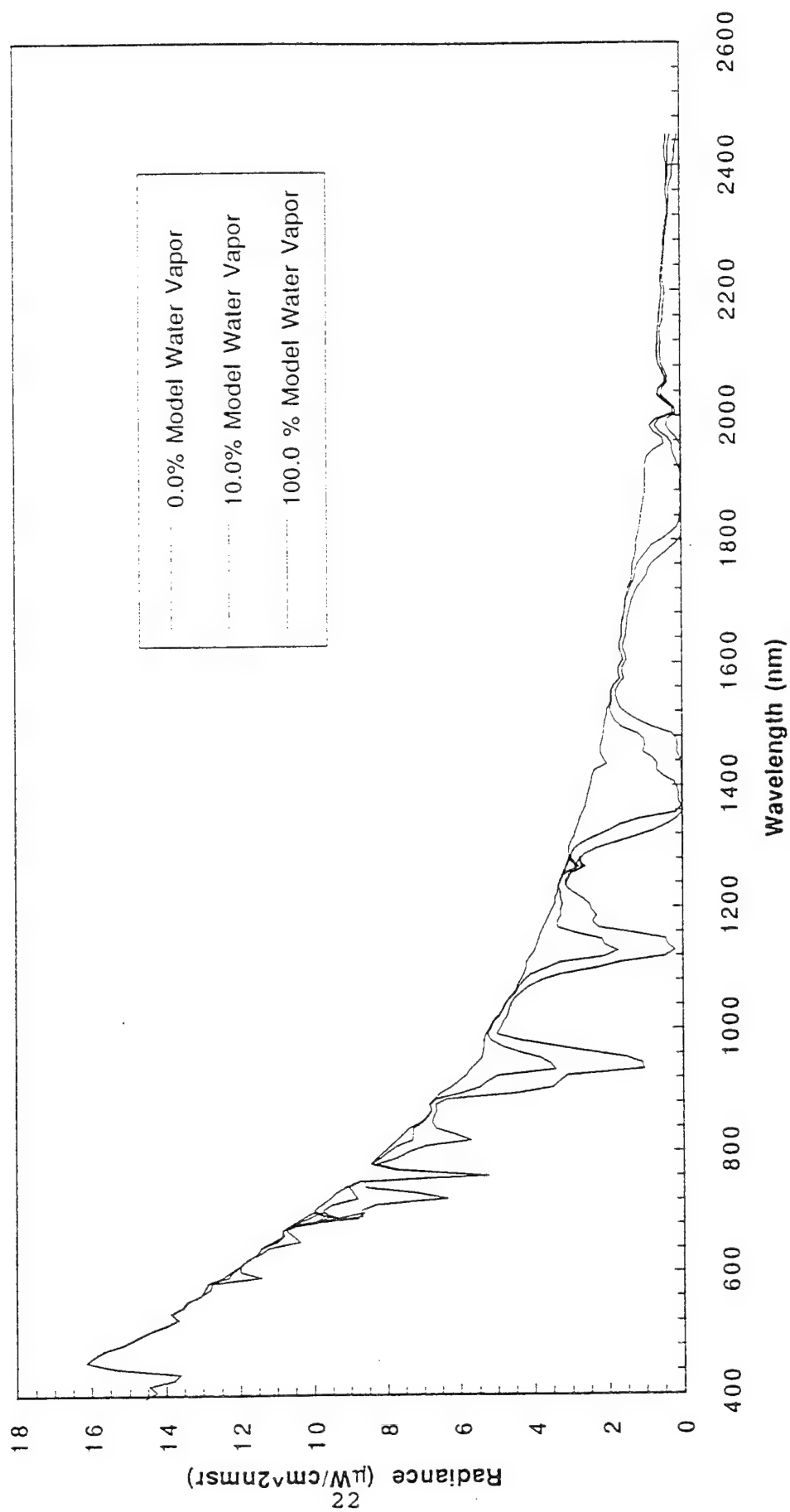


AVIRIS SIGNAL-TO-NOISE AT REFERENCE RADIANCE

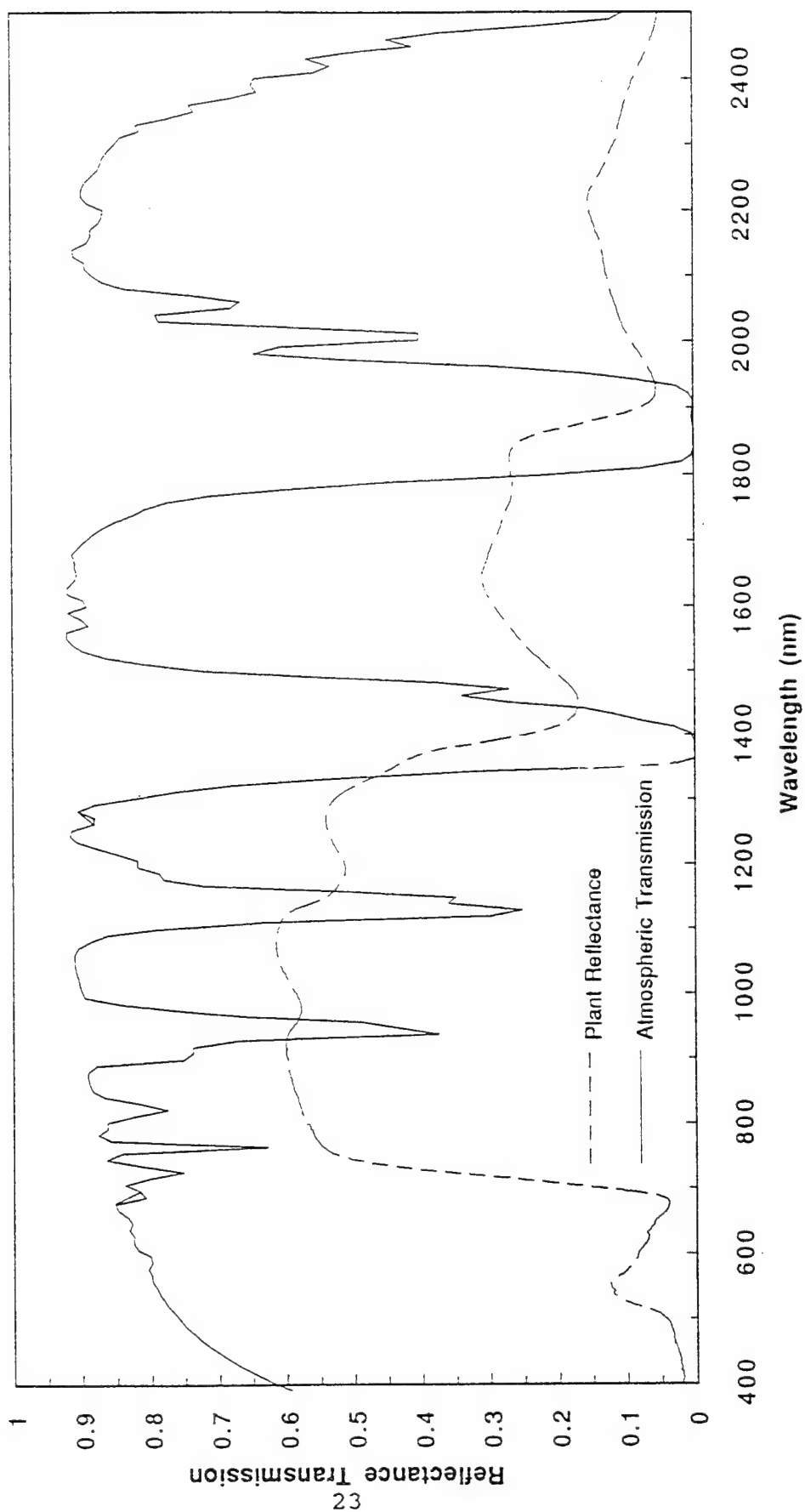


Water Vapor

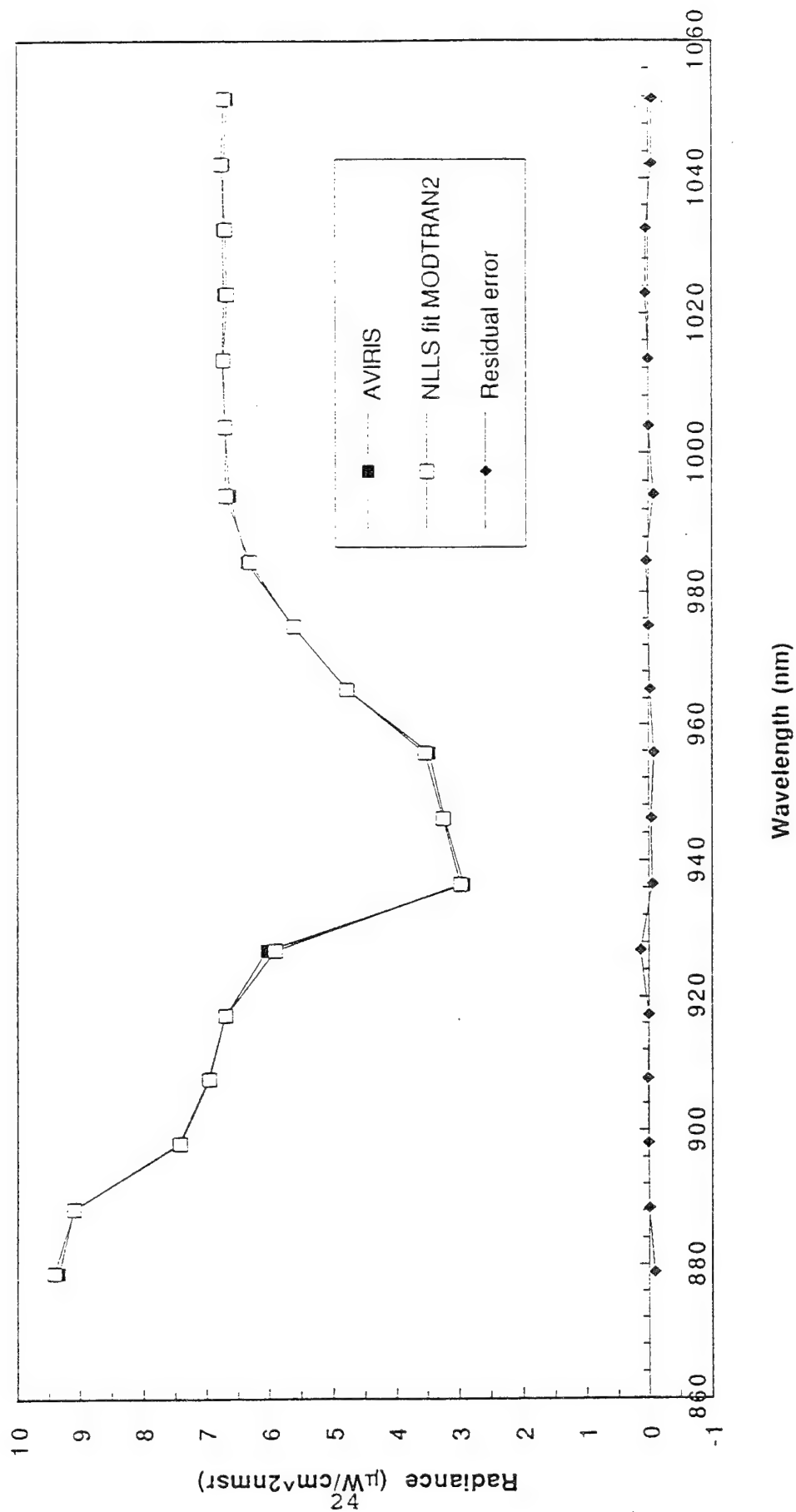
Influence of Water Vapor on AVIRIS Measured Radiance



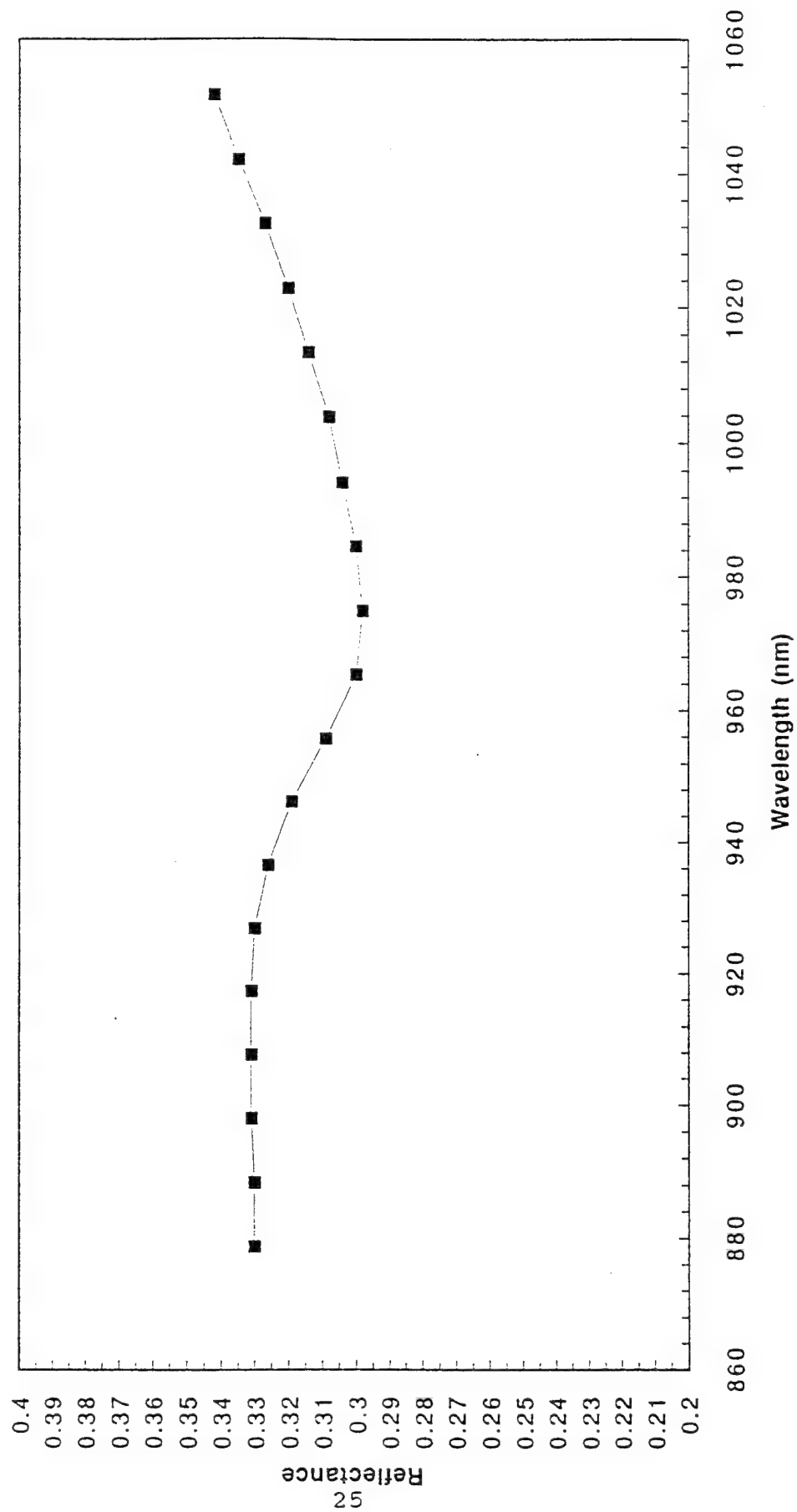
Atmospheric Transmission and Plant Reflectance



AVIRIS to NLLS Fit of MODTRAN2

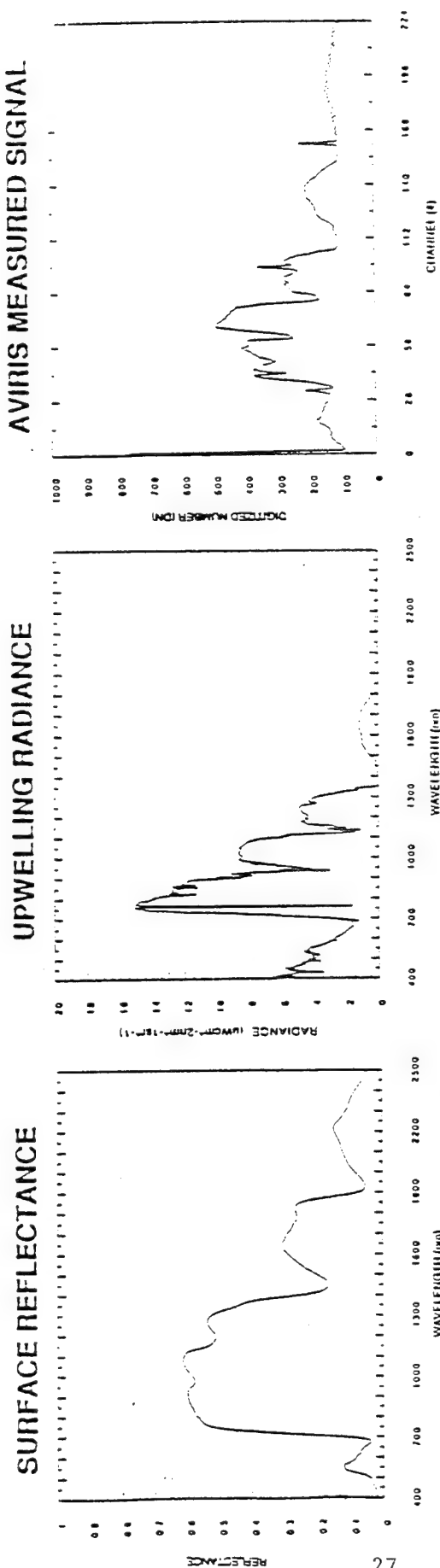


Reflectance for NLLS fit with MODTRAN2

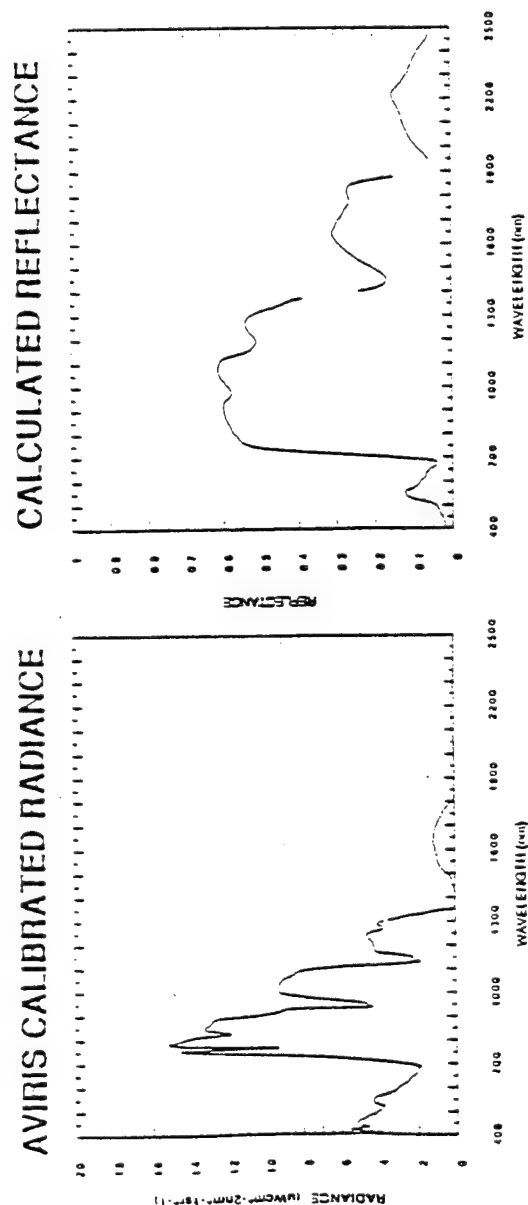


Reflectance Calculation

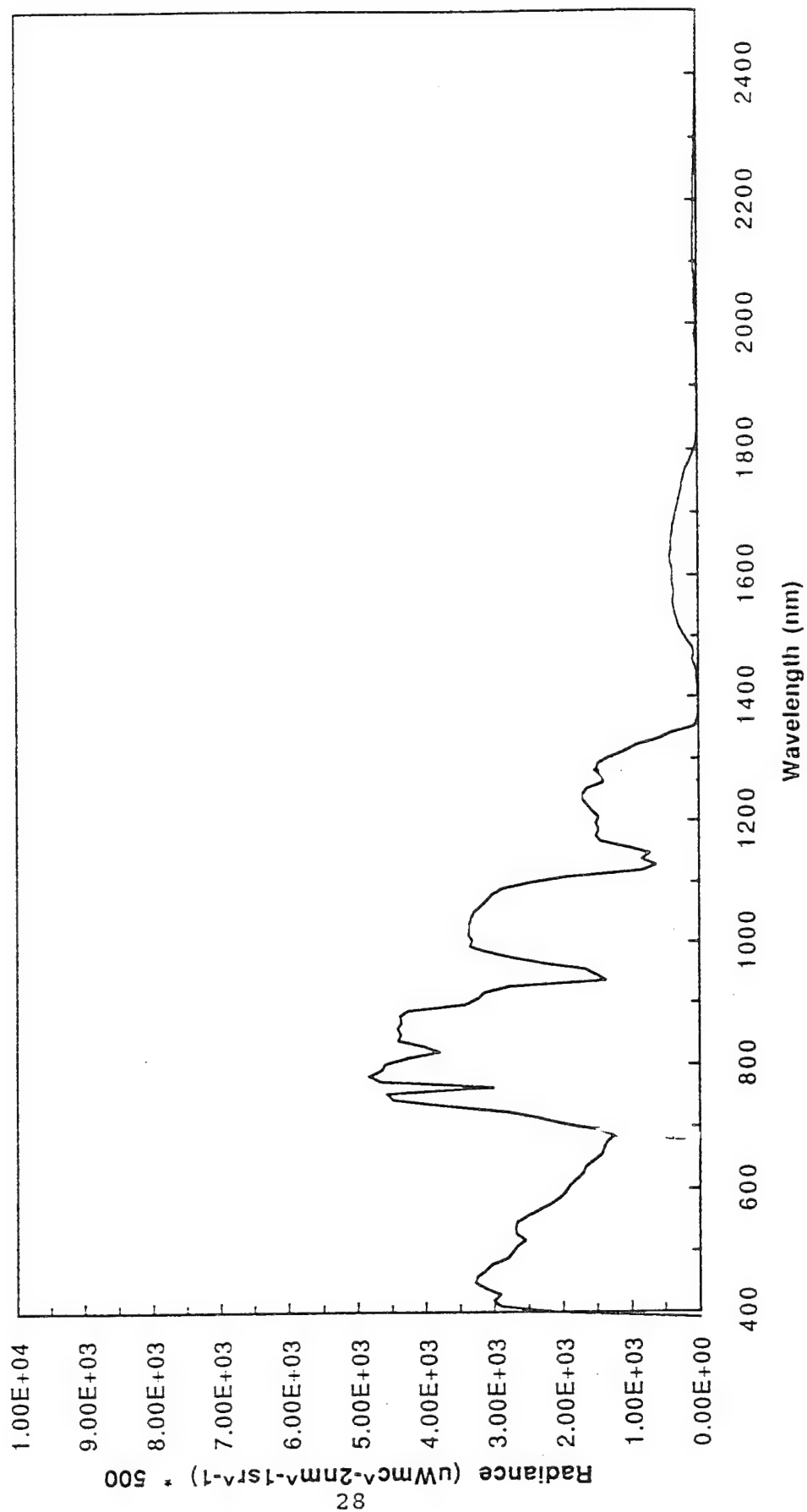
JPL AVIRIS: MEASUREMENT, CALIBRATION AND CALCULATED REFLECTANCE



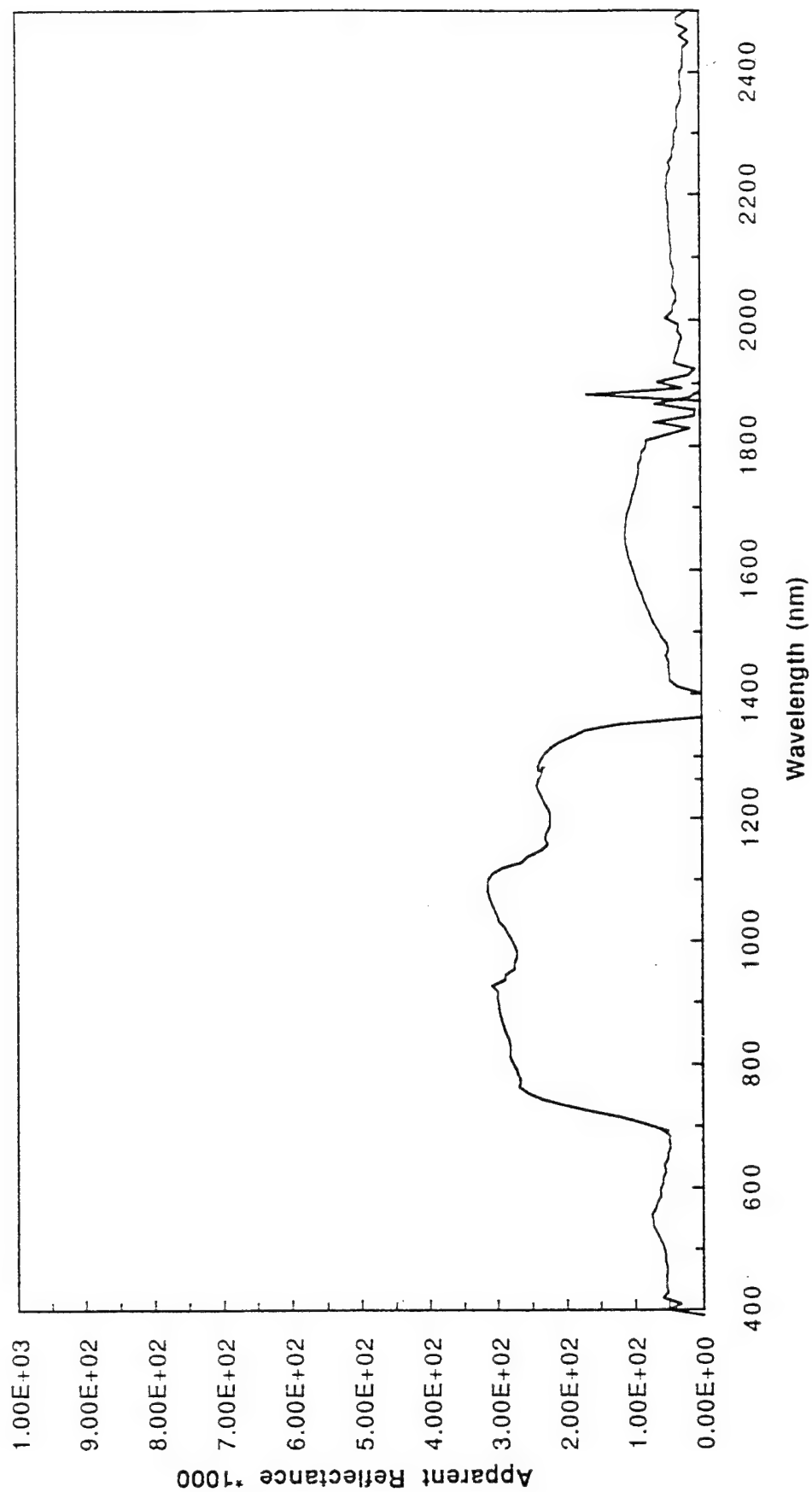
- PHYSICAL
PARAMETERS
DERIVED FROM
SURFACE
REFLECTANCE



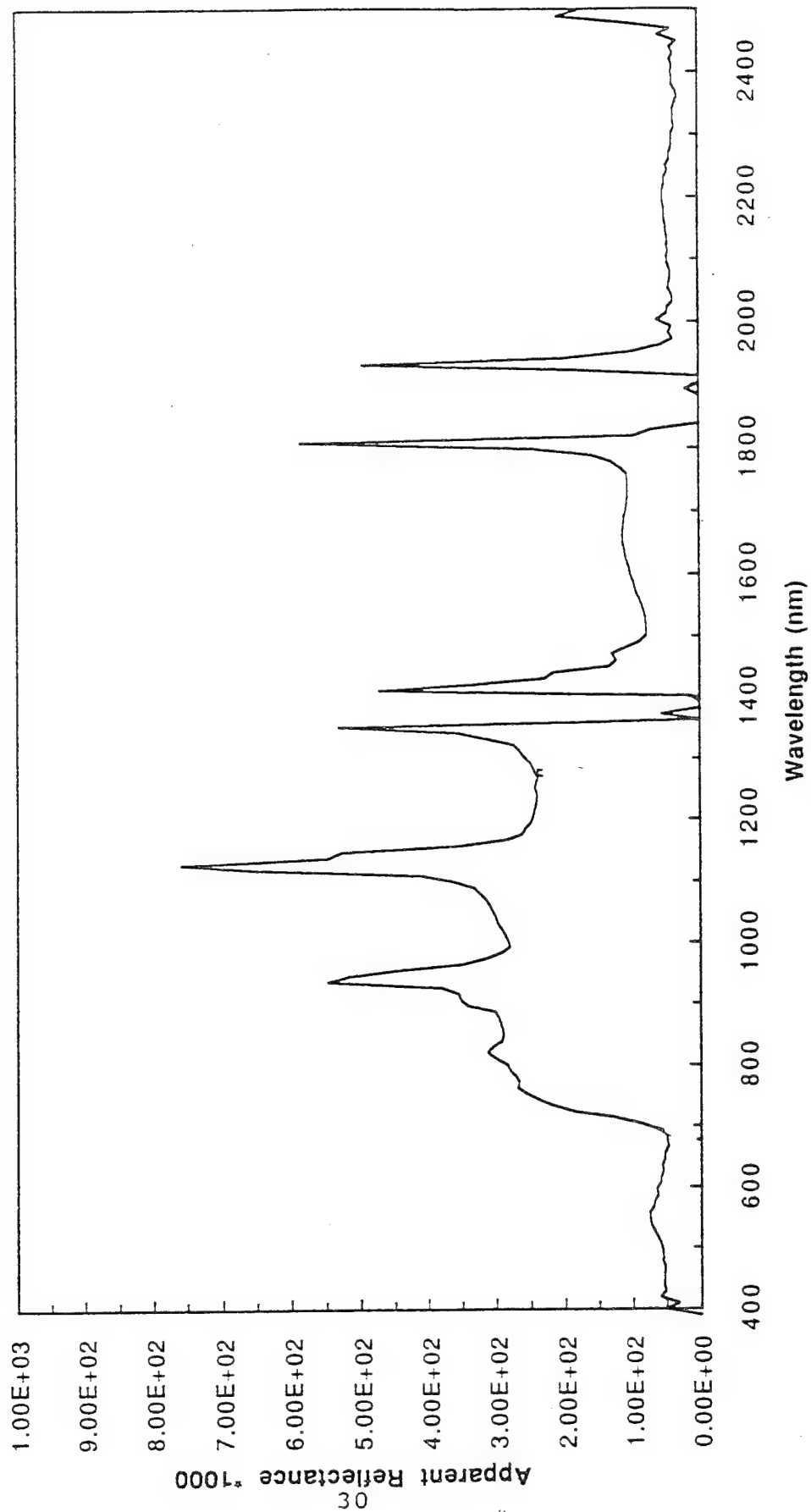
AVIRIS Calibrated Radiance, Jasper Ridge: Forest Target



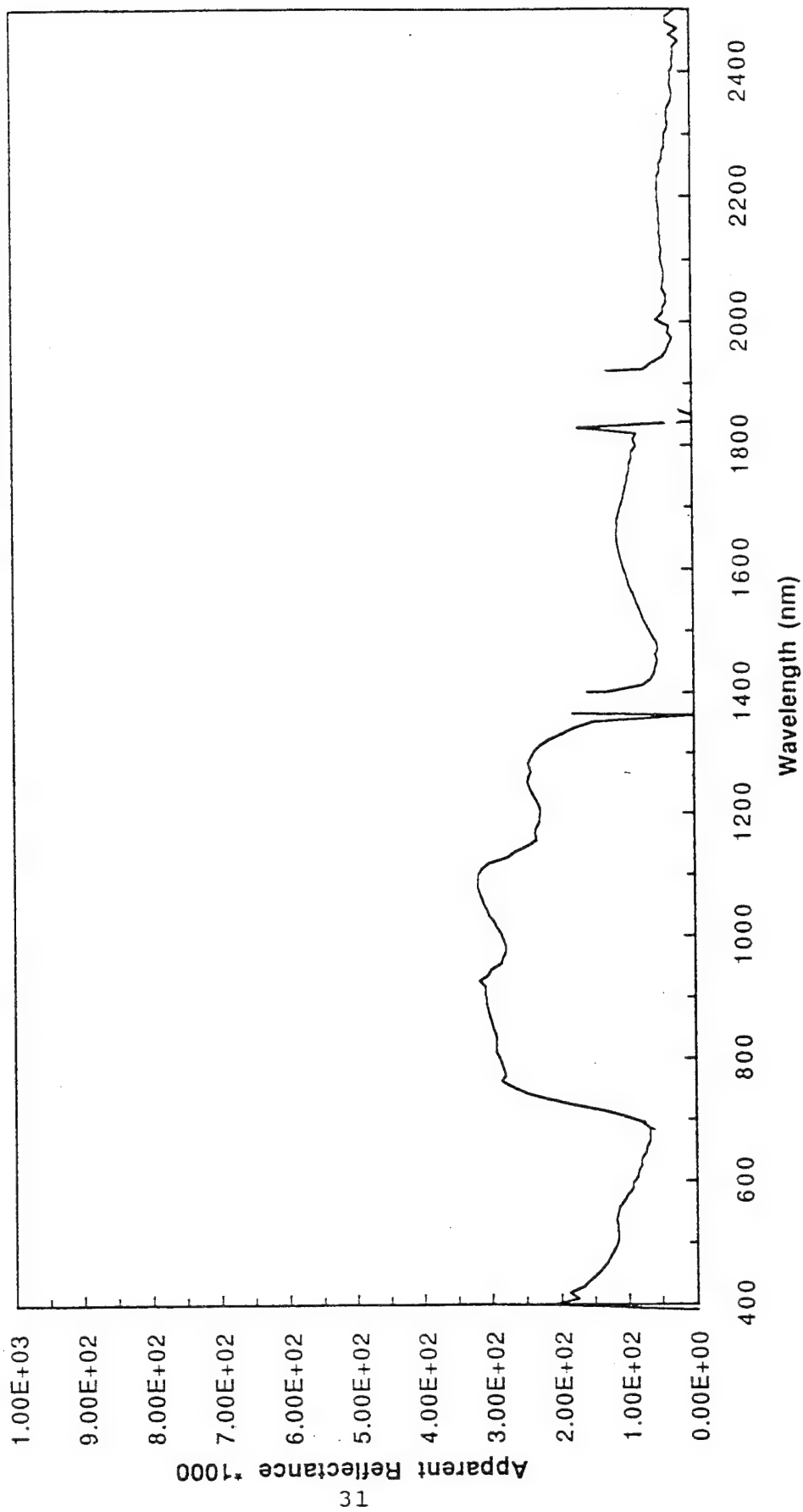
AVIRIS Apparent Reflectance, Jasper Ridge: Forest Target



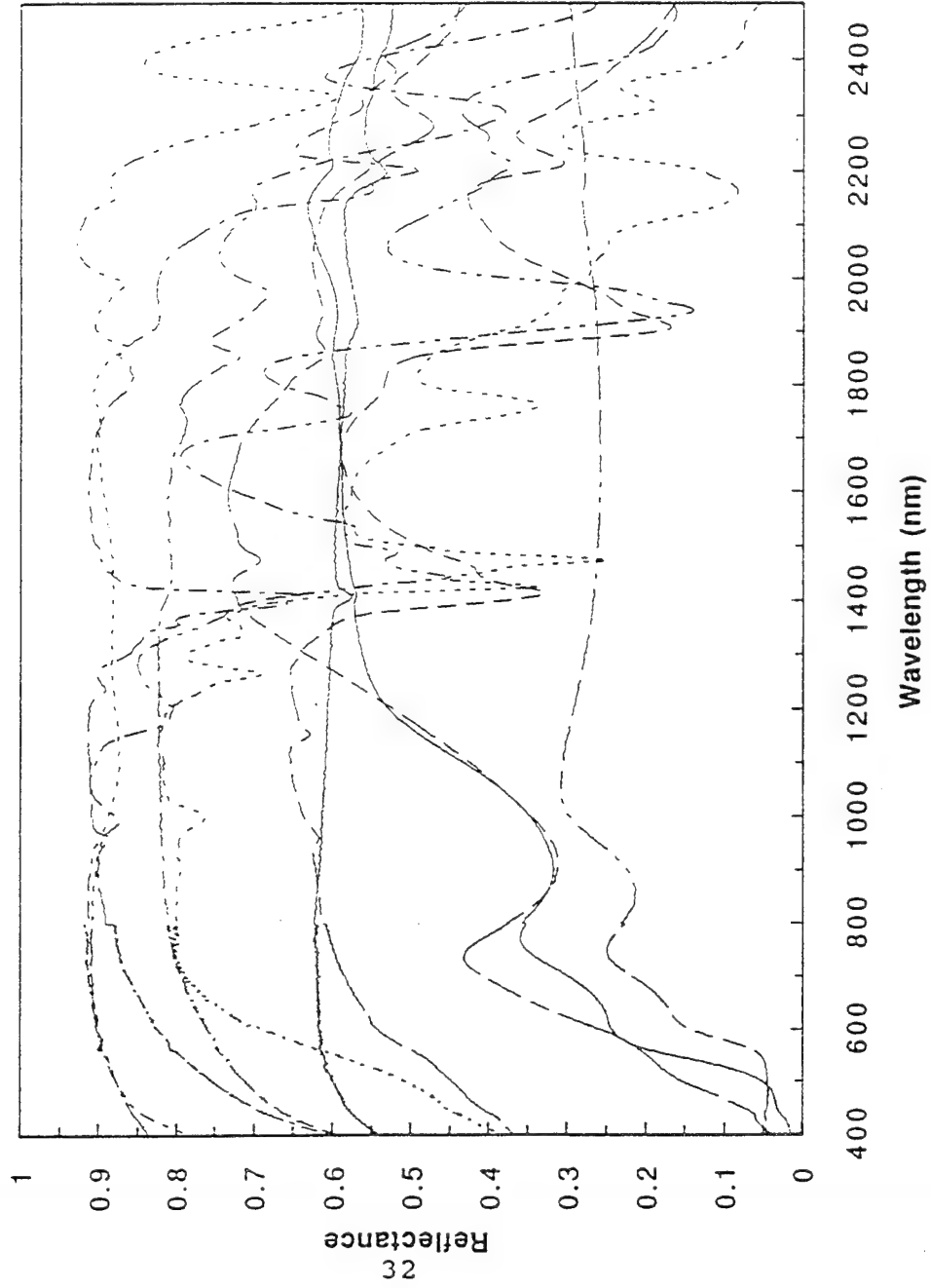
AVIRIS Apparent Reflectance, Jasper Ridge: Forest Target (incorrect water vapor)



AVIRIS Apparent Reflectance, Jasper Ridge: Forest Target (incorrect path radiance)



Mineral Spectra in the AVIRIS Spectral Range



MUSCOVITE

MONIMORILLONITE

ALUNITE

KAOLINITE

GYPSUM

GOETHITE

JAROSITE

CALCITE

DOLOMITE

HEMATITE

Possible Improvements to MODTRAN

Reflectance constraint

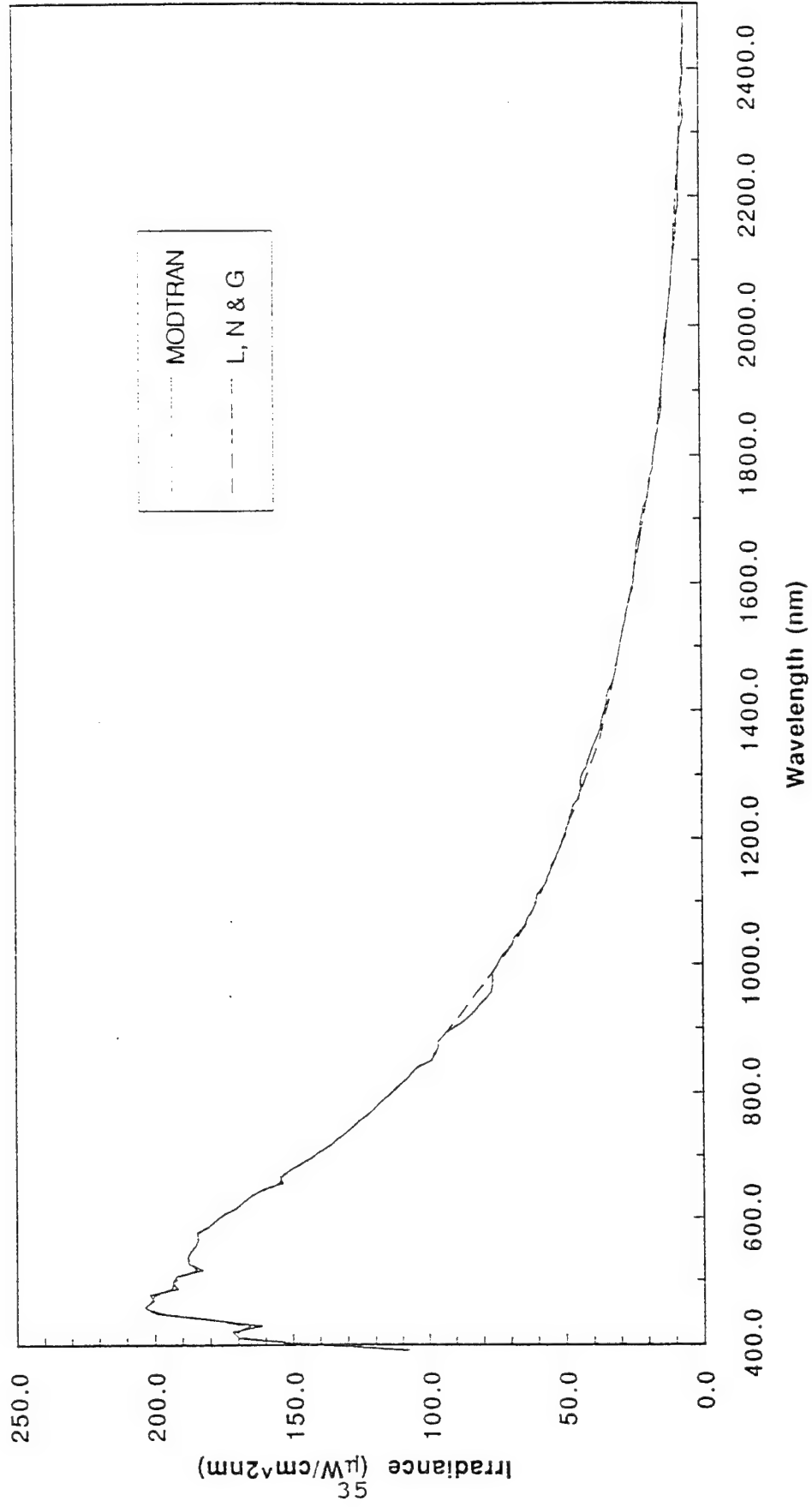
Solar Irradiance

Aerosols (350 to 1000 nm)

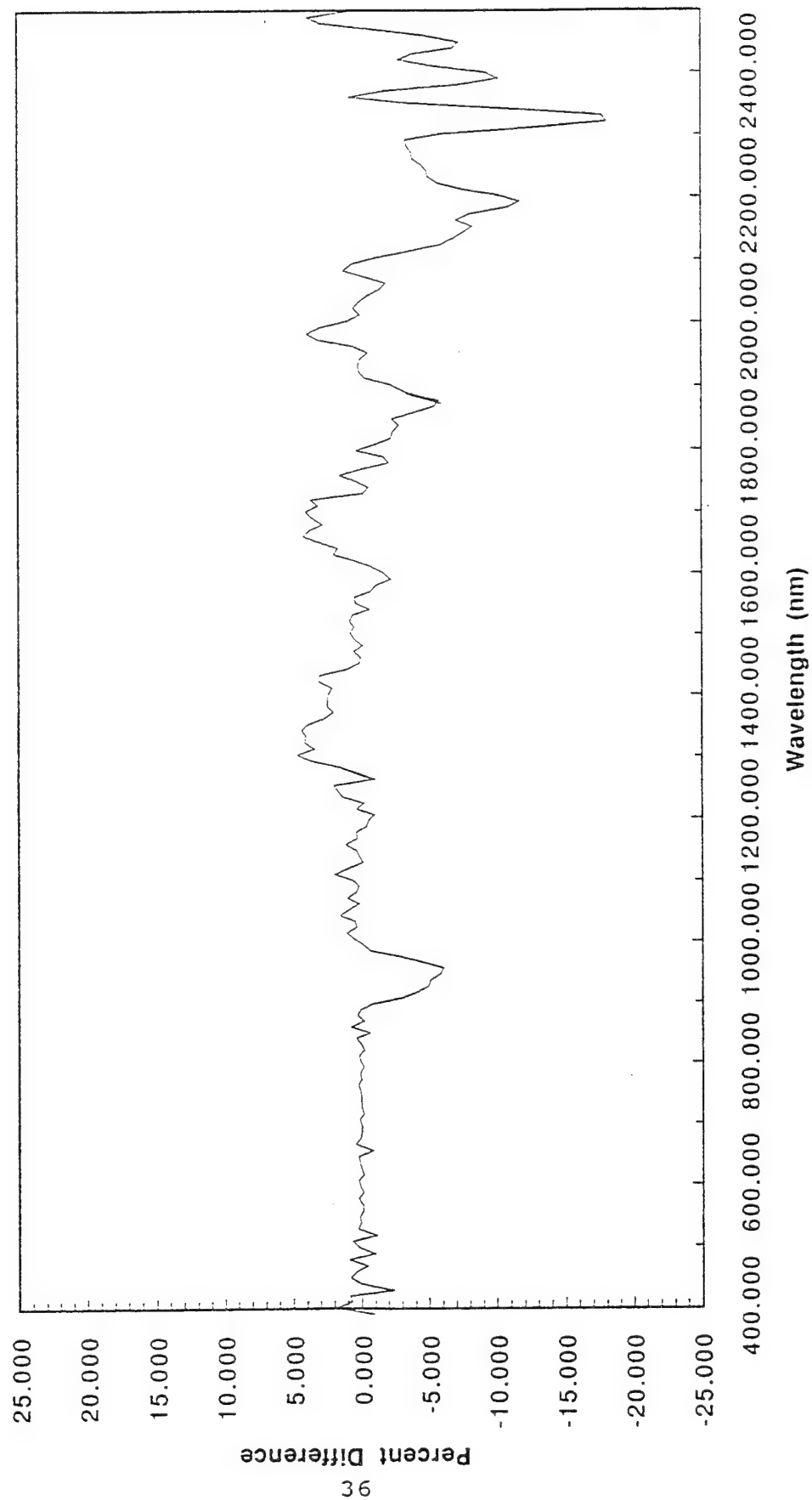
Water vapor models

Other gases

MODTRAN and L, N & G Exo Atmospheric Solar Irradiance



MODTRAN and L, N & G Exo Atmospheric Solar Irradiance Percent Difference



THE PRESENCE OF EARTH ATMOSPHERIC ABSORPTION BANDS IN THE LOWTRAN7 SOLAR IRRADIANCE CURVE

Author: Bo-Cai Gao

University Space Research Association (USRA)
NASA/Goddard Space Flight Center, Greenbelt, MD

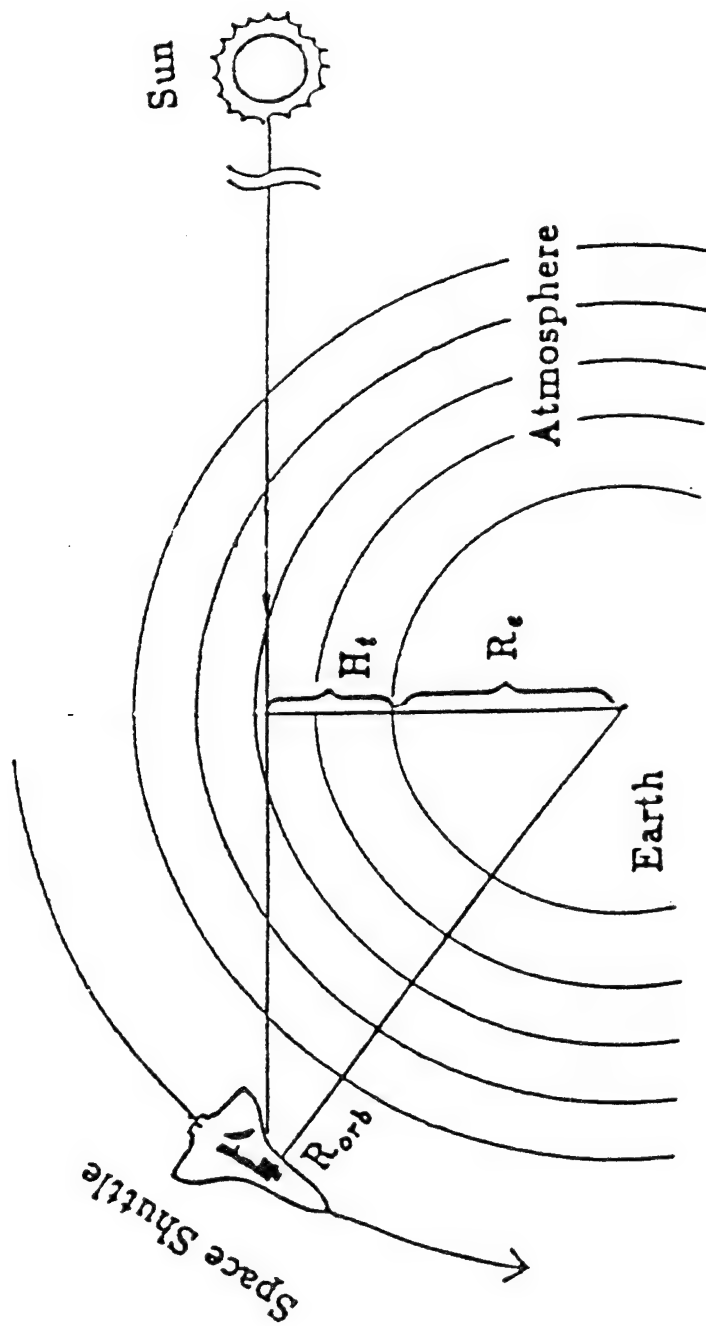
Presented by: Robert O. Green

Jet Propulsion Laboratory
California Institute of Technology, Pasadena, CA

INTRODUCTION

- The ATMOS Experiment during Spacelab 3 Mission in the Spring of 1985.
- Reduction of ATMOS spectra above the earth atmosphere to obtain a transmittance spectrum of the solar atmosphere
- Comparison of the ATMOS spectrum with LOWTRAN7 and other solar irradiance curves
- Problems with solar irradiance measurements in late 1960's and early 1970's.
- Improved measurements of solar irradiance spectra in the visible and near-IR from satellite platforms are necessary in the future.

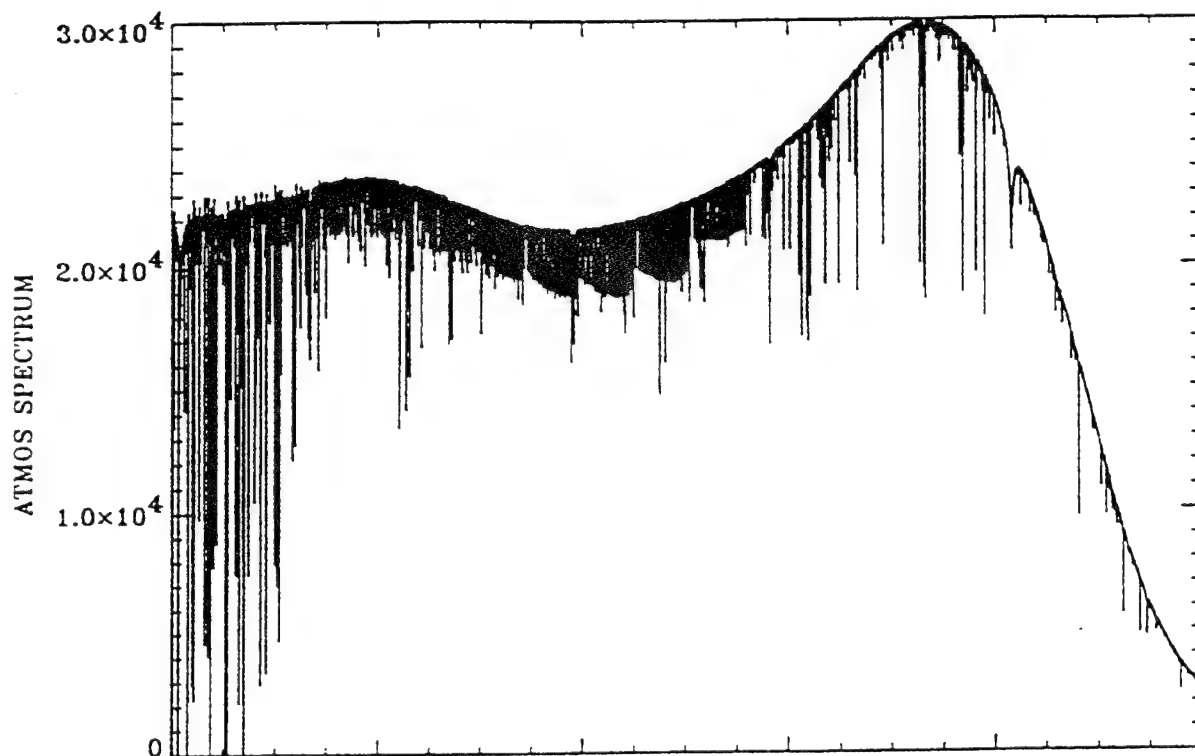
THE ATMOS EXPERIMENT



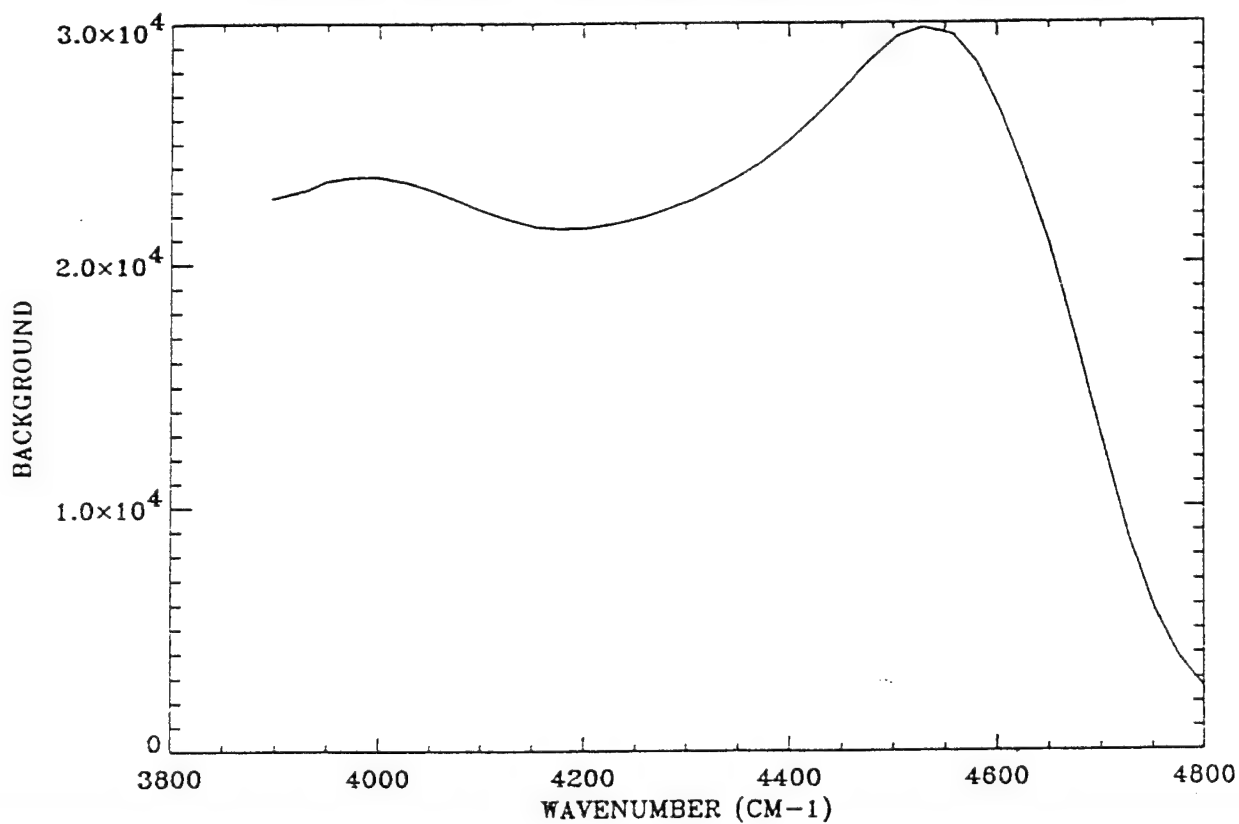
ATMOS instrument characteristics.

Spectral Interval Covered	550–4800 cm^{-1} (2.1–18 μm)
Spectral Resolution	0.01 cm^{-1} (unapodized)
Vertical Resolution	4 km
Field of View	1, 2, or 4 milliradian (selectable)
Scan Time	2.2 second
Detector	HgCdTe (cooled to 77 K)

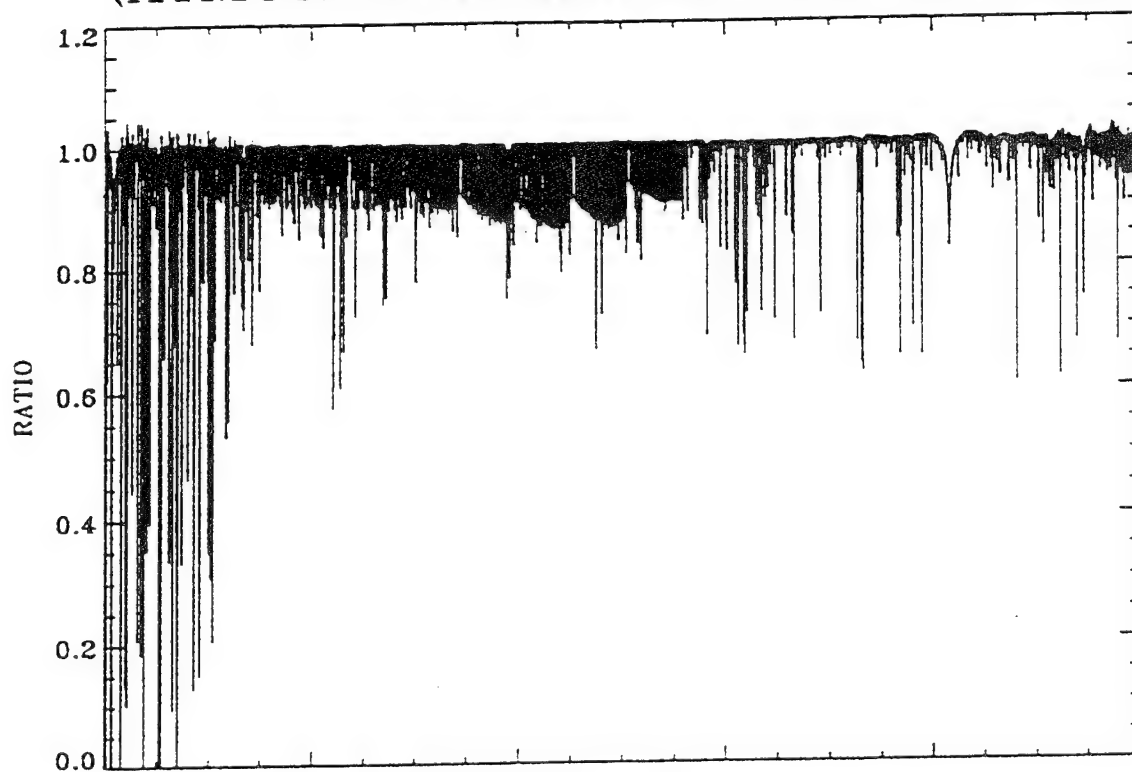
AN ATMOS SOLAR SPECTRUM ABOVE THE EARTH ATMOSPHERE



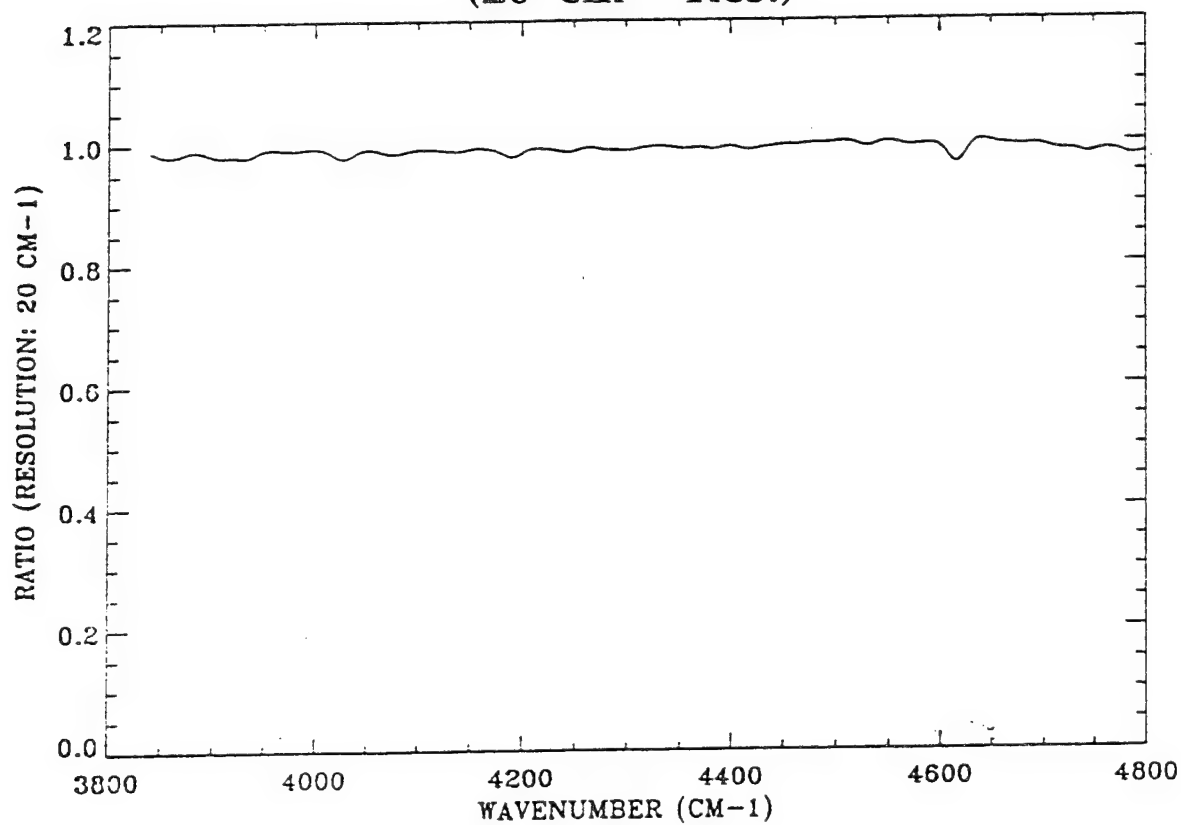
SPECTRAL BACKGROUND LEVEL



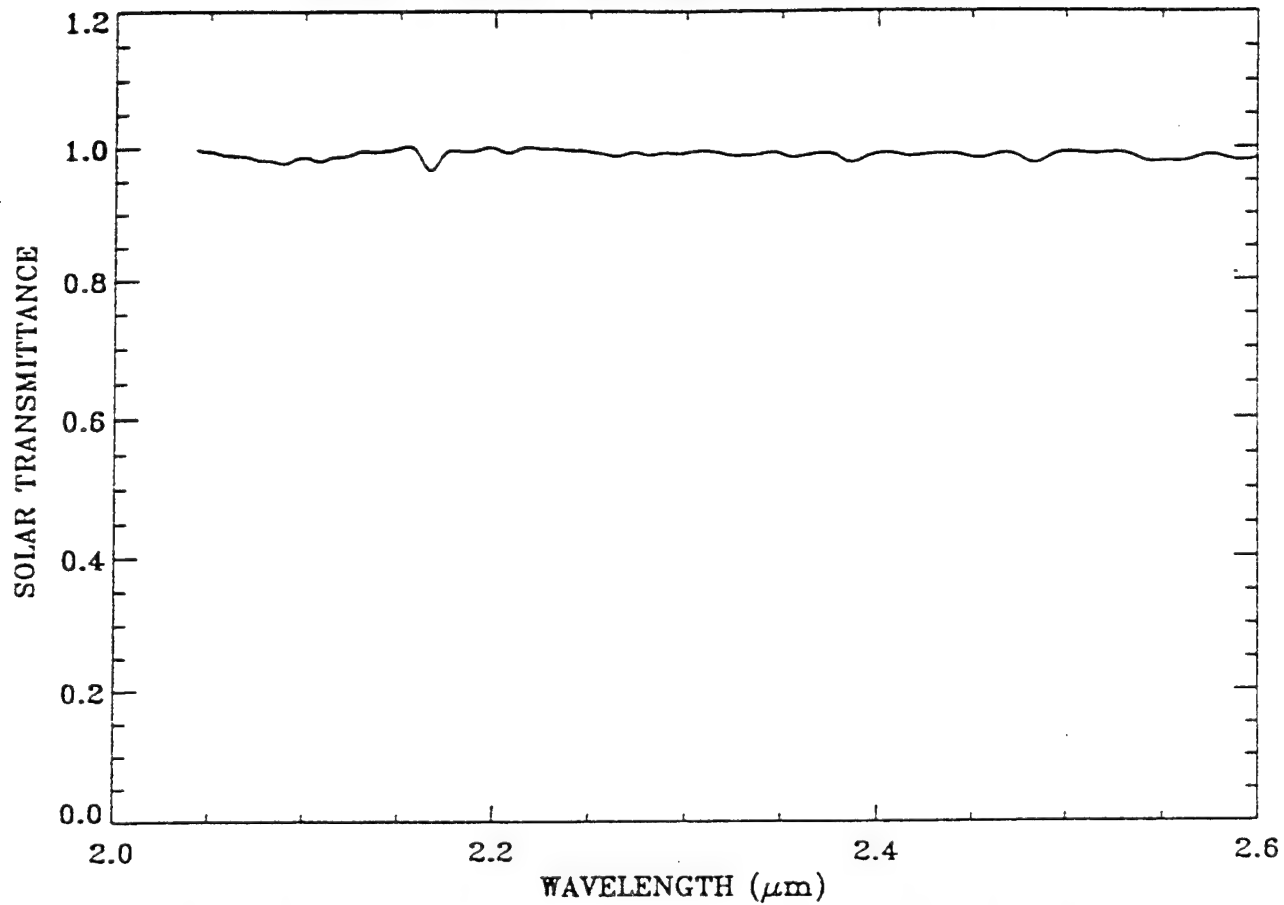
SOLAR TRANSMITTANCE SPECTRUM (ATMOS/BACKGROUND, 0.01 cm^{-1} Res.)



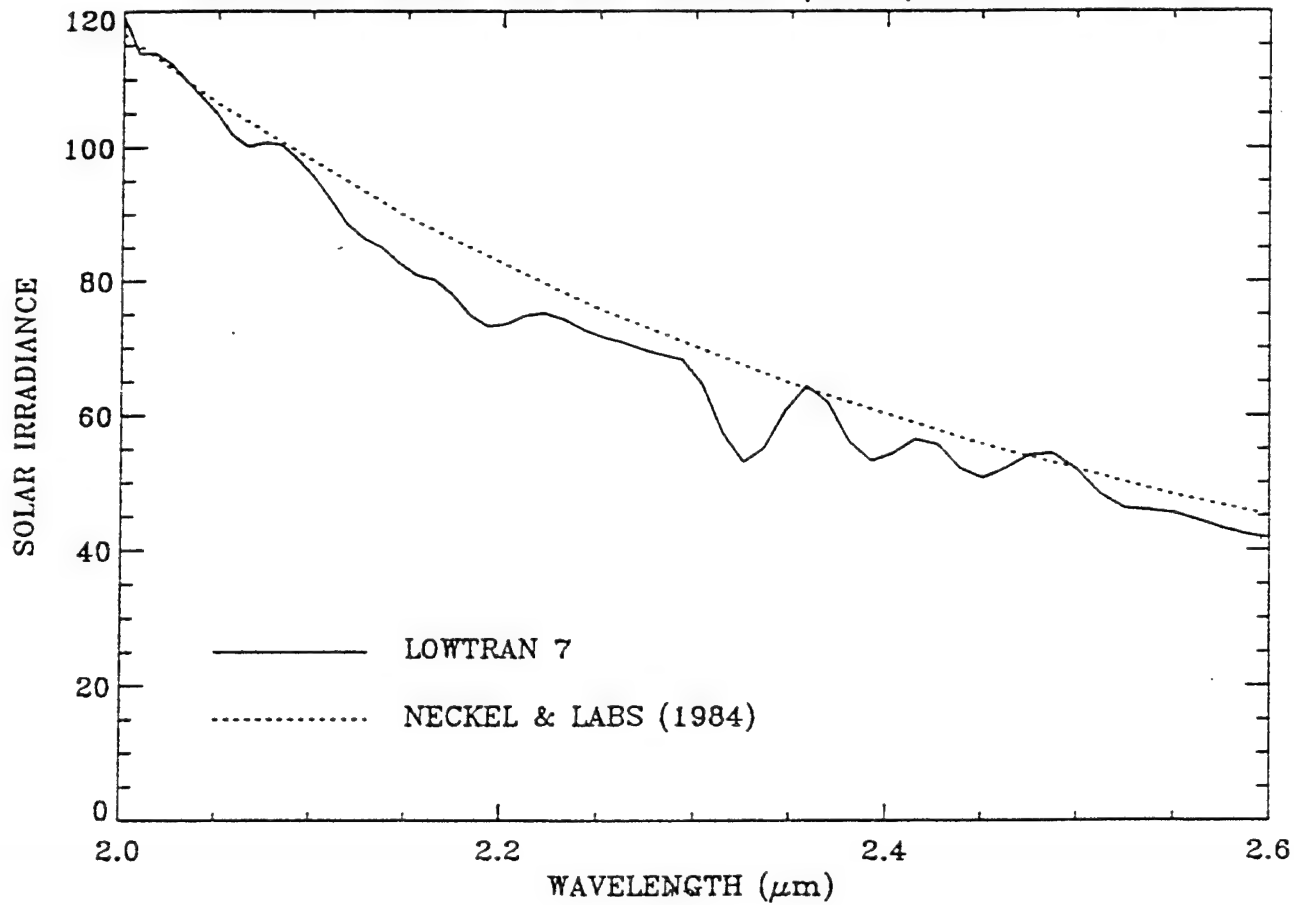
SOLAR TRANSMITTANCE SPECTRUM (20 cm^{-1} Res.)

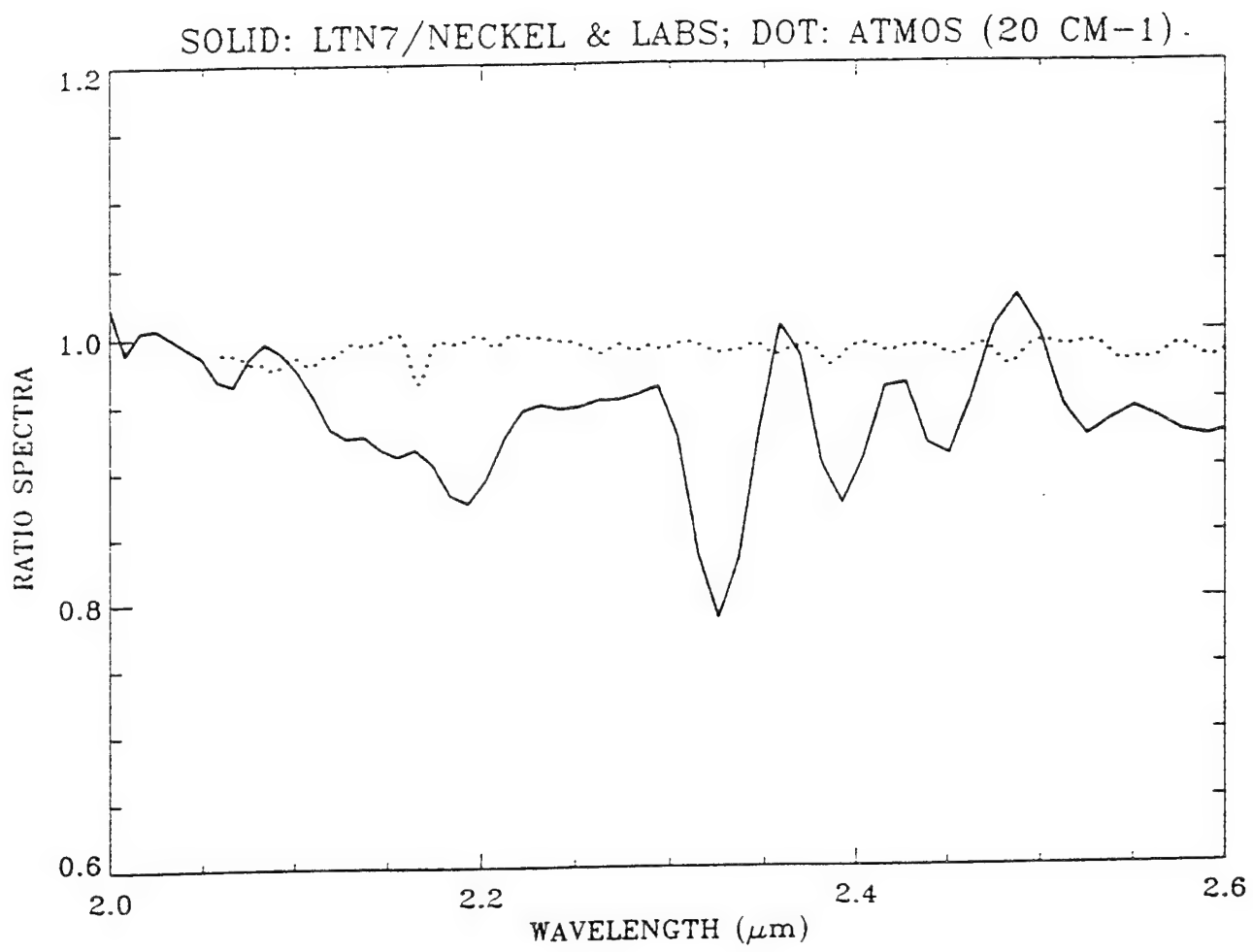


ATMOS SOLAR TRANSMITTANCE SPECTRUM

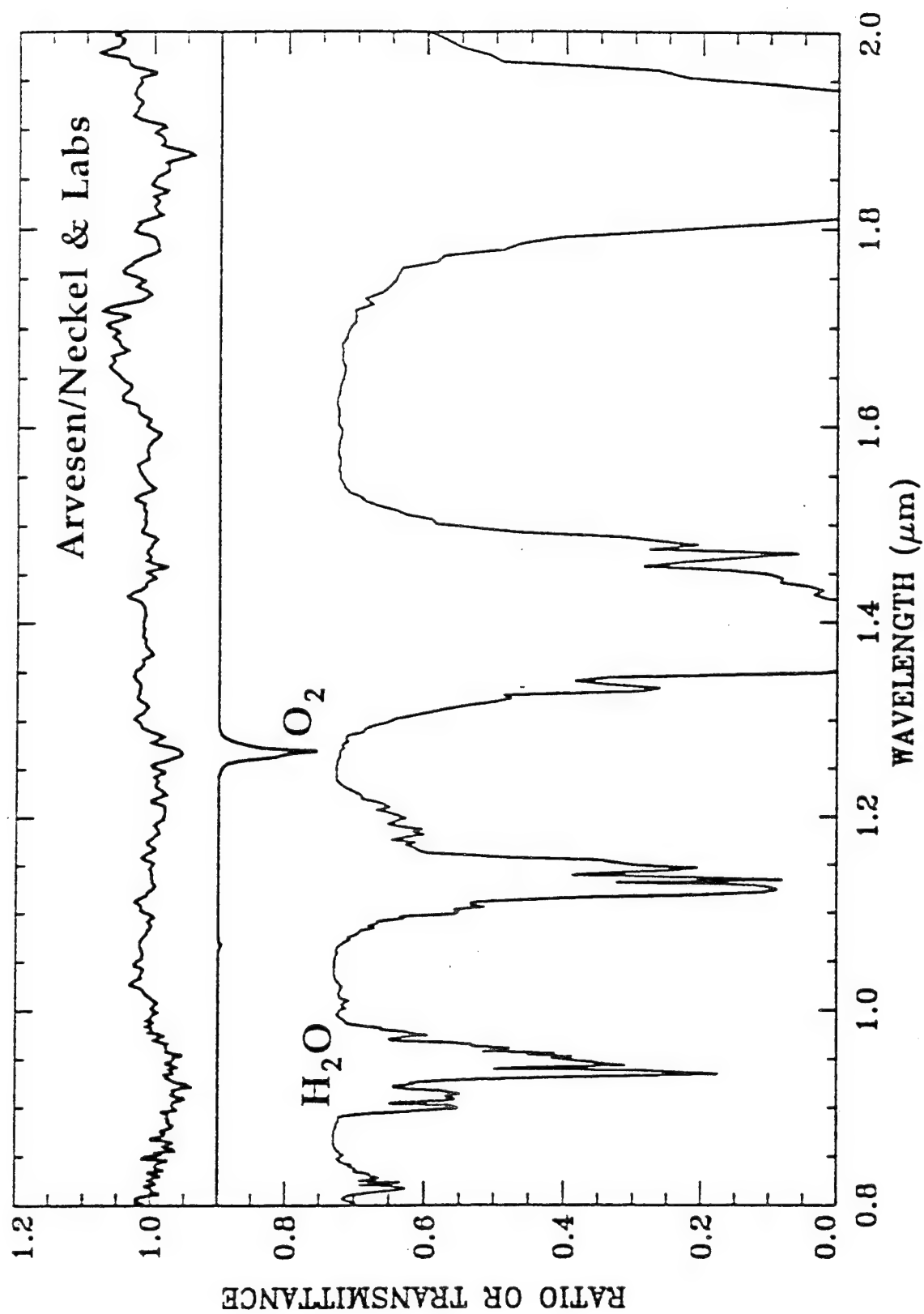


LOWTRAN7 and NECKEL & LABS (1984) SOLAR CURVES

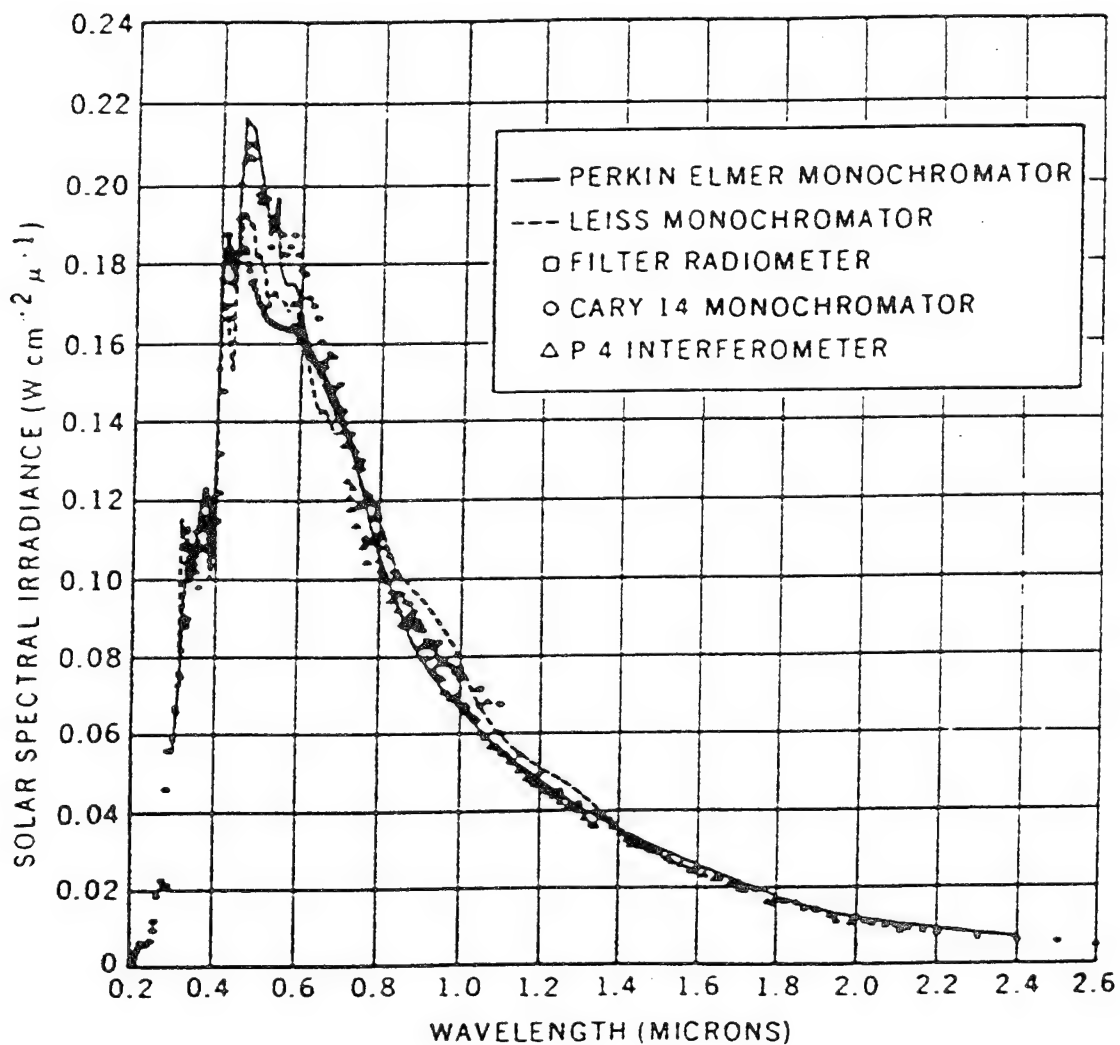




Atmospheric Bands in Arvesen's solar Curve



SOLAR SPECTRAL CURVES FROM INSTRUMENTS ON BOARD NASA 711



From Thekaekara (1974). Poor instrumental radiometric calibrations.

SUMMARY

- A solar transmittance spectrum has been derived from the ATMOS data. The spectrum shows weak solar features with peak absorptions of less than 3% at a spectral resolution of 20 cm^{-1} .
- The LOWTRAN 7 solar irradiance curve in the $2\text{-}2.5\text{ }\mu\text{m}$ region contains earth atmospheric features. The Neckel & Labs (1984) solar curve in the $2\text{-}2.5\text{ }\mu\text{m}$ region contains no solar features at all. The solar irradiance measurements from Thekaekara (1974) had radiometric calibration problems. The solar irradiance curve of Arvesen et al. (1969) contains atmospheric O_2 and H_2O features.
- Improved measurements of solar irradiances in the visible and near-IR region with accurate radiometric calibrations from satellite platforms are necessary in the future.

THE IMPACT OF THIN CIRRUS CLOUDS ON TERRAIN REMOTE SENSING

W.M. Cornette, J.G. Shanks

Photon Research Associates, Inc.
10350 N. Torrey Pines Road, Suite 300
La Jolla, CA 92037-1020

The existence of thin, or sub-visual, cirrus clouds within the field-of-view of a satellite sensor can alter the sensor's perception of the terrain radiance. Since the existence of sub-visual cirrus is frequently unknown, this alteration of the terrain radiance can lead to erroneous conclusions from analysis using this data. Even if the existence of thin cirrus is known to exist, the cirrus parameters (e.g., cloud optical depth, cloud altitude and thickness, particle size distribution) are not fully known. This paper will quickly review cirrus cloud parameters and how these parameters are used in MODTRAN to evaluate the impact of thin cirrus clouds on remote sensing. The difference between actual and predicted surface temperatures in the presence of cirrus will be presented. A couple of numerical problems with MODTRAN that were encountered during this study will be discussed.

THE IMPACT OF THIN CIRRUS CLOUDS ON TERRAIN REMOTE SENSING

Presented at the
Annual Review Conference on Atmospheric Models
Hanscom AFB, Massachusetts
8-9 June 1993

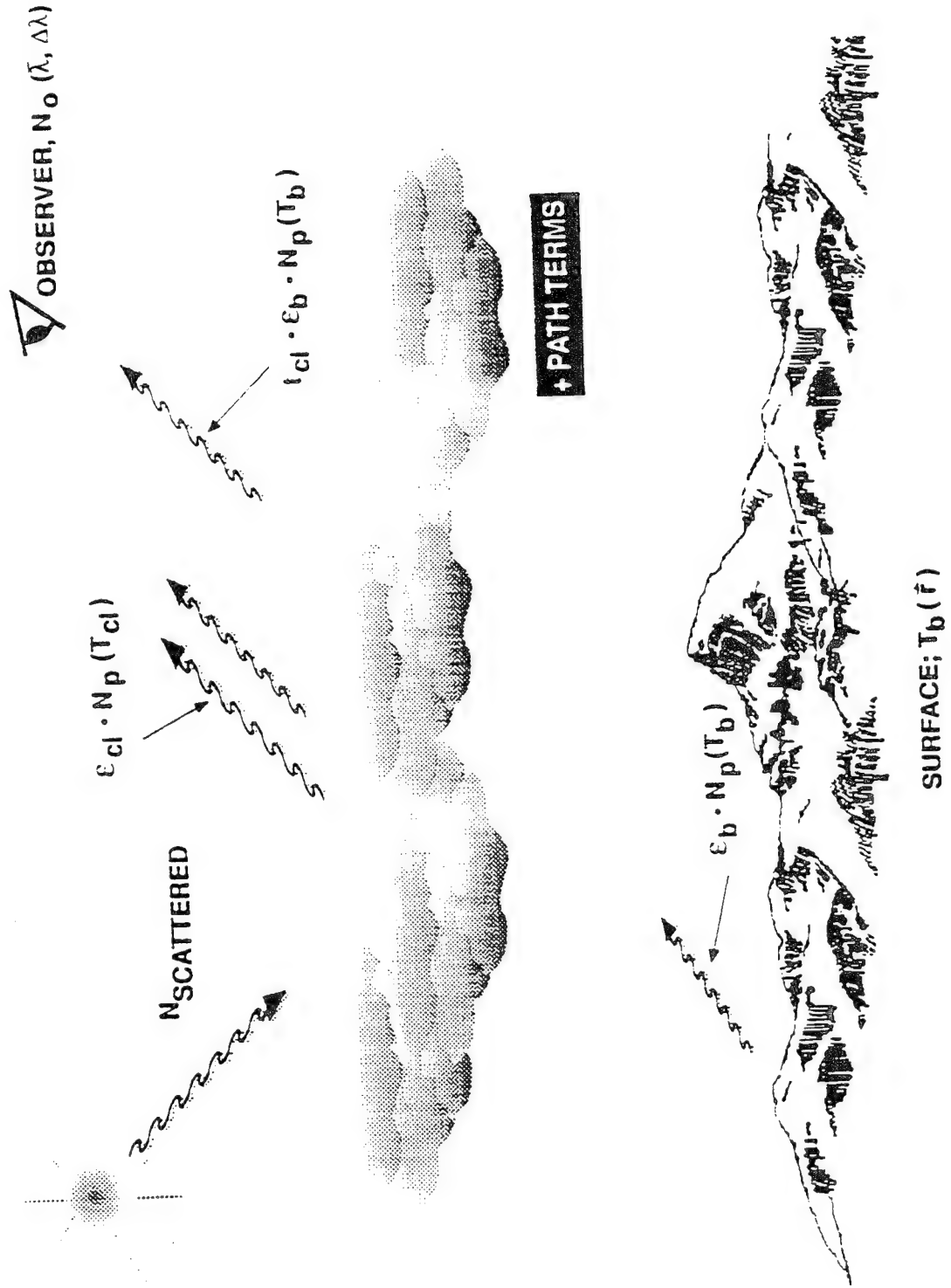
Presented By:
Dr. William M. Cornette
Dr. Joseph G. Shanks



Photon Research Associates, Inc.

10350 N. Torrey Pines Court, #300
La Jolla, California 92037-1020
(619) 455-9741
Fax: (619) 455-0658
e-mail: wmc@photon.com

INTRODUCTION





|<— 277. T_{apparent} 296. —>|
 Fig-A. Apparent Temperature Image, Thin Cirrus Over Desert

- * Spectral Band: [11.4, 12.4] (um), (= AVHRR Band 5)
- * 1024 x 1024 @ 0.12 (km) (from LANDSAT), Hist Eq. Scale
- * SSGM R 5.0 / Modified CLDSIM, GENESIS Scenes, 3/31/93
- > Joe Shanks, Photon Research Associates, Inc., La Jolla

IMPACT OF CIRRUS CLOUDS

- Increased Attenuation
 - Hydrometeors
 - Water Vapor
- Modified Path Radiance
 - Thermal Emissions
 - Scattered
- Modified Reflective Components
 - Direct Solar
 - Skyshine
- Modified Temperature
 - Solar Load
 - Thermal Load

TEMPERATURE INVERSION EQUATION

$$\Delta T = T_{\text{apparent}} - T_{\text{surface}}$$

$$= P^{-1} \left\{ \frac{N_{ci} - N_{\text{clear}} + (1 - \epsilon_b) \cdot \left(\frac{\phi_{ci} \cdot t_{ci} - \phi_{\text{clear}} \cdot t_{\text{clear}}}{\pi} \right) + \epsilon_b t_{ci} P(T_b)}{\epsilon_b t_{\text{clear}}} \right\} - T_b$$

53

$P(T), P^{-1}\{N\}$ \equiv Planck Function, Inverse

T_b, ϵ_b \equiv Terrain Temperature, Emissivity

N_{clear}, N_{ci} \equiv Total Path Radiance, Clear, Cirrus LOS

t_{clear}, t_{ci} \equiv Transmission (Terrain \rightarrow Observer) for Clear, Cirrus LOS

$\phi_{ci}, \phi_{\text{clear}}$ \equiv Irradiance Incident on Terrain With, Without Intervening C_i

INVERSION PROBLEMS

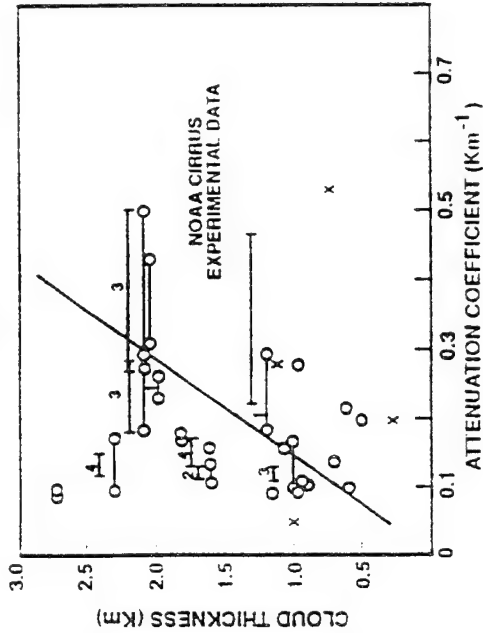
- In Some Cases, $\tau_{\text{clear}} < \tau_{\text{cirrus}}$ Which is Not Physically Reasonable
- Numerical Instability Causes Equivalent Blackbody Temperature to Exceed Reasonable Values. Currently Limited Between 100 - 330 K.
- Numerical Underflow Results in $\epsilon \tau_{\text{clear}} = 0$

CIRRUS CLOUD PARAMETERS

- Geographical Occurrence
- Altitude
- Thickness
- Particle Shapes
- Particle Size Distribution
- Index of Refraction
- Extinction Efficiency, Extinction Coefficient, and Optical Depth
- Single Scattering Albedo
- Phase Function and Asymmetry Parameter

CIRRUS CLOUD

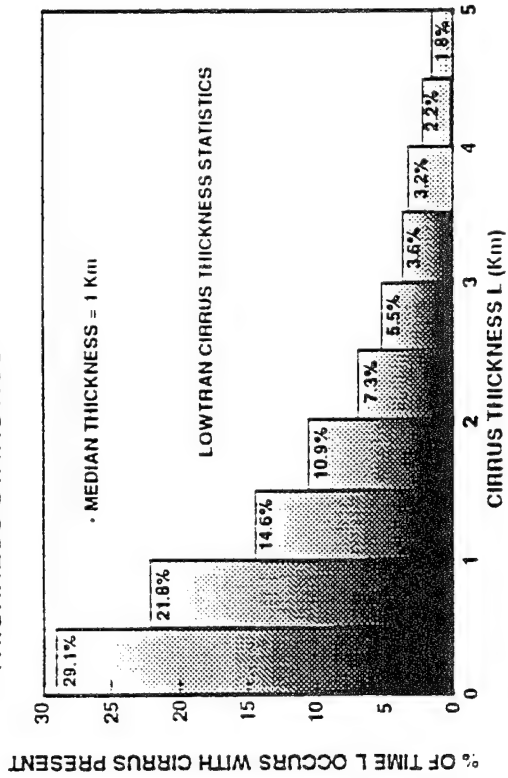
• ATTENUATION COEFFICIENT



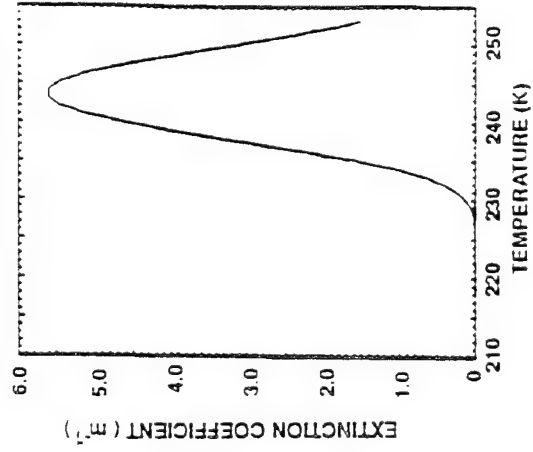
• Altitude Ranges (km)

Tropics	7.50 - 16.50
Temperate, Winter	4.50 - 14.00
Temperate, Summer	7.30 - 13.50
Polar, Winter	2.50 - 10.00
Polar, Summer	4.50 - 9.50

• THICKNESS STATISTICS

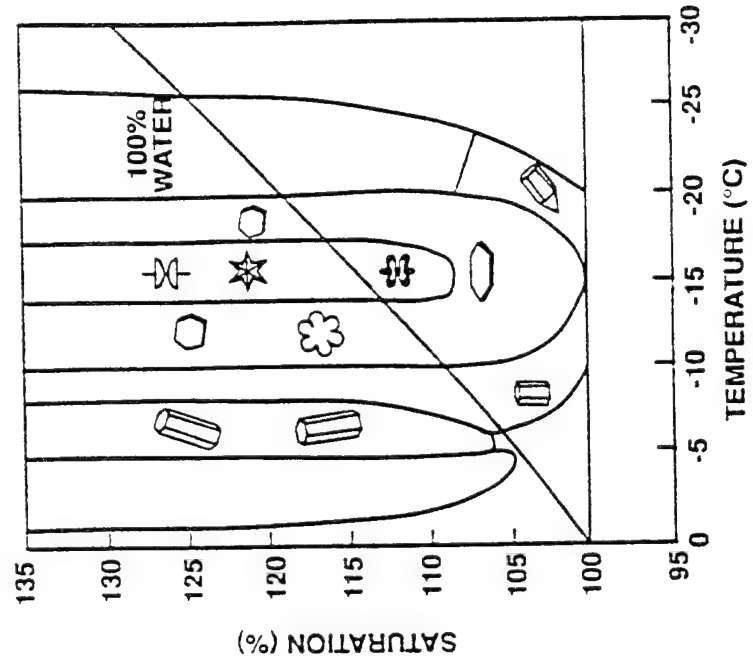
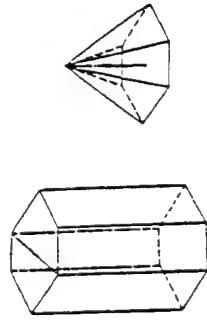


• TEMPERATURE DEPENDENCE



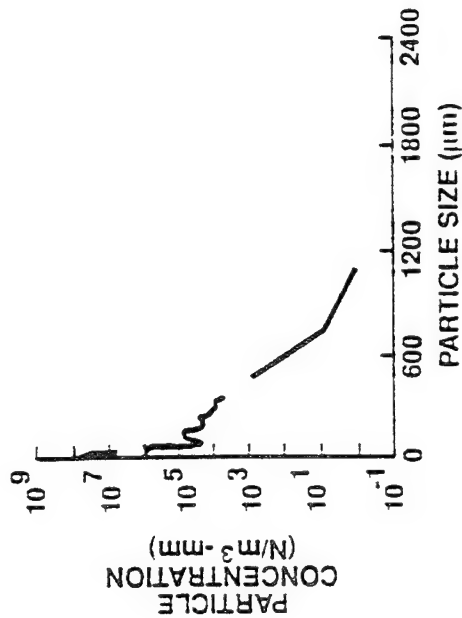
PARTICLE SHAPES

- Hexagonal Plates (Thick/Thin)
- Hexagonal Columns (Solid/Hollow/Hollow Ends)
 - Cirrostratus (40 x 100 μm)
 - Cirrocumulus (50 - 100 x 200 - 300 μm)
 - (Incompletely Built)
 - Cirrus Generating Cells (? x 60 - 100 μm)
- Bullet Rosettes (75%)
- Plates (25%)
- Hollow Cones
- Stars
- Pyramids
- Combinations and Polycrystalline Forms

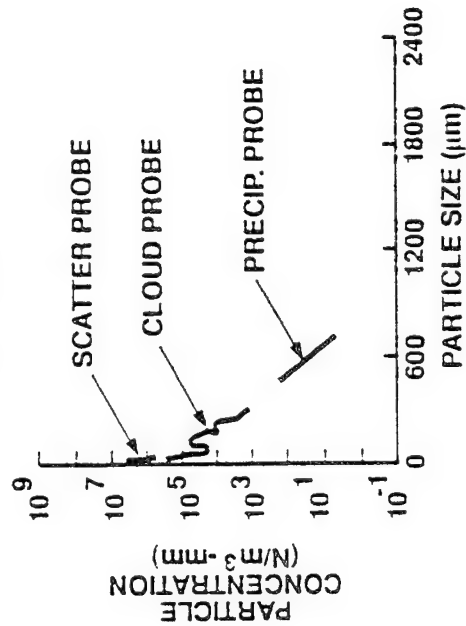


PARTICLE DISTRIBUTIONS (REF: BARNES)

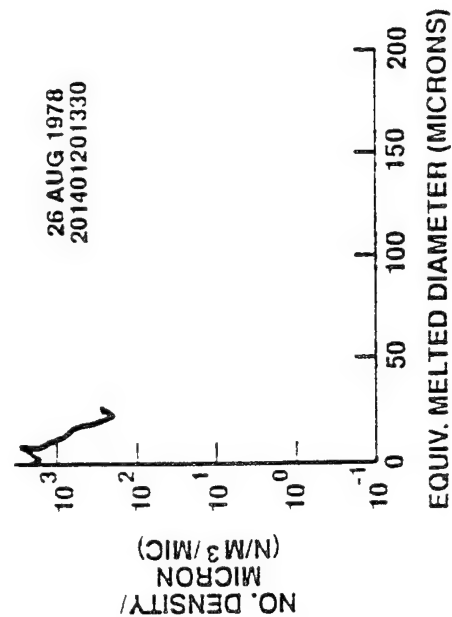
• Opaque Cirrus



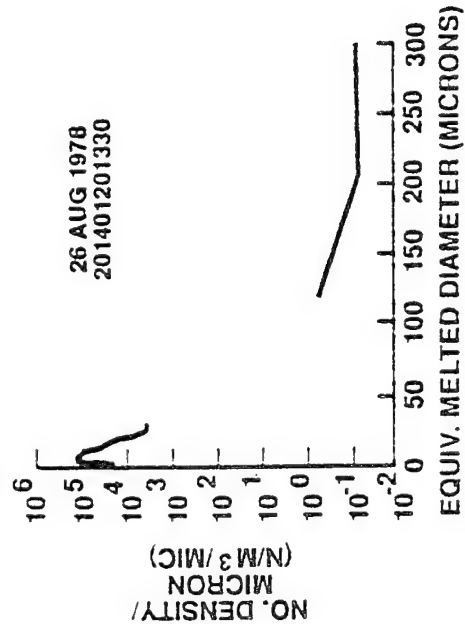
• Thin, Translucent Cirrus



• Type 1 Subvisual Cirrus



• Type 1 & 2 Subvisual Cirrus

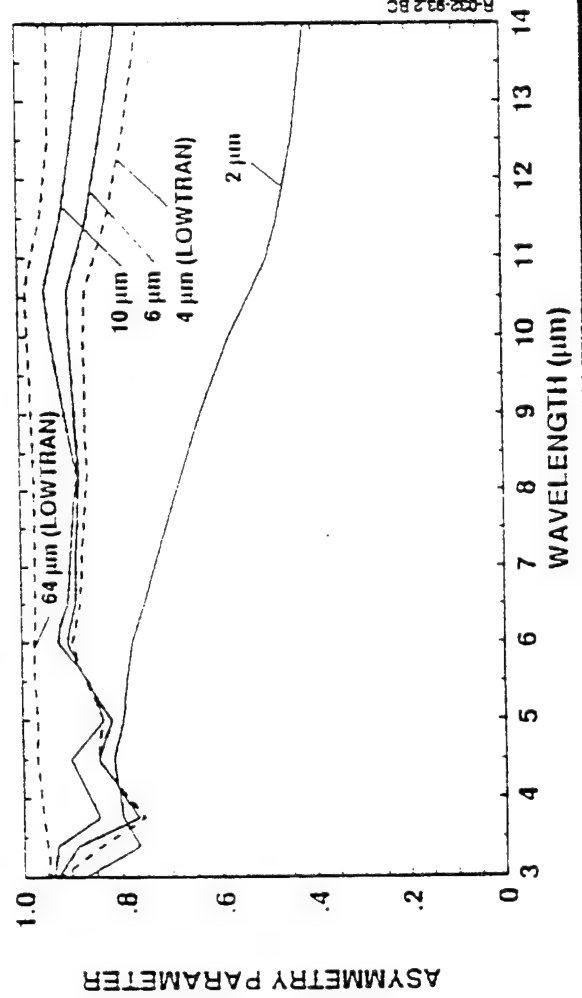
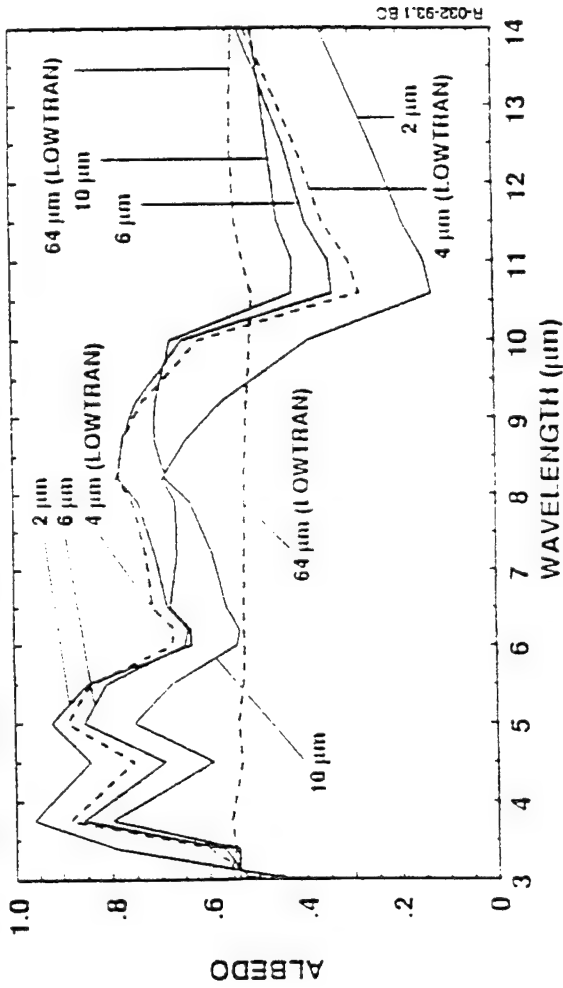


U 147 90 4 B/C

B 003 93:1-16.12

ALBEDO, ASYMMETRY PARAMETER FOR A LOG-NORMAL DISTRIBUTION

- Curves Labeled by Median Radius
- $\hat{\sigma} = 0.3$



PARAMETRIC VARIATIONS

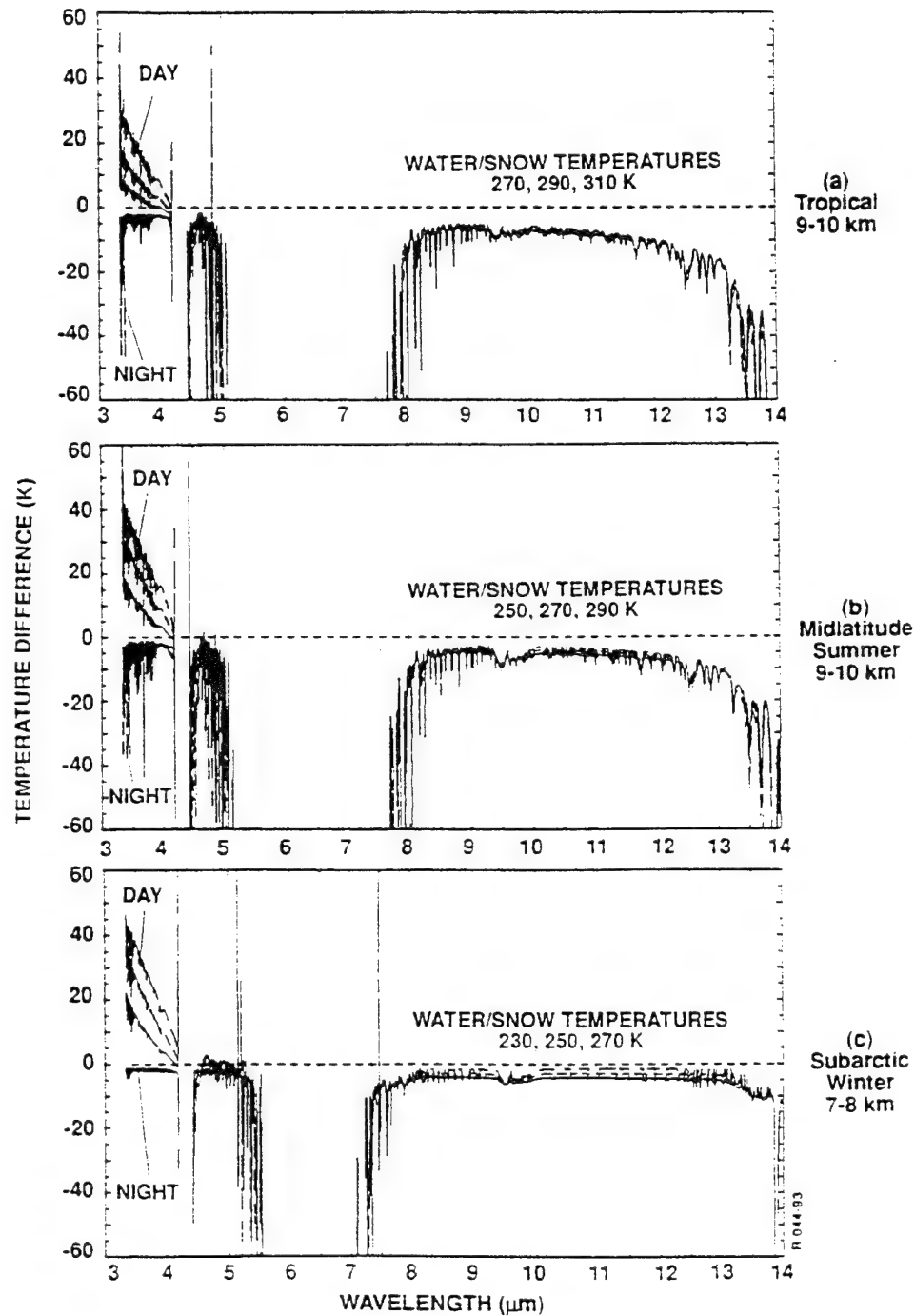
- Optical Depth
- Surface Temperature (230 - 310)
- Cloud Temperature (Tropical, Midlatitude Summer, Subarctic Winter)
- Surface Albedo (Water, Ice, Terrain)
- Cloud Altitude and Thickness

	Tropopause (km)	Altitude (km)	Thickness (km)
Tropical	16	10, 12, 16(*)	0.2, 1
Midlatitude Summer	12	8, 10, 12	0.2, 1
Subarctic Winter	8	8	0.2, 1

(*) Add 2, 3, 5 km Thickness

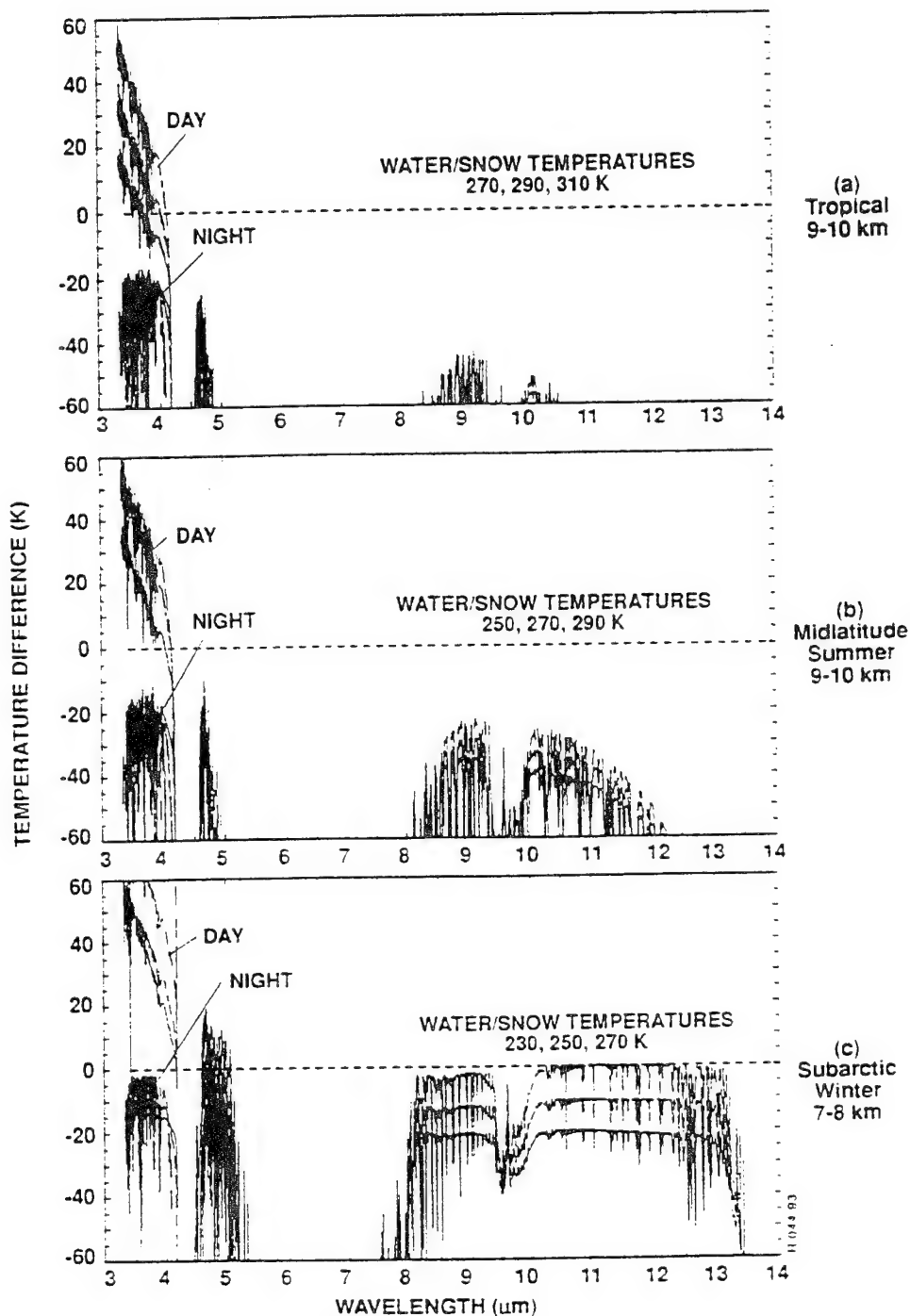
$$\Delta T \text{ vs } \lambda [R_{\text{median}} = 64 \mu\text{m}, \tau (\lambda = 0.55 \mu\text{m}) = 0.1]$$

Temperature Differences for 64 μm Median Radius Cloud with
Optical Depth = 0.1 at 0.55 μm



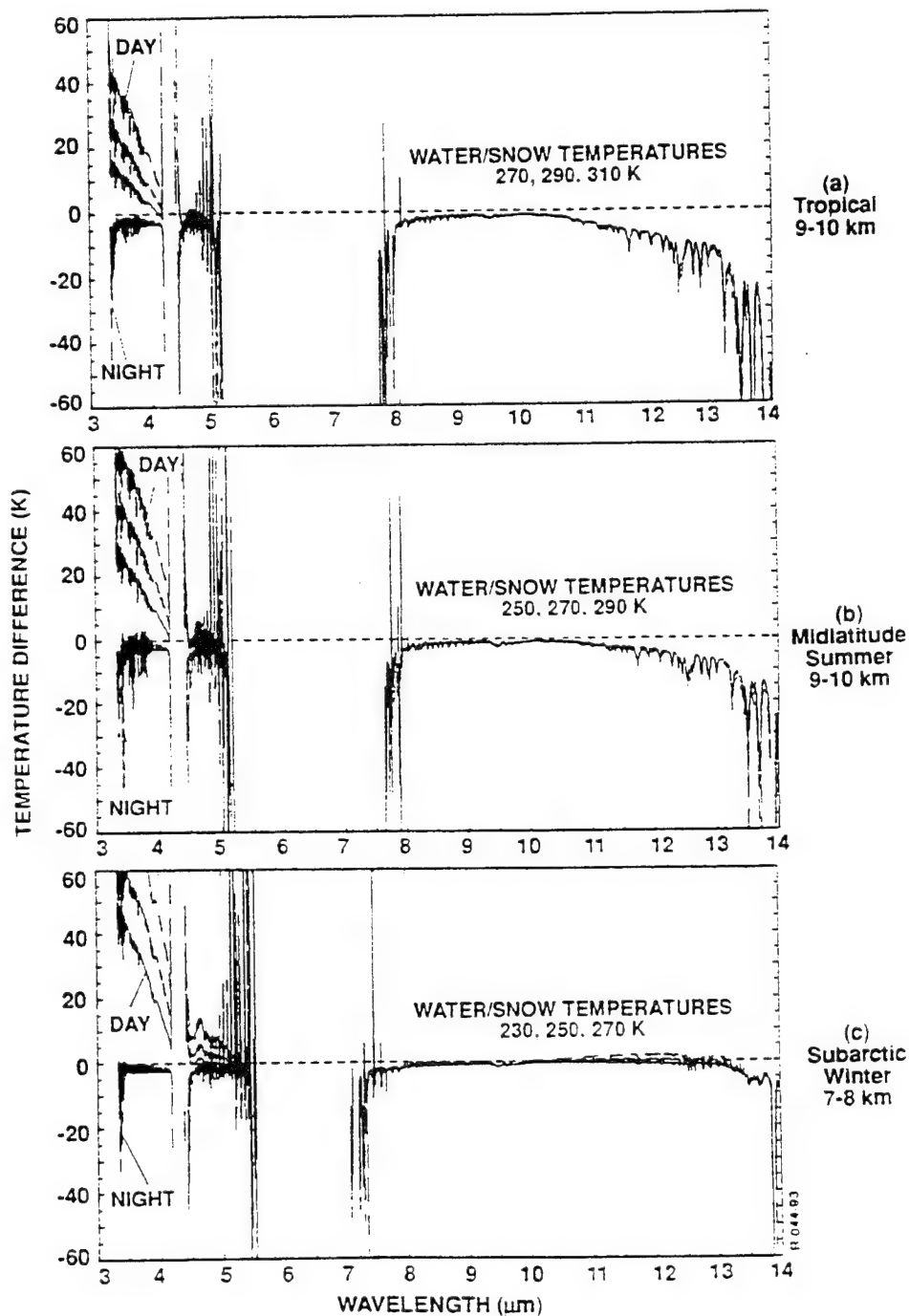
$$\Delta T \text{ vs } \lambda [R_{\text{median}} = 64 \mu\text{m}, \tau(\lambda = 0.55 \mu\text{m}) = 0.8]$$

Temperature Differences for 64 μm Median Radius Cloud with
Optical Depth = 0.8 at 0.55 μm



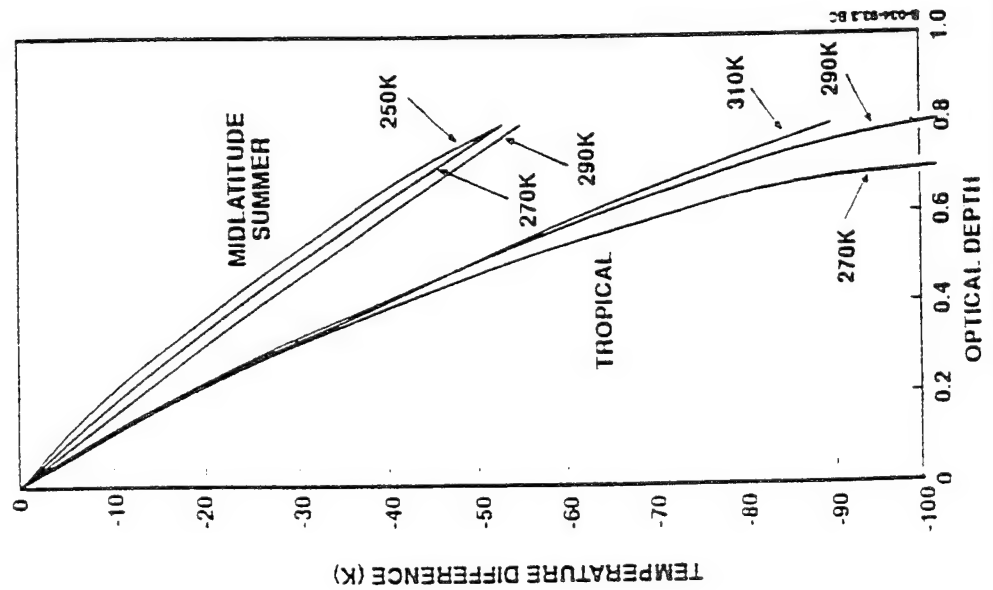
$$\Delta T \text{ vs } \lambda \text{ [} R_{\text{median}} = 2 \mu\text{m, } \tau (\lambda = 0.55 \mu\text{m}) = 0.1 \text{]}$$

Temperature Differences for 2 μm Median Radius Cloud with
Optical Depth = 0.1 at 0.55 μm

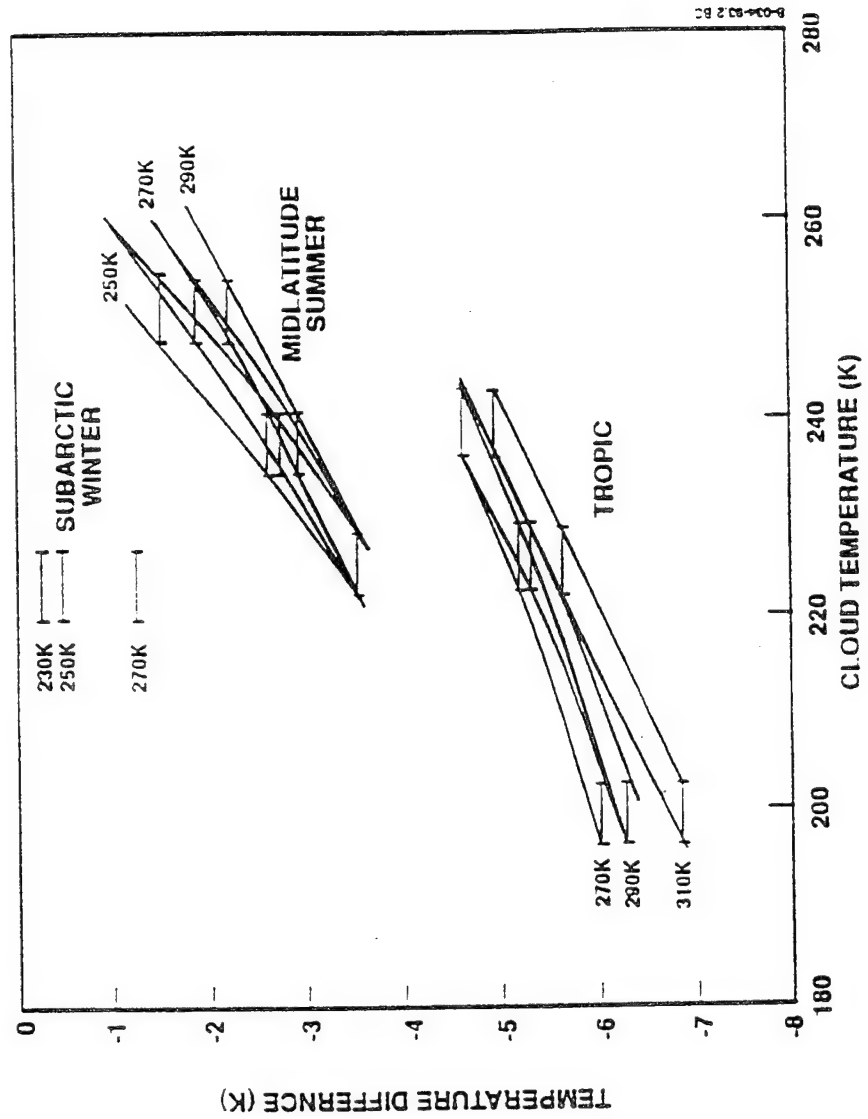


ΔT vs OPTICAL DEPTH, CLOUD TEMPERATURE

Cloud Optical Depth Effects at $11\text{ }\mu\text{m}$ for a $64\text{ }\mu\text{m}$ Median Radius Cirrus Cloud Between 9 and 10 km for Various Terrain Temperatures.

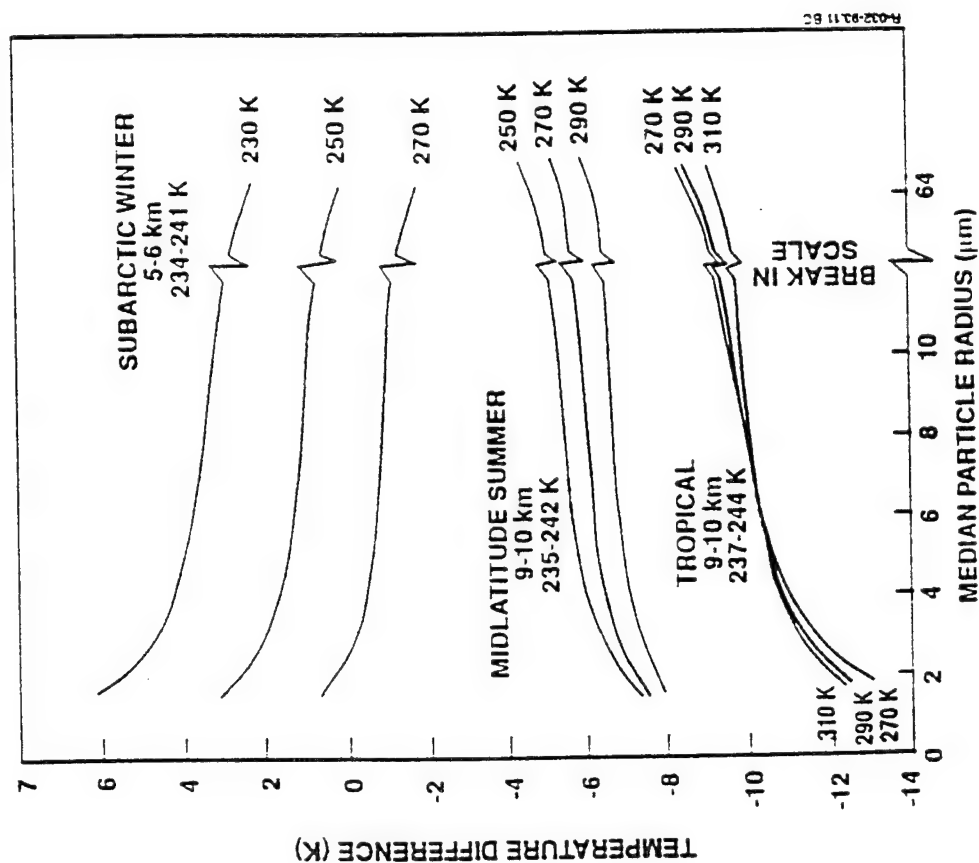


Cloud Temperature Effects at $11\text{ }\mu\text{m}$ for a $64\text{ }\mu\text{m}$ Median Radius Cirrus Cloud Between 9 and 10 km. Optical depth at $0.55\text{ }\mu\text{m}$ is 0.10. Only one temperature for a Subarctic Winter atmosphere is shown.



ΔT vs MEDIAN PARTICLE RADIUS [$\tau (\lambda = 11 \mu m) = 0.1$]

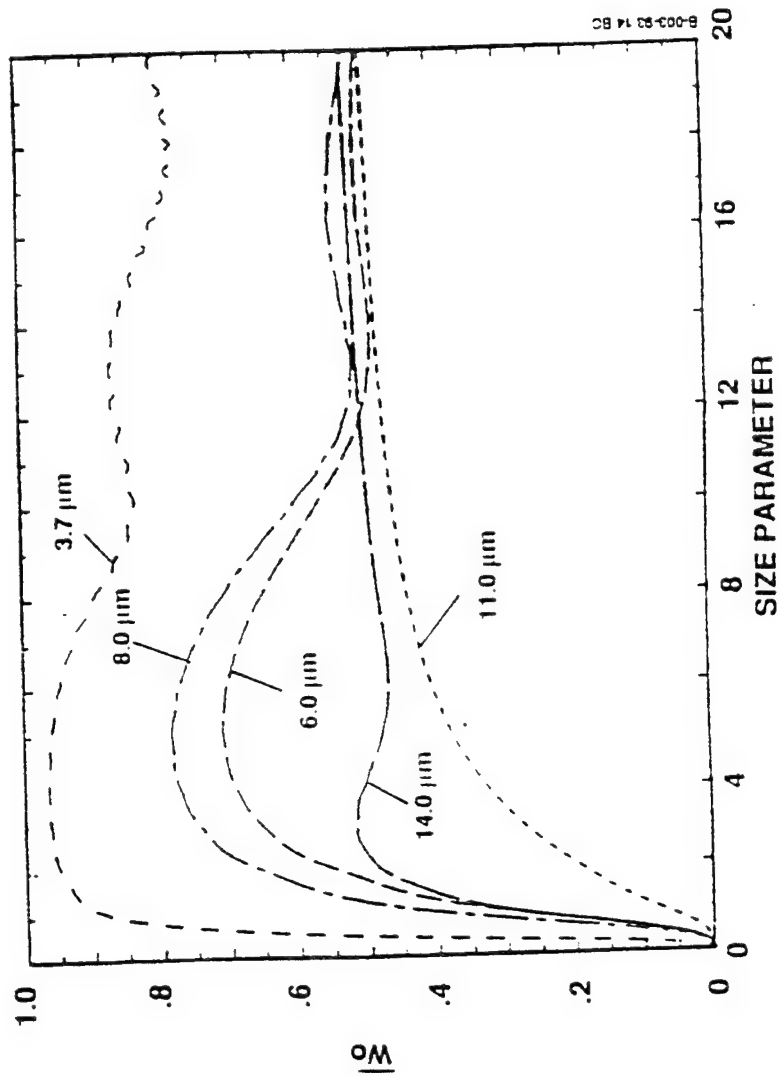
Cloud Temperatures are Shown for each Model Atmosphere and Appropriate Terrain Temperatures.



PARAMETRIC ANALYSIS

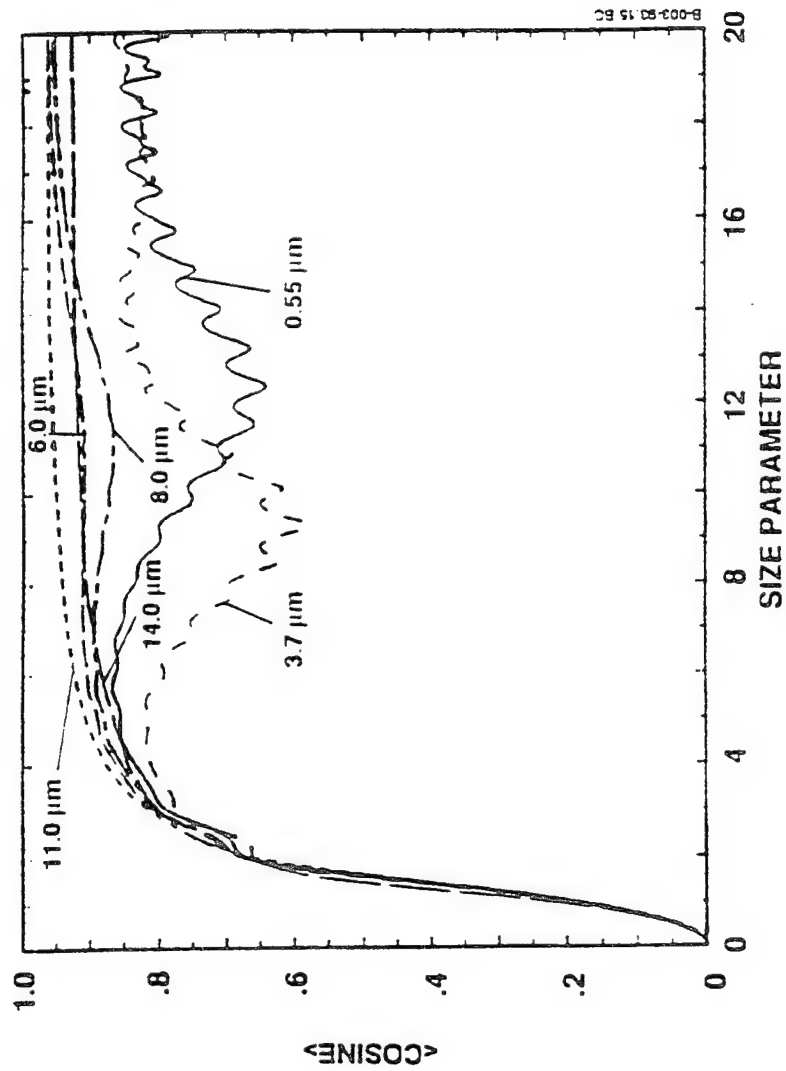
- Optical Depth:
 - Major Impact ($\sim 100 \text{ K}/\tau$)
- Model Atmosphere:
 - Moderate Impact ($\sim 2\text{-}4 \text{ K}/15^\circ \text{ Lat}$)
- Cloud Temperature and Altitude:
 - Minor Impact ($\sim 0.05 \text{ K}/1 \text{ K}$)
- Cloud Thickness:
 - Minor Impact ($< 0.2 \text{ K}/\Delta H$)
- Particle Size Distributions:
 - Single Scattering Albedo
 - Asymmetry Parameter
 - Moderate Impact ($\sim 2\text{-}3 \text{ K}/r_{\text{mean}}$)

MIE SCATTERING ALBEDO



• Spherical Ice

ASYMMETRY PARAMETER



• Spherical Ice

APPLICATION OF LOWTRAN-7 TO AVHRR THERMAL DATA IN FIFE

T. Schmugge, P. Bougarel

M. Sugita

W. Brutsaert

USDA Hydrology Lab
Beltsville, MD

Env. Res. Ctr.
Univ. of Tsukuba
Japan

Cornell University

LOWTRAN-7 was used with near coincident radio soundings of the atmosphere to estimate surface brightness temperatures from the NOAA-9 AVHRR data. The data were obtained for 8 days during the First ISLSCP Field Experiment (FIFE) conducted in central Kansas between the end of June and October of 1987. In general the channel 4 results were up to 2° K warmer than those from channel 5 indicating that we were undercorrecting for the atmospheric water vapor. However on one day the reverse was true and the channel 5 result was higher. In this case we were able to get agreement by reducing water vapor content to 80% of its measured value. The results were compared also with various split window approaches for estimating surface temperature and with ground based broad band radiometers with AVHRR results being generally warmer.

Application of LOWTRAN-7 to AVHRR Thermal Data In FIFE

T. Schmugge and P. Bougarel, USDA Hydrology Lab, Beltsville MD

M. Sugita, Environmental Research Center, Univ. of Tsukuba, Japan

W. Brutsaert, Cornell University

ABSTRACT for Annual Review Conference on Atmospheric Transmission Models

Application of LOWTRAN-7 to AVHRR Thermal Data In FIFE

T. Schmugge and P. Bougarel, USDA Hydrology Lab, Beltsville MD

M. Sugita, Environmental Research Center, Univ. of Tsukuba, Japan

W. Brutsaert, Cornell University

LOWTRAN-7 was used with near coincident radio soundings of the atmosphere to estimate surface brightness temperatures from the NOAA-9 avhrr data. The data were obtained for 8 days during the First ISLSCP Field Experiment (FIFE) conducted in central Kansas between the end of June and October of 1987. In general the channel 4 results were up to 2 K warmer than those from channel 5 indicating that we were undercorrecting for the atmospheric water vapor. However on one day the reverse was true and the channel 5 result was higher. In this case we were able to get agreement by reducing water vapor content to 80% of its measured value. The results were compared also with various split window approaches for estimating surface temperature and with ground based broad band radiometers with avhrr results being generally warmer.

AVHRR DATA for 8 days during the summer 1987 from FIFE

- 256 X 256 Images from FIFE Information System (FIS))

Supporting radiosoundings before and after the overpass

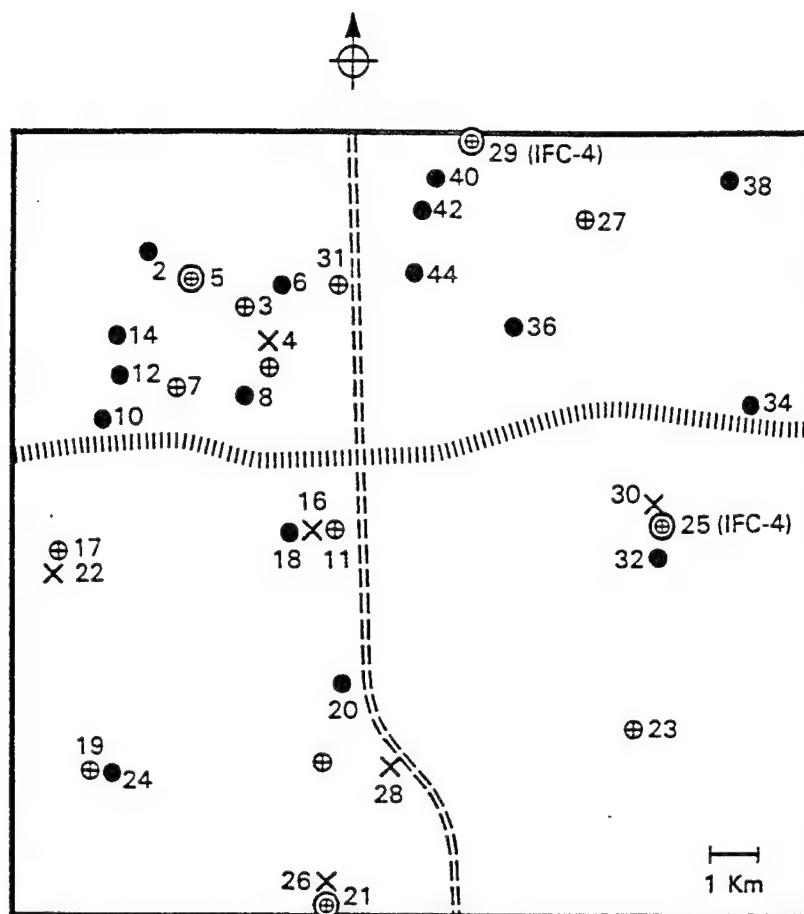
- Calculations done with both Lowtran7 and Modtran

Ground measurements from 8 to 10 stations over a 15 x 15 km area

- Obtained from FIS

Differences:

- Spatial Scale: 1 km vs ~ 1 m
- Spectral: narrow band 10-11 μm vs 8-14 μm



- ⊕ P-PAM
 - ⊕ D-DCP
 - ⊕ SP-Super PAM
 - ⊕ SD-Super DCP
 - B-Bowen Ratio Flux Measurement
 - X E-Eddy Correlation Flux Measurement
 - Site Boundary
 - ||||| I-70
 - === R-177
- } Ground IRT Sites

Figure 2.2b: Map of FIFE sites showing flux stations and AMS as actually located during FIFE-1987. Stations are marked by station number: even numbers for flux stations, odd numbers for AMS.

Note (i) No DCPs displayed, as data is currently inaccessible

(ii) Stations 40 (flux) and 31 (AMS) moved from positions as marked in EXPLAN

(iii) 25 (east) and 29 (north) operating in IFC-4 only.

See also Table 2.2b and Figure/Table 2.4b in EXPLAN

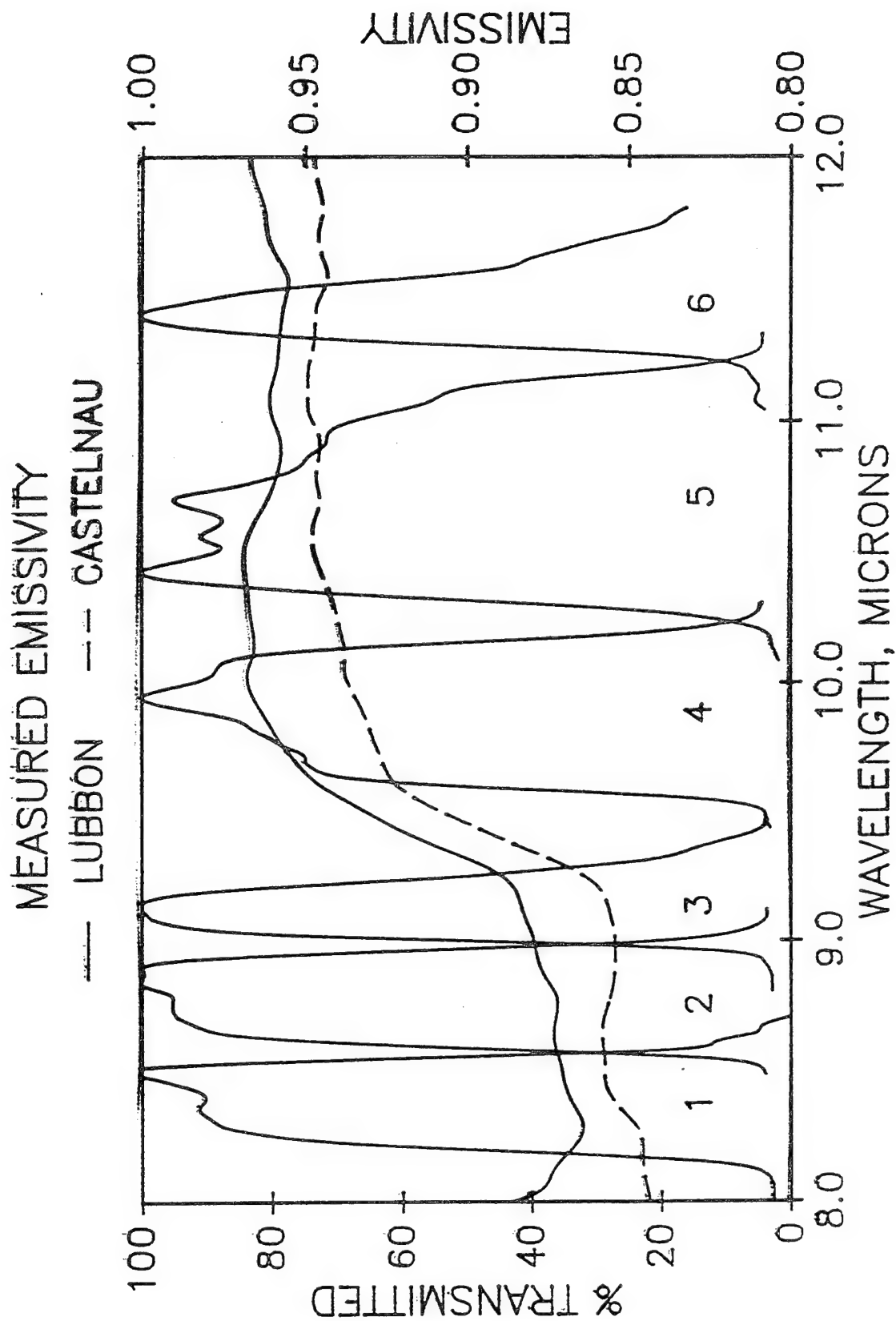
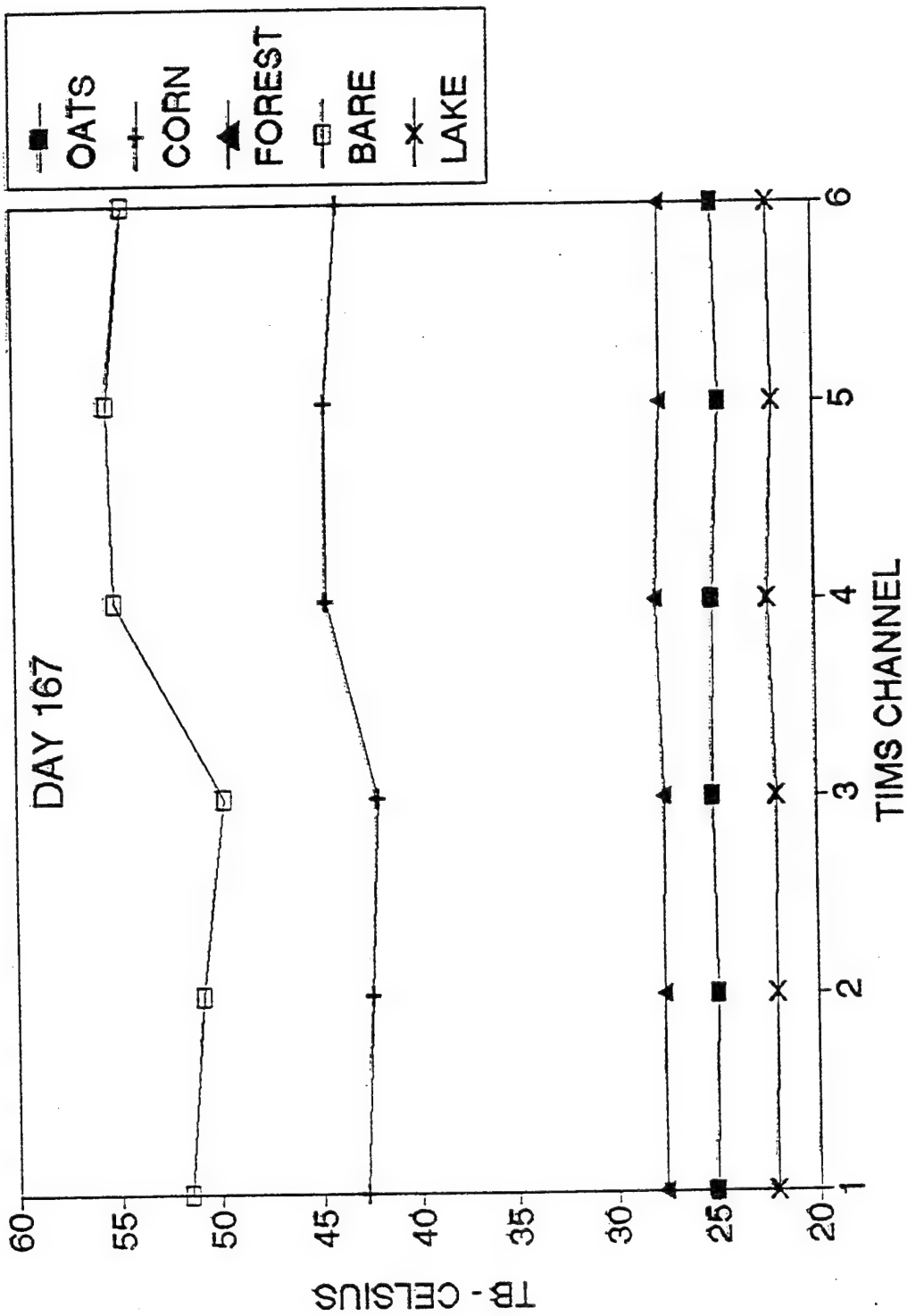


Figure 1. The filter functions for the 6 TIMS channels superimposed on the laboratory measurements of emissivity for two soils from the HAPEx test area (Nerry et al., 1988).



KERR Split Window approach

- Developed by comparison with ground measurements

- For vegetated surfaces:

$$T_{\text{surf}} = -2.4 + 3.6 \bullet T_4 - 2.6 \bullet T_5$$

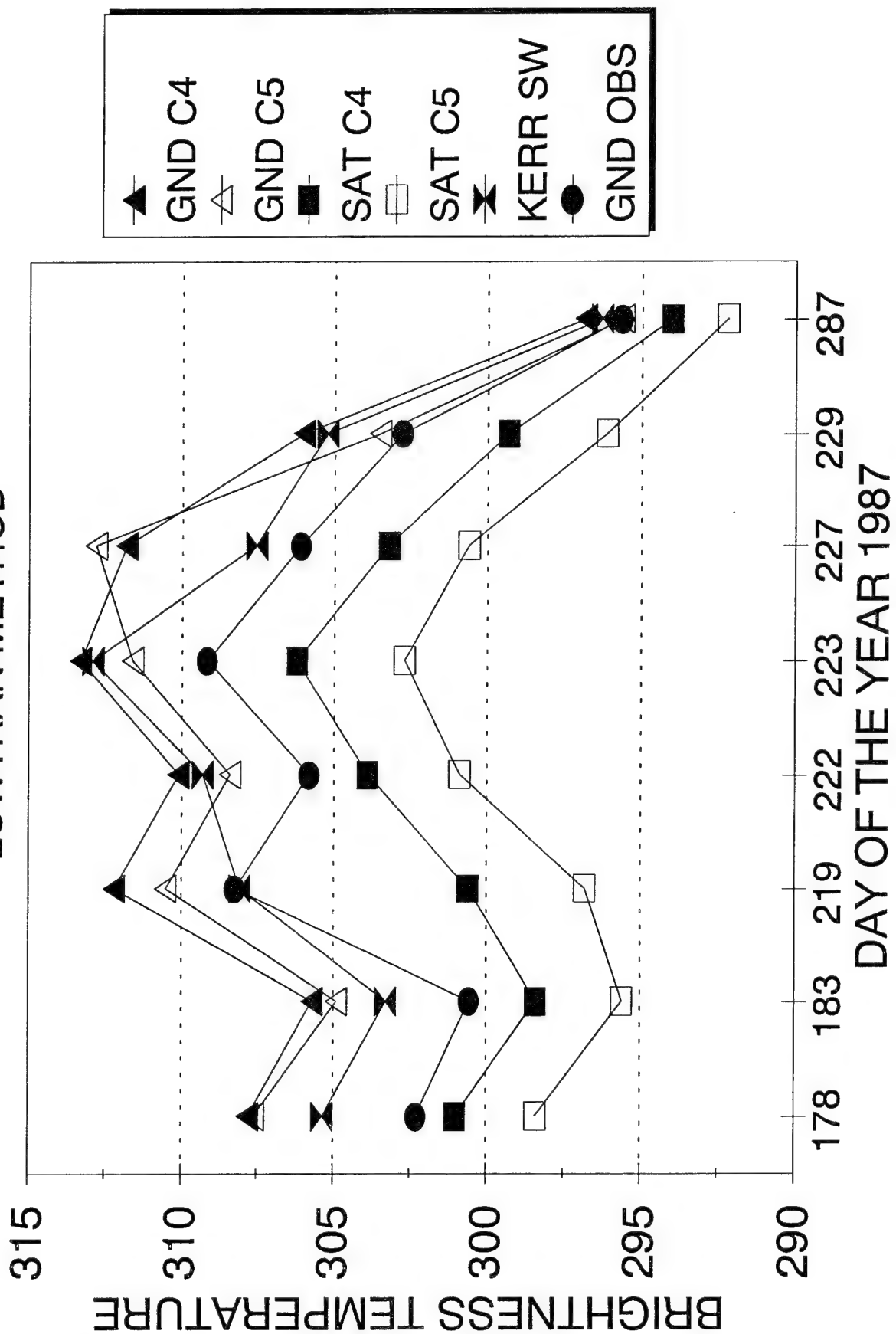
- For bare soil:

$$T_{\text{surf}} = 3.1 + 3.1 \bullet T_4 - 2.1 \bullet T_5$$

We assumed vegetated surfaces for each of the ground sites.

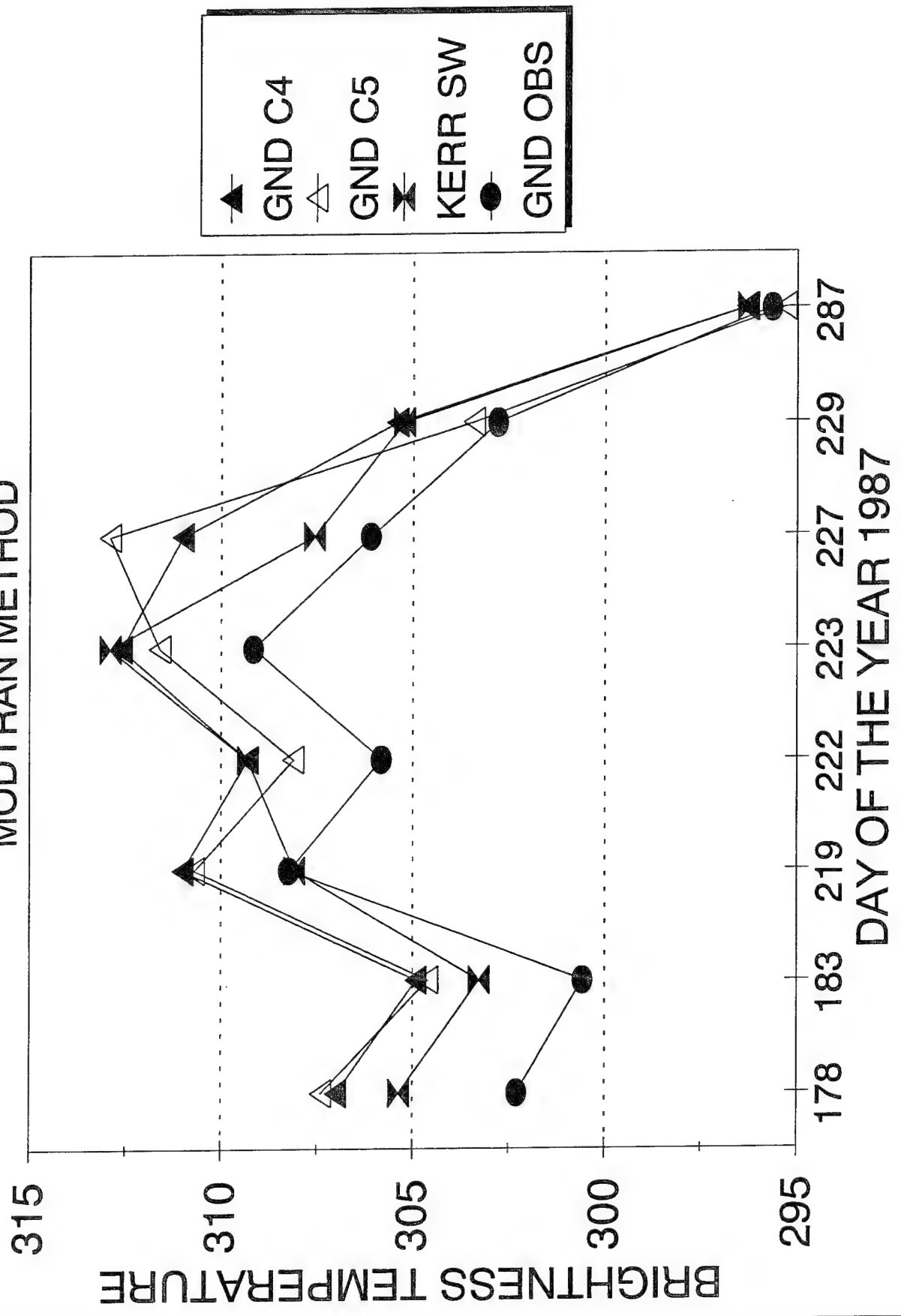
FIFE 1987

LOWTRAN METHOD

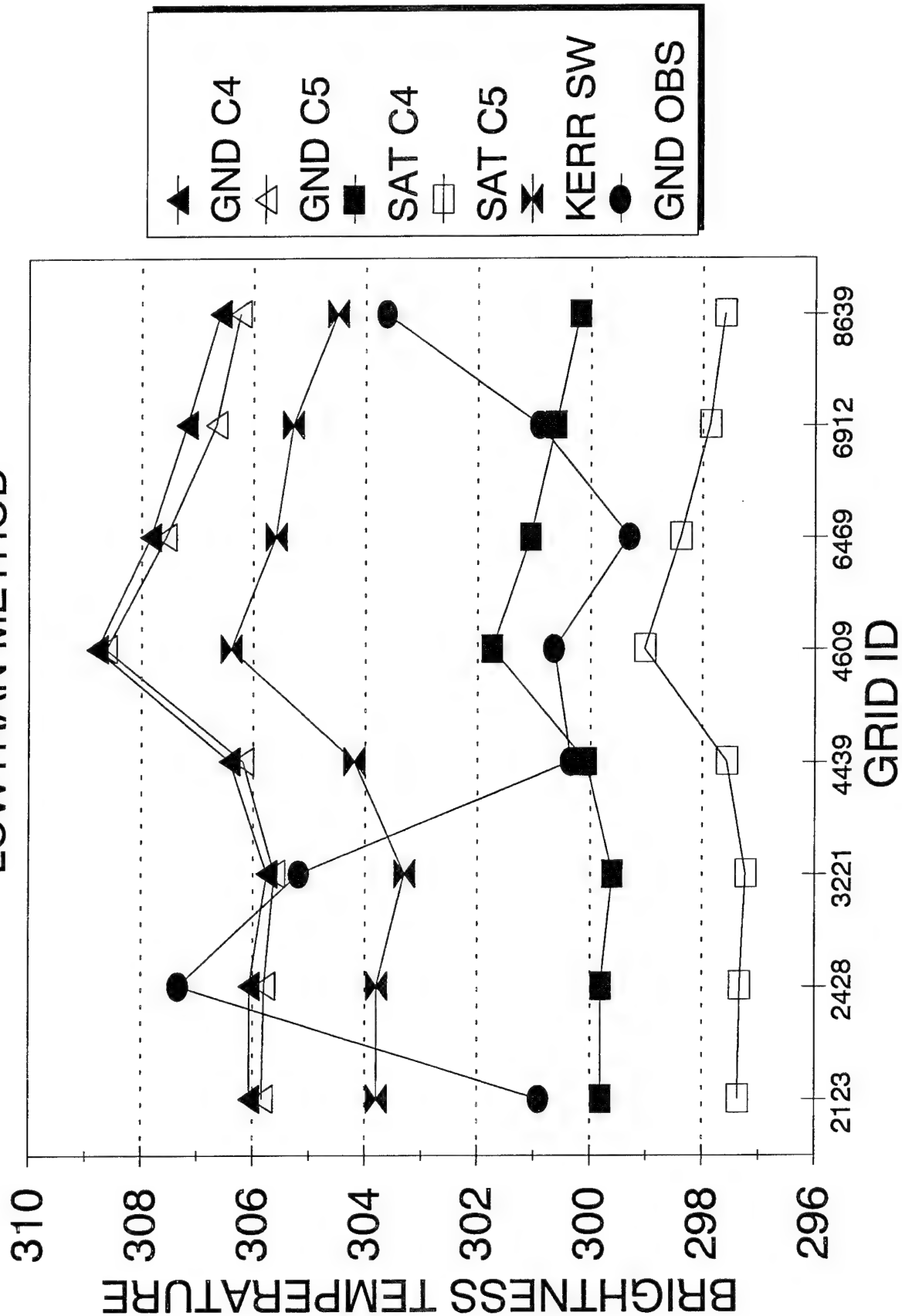


FIFE 1987

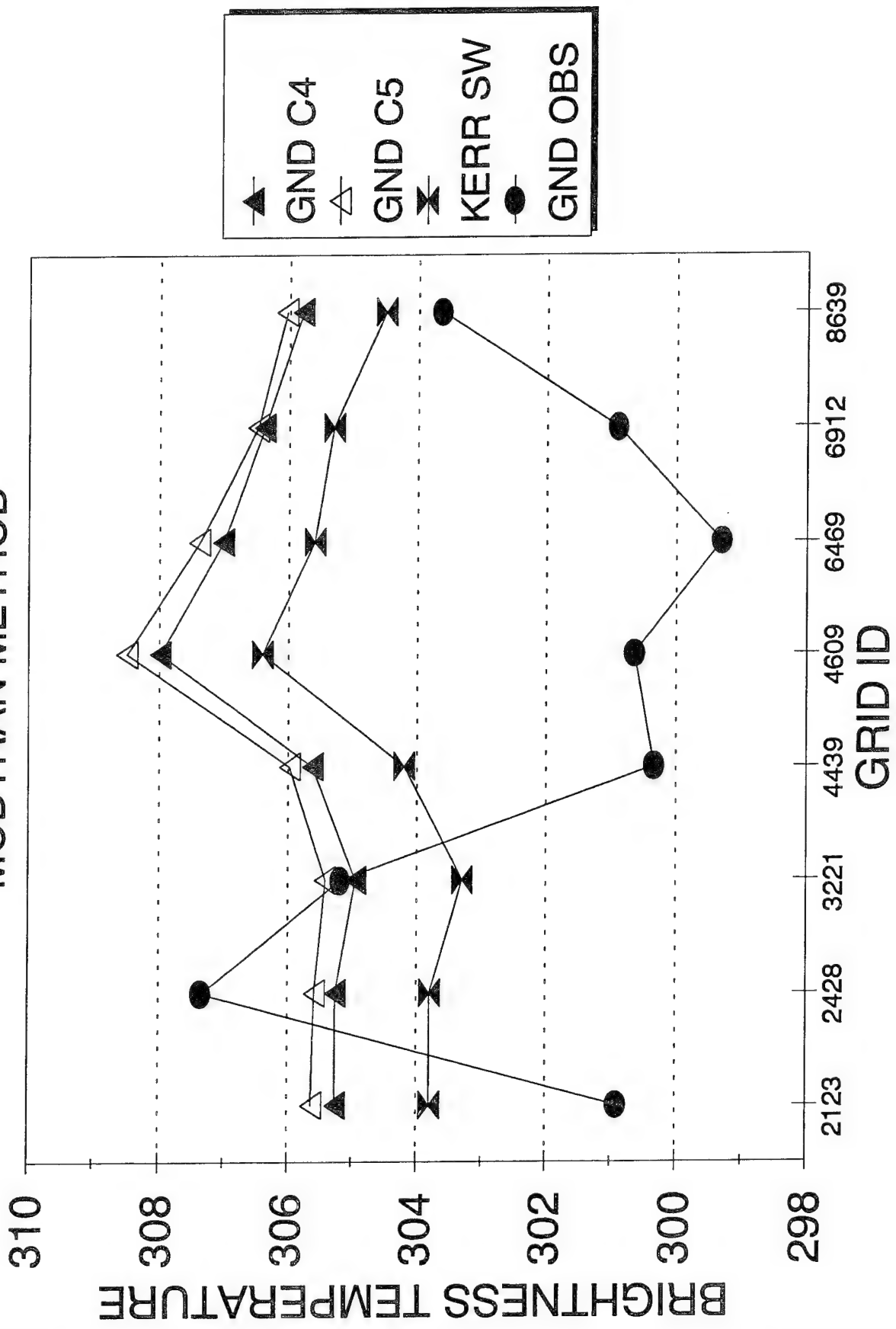
MODTRAN METHOD



FIFE - JUN 27 1987 LOWTRAN METHOD

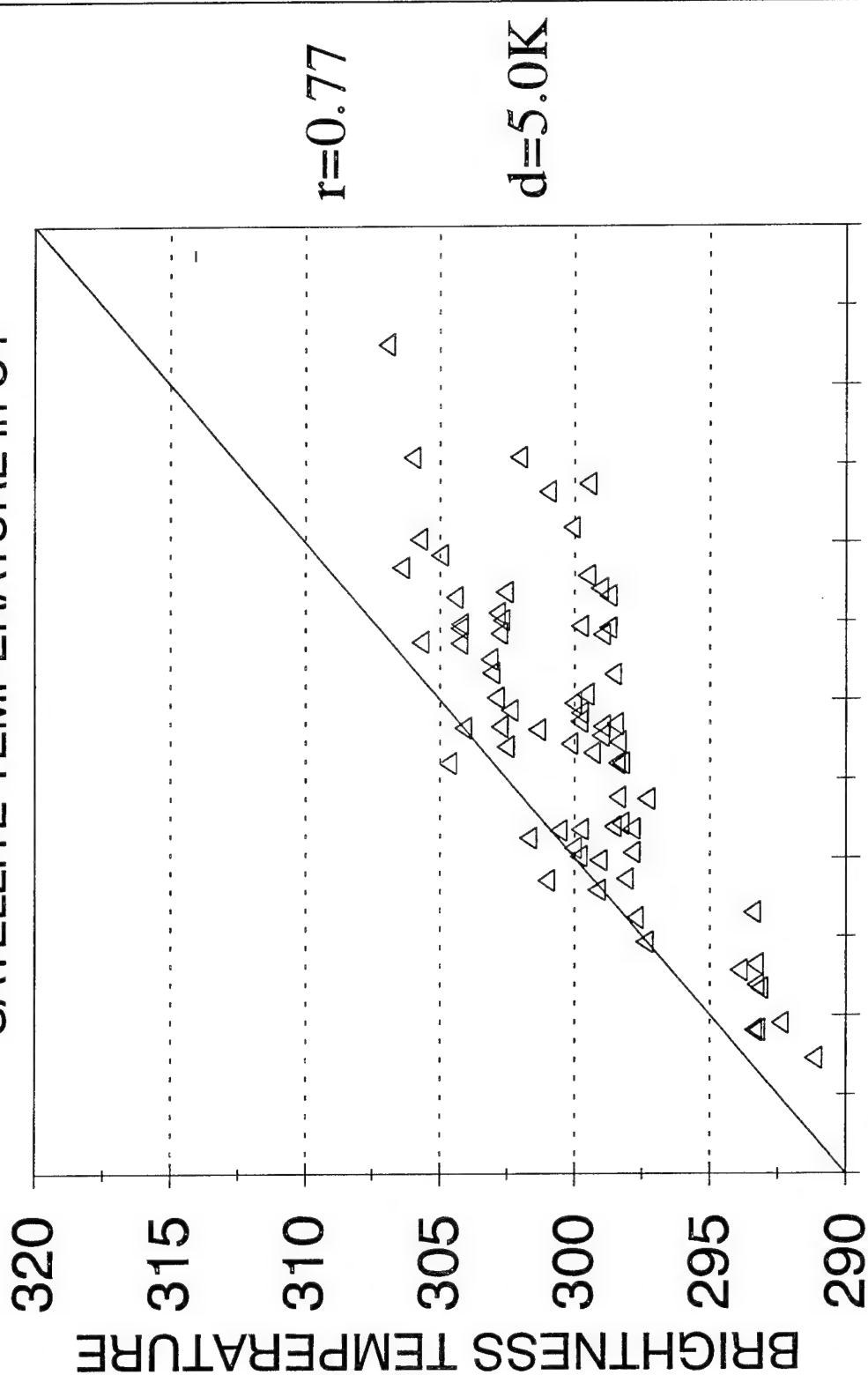


FIFE - JUN 27 1987 MODTRAN METHOD



FIFE 1987

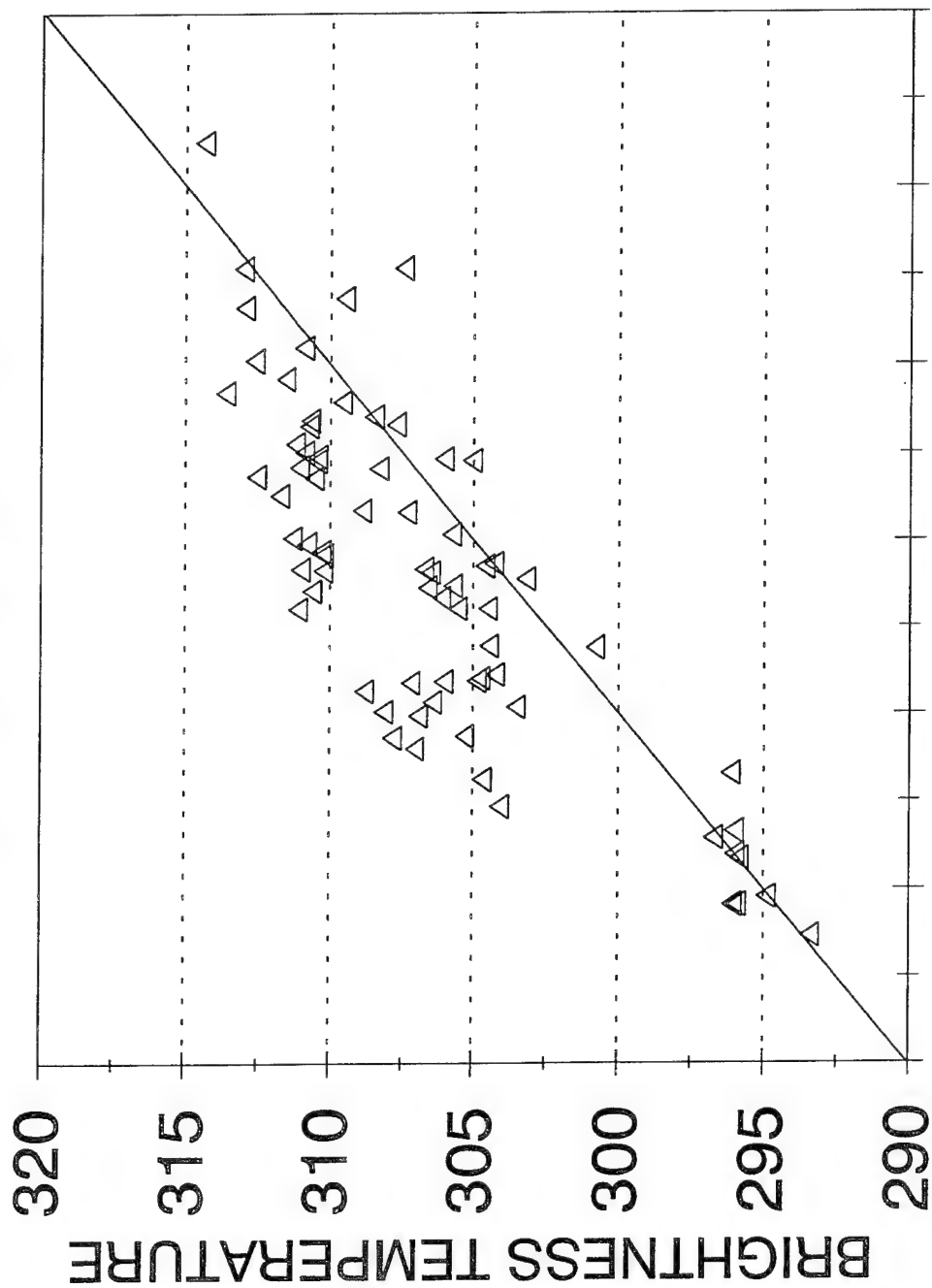
SATELLITE TEMPERATURE in C4



290 295 300 305 310 315 320
GROUND BRIGHTNESS TEMPERATURE OBSERVED

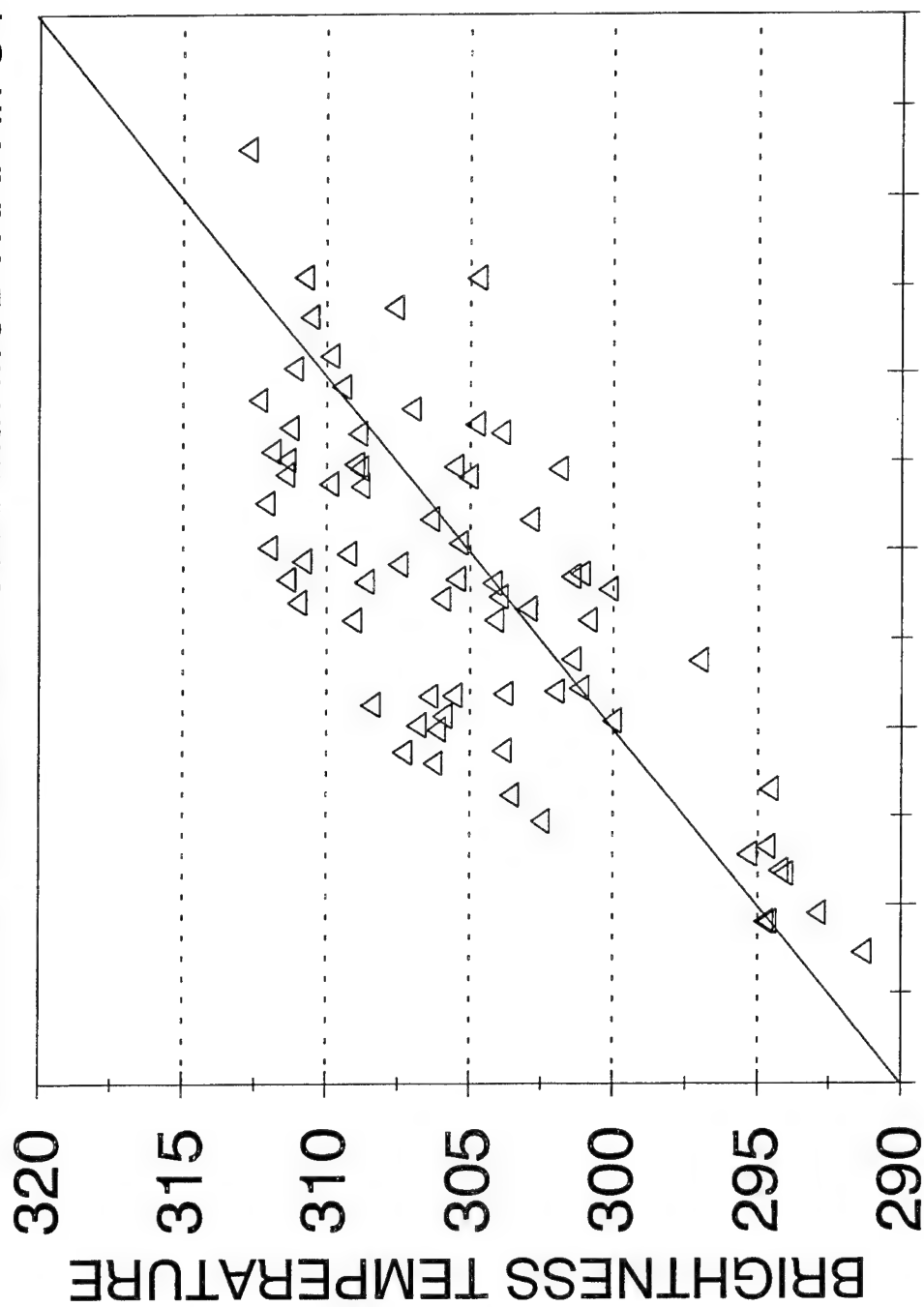
FIFE 1987

GND TEMPERATURE with LOWTRAN in C4



FIFE 1987

GROUND TEMPERATURE with MODTRAN in C4

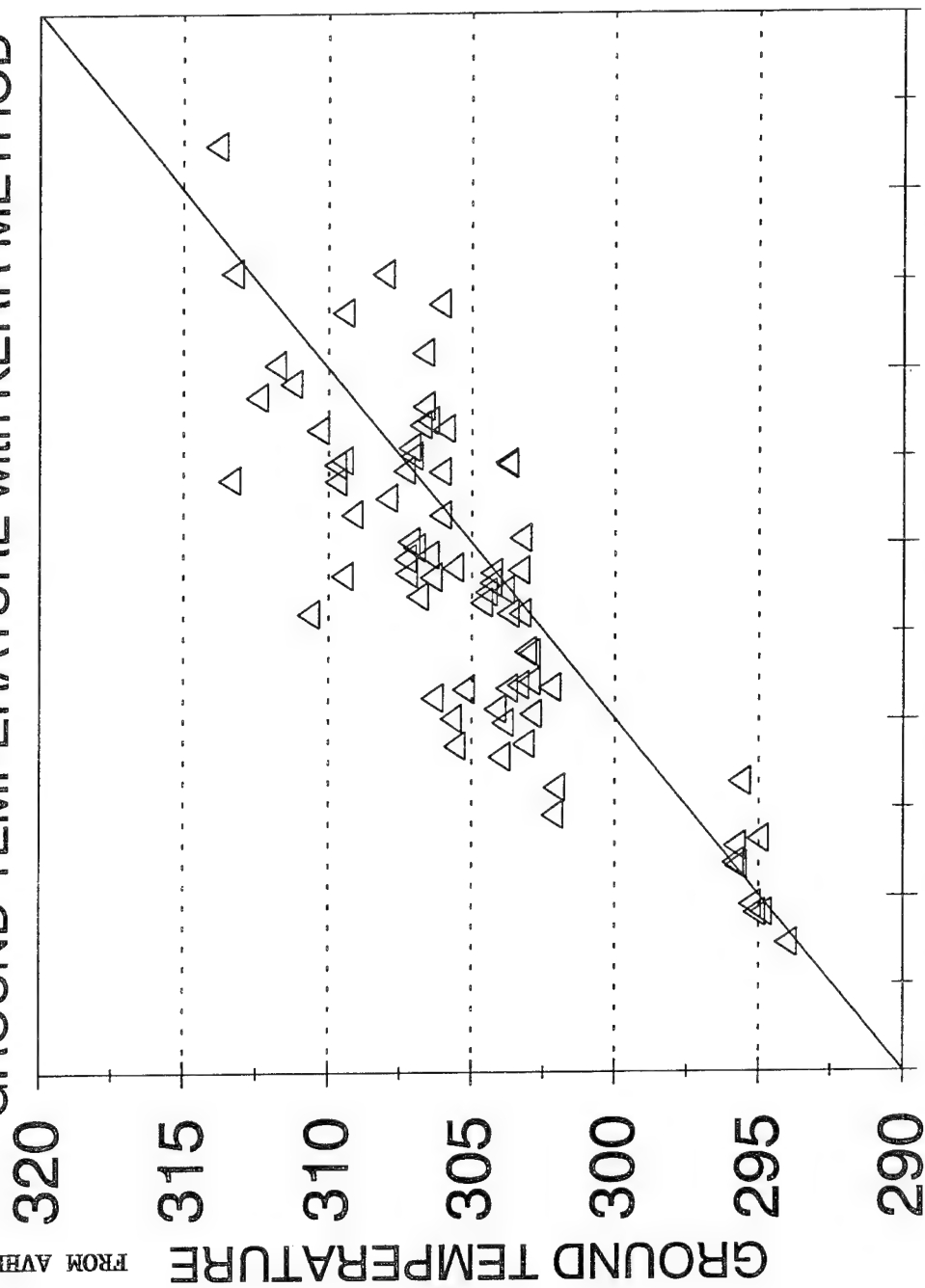


290 295 300 305 310 315 320
GROUND BRIGHTNESS TEMPERATURE OBSERVED

FIFE 1987

GROUND TEMPERATURE with KERR METHOD

FROM AVHRR



CONCLUSIONS

Lowtran/Modtran appears to work reasonably well with concurrent radiosoundings of the atmosphere

- Differences ~ 2 to 3C with ground observations
 - even at large angles
- Modtran works slightly better

What are the causes of the remaining differences?

- Uncertainties in the profile determinations?
- or in the models??

AN URGENT NEED OF VALIDATING WATER VAPOR ABSORPTION COEFFICIENTS FOR THE DEVELOPMENT OF EOS'S EARTH SURFACE TEMPERATURE ALGORITHMS

Z. Wan, J. Dozier

Computer Systems Laboratory
Center for Remote Sensing & Env. Optics
Univ. of California
Santa Barbara, CA 93106

In order to remotely measure surface temperature from space to an accuracy of 0.2°K for oceans and 1°K for land, as required by NASA's Earth Observing System (EOS), radiative transfer simulations should be accurate to tenths of a percent. Through "exponential-sum-fit" tables, the atmospheric transmission models in LOWTRAN and MODTRAN have been incorporated into accurate radiative transfer models based on adding/doubling or discrete-ordinate methods. Simulated cross-comparisons show that approximations used in LOWTRAN and MODTRAN can cause AVHRR band radiances to differ by as much as 1%, and the uncertainties caused by absorption by the water vapor continuum are larger. In combination with the water vapor band absorption coefficients in MODTRAN, with a finer spectral resolution and dependence on temperature and pressure, an exponential form of water vapor continuum absorption with a factor of 1.157 on the coefficient at 296°K used in LOWTRAN7 gave a better agreement between AVHRR data and simulations that were based on radiometric SST data and measured atmospheric temperature and humidity profiles. Accurate measurements and validations of water vapor absorption in a wide temperature range at a moderate spectral resolution, 5 cm⁻¹, are recommended.

A URGENT NEED OF VALIDATING WATER VAPOR ABSORPTION COEFFICIENTS FOR THE DEVELOPMENT OF EOS'S EARTH SURFACE TEMPERATURE ALGORITHMS

Zhengming Wan and Jeff Dozier

Computer Systems Laboratory / CRSEO

University of California, Santa Barbara, CA 93106, USA

Abstract — In order to remotely measure surface temperature from space to an accuracy of 0.2 °K for oceans and 1 °K for land, as required by NASA's Earth Observing System (EOS), radiative transfer simulations should be accurate to tenths of a percent. Through "exponential-sum-fit" tables, the atmospheric transmission models in LOWTRAN and MODTRAN have been incorporated into accurate radiative transfer models based on adding/doubling or discrete-ordinate methods. Simulated cross-comparisons show that approximations used in LOWTRAN and MODTRAN can cause AVHRR band radiances to differ by as much as 1%, and the uncertainties caused by absorption by the water vapor continuum are larger. In combination with the water vapor band absorption coefficients in MODTRAN, with a finer spectral resolution and dependence on temperature and pressure, an exponential form of water vapor continuum absorption with a factor of 1.157 on the coefficient at 296 °K used in LOWTRAN7 gave a better agreement between AVHRR data and simulations that were based on radiometric SST data and measured atmospheric temperature and humidity profiles. Accurate measurements and validations of water vapor absorption in a wide temperature range at a moderate spectral resolution, 5 cm⁻¹, are recommended.

INTRODUCTION

- Accuracy requirements for the Earth surface temperature:
 - SST of 0.3 °K specified by the International Tropical Ocean Global Atmosphere (TOGA) program for global numerical models of climate.
 - Earth Observing System (EOS) specified 0.2 °K for SST.
 - Earth Observing System (EOS) specified 1 °K for LST in 270-340 °K.
- The accuracy of radiative transfer simulations is required better than 0.25% according to a simple error analysis of NOAA7 MCSST.
 - $T_{ss} = 3.6125T_4 - 2.5779T_5 - 10.05 \rightarrow \delta T_{ss} = 6.19\delta T_b$ if $\delta T_4 = \delta T_5 = \delta T_b$
- EOS MODIS and ASTER will provide an unique opportunity for LST, and give a challenge for the high accuracy of radiative transfer simulations
 - at a higher spectral resolution (Table 1),
 - need to check various approximations used in radiative transfer models,
 - need more accurate water vapor absorption coefficients.

TABLE 1. Specifications of MODIS and ASTER thermal infrared bands for surface temperature

MODIS band	center (μm)	width (μm)	NE Δ T ($^{\circ}\text{K}$)	T _{max} ($^{\circ}\text{K}$)	ASTER band	center (μm)	width (μm)	NE Δ T ($^{\circ}\text{K}$)
20	3.75	0.18	0.05	335				
22	3.96	0.05	0.07	328	10	8.30	0.35	< 0.3
23	4.05	0.05	0.07	328	11	8.65	0.35	< 0.3
29	8.55	0.30	0.05	324	12	9.10	0.35	< 0.3
31	11.03	0.50	0.05	324	13	10.6	0.70	< 0.3
32	12.02	0.50	0.05	324	14	11.3	0.70	< 0.3

COMPARISON BETWEEN ATMOSPHERIC RADIATIVE TRANSFER MODELS

- Radiative transfer models used in comparison:
 - LOWTRAN 6 uses
 - temperature-independent band model absorption coefficients C_i for H_2O , CO_2 , and for O_3 , at spectral interval 5 cm^{-1} .
 - The transmission function is expressed as

$$\tau_i = \exp\{-C_i W_i\}, \quad W_i = \left(\frac{P}{P_0}\right)^{2n_i} \left(\frac{T_0}{T}\right)^{n_i} U_i. \quad (1)$$

- Approximations: two-stream method with single scattering.

— LOWTRAN 7 uses

- temperature-independent band model absorption parameter C' (nominally sea level at 296 °K) for eleven atmospheric molecules at spectral interval 5 cm^{-1} .
- The transmission function expressed in the double exponential form

$$\tau = \exp\{-(C W)^a\}, \quad C = 10^{C'}, \quad W = \left(\frac{P}{P_0}\right)^m \left(\frac{T_0}{T}\right)^n U. \quad (2)$$

- updated water vapor continuum absorption.
- Approximations: two-stream method and a three-term K-distribution multiple scattering parameterization.

— MODTRAN uses

- band model parameters formulated from the HITRAN line atlas for twelve atmospheric molecules. They were calculated for 1 cm^{-1} bins from 0-17900 cm^{-1} and at five temperatures from 200 to 300 °K.
- The transmission function is based on a statistical model for a finite number of lines within the spectral bin, and is given by

$$\tau = (1 - \langle W_{sl} \rangle^{<n>}) \quad (3)$$

- the same water vapor continuum absorption as in LOWTRAN 7.
- Approximations: two-stream method, a multiple scattering approximation without K-distribution, the Curtis-Godson approximation for transmission, and the Beer's Law for calculation of layer optical depths.

— ATRAD

- deals with accurate multiple scattering based on the interaction principle and adding/doubling method
- and uses an exponential-sum for each atmospheric molecular's transmission function. All cross terms in the product of exponential-sums for H_2O , CO_2 and O_3 are included in radiative transfer calculations.
- It has been validated with the discrete-ordinate method.

• Comparison between MODTRAN and LOWTRAN

TABLE 2. The band transmission and brightness temperature of MODIS and ASTER thermal bands for a land surface with $\epsilon = 0.98$ and at $T_s = T_{air} = 299.7^\circ\text{K}$ under tropical atmosphere with surface visibility 23 km at $0.55\text{ }\mu\text{m}$ and nadir viewing.

sensor band no.	band range (μm)	$\Delta(\text{transmittance})$ $t_m - t_l$	$T_{mod} - T_{low7}$ ($^\circ\text{K}$)	$T_{mod} - T_{low6}$ ($^\circ\text{K}$)
MODIS				
20	3.660-3.840	+6.0%	-2.1%	0.48
22	3.934-3.984	+1.9%	-1.3%	0.44
23	4.025-4.075	+3.7%	-2.0%	0.29
29	8.400-8.700	-0.7%	+1.2%	0.62
31	10.78-11.28	-0.1%	+7.7%	1.23
32	11.77-12.27	+2.7%	10.9%	1.47
ASTER				
10	8.125-8.475	-2.7%	-1.6%	0.74
11	8.475-8.825	-0.4%	+0.8%	0.68
12	8.925-9.275	+1.3%	+9.8%	1.90
13	10.25-10.95	+1.0%	+9.6%	1.80
14	10.95-11.65	-0.6%	+6.8%	1.06

• Factor Analysis

TABLE 3. Comparison of molecular absorptions in different models with MODTRAN.

no.	model	spectral interval	H ₂ O-band	CO ₂ +	O ₃	H ₂ O-cont
1	MODTRAN	1 cm ⁻¹	model 1	model 1	model 1	=model 4
2	ATRAD-MOD1	5 cm ⁻¹	≈model 1	≈model 5	≈model 4	=model 4
2'	ATRAD-MOD2	5 cm ⁻¹	≈model 1	≈model 4	≈model 4	=model 4
3	ATRAD-LOW1	5 cm ⁻¹	≈model 4	≈model 5	≈model 4	=model 4
3'	ATRAD-LOW2	5 cm ⁻¹	≈model 4	≈model 4	≈model 4	=model 4
4	LOWTRAN7	5 cm ⁻¹	+, --	≈, +	≈, ≈	model 4
5	LOWTRAN6	5 cm ⁻¹	+, -	≈, +	+, ≈	++, +

Note: (+, -) means that it is larger in NOAA-7 AVHRR channel 4 but smaller in channel 5.

TABLE 4. Quantitative comparisons between different models in NOAA7 AVHRR band brightness temperature and MCSST values simulated for tropical atmosphere, surface visibility 23 km at $0.55\ \mu\text{m}$, $\varepsilon = 0.98$, $T_{ss} = T_{air} = 299.7\ ^\circ\text{K}$, viewing at 11.4° .

no.	MODEL	T_4 ($^\circ\text{K}$)	T_5 ($^\circ\text{K}$)	$T_4 - T_5$ ($^\circ\text{K}$)	MCSST ($^\circ\text{K}$)	MCSST - SST
1	MODTRAN	295.434	293.509	1.925	300.57	+0.87
2	ATRAD-MOD1	295.175	293.760	1.415	298.99	-0.71
2'	ATRAD-MOD2	295.117	293.531	1.586	299.37	-0.33
3	ATRAD-LOW1	294.674	293.207	1.467	298.60	-1.10
3'	ATRAD-LOW2	294.611	292.971	1.640	298.98	-0.72
4	LOWTRAN7-MS	294.872	293.261	1.611	299.18	-0.52
4'	LOWTRAN7-SS	294.441	292.814	1.627	298.77	-0.93
5	LOWTRAN6	293.641	292.422	1.219	296.89	-2.81
5'	LOWTRAN6 using H ₂ O-continuum in LOWTRAN7	293.993	292.714	1.279	297.41	-2.29

compare models	ΔT_4 ($^\circ\text{K}$)	ΔT_5 ($^\circ\text{K}$)	$\Delta(T_4 - T_5)$ ($^\circ\text{K}$)	ΔMCSST ($^\circ\text{K}$)	factors
2' - 3'	+0.51	+0.56	-0.05	+0.39	H ₂ O band difference
5' - 5	+0.35	+0.29	+0.06	+0.52	H ₂ O-cont difference
3' - 3	-0.06	-0.24	+0.17	+0.38	CO ₂ band difference
4 - 4'	+0.43	+0.45	-0.02	+0.41	multiple scattering
3' - 4	-0.26	-0.29	+0.03	-0.20	overlap effect
1 - 2	+0.26	-0.25	+0.51	+1.58	following effects in model 1
	+0.02	+0.01	+0.01	+0.04	no k-distribution
	+0.26	+0.29	-0.03	+0.20	no overlap
	+0.13	+0.42	-0.29	-0.61	Curtis-Godson approx.
	-0.15	-0.97	+0.82	+1.95	Beer's law & others

- Comparison between Simulations and SST Measurements.
- SST data sets of Barton (Applied Optics, pp. 2929-2934, 1991).

TABLE 5. Sea surface temperature measurements data sets.

data id.	date d/m/y	Lat. (°S)	Long. (°E)	zenith angle	SST (°C)	satellite T ₄	satellite T ₅	wind speed knots/direction	T _a (°C)	RH _s (%)	RH _{max} (%)	at elev. (km)
Base Strait (NOAA-7)												
d01	05/07/84	40.77	147.92	33°	12.6	9.6	8.7		9.75	56	95	1.39
d02	08/08/84	34.88	151.22	59°	18.0	13.7	12.1	18/080	13.65	70	76	0.28
d03	08/08/84	36.57	150.35	27°	15.6	13.6	12.6	2/275	15.05	58	60	3.39
d04	07/10/84	32.90	153.53	16°	20.7	17.5	16.2		21.35	40	93	1.09
d05	12/10/84	31.58	153.90	46°	20.3	18.1	17.1		20.65	70	88	0.32
d06	13/10/84	31.75	153.18	49°	21.2	18.0	17.0		14.65	72	85	0.01
d07	01/12/84	38.80	148.33	26°	16.1	14.6	13.6	15/090	19.35	60	81	1.02
d08	02/12/84	38.67	148.12	3°	15.0	13.5	12.9	25/010	15.55	94	94	0.00
Coral Sea (NOAA-9)												
d09	25/10/85	18.42	153.50	50°	26.7	19.9	17.7	8/150	29.85	95	95	0.00
d10	28/10/85	15.57	156.53	65°	28.4	15.6	12.6	3/240	22.25	70	91	2.73
d11	29/10/85	13.37	154.93	54°	29.2	19.1	16.0	4/160	30.25	62	98	8.60
d12	31/10/85	13.03	151.75	36°	27.3	22.9	21.4	13/270	26.35	59	105	9.40
d13	31/10/85	13.53	150.75	5°	27.1	22.5	20.7	9/280	28.35	59	91	1.86
d14	04/11/85	16.57	147.68	43°	26.9	17.9	15.1	17/175	24.75	82	98	5.09

— Comparison with radiative transfer simulations

TABLE 6. RT simulation results compared with SST measurements.

band	water vapor absorption continuum	model $T_4 - T_4$ (°C)	model $T_5 - T_5$ (°C)	model MCSST - SST (°C)
{ data id. = d03, precip. water = 1.33 cm, SST = 15.6°C,				
exptbl (lowtran7)	lowtran7	-0.29	-0.20	-0.10
exptbl (modtran)	lowtran7	0.08	0.30	-0.02
exptbl (modtran)	exp. form	0.03	0.18	0.09
exptbl (modtran)	1.157 × exp. form	-0.05	0.07	0.11
{ data id. = d09, precip. water = 4.13 cm, SST = 26.7°C,				
exptbl (lowtran7)	lowtran7	0.23	0.47	-0.79
exptbl (modtran)	lowtran7	0.60	0.93	-0.66
exptbl (modtran)	exp. form	0.59	0.84	-0.46
exptbl (modtran)	1.157 × exp. form	0.16	0.31	-0.58
{ data id. = d10, precip. water = 4.01 cm, SST = 28.4°C,				
exptbl (lowtran7)	lowtran7	0.61	0.66	-3.72
exptbl (modtran)	lowtran7	0.97	1.09	-3.55
exptbl (modtran)	exp. form	0.75	0.58	-3.02
exptbl (modtran)	1.157 × exp. form	0.02	-0.28	-3.38
{ data id. = d13, precip. water = 3.40 cm, SST = 27.1°C,				
exptbl (lowtran7)	lowtran7	0.22	0.54	-0.21
exptbl (modtran)	lowtran7	0.56	0.96	-0.09
exptbl (modtran)	exp. form	0.56	0.92	0.02
exptbl (modtran)	1.157 × exp. form	0.28	0.55	-0.02

— Notes:

- The sea-surface emissivity model (Masuda et al., 1988) has been used.
- "exptbl(lowtran7)" means the exponential-sum-fitting table from the transmission values used in LOWTRAN7.
- "exp. form" means the exponential form of the H₂O self-broadening coefficient $\ln C_s^0 = \Theta/T + \text{constant}$ based on the coefficient at 296 °K in LOWTRAN7, and data of Burch and Gryvnak (1980).

STATUS OF VALIDATION OF WATER VAPOR ABSORPTION COEFFICIENTS

- Atmospheric CVF transmissometer measurements at low spectral resolutions (2-6% of the wavelength).
 - Kneizys et al., 1984
 - Oppenheim & Lipson, 1985
- Atmospheric transmission measurements in the 2.8-5.5 μm region with Fourier interferometric transmissometer.
 - Theriault et al., 1990

RECOMMENDATIONS ON VALIDATION OF WATER VAPOR ABSORPTION

- At a moderate spectral resolution, 5 cm^{-1} .
- For a wide temperature range from 240 to 330 $^{\circ}\text{K}$.
- The desirable accuracy of absorption coefficients, 5%.

— Quantitative results (Table 4).

TABLE 4. table 4

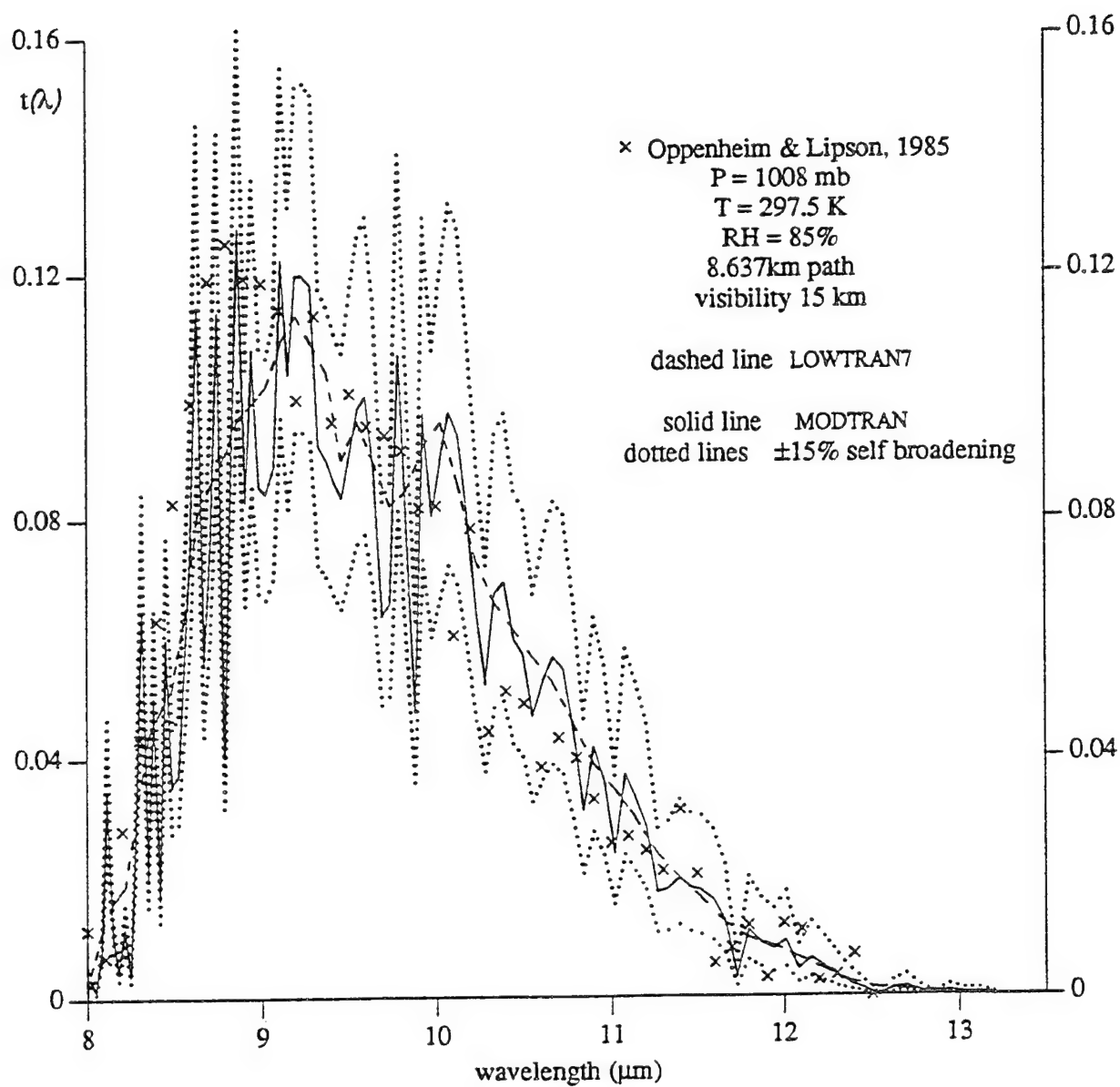
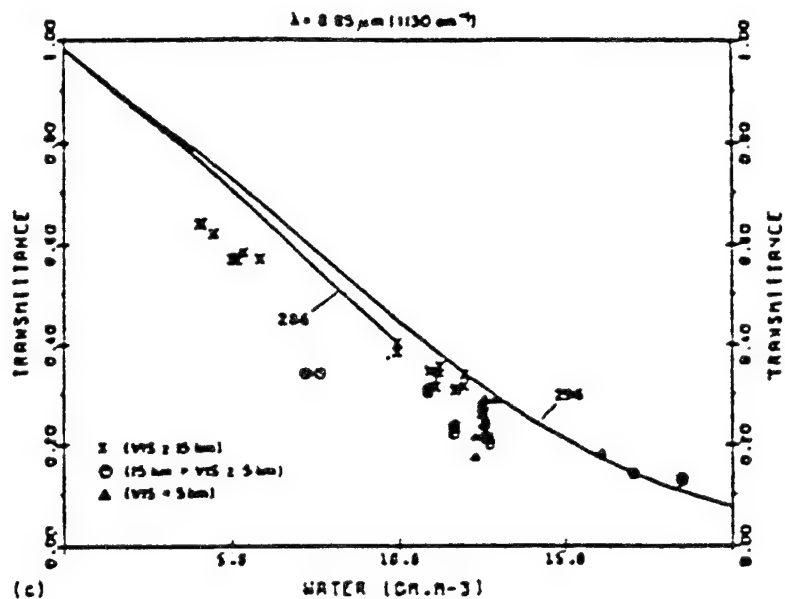
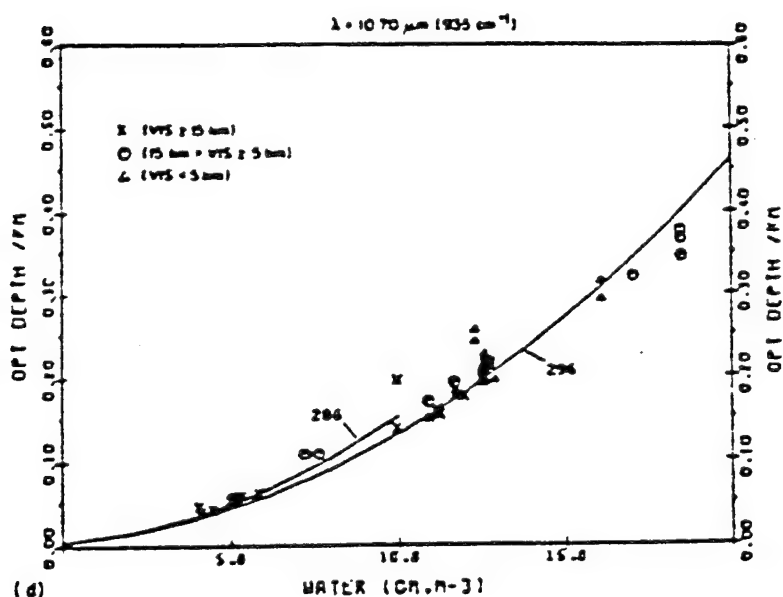


Figure 4. Comparison between atmospheric transmission data and RT simulations.



(c) $8.85\text{-}\mu\text{m}$ Filter, Transmittance Scale, All Data



(d) $10.70\text{-}\mu\text{m}$ Filter, Optical Depth/km Scale, All Data

Figure 15. Measured Transmittances (Symbols) and LOWTRAN Calculations (Solid Lines) at 286 and 296 K for the 8- to $12\text{-}\mu\text{m}$ Region and the 8-km Path

ANALYSIS OF CLOUD-TOP HEIGHT AND RELATED CLOUD PARAMETERS FROM SATELLITES USING THE O₂ A AND B BANDS

A. Kuze, K. Chance

Harvard-Smithsonian Ctr.
for Astrophysics
Atomic & Molecular Physics Div.
60 Garden Street
Cambridge, MA 02138

Cloud height and cloud coverage detection are important for total ozone retrieval using ultraviolet scattered light. Use of the O₂ A and B bands, around 762 and 688 nm, make it possible to detect both cloud top height and cloud percentage. The measured values of a space borne high resolution spectrometer are convolutions of the instrument slit function and the atmospheric transmittance between cloud top and satellite. Optical thicknesses between the satellite orbit and each height are calculated with high accuracy using FASCODE3P. Cloud parameters are determined by least-squares fitting. A grid-search method is used to search the parameter space of cloud top height and percentage to minimize the variance. For this search, nonlinearity of atmospheric transmittance is important. Using the above-mentioned method, operational cloud detection is possible with minimal computation time. Measurement of clouds and atmospheric trace gases in the same IFOV are also possible.

Analysis of
Cloud-top Height and Related Cloud Parameters
from Satellites Using the O₂ A and B Bands

June 8, 1993

AKIHIKO KUZE AND KELLY V. CHANCE

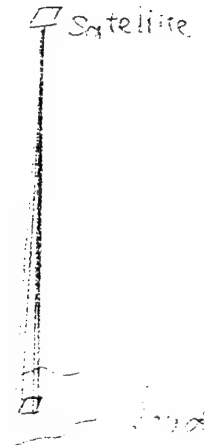
Harvard-Smithsonian Center for Astrophysics

IFOV of Satellite Borne High Resolution Spectrometer



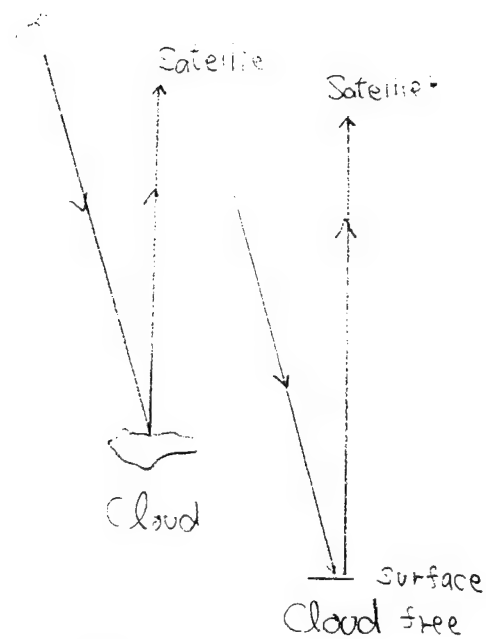
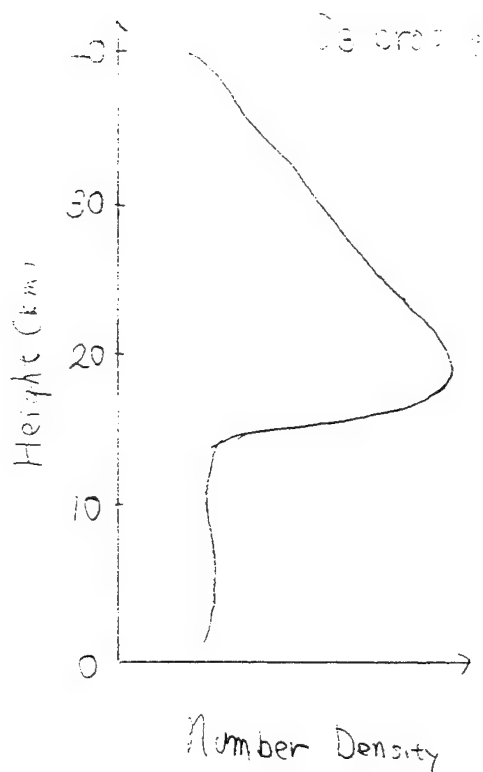
typically $100 \text{ km} \times 100 \text{ km}$

IFOV of Radiometer



typically $100 \text{ m} \times 100 \text{ m}$

Ozone Profile and Cloud Effect on Measurement



GOME and SCIAMACHY Project

Satellite Borne High Resolution Spectrometer

Orbit : Sun-Synchronous

Altitude : 800 km

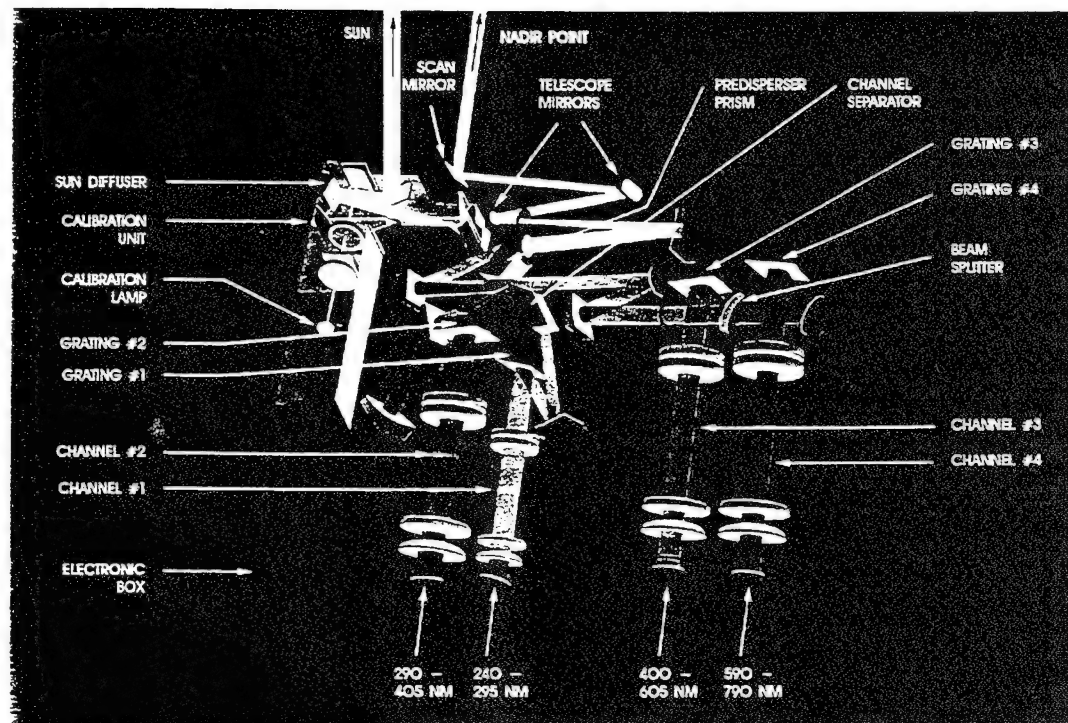
Nadir Looking

Solar Backscattering Radiance Observation

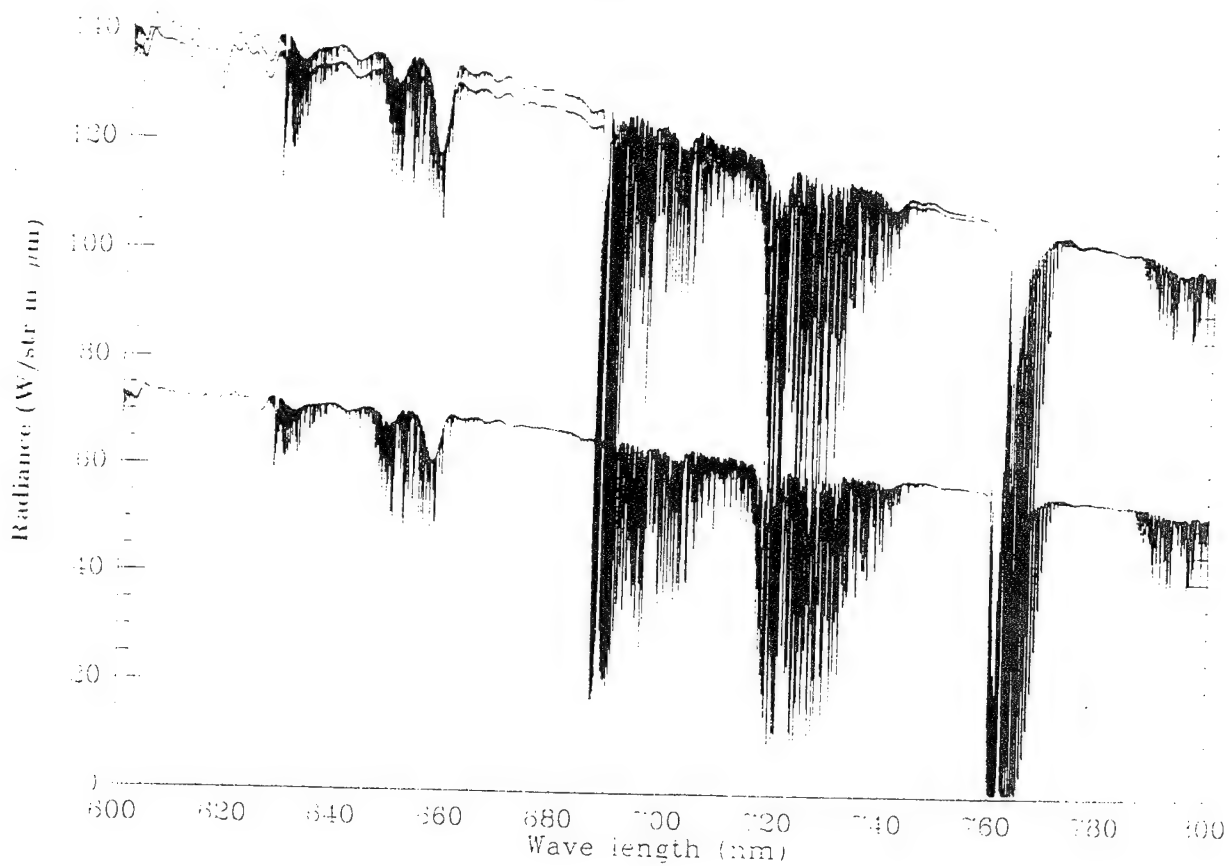
IFOV : $320 \text{ km} \times 40 \text{ km}$

Spectral Coverage : 240 - 790 nm

Spectral Resolution : 0.1 - 0.2 nm



Measured Radiance and O₂ Absorption



Radiative Transfer in the O₂ Absorption Region

$$I(j) = \sum_{i=1}^N \alpha_{ij} r_i \int f_j(\nu) F(\nu) \exp(-s\tau(\nu, h_i)) \frac{d\nu}{\Delta\nu} \\ + \beta_j \left(1 - \sum_{i=1}^N r_i\right) \int f_j(\nu) F(\nu) \exp(-s\tau(\nu, 0)) \frac{d\nu}{\Delta\nu} ,$$

α_{ij} : the cloud top reflectivity

β_j : the earth's surface diffusive albedo

$\tau(\nu, h)$: the optical depth between cloud top and satellite
(proportional to total O₂ column amount above cloud top)

$f_j(\nu)$: the slit function of channel

$F(\nu)$: the solar spectrum

r_i : the coverage of type i cloud

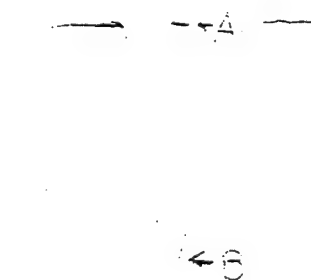
h_i : the top height of type i cloud

$\Delta\nu$: FWHM of the instrument

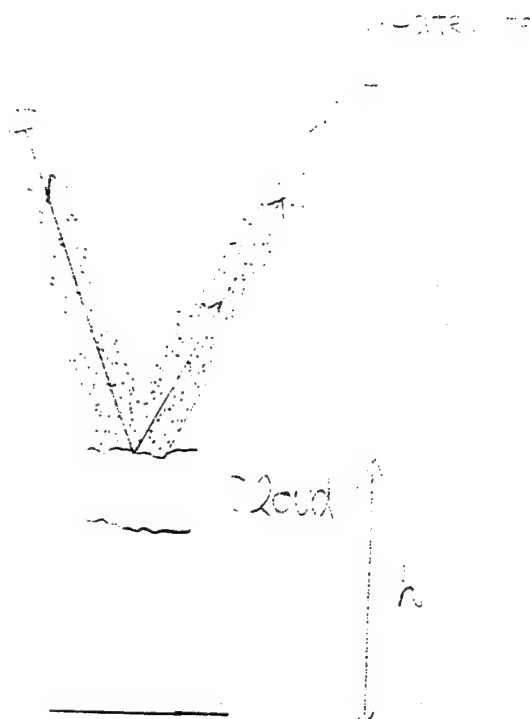
O₂ Absorption

O₂ Total Amount above Clouds

Clouds Top Estimation

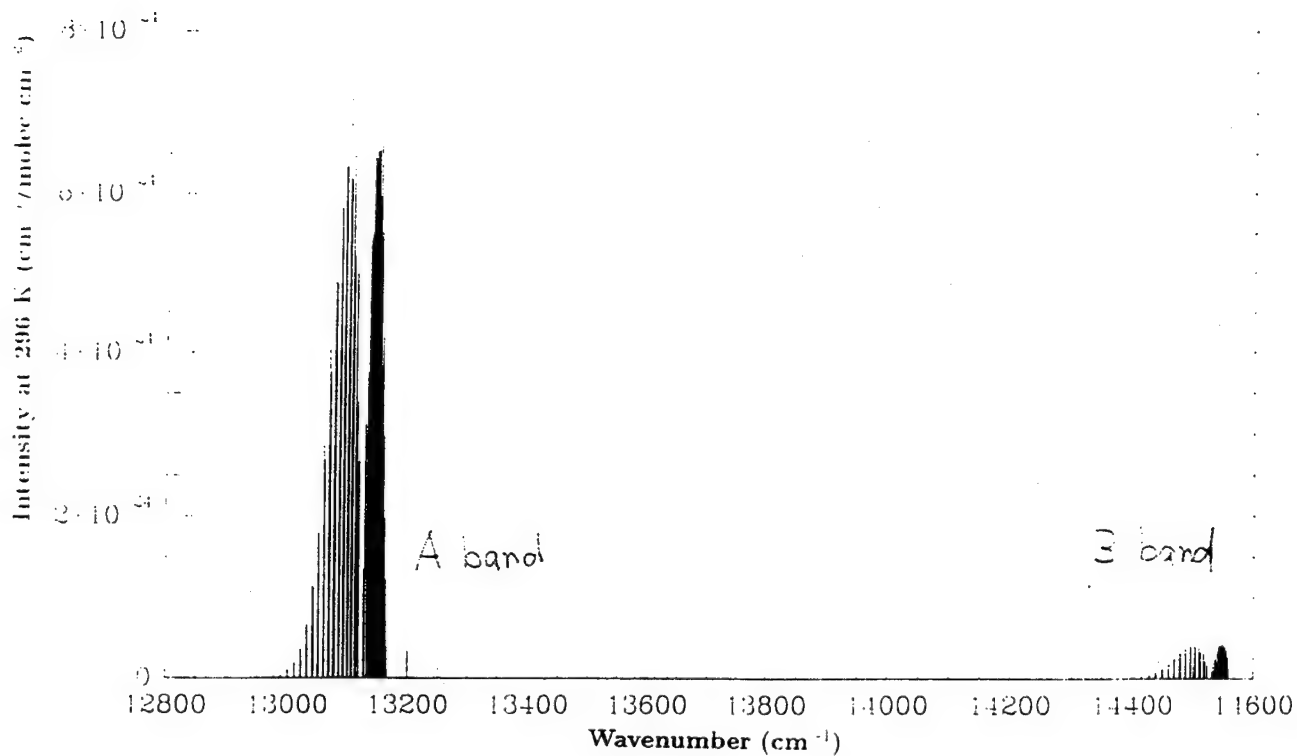


$$\frac{1}{1.0} = 1.0$$

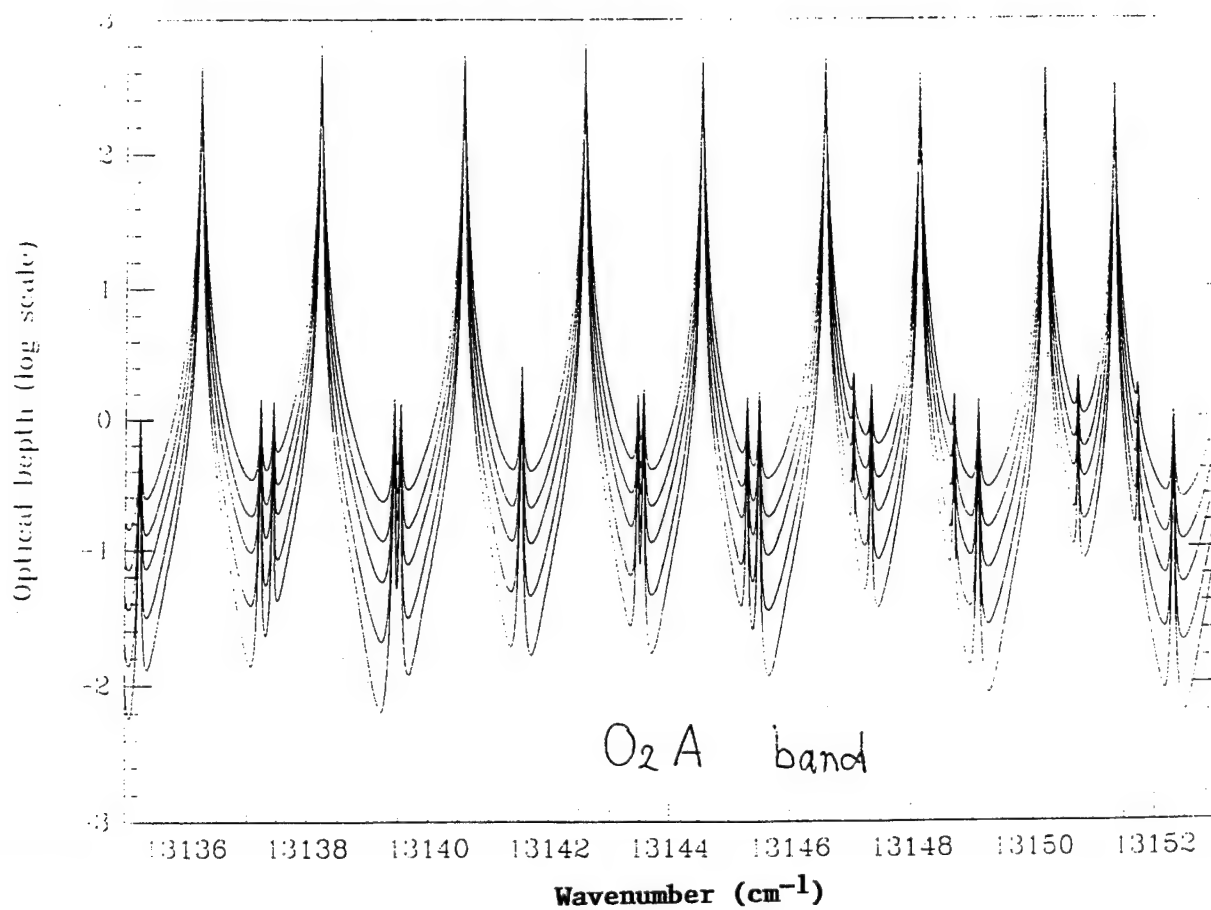


32 and 1
1000000 to be
14 known

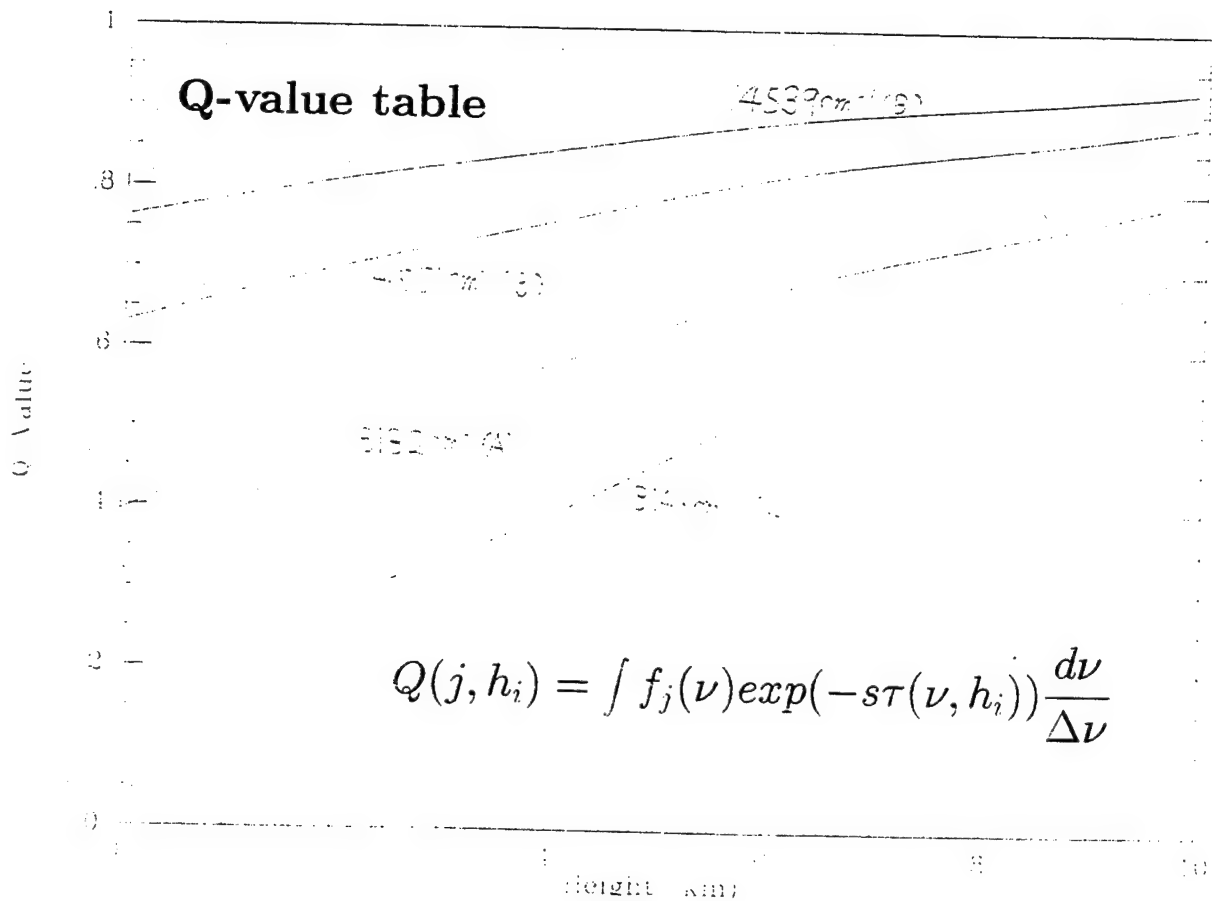
O₂ A and B band



Calculated Optical Depth by FASCODE3



Algorithm



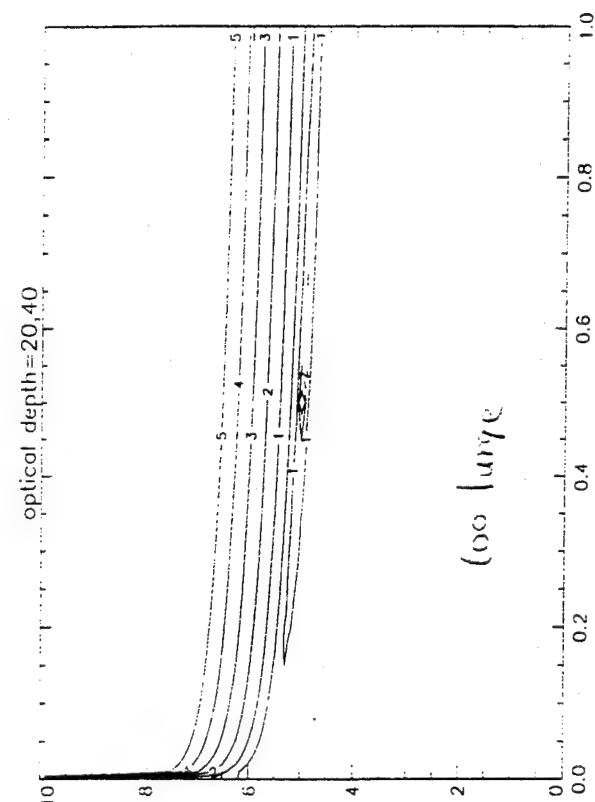
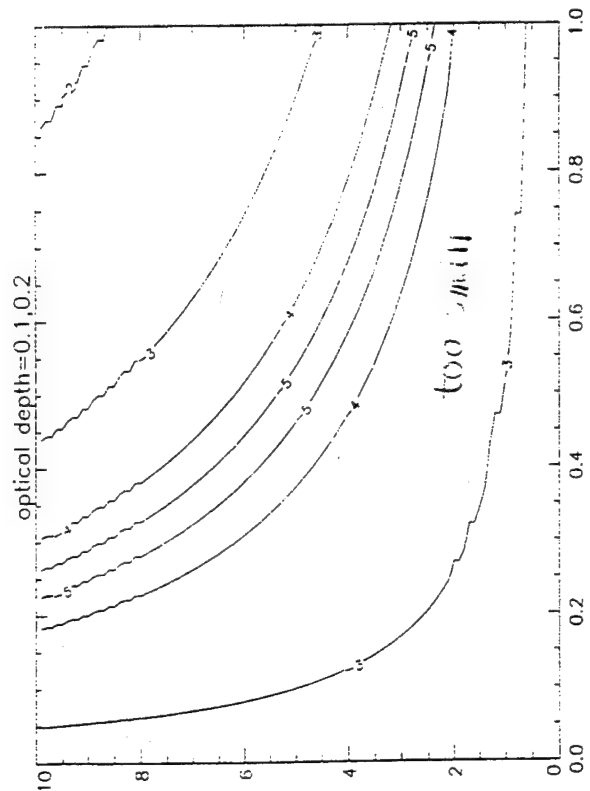
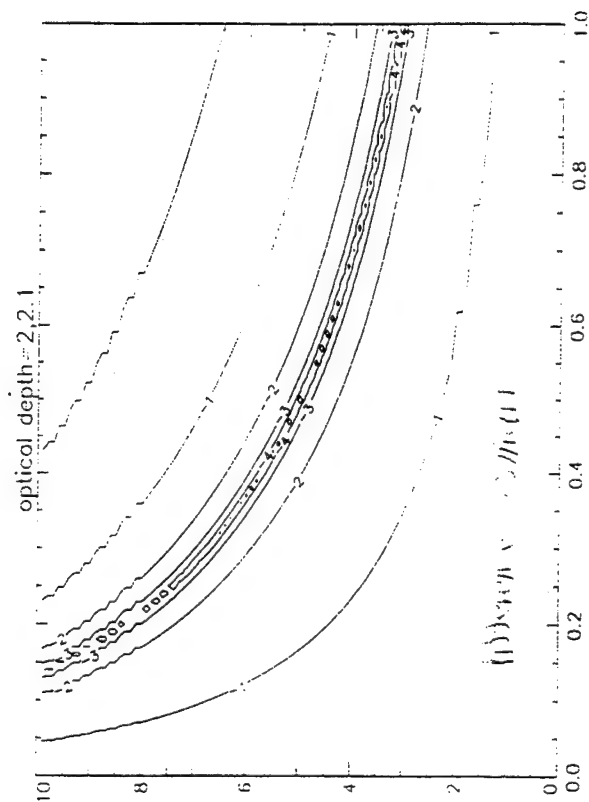
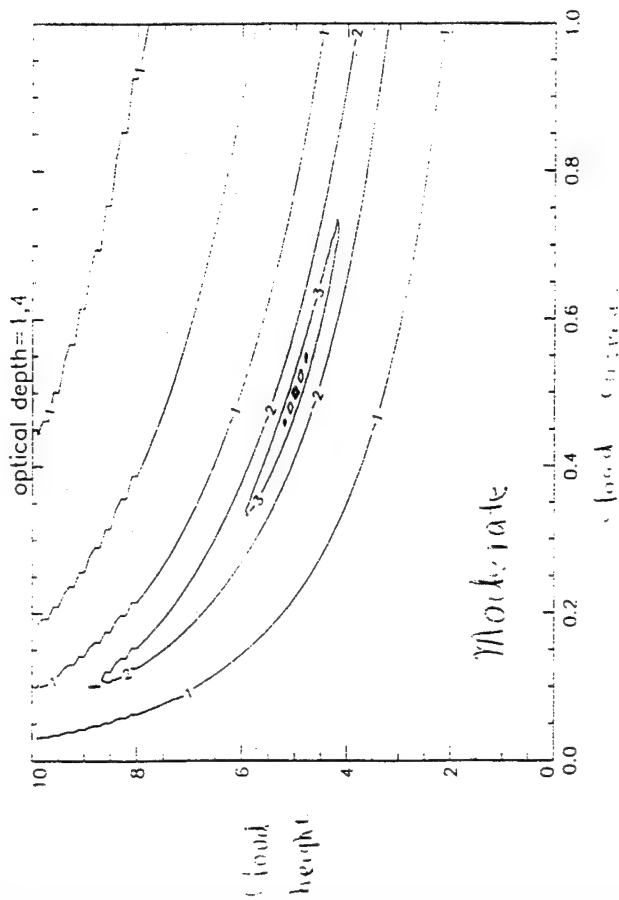
χ^2 Grid Search

Height vs Cloud Coverage

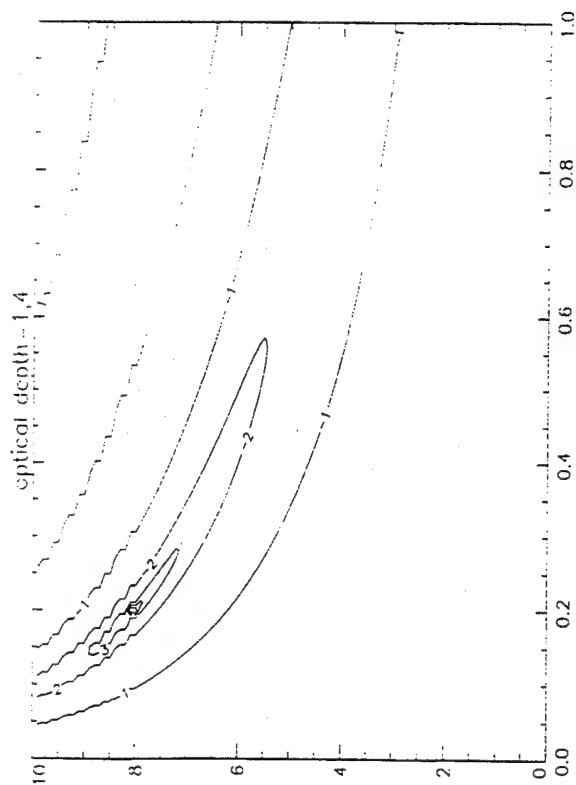
$$\chi^2 = \sum_{j=1}^M \left(\frac{R_{obs}(j, h_i, \alpha_{ij}r_i) - R_{calc}(j, h_i, \alpha_{ij}r_i)}{R_{obs}(j, h_i, \alpha_{ij}r_i)} \right)^2 / M$$

$$\begin{aligned} R(j, h_i, \alpha_{ij}r_i) &= \frac{I(j)}{F(\nu)} = \sum_{i=1}^N \alpha_{ij}r_i Q(j, h_i) + \beta_j \left(1 - \sum_{i=1}^N r_i \right) Q(j, 0) \\ &= \sum_{i=1}^N \alpha_{ij}r_i Q(j, h_i) + (\gamma_j - \sum_{i=1}^N \alpha_{ij}r_i) Q(j, 0) \end{aligned}$$

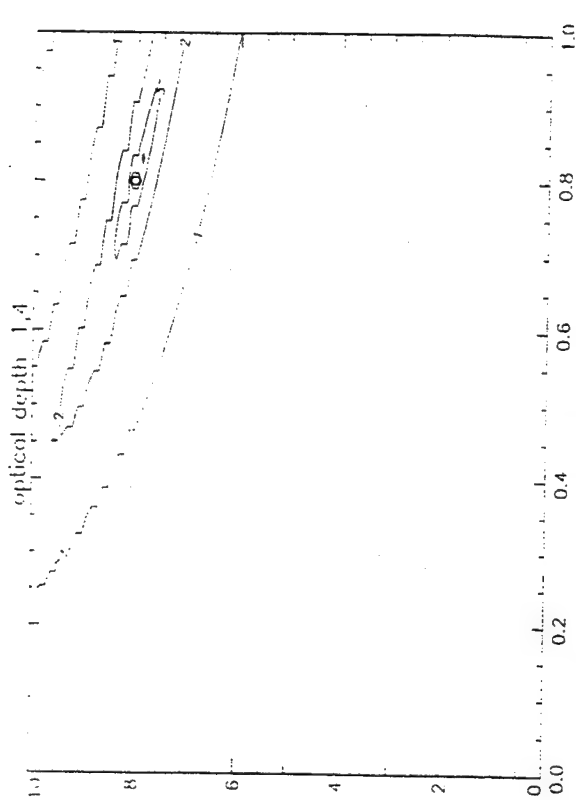
Height and Coverage Detection Optical Depth Effect



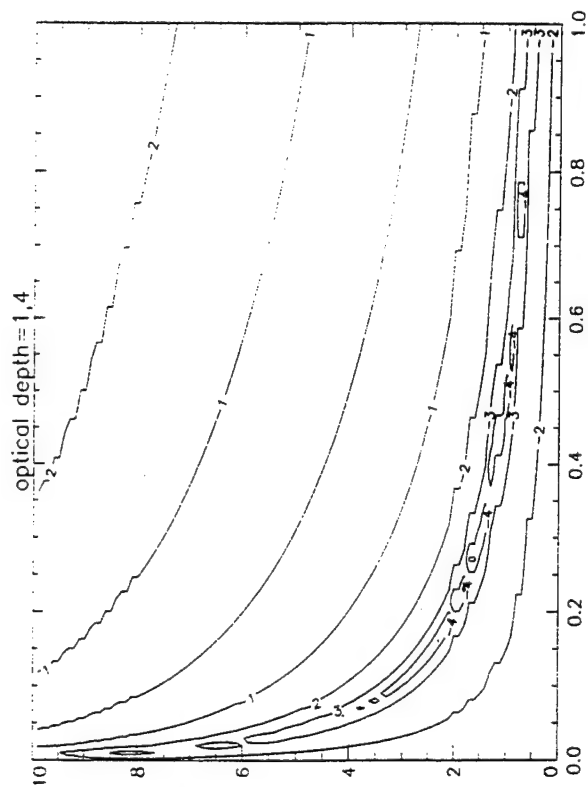
Height and Coverage Detection



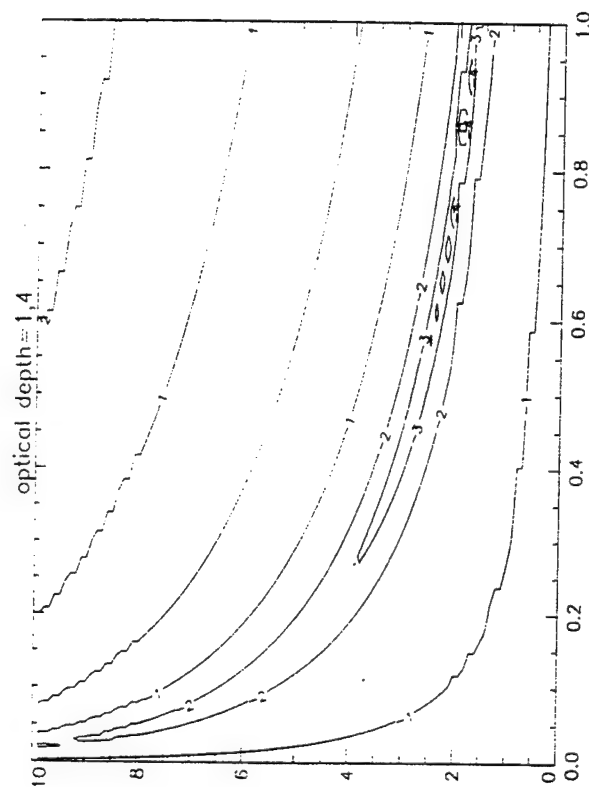
Height Height & Low Coverage



Height Height & High Coverage

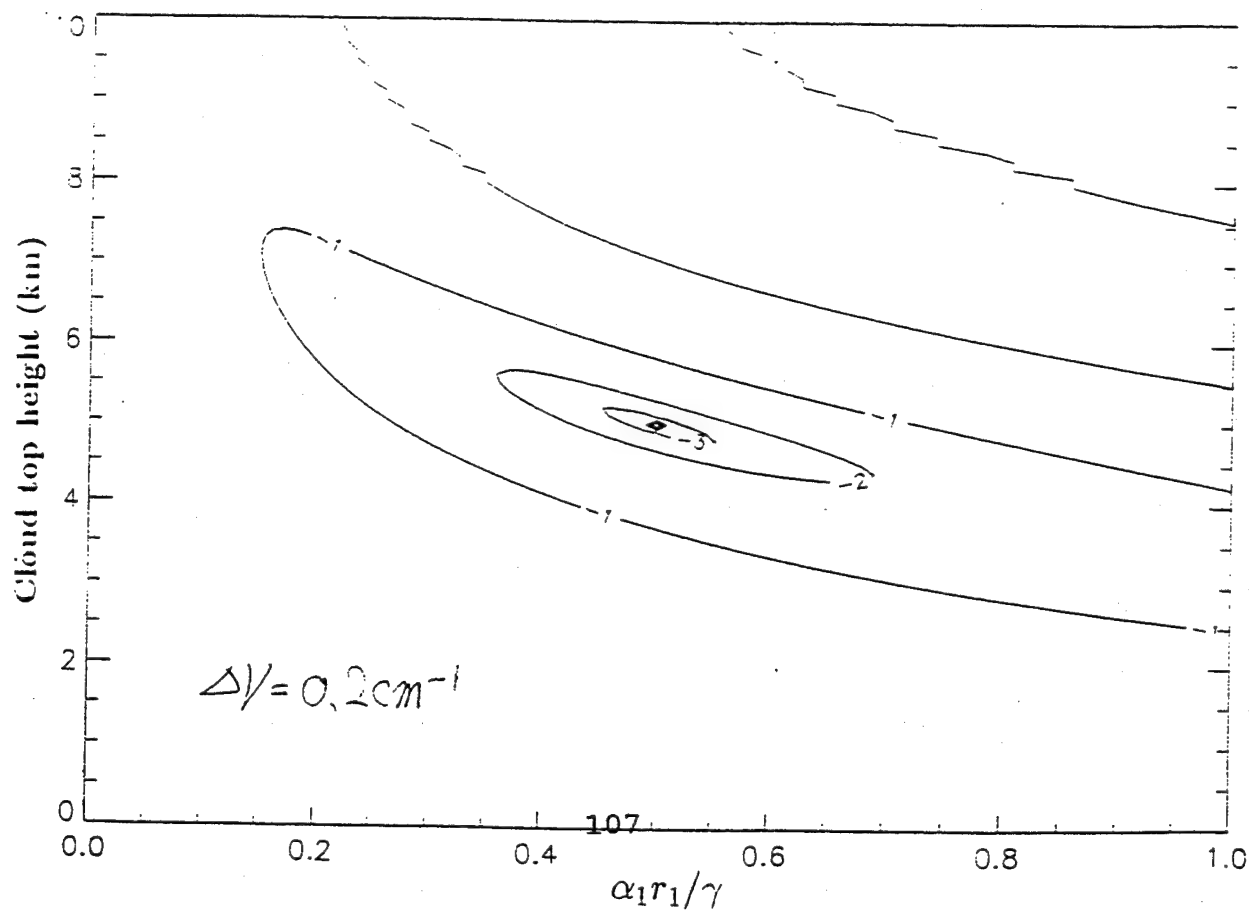
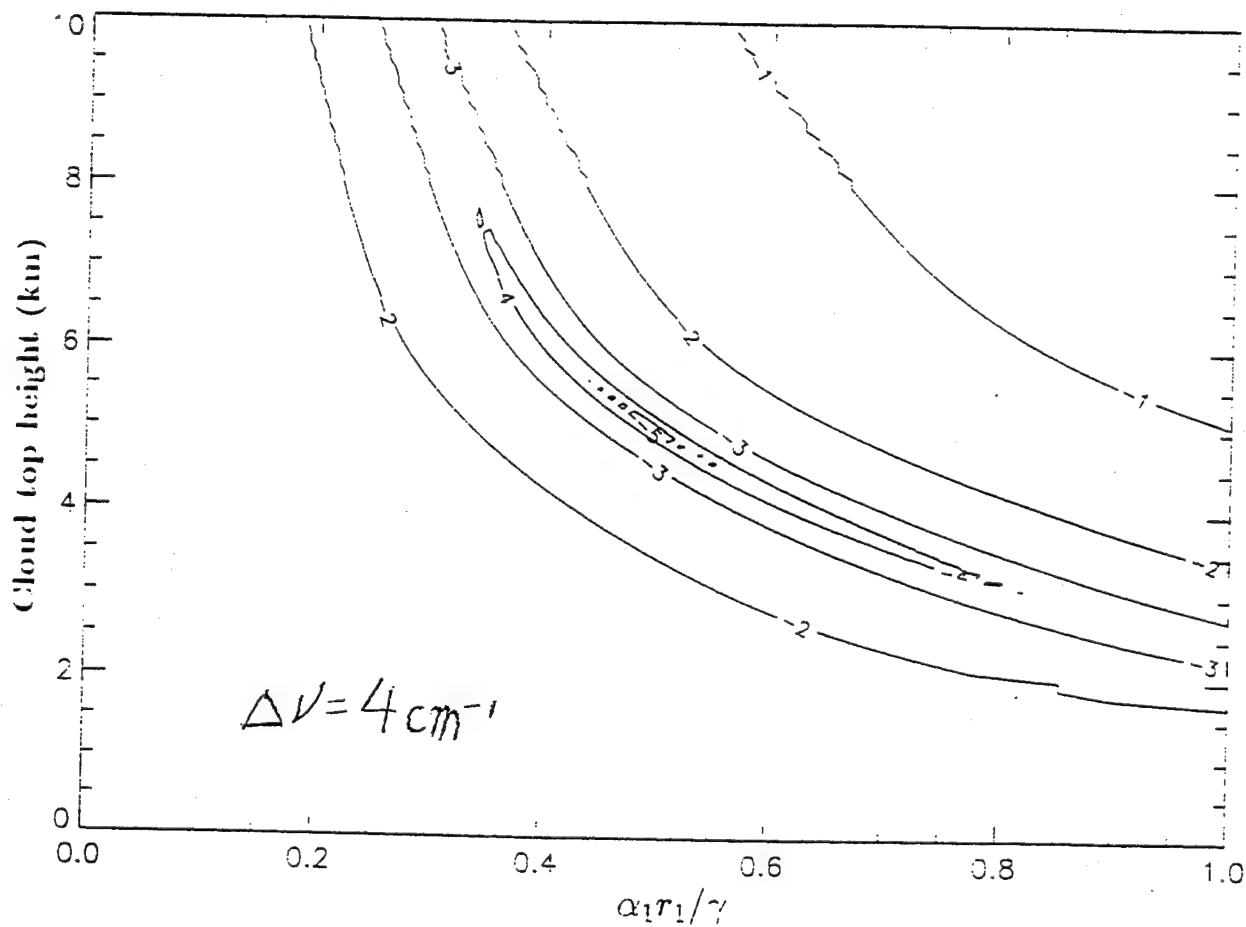


Low Height & Low Coverage

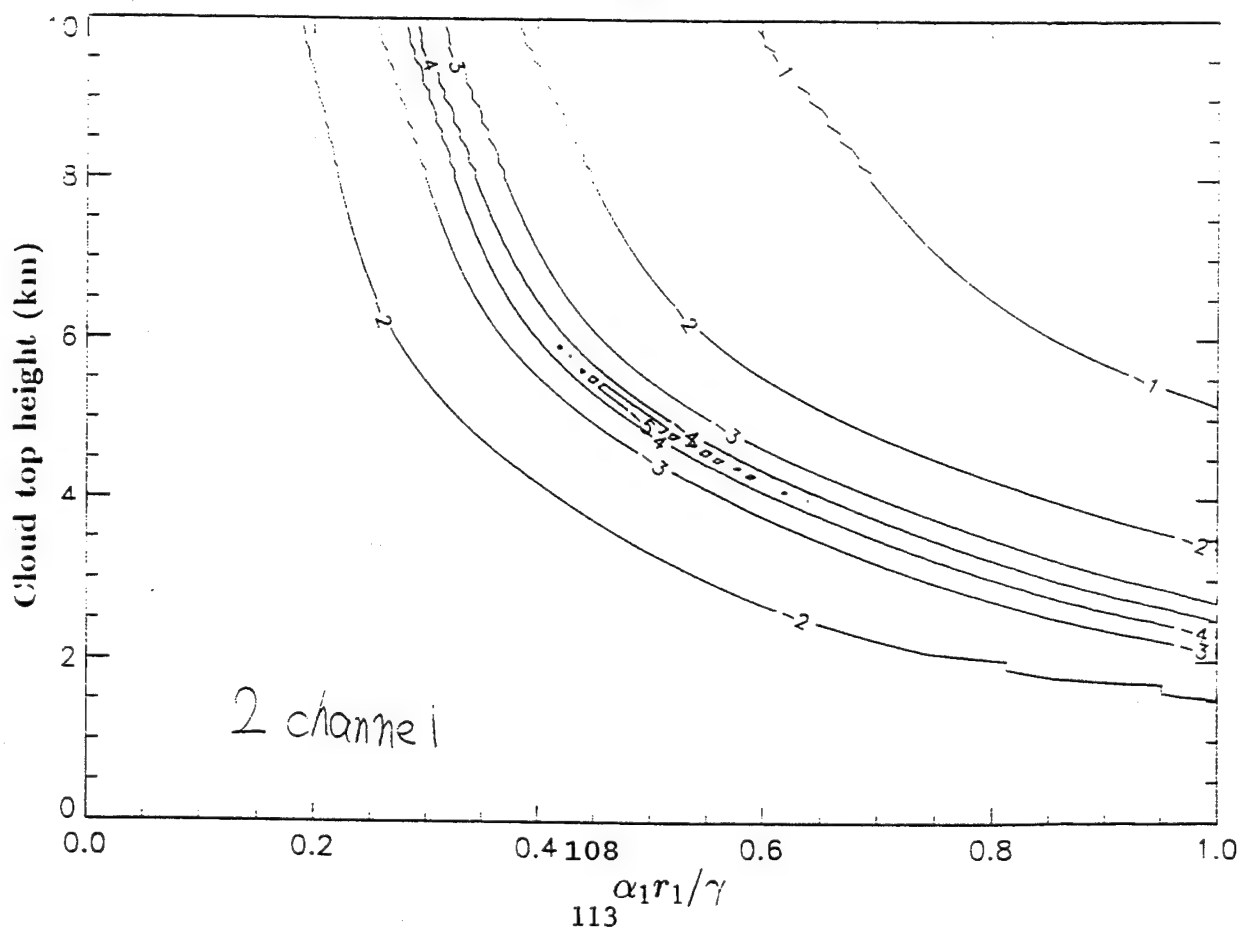
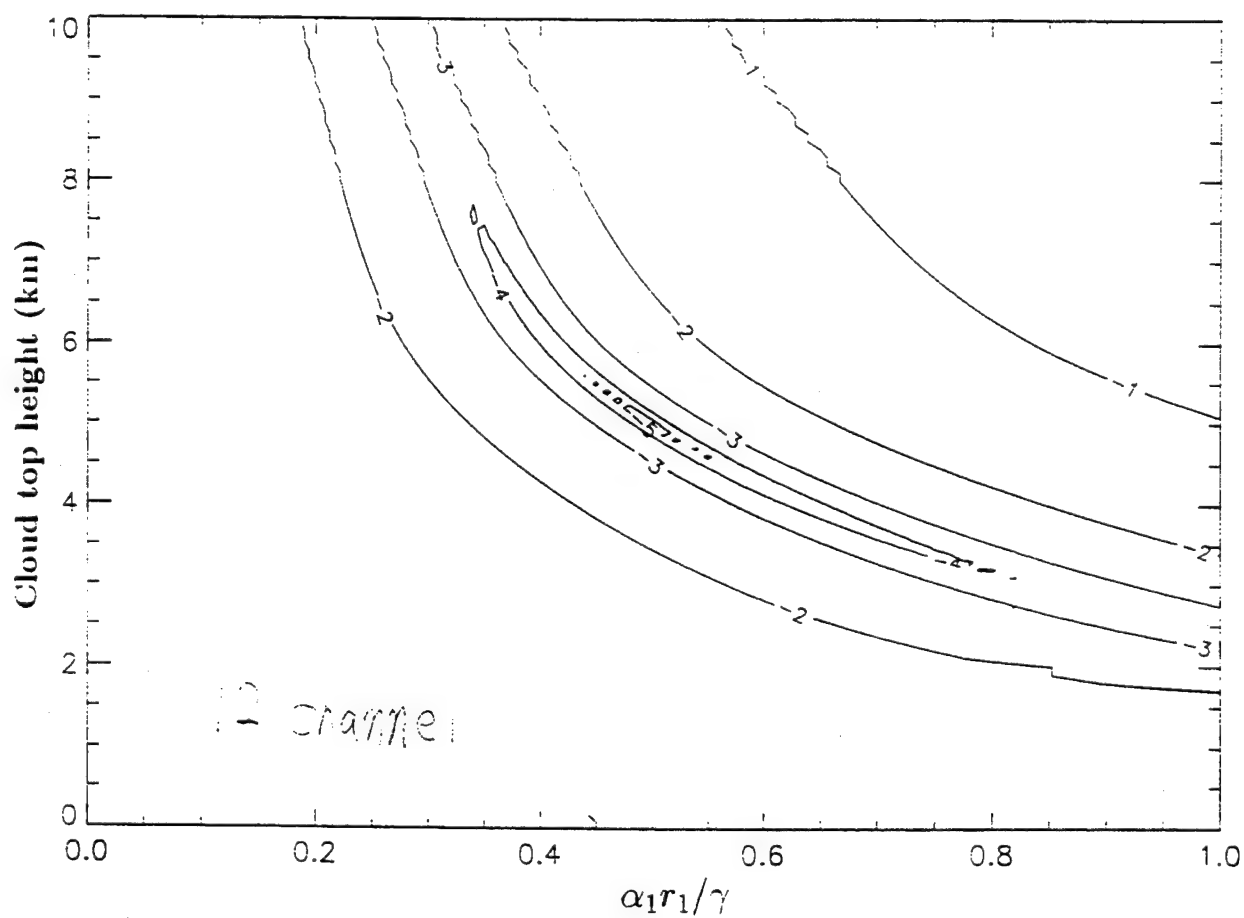


Low Height & High Coverage

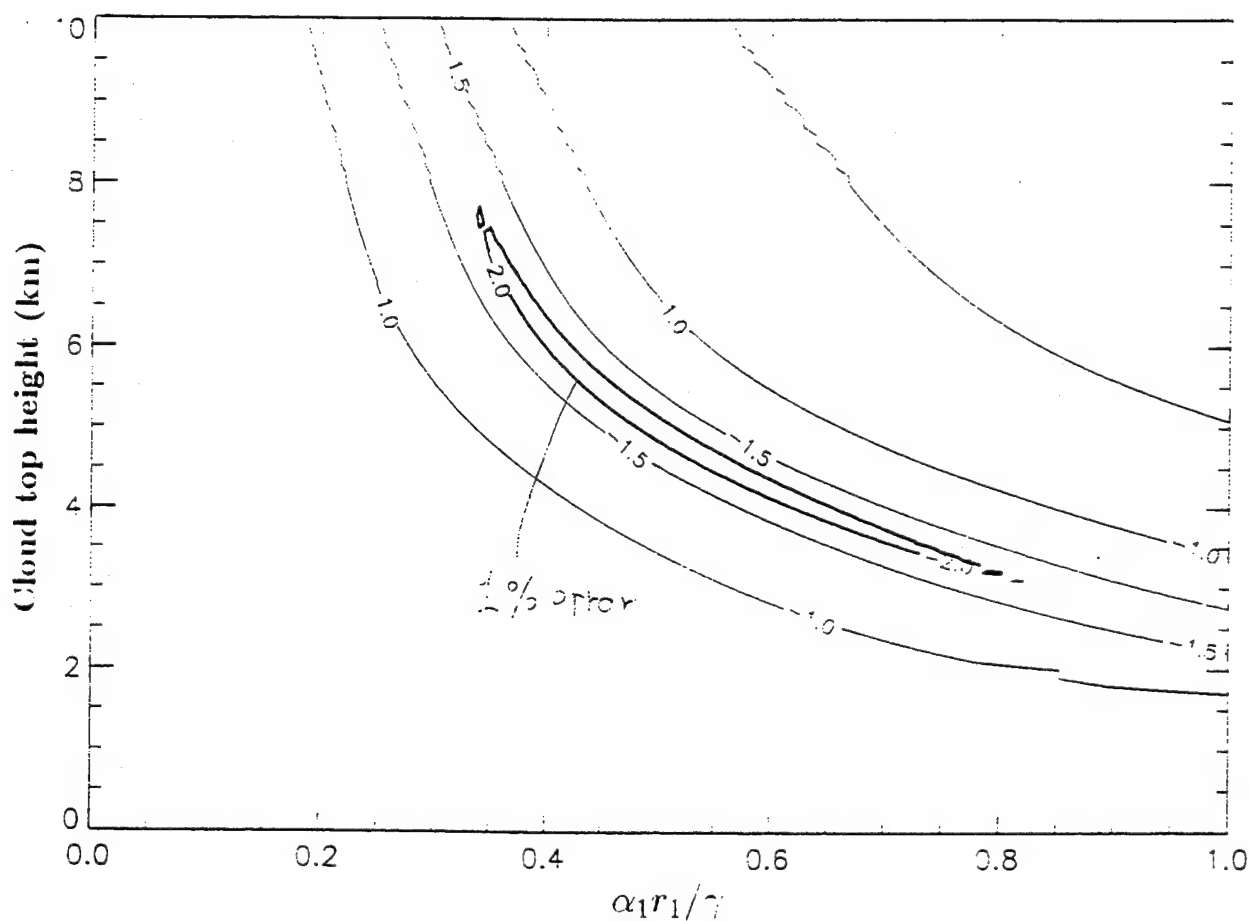
Height and Coverage Detection Spectral Resolution Effect



Channel Number Effect



Accuracy Requirements



Error Analysis

Measurement Error

Model Calculation Error

Scattering

Earth Albedo Data

Spectral Band Database

Intensity and Line Width

Slit Function

Conclusion

Characteristic of this Method

**Both Cloud Top Height and Coverage Detection
with Minimal Computation Time
in Moderate Accuracy**

Further Studies

**Spectral Band Database
Earth Surface Albedo Information**

THE USE OF SPACE BASED REMOTE SENSING FOR ESTIMATION OF THE METHANE MIXING RATIO IN THE MIXING LAYER

P. Ashcroft

Dept. of Engineering & Public Policy
Carnegie Mellon University
Pittsburg, PA 15213

This investigation explores the limits of space based remote sensing for methane characterization, and the extent to which those limits are affected by uncertainty in other atmospheric attributes. Central to this analysis is the fact that the attribute considered, (enhancement of the methane mixing ratio in the mixing layer), is not directly observable, but must be obtained through inversion of the spatially integrated signal received by the instrument.

MODTRAN is used to simulate atmospheric transmission in the neighborhood of the 3.3μ methane absorption band. This signal is then inverted to determine the importance of ancillary information, (e.g., the vertical profile of H_2O and temperature), for methane retrieval. Thus, this research provides quantitative description of the importance of simultaneous observation of methane with other atmospheric conditions, and the relative utility of space based observation relative to other measurement methods.

Remote Sensing Policy

Peter Ashcroft

Department of Engineering and Public Policy

Carnegie Mellon University

Examples of Remote Sensing Policy Questions:

- What phenomena should be observed?
- What spatial, temporal, and spectral resolution is necessary or desirable?
- Simultaneity - What observations must be made simultaneously?
- How should space based observations best be integrated with observations by other mechanisms and from other platforms?

Case Study: Atmospheric Methane Characterization

- Methane is a radiatively active trace gas in the atmosphere.
- Sources are not well characterized.
- Methane is produced at the Earth surface, hence enhancement is expected to be most pronounced in the mixing layer, and less at higher altitudes.
- Long atmospheric lifetime, (8-10 years).
- Local enhancement due to sources is small. 1% change in the total vertical column would be unusual.

Specific Question

- To what extent does uncertainty about the water profile limit the accuracy of methane retrieval?
- Consider an ideal, nadir-viewing instrument.
- Model the atmosphere as three homogeneous layers for both methane and water.

Analytic Approach

- Simulate with MODTRAN the solar flux received by the instrument for various water and methane enhancement scenarios.
- Using simulated results, obtain a linear expression for flux as a function of the water column and methane column.
- Use various filter functions to generate signals.
- Use inversion algorithm to estimate methane profile based on simulated signals.
- This is the "Best Case" for methane retrieval subject to uncertainty in the water column, but assuming that there are no other sources of uncertainty.

Assumptions for this Case Study

- Methane enhancement is most pronounced in the mixing layer.
- Water enhancement is in all three layers
- Temperature profile is known exactly
- No clouds
- Solar irradiance is known exactly
- Earth albedo is known exactly

Linearized Inversion of Total Methane and Water Column

$$S = Mm$$

$$S_0 = \int d\nu I(\nu) \tau^2(\nu) \\ = \int d\nu I(\nu) \tau_0^2(\nu) - 2 \sum_i m_i \int d\nu I(\nu) \tau_0^2(\nu) k_{mi}(\nu)$$

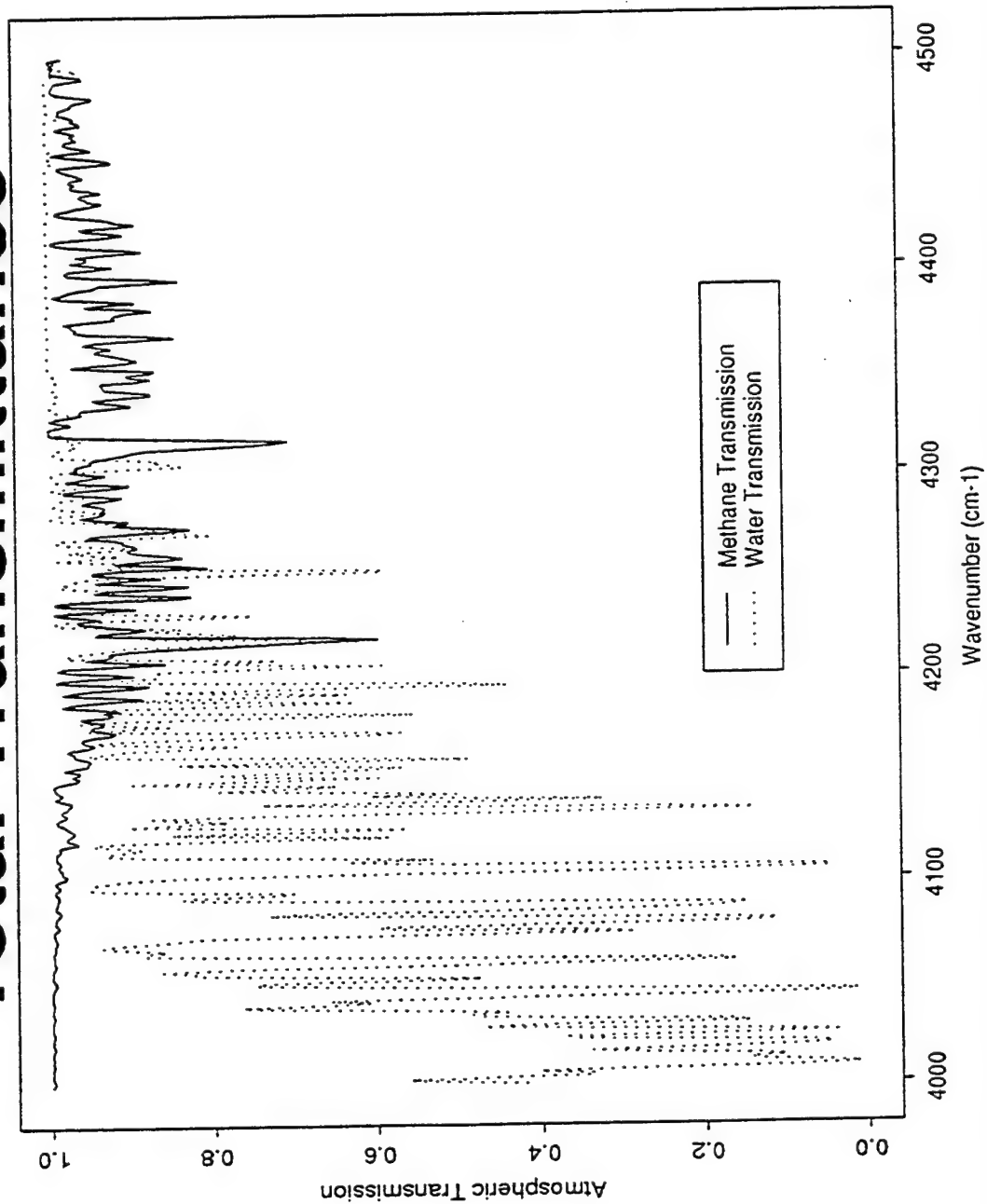
$$\sum_0 - \int_{\Delta\nu} d\nu I(\nu) \tau_0^2(\nu) = -2 \sum_i m_i \int_{\Delta\nu} d\nu I(\nu) \tau_0^2(\nu) k_m(\nu)$$

$$S_1 - \int_{\nu_1}^{\nu_2} I(\nu) F_1(\nu) \tau_o^2(\nu) = -2 \sum_i m_i \int d\nu I(\nu) F_i(\nu) \tau_o^2(\nu) k_m; (\nu)$$

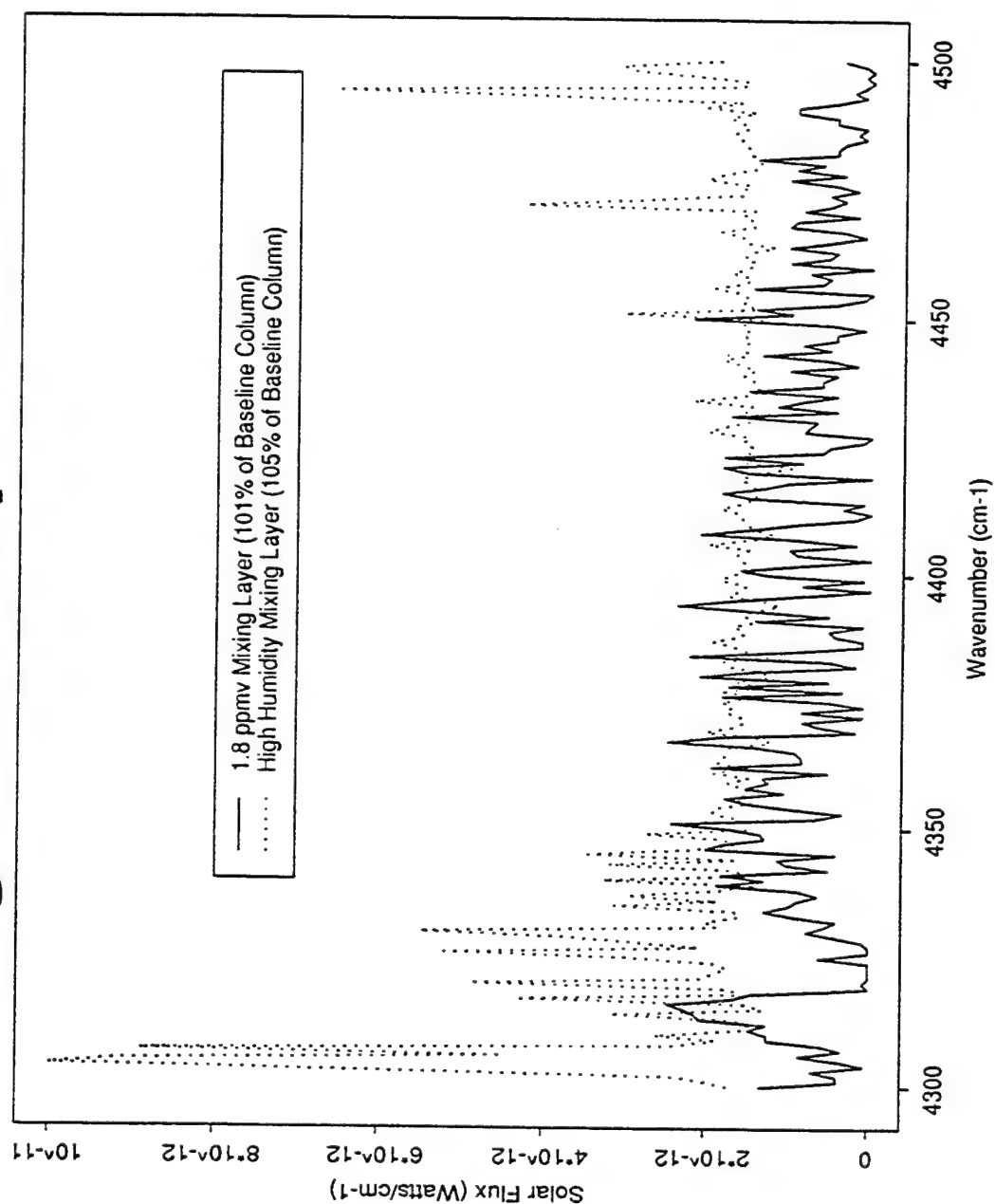
$$S_2 - " F_2^{(V)} = " F_2^{(V)}$$

$$S_3 - \quad " \quad F_3(\nu) = \quad " \quad F_3(\nu)$$

Total Transmittance

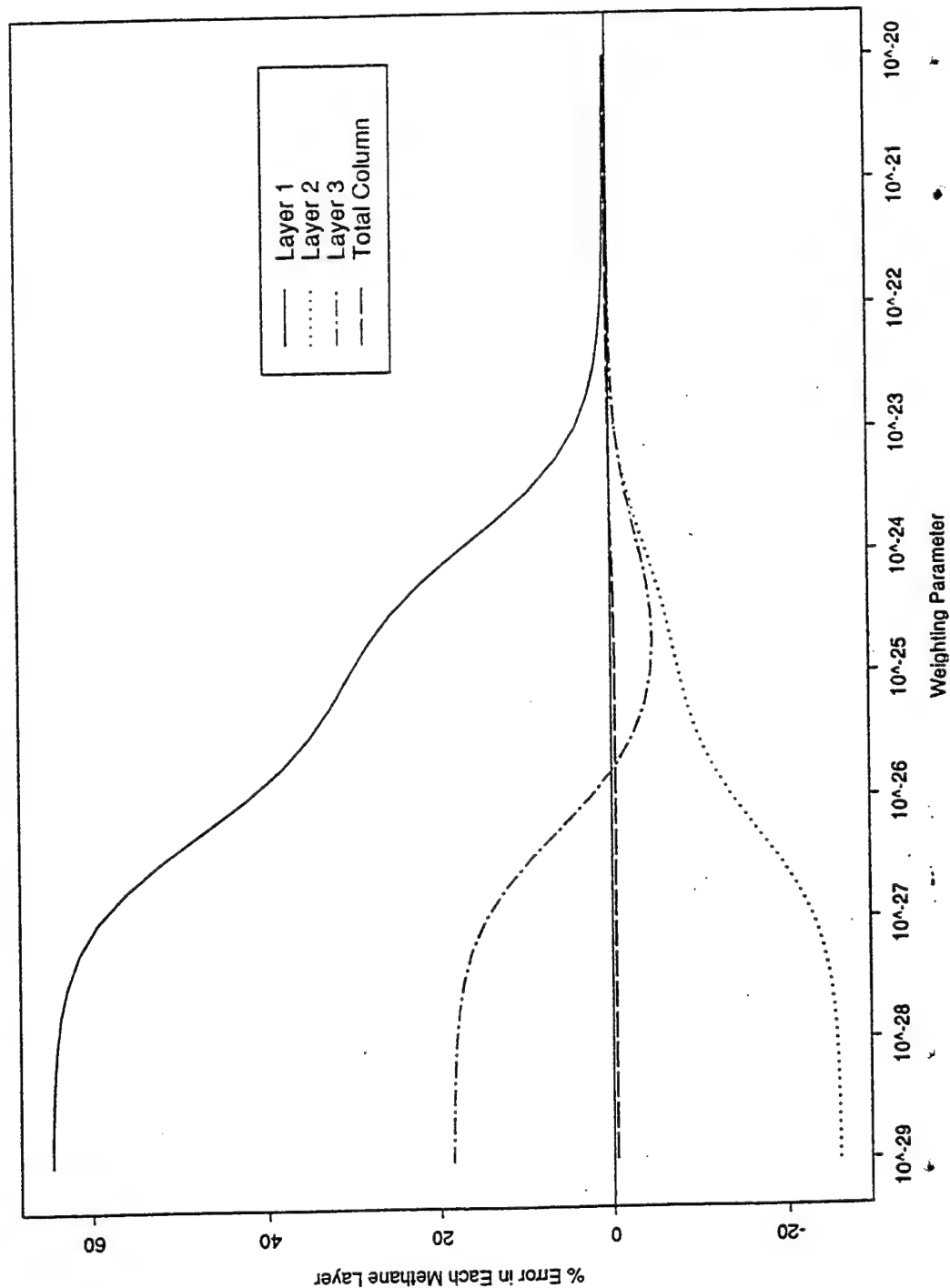


Gross Water and Methane Signal Comparison

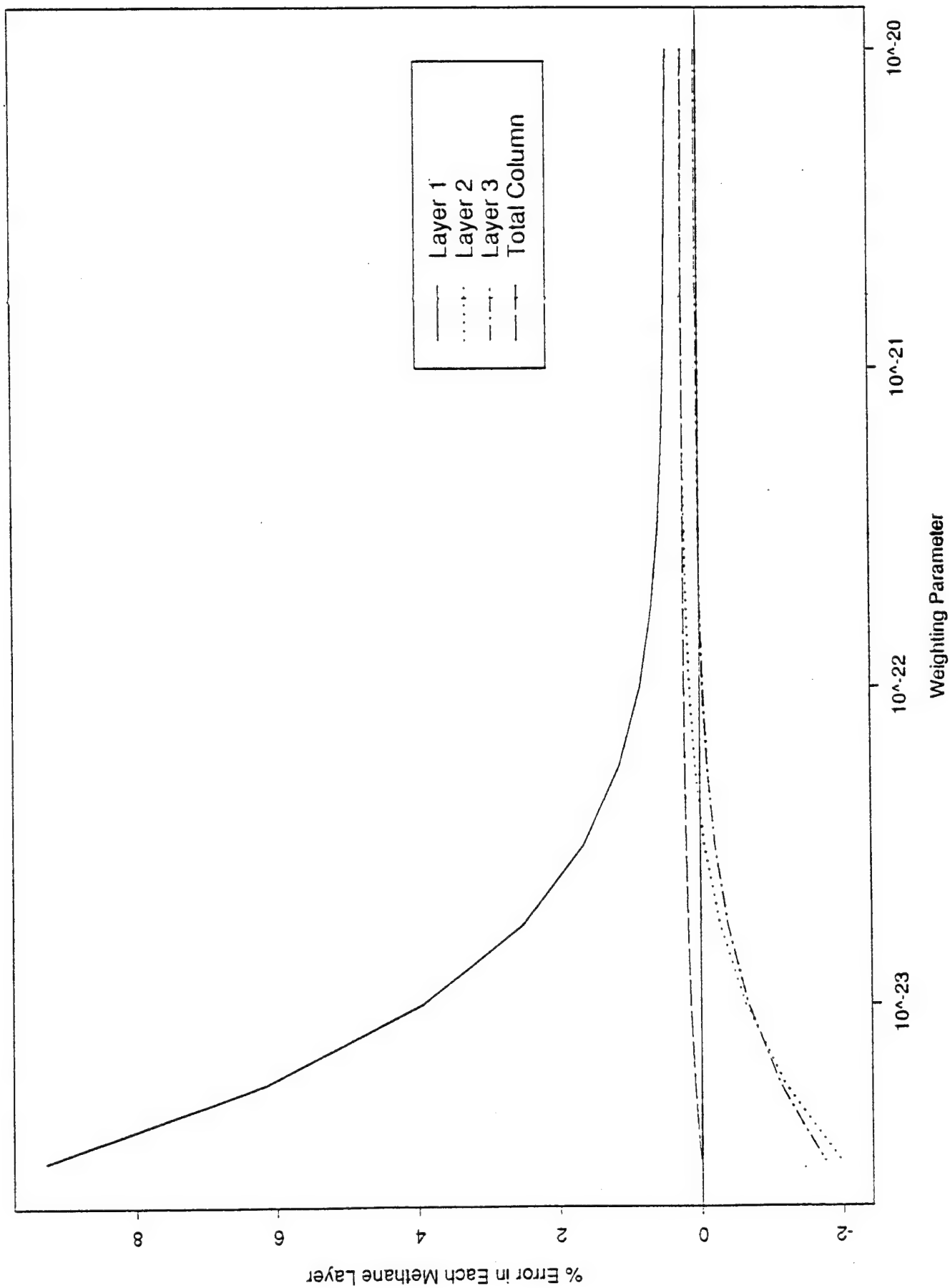


Error in Methane Retrievals Resulting from 1% Water Error

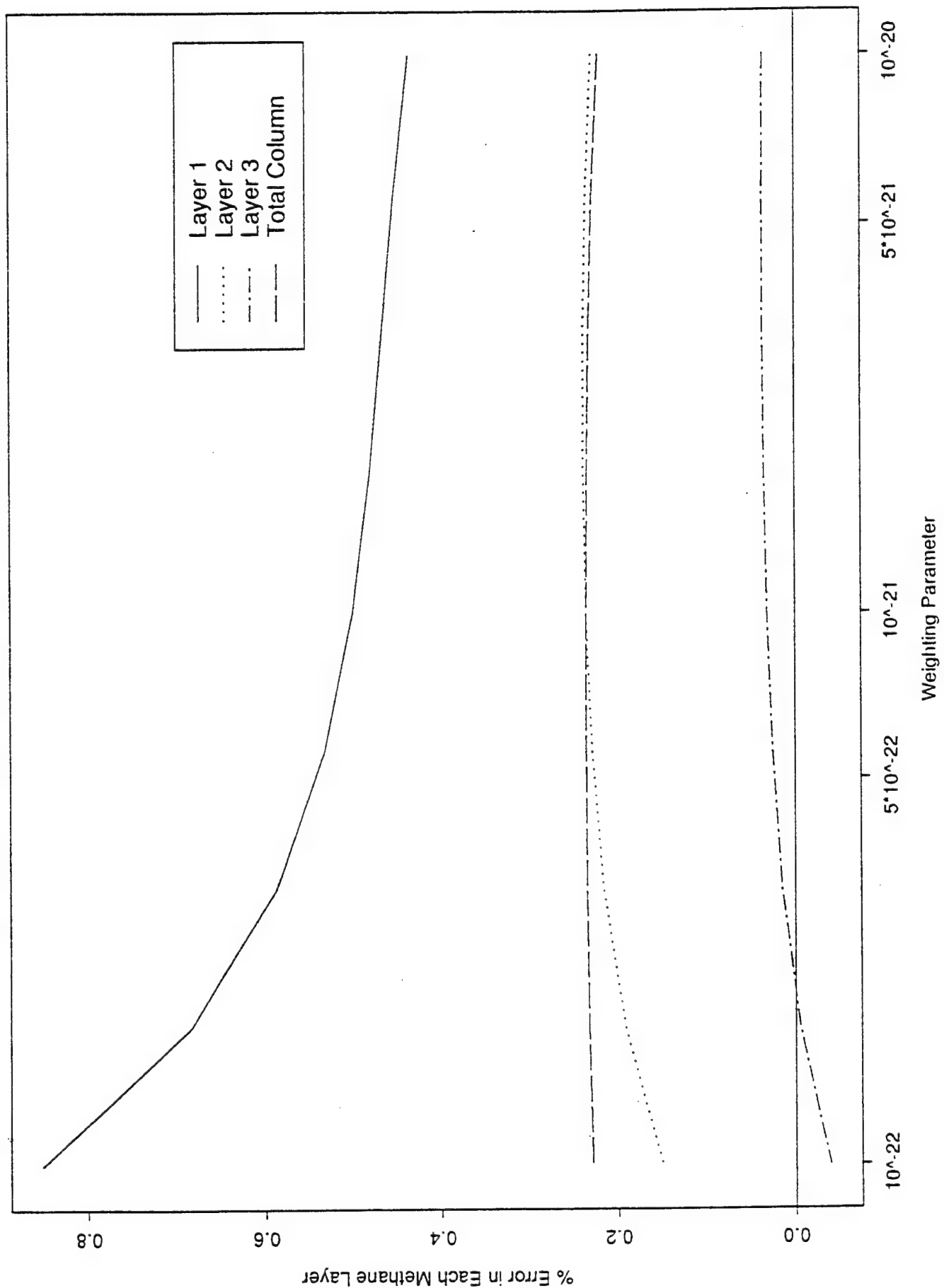
Error in Methane Retrievals as a Result of 1% Error in Water Profile



Error in Methane Retrievals as a Result of 1% Error in Water Profile



Error in Methane Retrievals as a Result of 1% Error in Water Profile



Conclusions

- Any signal due to methane enhancement is extremely small.
- Even in areas of minimal water absorption, the expected gross signal due to variations in water exceeds that of methane unless some spectral filtering is performed.
- Separating the water measuring instruments from the methane measuring instruments may critically threaten the ability to measure methane at all.

Future work

- Confirm water and methane variances.
- Better justify choice of weighting parameter.
- Incorporate temperature uncertainty.
- Include instrument noise limitations (using specifications of actual instrument).
- Calculate water and methane overlap more accurately using HITRAN.

Open Questions

- Is this a reasonable approach to assessing instrument performance?
- I had trouble specifying the methane profile. Why?
- How will HITRAN results compare to these?
- What problems should I anticipate in implementation?

A CORRELATED K-DISTRIBUTION MODEL OF THE ATMOSPHERIC HEATING RATES FOR OVERLAPPING SPECTRA OF CO₂/H₂O AND CH₄/N₂O

**ALLEN S. GROSSMAN
KEITH E. GRANT**

Global Climate Research Division
Lawrence Livermore National Laboratory

The problem of overlapping the spectra of CO₂ and H₂O in the 0-2500 cm⁻¹ wavenumber region has been considered using a correlated k-distribution model for the transmission in the atmosphere between 0 and 60 km. Individual k-distributions for the two gases have been combined using an overlapping algorithm to produce k-distributions for the mixture of CO₂ plus H₂O. A prototype radiative transfer model has been used to calculate atmospheric fluxes and heating rates. The heating rates for the overlapped mixture agree to better than eight percent with those calculated for a single pre-combined mixture of CO₂ and H₂O.

A Correlated K-distribution Model of the Atmospheric Heating Rates for Overlapping Spectra of $\text{CO}_2/\text{H}_2\text{O}$ and $\text{CH}_4/\text{N}_2\text{O}$



**Allen S. Grossman
Keith E. Grant**

**Lawrence Livermore National Laboratory
Global Climate Research Division**

**Presentation at the Annual Revue Conference on
Atmospheric Transmission Models
Hanscom Air Force Base, MA**

June 8-9, 1993



OUTLINE OF PRESENTATION

- 1. Review of Correlated K-Distribution Model**
- 2. Results For Single Molecule Calculations**
- 3. Theory Of Overlapping K-Distributions**
- 4. Results Of Overlapping Calculations**

TRANSMISSION MODEL

- If $f_\nu(\tau_\nu) \sim \text{constant over } \Delta\nu$, a transmission model can be developed

$$F_{\Delta\nu} \approx \bar{f}_{\Delta\nu} \int_{\Delta\nu} e^{-\tau_\nu} d\nu = \bar{f}'_{\Delta\nu} T_{\Delta\nu}$$

$$T_{\Delta\nu} \equiv \int_{\Delta\nu} e^{-\tau_\nu} \frac{d\nu}{\Delta\nu}$$

- For the case of a nonhomogeneous atmospheric path

$$T_{\Delta\nu}(w) = \frac{1}{\Delta\nu} \int_{\Delta\nu} \exp\left[-\sum_j k_{\nu_j} w_j\right] d\nu$$

- Start with a homogeneous atmospheric layer at temperature T , and pressure, P .
- Instead of dealing with the structured k , vs ν function in the transmission expression, a different strategy will be adopted.
- Define the opacity distribution function over the band $\Delta\nu$,

$$f(k)dk = \text{fraction of the frequency domain occupied by absorption coefficients between } k \text{ and } k + dk.$$

- It can be shown that the transmission $T_{\Delta\nu}$ is

$$T_{\Delta\nu} = \int_0^{\infty} f(k) e^{-k_{\nu} \nu} dk$$

- Define the cumulative probability

$$g(k) = \int_0^k f(k) dk,$$

and it can also be shown that

$$T_{\Delta\nu} = \int_0^1 e^{-k_{\nu} \nu} dg$$



- The transmission expression

$$T_{\Delta\nu} = \int_0^1 \exp\left[-\sum_j k_{g,j} w_j\right] dg$$

can be approximated as

$$T_{\Delta\nu} \approx \sum_{i=1}^N a_i \exp\left[-\sum_j k_{g,i,j} w_j\right] \Delta g_i$$

where the a_i 's are the integration weights.

- The prototype calculations for CH₄ and N₂O had 201 opacity bins and thus a maximum of 201 k(g)-g values. The 201 g values are equally spaced between 0 and 1. A 43 point variable spaced trapezoidal integration routine was chosen for the calculations presented here.
- The number of points required depends on the altitude range. For example, only ten points were needed to reproduce fluxes and heating rates accurately at altitudes below ~ 20km.

- Can the k-distribution method be extended to a nonhomogeneous atmospheric path. Is

$$T_{\Delta\nu}(w') = \frac{1}{\Delta\nu} \int_{\Delta\nu} \exp\left[-\sum_j k_{\nu_j} w_j\right] d\nu$$

equivalent to

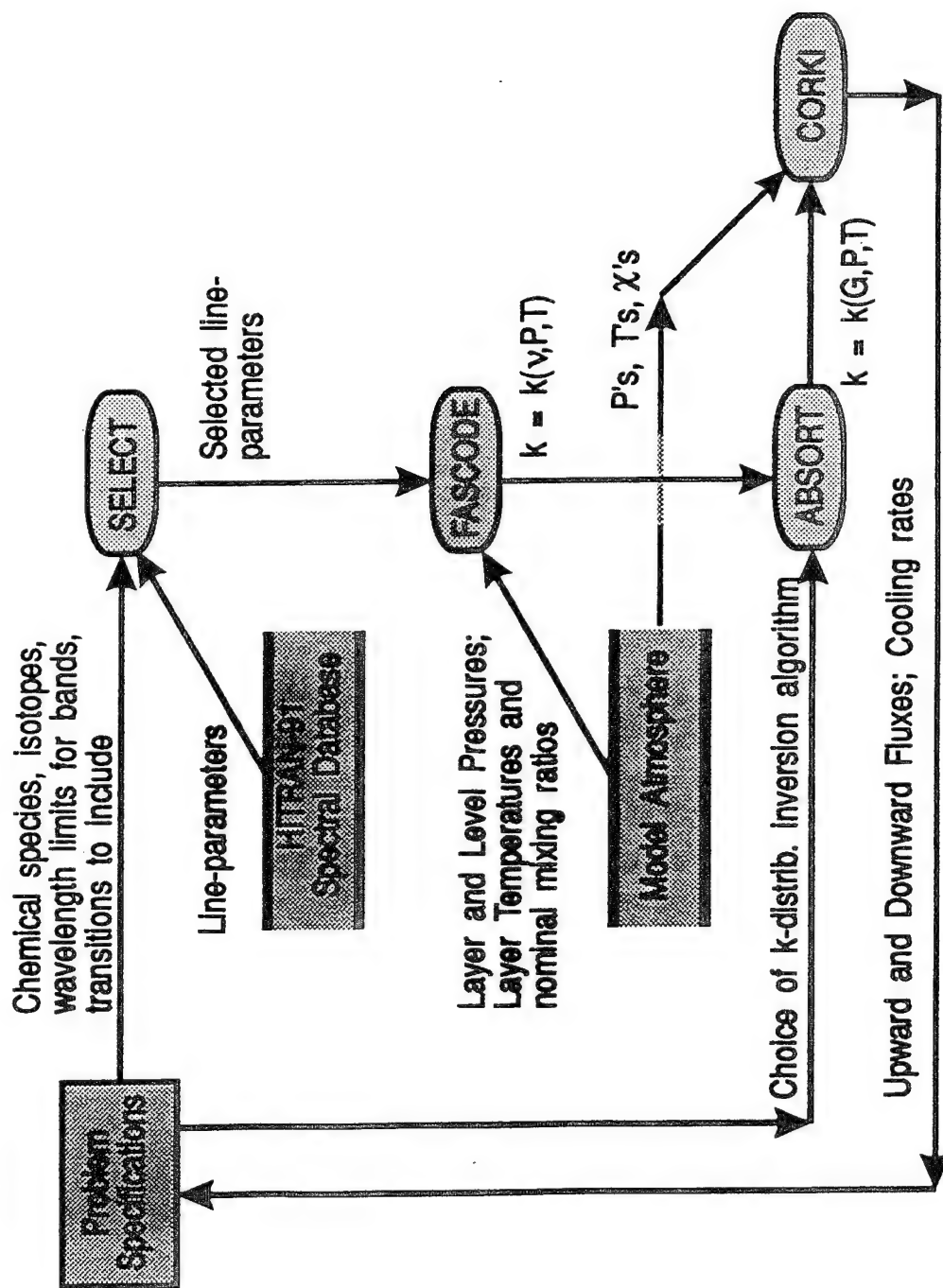
$$T_{\Delta\nu}(w') = \int_0^1 \exp\left[-\sum_j k_{g_j} w_j\right] dg$$

- Essentially this involves a mapping of the k_ν vs ν relation into a k_g vs g relation and the mapping must be unique for all the layers for the two expressions to be equivalent.
- For the case $k_{\nu_j} = k_{\nu_0} f_{\lambda_j}(T_{\lambda_j}, P_{\lambda_j})$, the expressions are equivalent (strong pressure broadened lines).
- If the exponential terms are expanded and the integrals are compared term by term, a more detailed equivalence test can be made. In the "weak line limit", where only the linear terms are kept, the two expressions are equivalent
HIGHER ORDER TERMS $\left[\sum_j k_{\nu_j} w_j\right]^m$ CONTAIN $(k_{\nu_j} w_j)^m$ TERMS WHICH ARE EQUIVALENT



- For the k-distribution method to be valid :
 1. A particular value of g must select the same ν 's layer to layer, i.e., the opacity-frequency relations are exactly correlated.
 2. The frequency ordering of the opacity groups must be preserved layer to layer.
- Since major contributions to the flux in a frequency band come from relatively small regions of the atmosphere, the correlated-k method should be very accurate.
- The method cannot be rigorously shown to be valid for all conditions and its use under all circumstances must be accompanied by appropriate numerical tests.
- The monotonic nature of the k-distributions can provide sufficient computational economy in transmission calculations to warrant such tests.

Structure of the C-K Model Generation Process

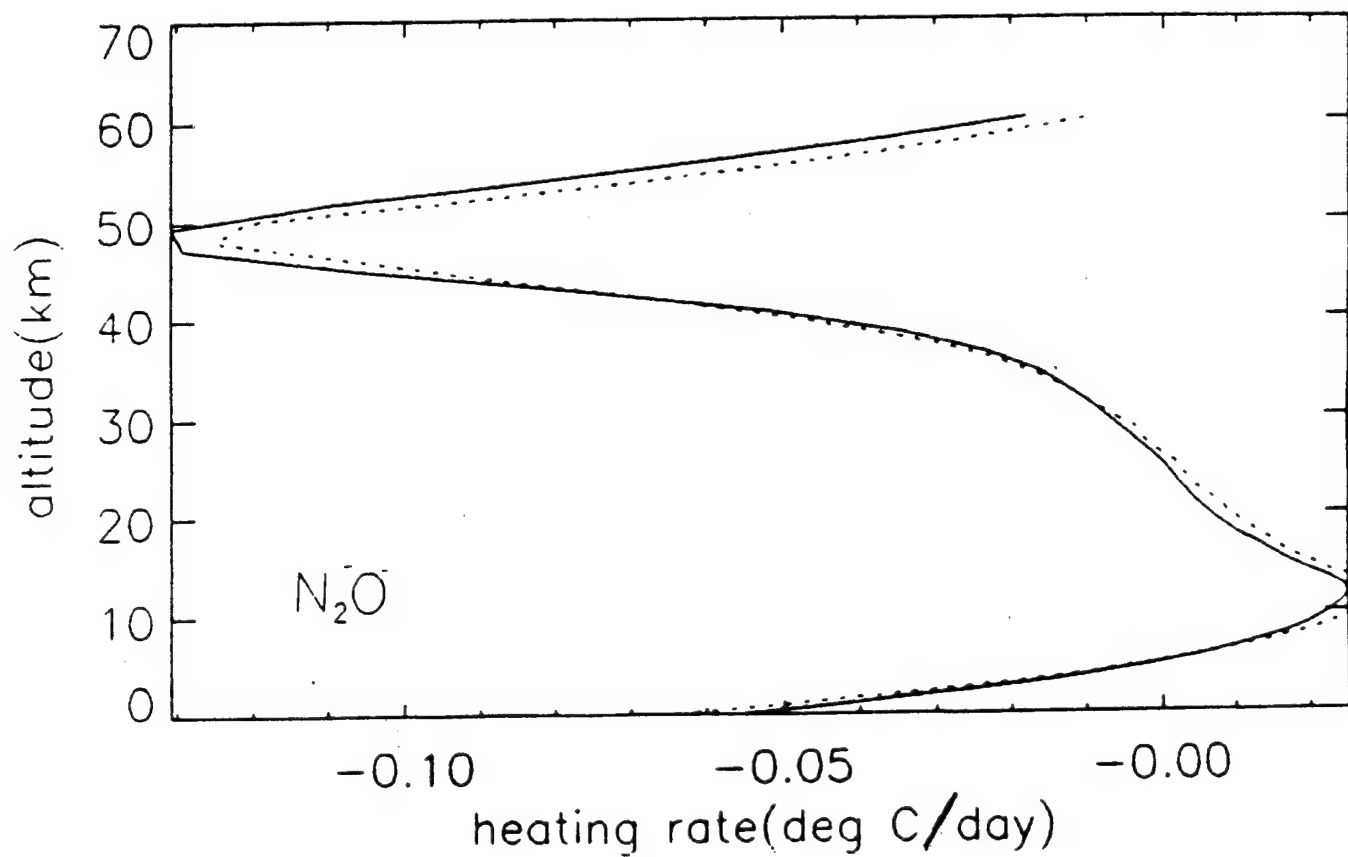
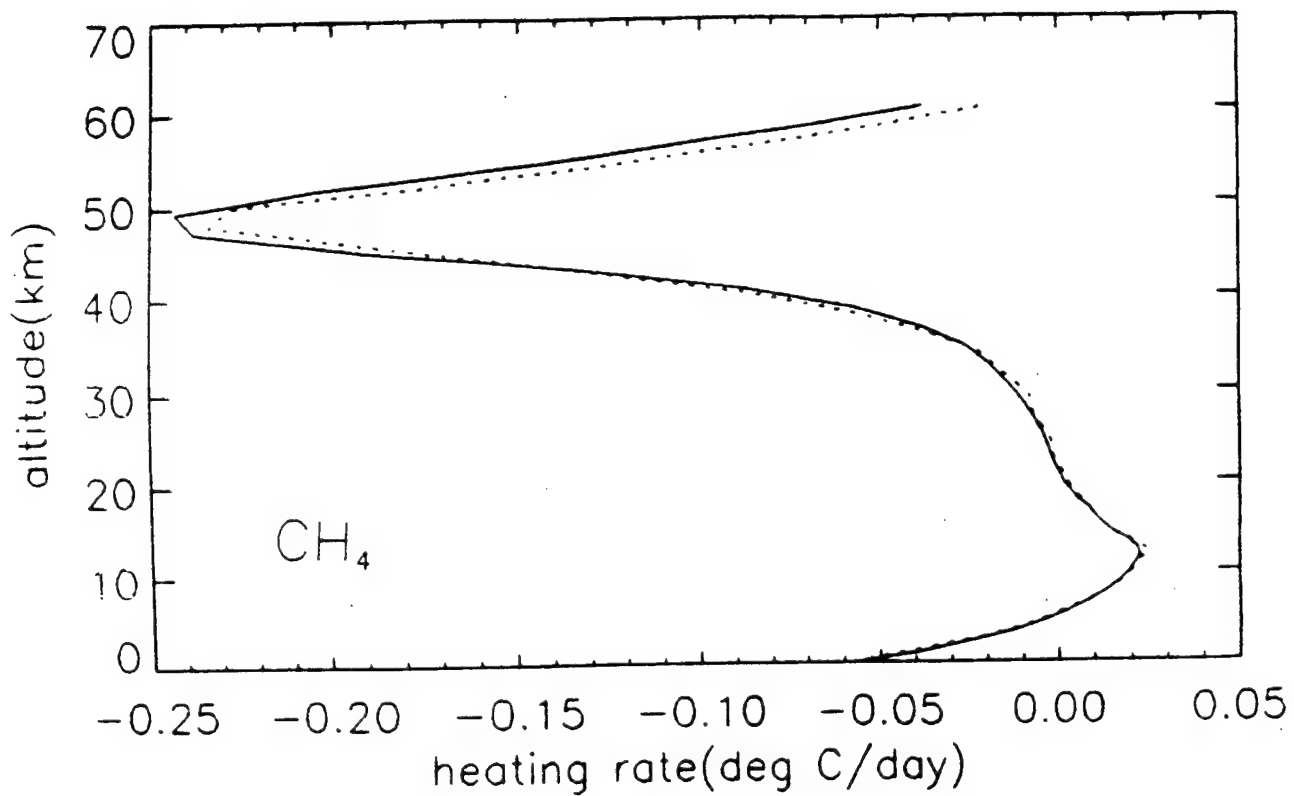




MODEL ATMOSPHERE

- The model atmosphere used is the McClatchey mid-latitude, summer model.
- The altitude resolution is;

1km	0-20km altitude
2km	20-40km altitude
- The ground temperature is 294K
- The CH₄ mixing ratio is 1.75 ppm - constant with altitude
- The N₂O mixing ratio is 0.31 ppm - constant with altitude

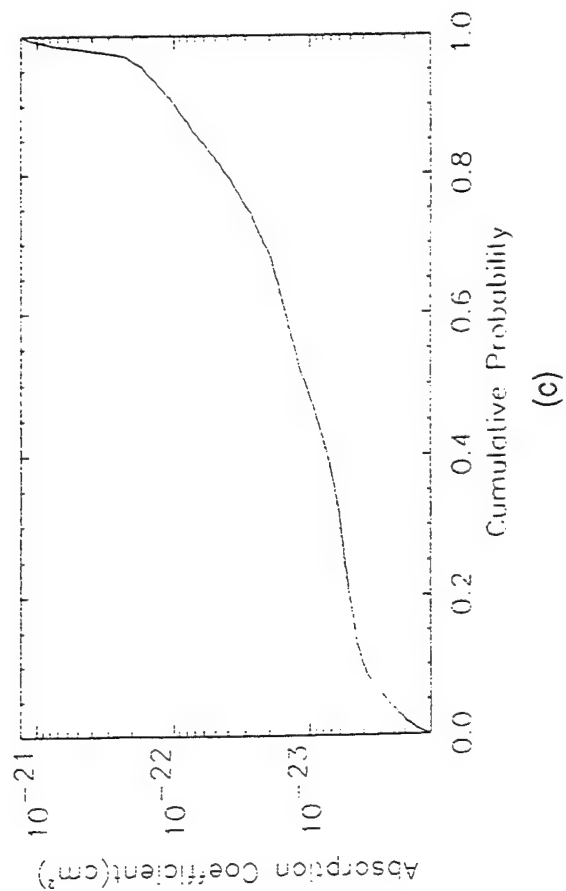
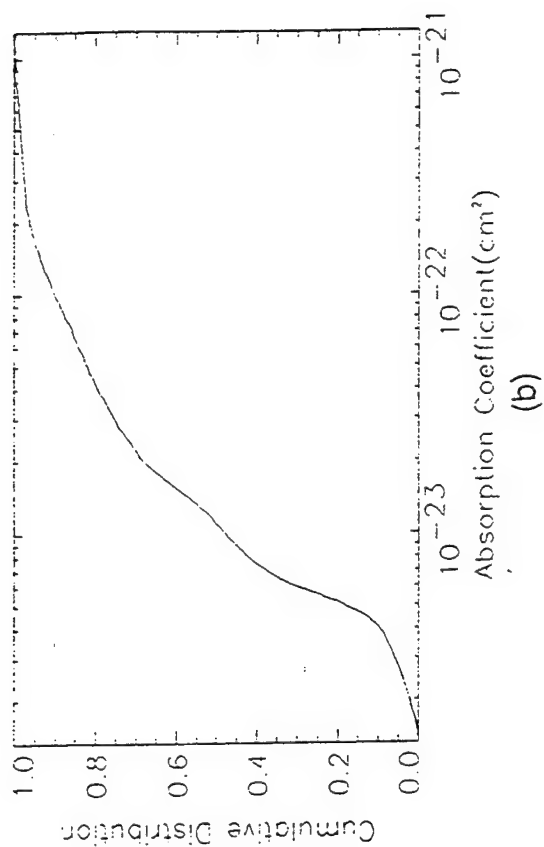
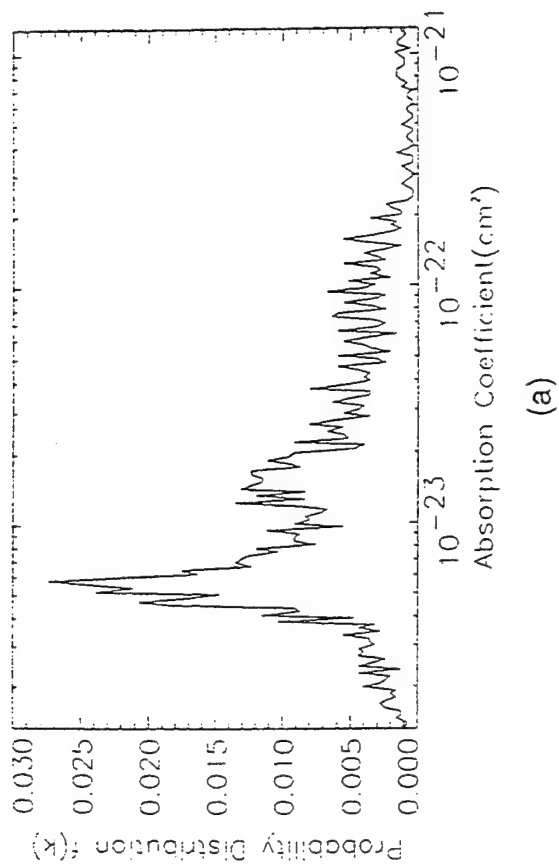


H₂O and CO₂ model parameters



- Abundances
 - CO₂
 - 300 ppm, constant with altitude
 - H₂O
 - As specified in MLS model, variable with altitude
- Wave number intervals
 - CO₂
 - 550–850 cm⁻¹, 40 cm⁻¹ intervals, 15 micron band
 - 840–1200 cm⁻¹, 40 cm⁻¹ intervals, 10 micron band
 - 2000–2520 cm⁻¹, 40 cm⁻¹ intervals, 4.3 micron band
 - H₂O
 - 0–2500 cm⁻¹, 25 cm⁻¹ intervals

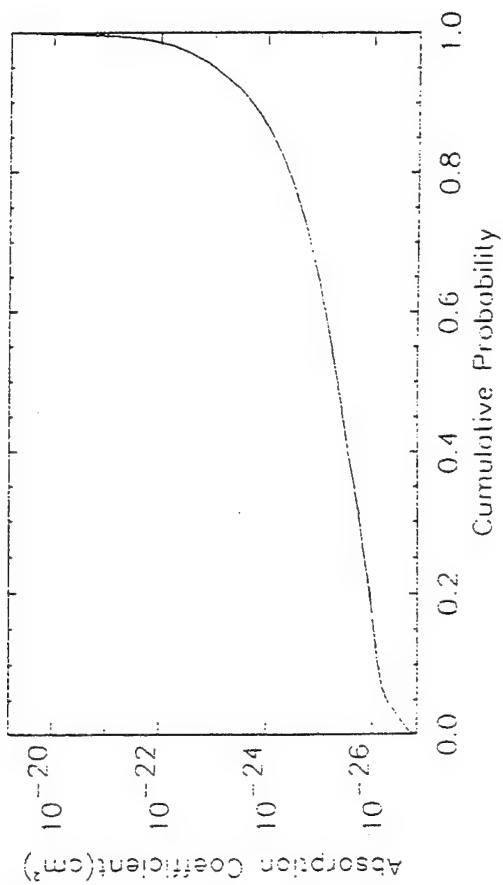
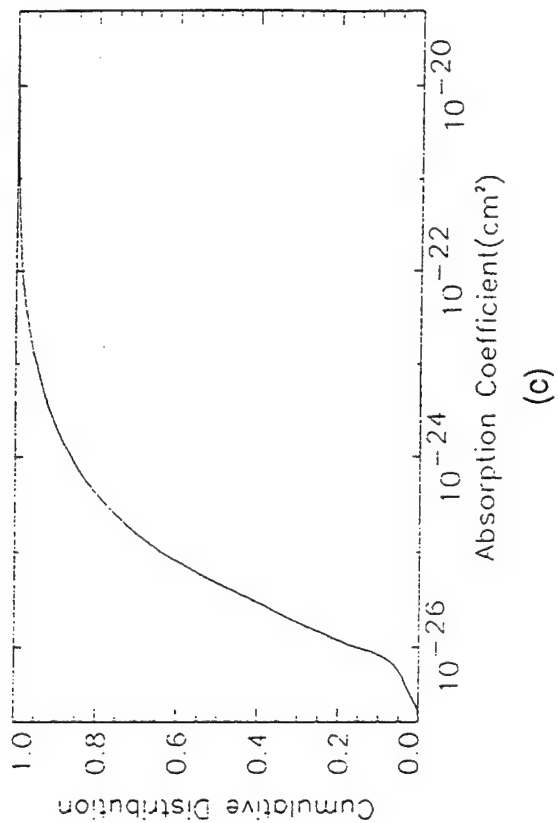
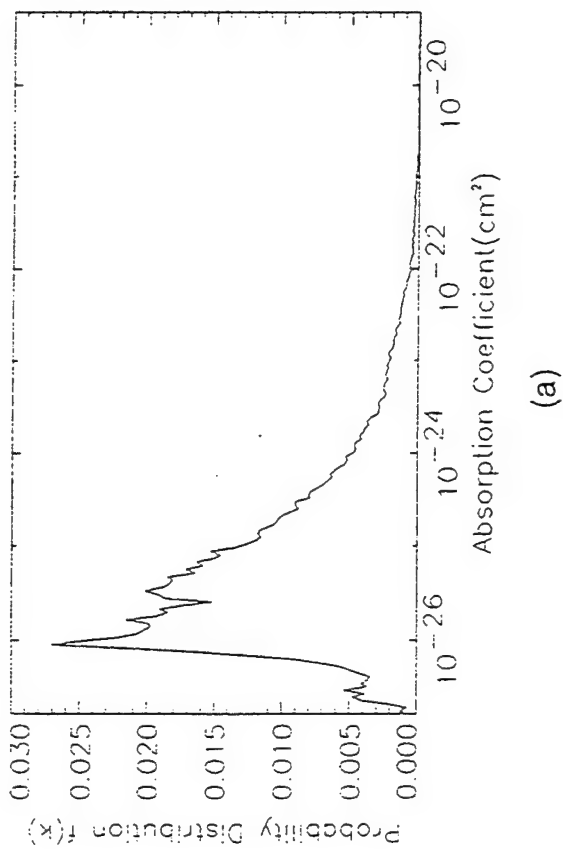
CO₂



Pressure	945.2
Temperature	291.66
Band Low	650.00
Band High	700.00

Figure 1

CO₂



Pressure	1.480
Temperature	272.23
Band Low	650.00
Band High	700.00

Figure 2

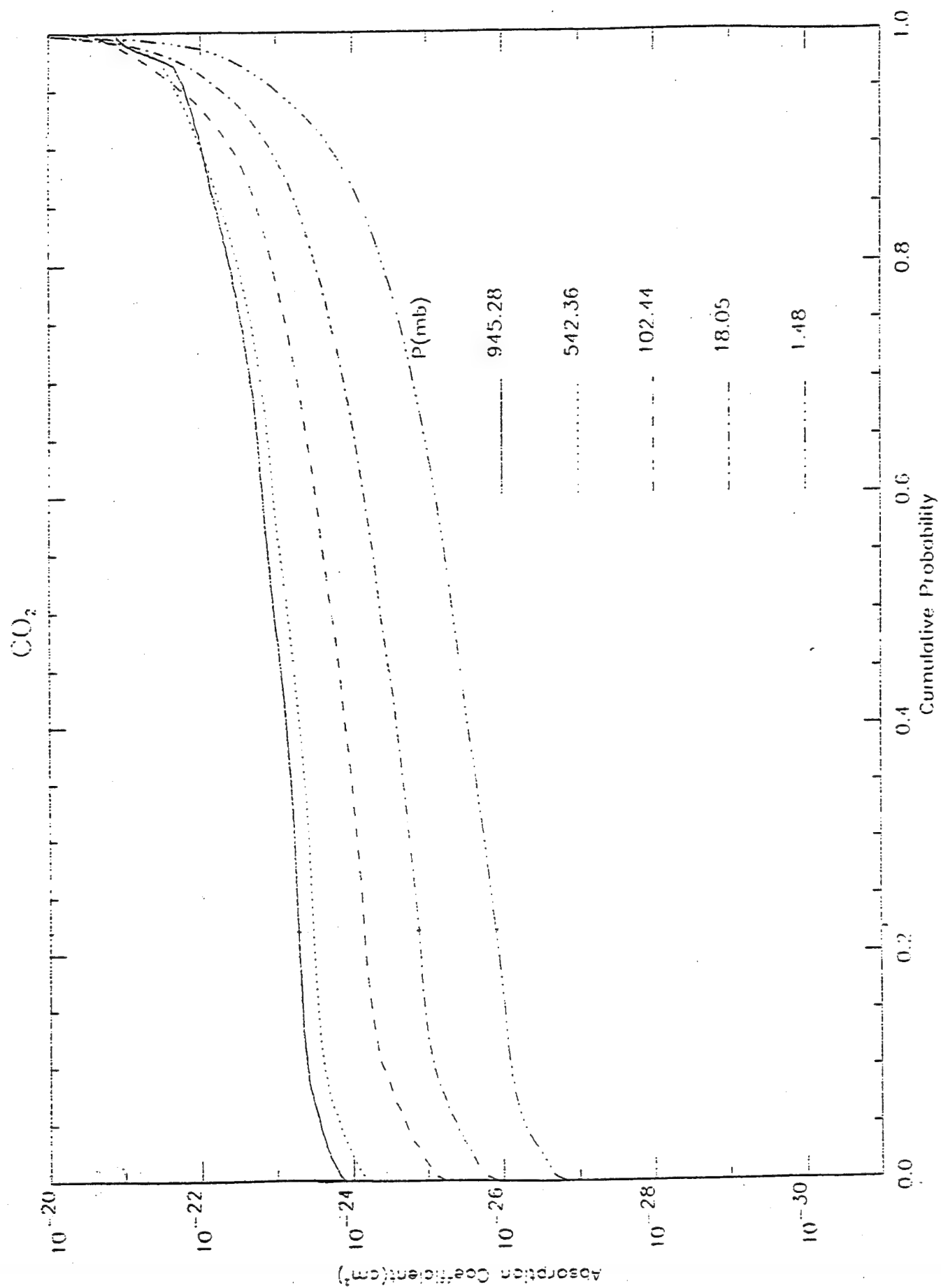


Figure 3

CO₂ 50 points 15 micron

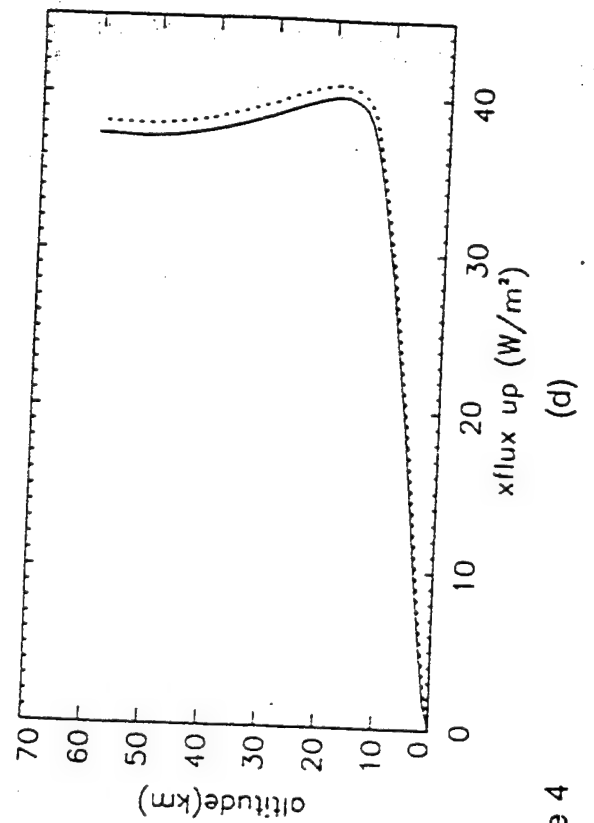
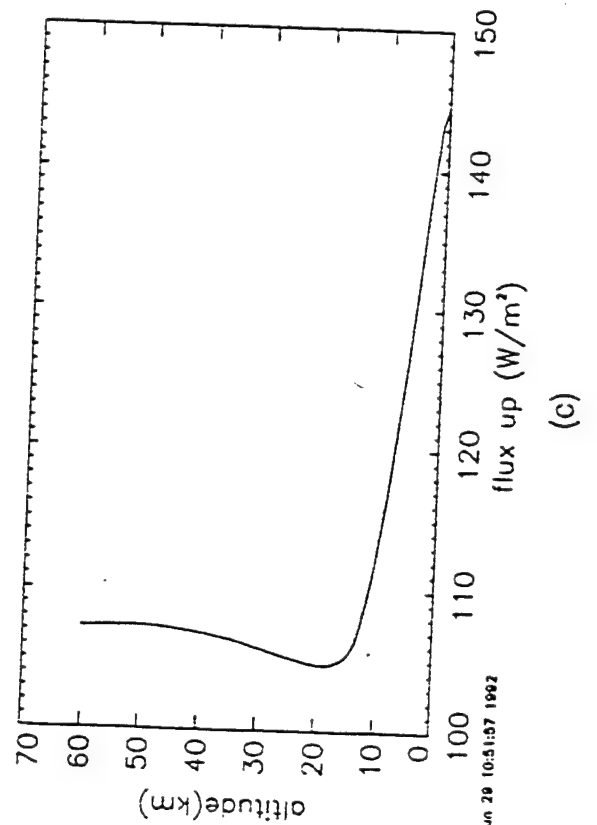
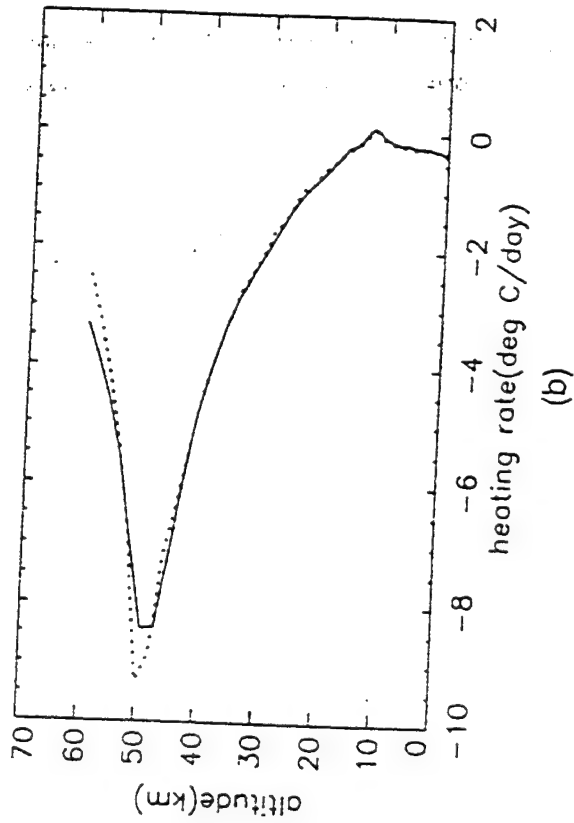
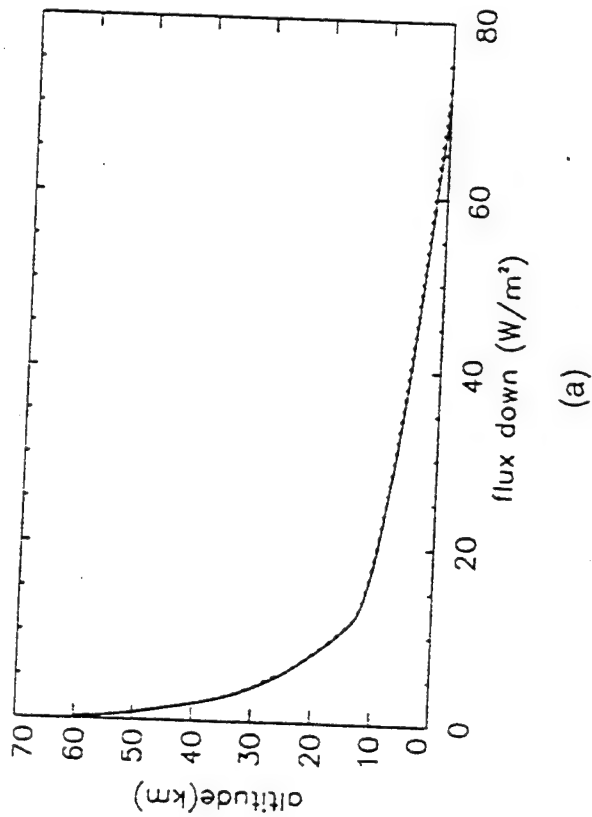
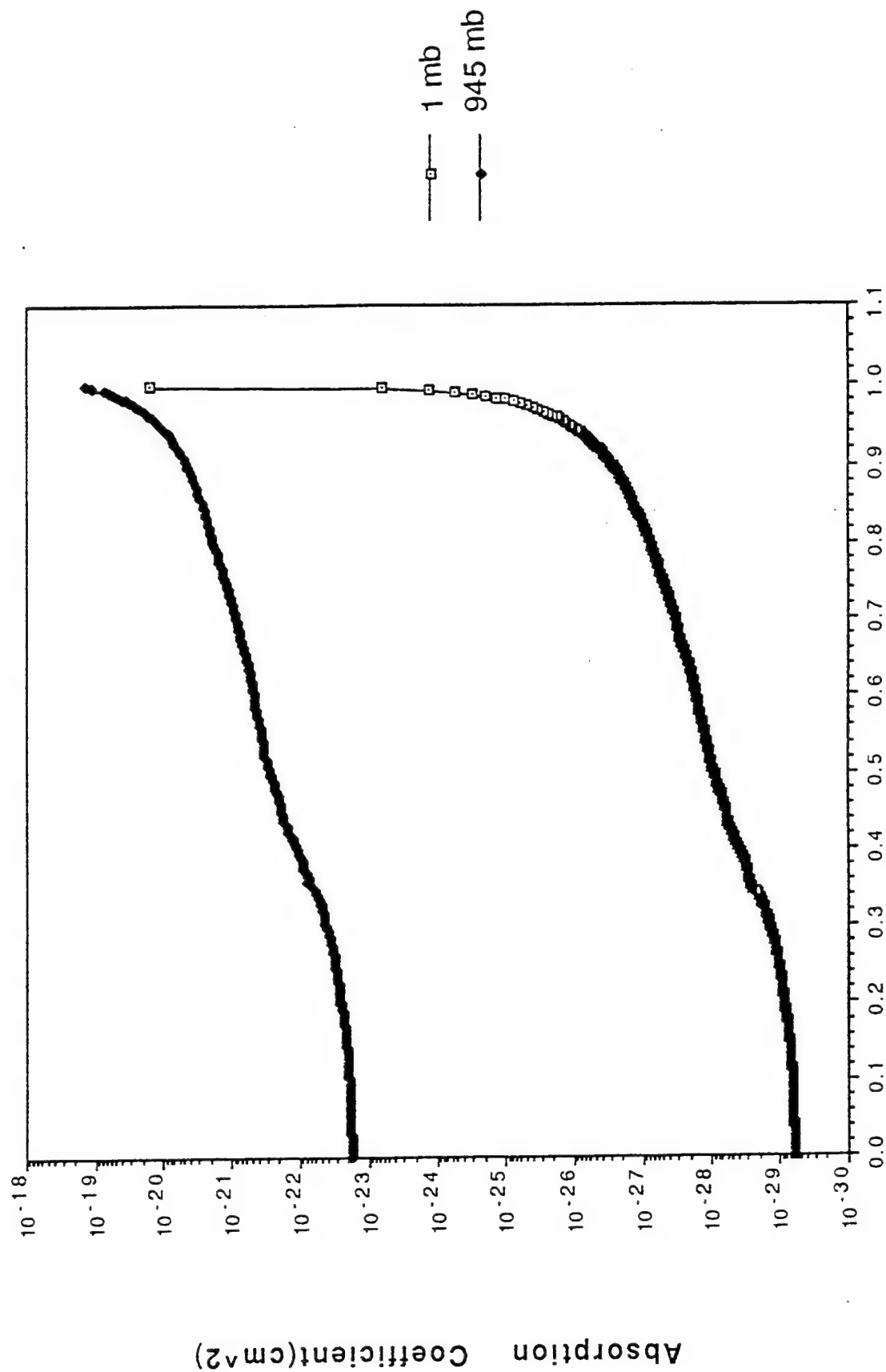


Figure 4

K(g) vs g H2O BIN9 225-250cm⁻¹



Cumulative Probability

Figure 1

HEATING RATE H2O BIN9 225-250cm⁻¹-1

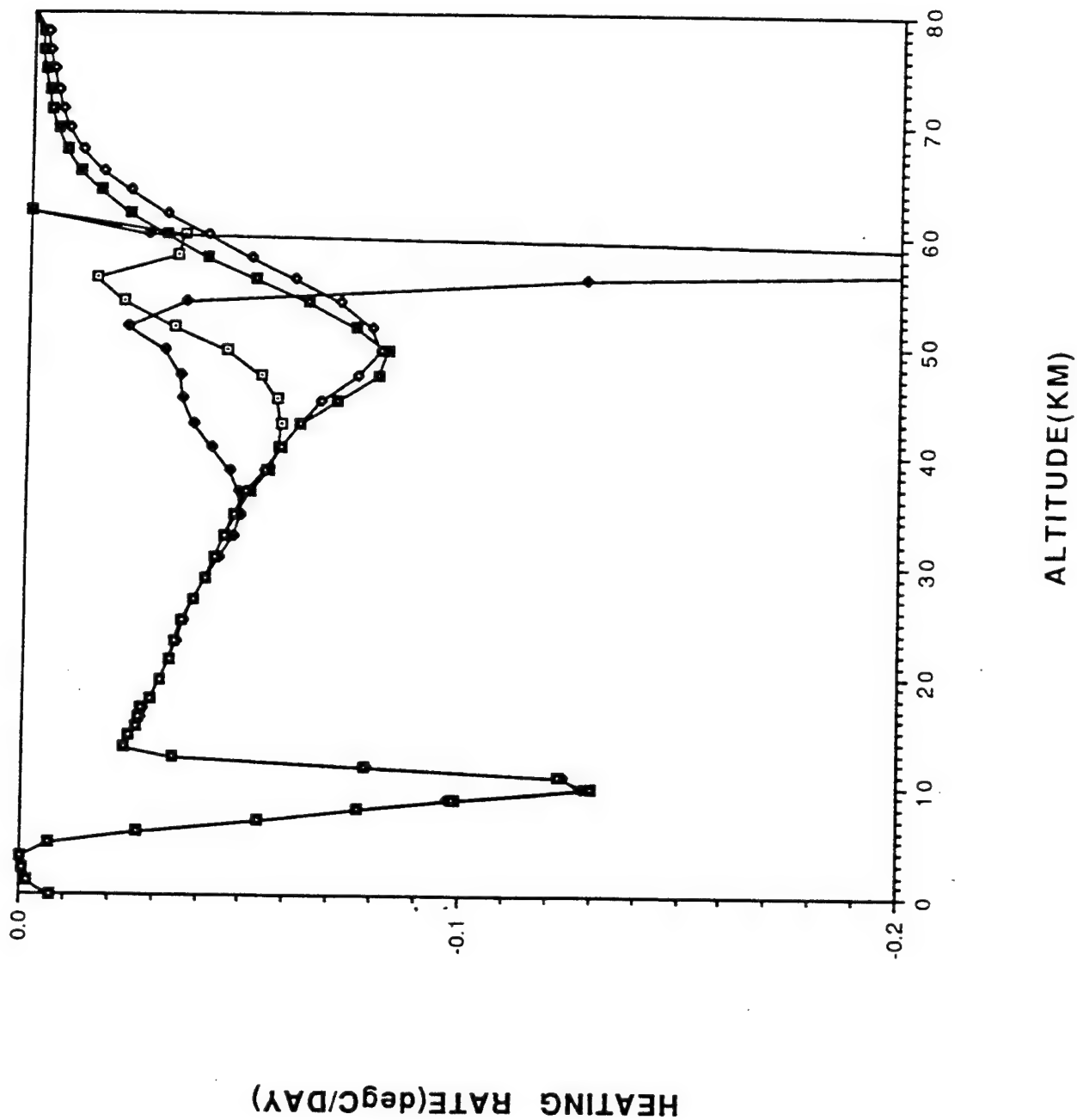


Figure 2

H₂O 50 points

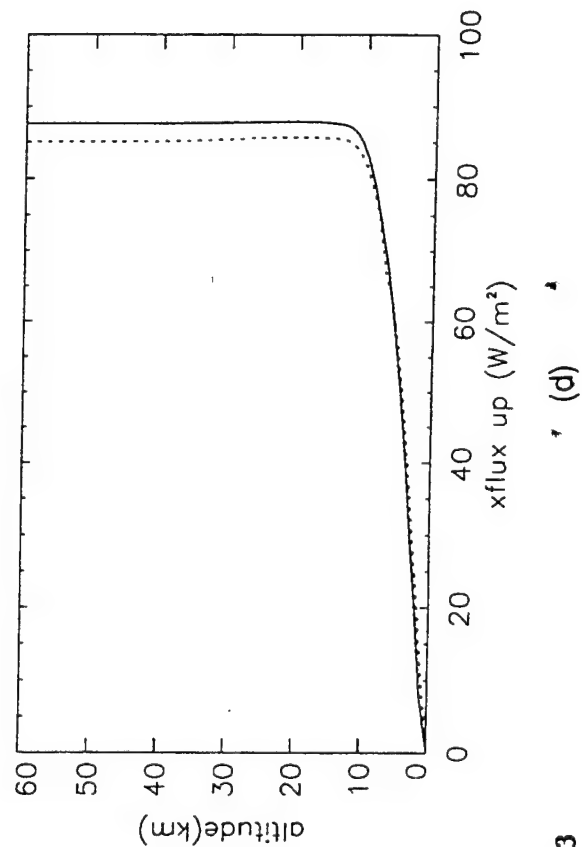
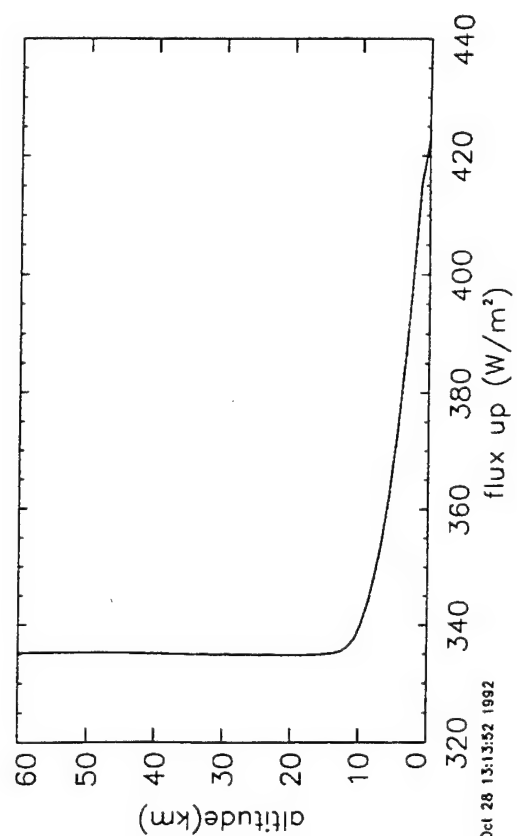
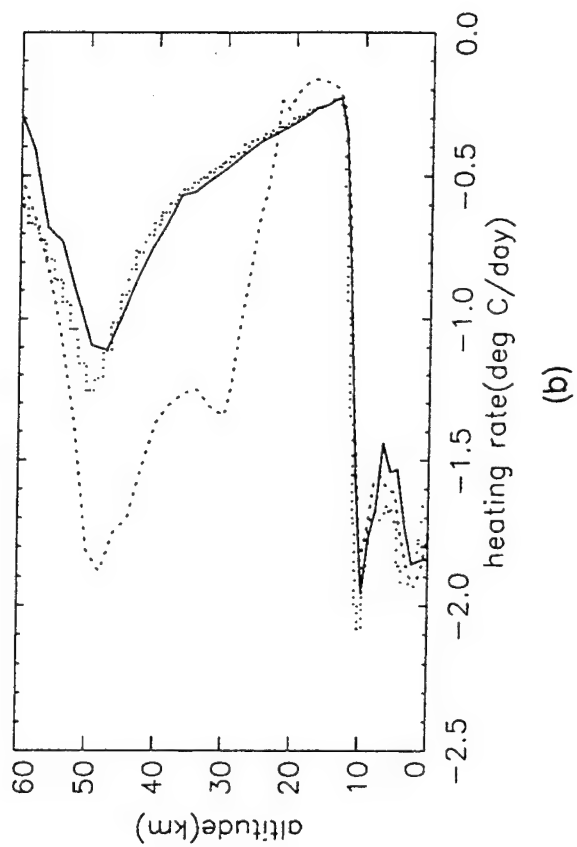
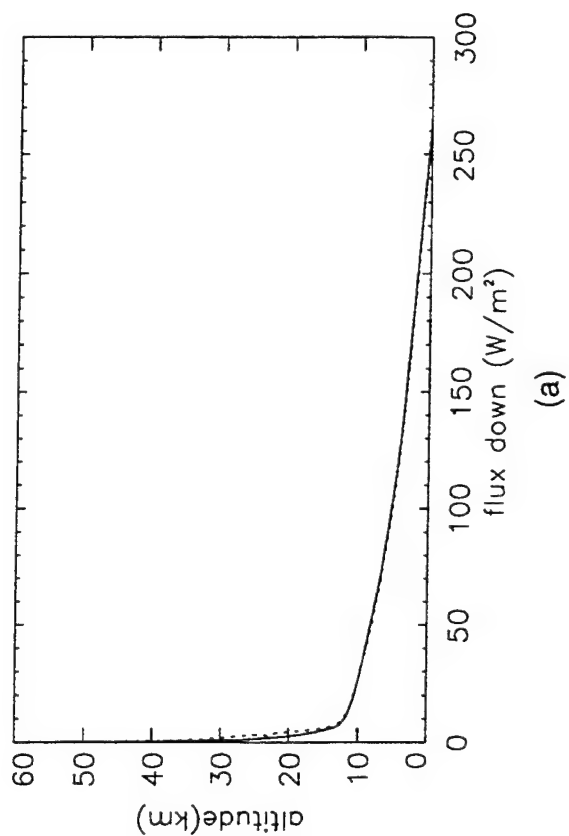


FIGURE 3



OVERLAP MODEL

Consider a spectral region over which two gases have overlapping but uncorrelated spectra. According to G1, the opacity distribution function for the combined gas can be written as,

$$F_{12}(\tau)d\tau = f_{12}(k)dk,$$

where τ is the optical depth defined by the relation, $d\tau = mdk$, k is the absorption coefficient, and m is the column density of the mixture;

$$F_{12}(\tau) = f_{12}(k)/m.$$

Assuming that the spectra of each gas is independent of the other, a separate opacity distribution function can be written for each component;

$$F_1(\tau_1) = f_1(k_1)/m_1, \quad F_2(\tau_2) = f_2(k_2)/m_2,$$

$$\tau = \tau_1 + \tau_2 = k_1/m_1 + k_2/m_2.$$

G1 gives an expression for the distribution function for the combined mixture in terms of the individual distributions;

$$dF_{12}(\tau) = F_2(\tau_2)F_1(\tau - \tau_2)d\tau_2$$

and

$$F_{12}(\tau) = \int_0^\tau F_2(\tau_2)F_1(\tau - \tau_2)d\tau_2.$$

G1 states that there were numerical difficulties using the above expression for the combined distribution function and provides, without proof, an alternate expression giving the combined cumulative probability function $G_{12}(\tau)$ in terms of the individual gas cumulative probability functions $G_1(\tau_1)$ and $G_2(\tau_2)$;

$$G_{12}(\tau) = \int_0^\tau G_1(\tau - \tau_2)dG_2(\tau_2),$$

$$G(\tau) = \int_0^\tau F(\tau')d\tau'.$$

The derivation of Eq. 4 can be accomplished as follows. The form of Eq. 4 in terms of the distribution functions $F_1(\tau_1)$, $F_2(\tau_2)$, and the general expression, Eq. 5, is

$$G_{12}(\tau) = \int_0^\tau F_{12}(\tau') d\tau'$$

$$G_{12}(\tau) = \int_0^\tau \int_0^{\tau'} F_1(\tau' - \tau_2) F_2(\tau_2) d\tau_2 d\tau'.$$

From Eq. 5 the expression $dG_2(\tau_2)$ is

$$dG_2(\tau_2) = F_2(\tau_2) d\tau_2.$$

Let

$$F_1(\tau' - \tau_2) F_2(\tau_2) = \mathcal{F}(\tau', \tau_2),$$

and

$$G_{12}(\tau) = \int_0^\tau \int_0^{\tau'} \mathcal{F}(\tau', \tau_2) d\tau_2 d\tau' = \int_0^\tau F_{12}(\tau') d\tau'. \quad (7)$$

Using the Iterated Integral Theorem for interchanging the integration limits, the following expression can be obtained;

$$\begin{aligned} \int_0^\tau \int_0^{\tau'} \mathcal{F}(\tau', \tau_2) d\tau_2 d\tau' &= \int_0^\tau \int_{\tau_2}^{\tau'} \mathcal{F}(\tau', \tau_2) d\tau' d\tau_2 \\ &= \int_0^\tau \int_{\tau_2}^{\tau} F_1(\tau' - \tau_2) d\tau' F_2(\tau_2) d\tau_2. \end{aligned} \quad (8)$$

Examination of the term

$$\int_{\tau_2}^{\tau} F_1(\tau' - \tau_2) d\tau', \quad (9)$$

in Eq. 8, by itself, reveals that the transformation

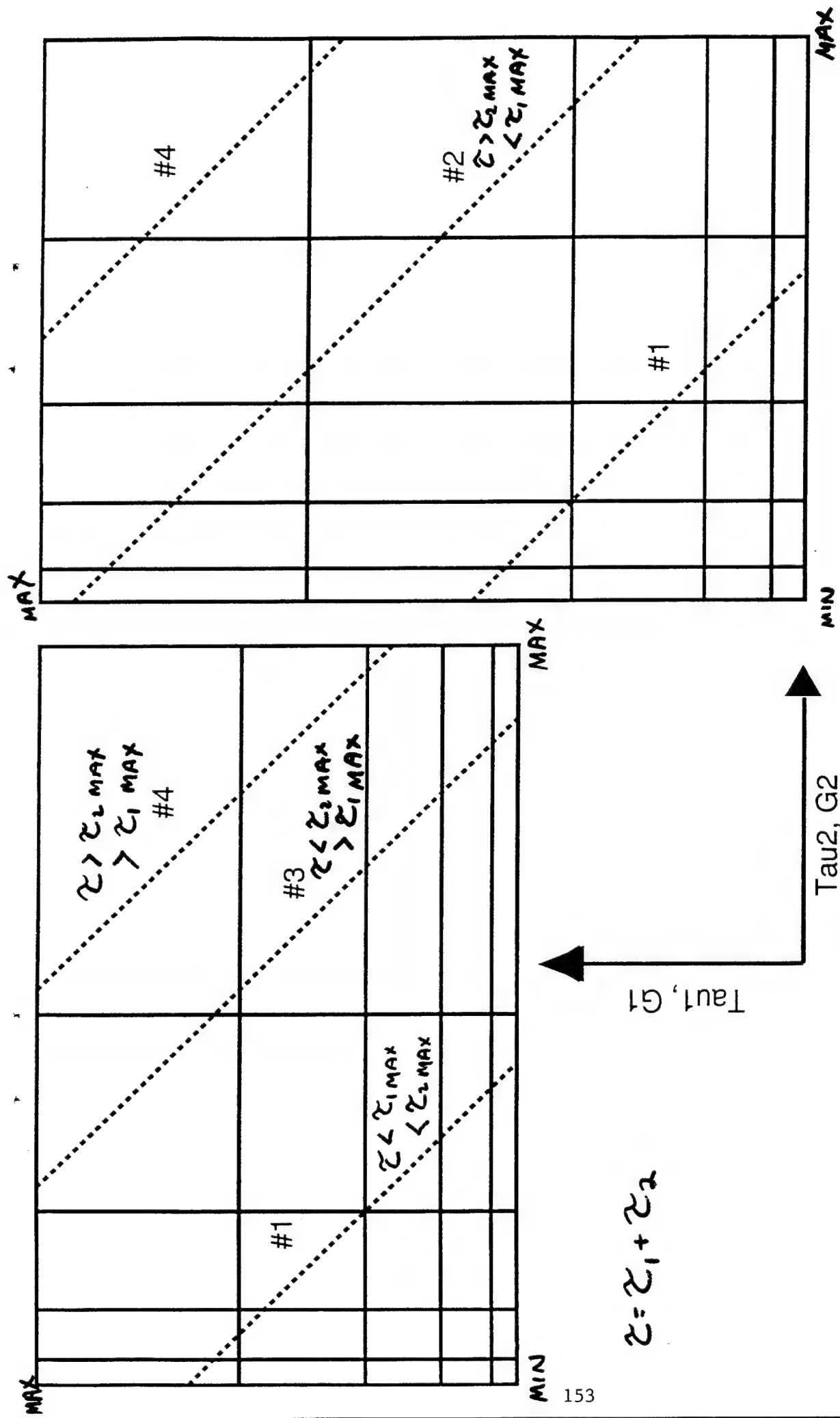
$$\begin{aligned} u &= \tau' - \tau_2, \\ du &= d\tau' \\ u &= \tau - \tau_2, \quad \tau' = \tau \\ u &= 0, \quad \tau' = \tau_2 \end{aligned}$$

can be made (τ_2 is treated as a constant). Thus Eq. 9 becomes

$$\int_0^{\tau - \tau_2} F_1(u) du = G_1(u) = G_1(\tau - \tau_2)$$

and

$$\begin{aligned} \int_0^\tau F_2(\tau_2) d\tau_2 G_1(\tau - \tau_2) &= \int_0^\tau G_1(\tau - \tau_2) dG_2(\tau_2) \\ &= G_{12}(\tau). \end{aligned} \quad (10)$$



$$\tau = \tau_1 + \tau_2$$

Graphical representation of the possible cases for integrating $dG_{12} = G_1(\tau_1 - \tau_2)dG_2(\tau_2)$ over the interval 0 to τ . This yields a single pair of values $(G_1(\tau_1), \tau_1)$ for overlapping two gases in the correlated-k formulation of gaseous absorption bands. The lines of constant τ are shown in τ -space. The actual integration must be done in G -space.

CO2+H2O & OVERLAP points

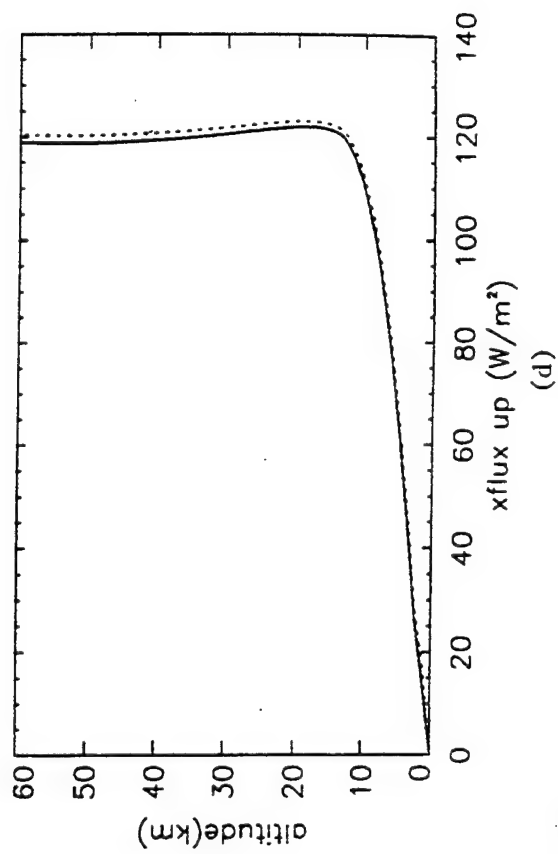
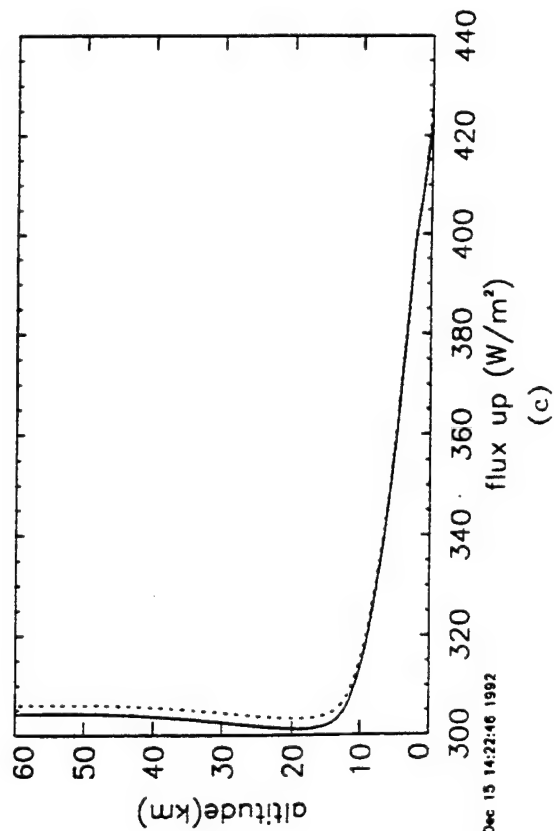
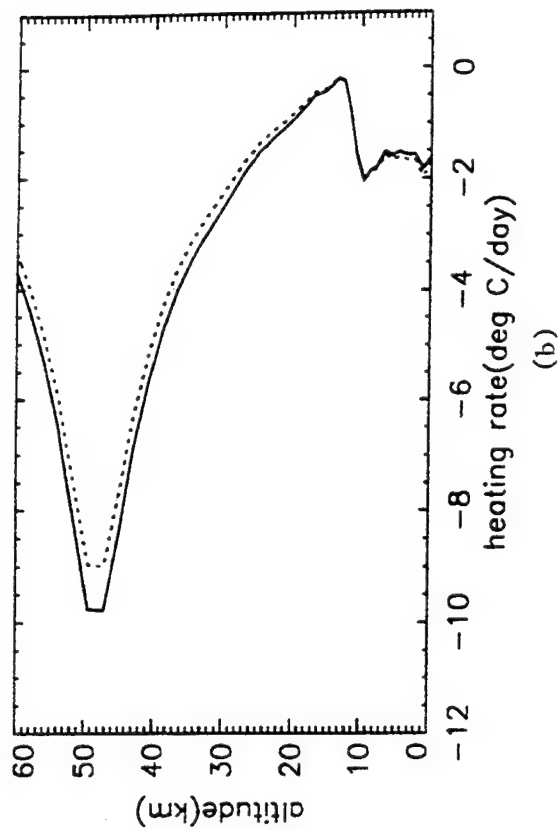
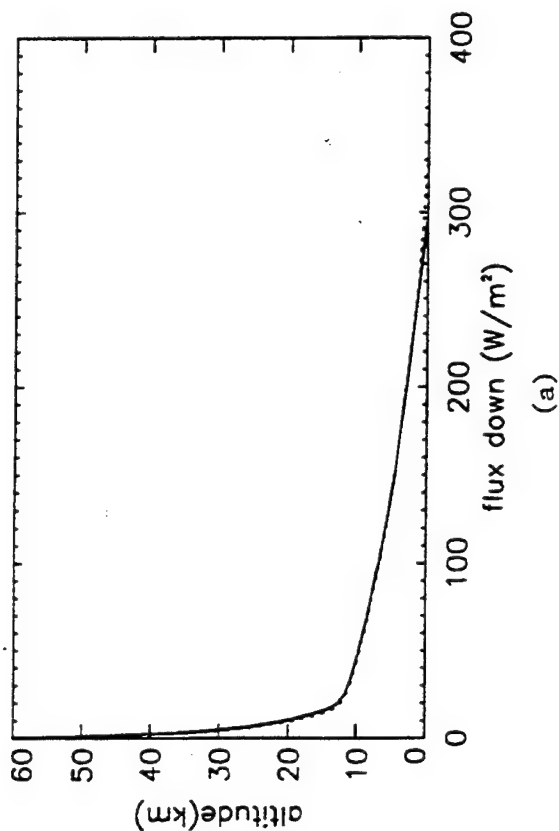


Figure 1.

CH₄/N₂O 40 points Overlap/401 PTS

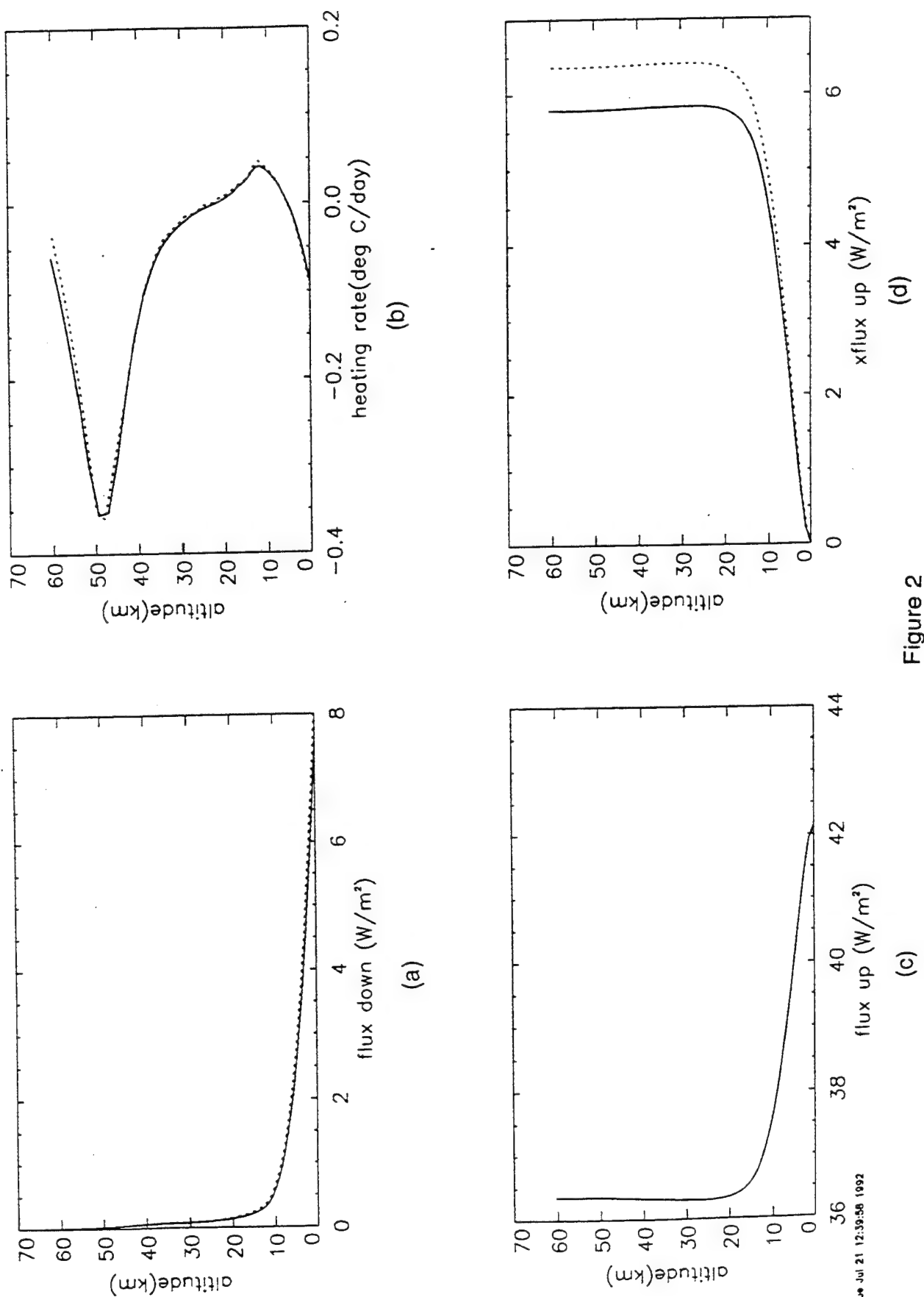


Figure 2

Tuesday 8 June 1993 p.m.

SESSION B: RADIATIVE TRANSFER CODE DEVELOPMENT

Chair: William A.M. Blumberg, PL/GPOS

FASCODE/MODTRAN: VALIDATION AND APPLICATIONS

¹G.P. Anderson, J.H. Chetwynd, F.X. Kneizys*
²A. Berk, L.S. Bernstein, D.C. Robertson, P. Acharya
³J.-M. Theriault, ⁴L.W. Abreu, ⁵S.A. Clough, J.L. Moncet

¹PL/Geophysics Directorate
29 Randolph Road
Hanscom AFB, MA 01731-3010

²Spectral Sciences, Inc.
99 South Bedford St.
Burlington, MA 01830

³DREV-Defence Research
Establishment Valcartier
P.O. Box 8800
Quebec, Canada, GOA 1R0

⁴ONTAR Corp.
129 University Road
Brookline, MA 02146

⁵Atmospheric And Environmental Research, Inc.
Cambridge, MA 02139

(* Retired)

During the previous year the merit of MODTRAN2 has been demonstrated, particularly through comparisons with both measured interferometric data and line-by-line (LBL) flux divergence (cooling rate) calculations. MODTRAN2 differs from MODTRAN in three major areas: (1) its spectral data bases (based on a two-parameter band model) are derived from HITRAN92 rather than the '86 version; (2) the line-of-sight geometry routines have been modified to eliminate sets of errors; and (3) the radiance algorithm has been upgraded to respond appropriately to optically thick layers. This latter correction is similar to those suggested by Clough et al. (1992) and Cornette (1992) for FASCODE and LOWTRAN, respectively.

The current and future directions of the DoD radiance-transmittance codes remain robust. For instance, DOE is collaborating on a new effort to bring about convergence between the DOE FASCODE-based code (LBLTRN) and FASCOD3P, fostering commonality in vectorization, continua, non-LTE, laser, line-of-sight and flux divergence applications. In addition, the cross section capabilities (IR CFC's) from FASCODE are being incorporated into MODTRAN2, and the development of joint FASCODE/MODTRAN inversion algorithms are being explored.

ATMOSPHERIC TRANSMISSION MODELING
ANNUAL REVIEW CONFERENCE

8 JUNE 1993

GEOPHYSICS DIRECTORATE/PHILLIPS LABORATORY

FASCODE/MODTRAN: Validation and Applications

G.P. Anderson, J.H. Chetwynd, F.X. Kneizys
Geophysics Directorate/PL

A. Berk, L.S. Bernstein, D.C. Robertson, P. Acharya
Spectral Sciences Inc.

J.-M. Theriault
DREV/Defence Research Establishment Valcartier

L.W. Abreu
ONTAR, Inc.

S.A. Clough, J.-L. Moncet
Atmospheric and Environmental Research, Inc.

HISTORY

DoD Plan for Atmospheric Transmission Research and Development

AIR FORCE

- o Maintain DoD Standard Atmospheric Optical/IR models:
(LOWTRAN), MODTRAN, FASCODE, HITRAN Database
- o Publish and Brief Model Updates
- o Conduct Annual Tri-Service Review
- o Measure and Model Propagation Effects of the
Free Atmosphere

ARMY

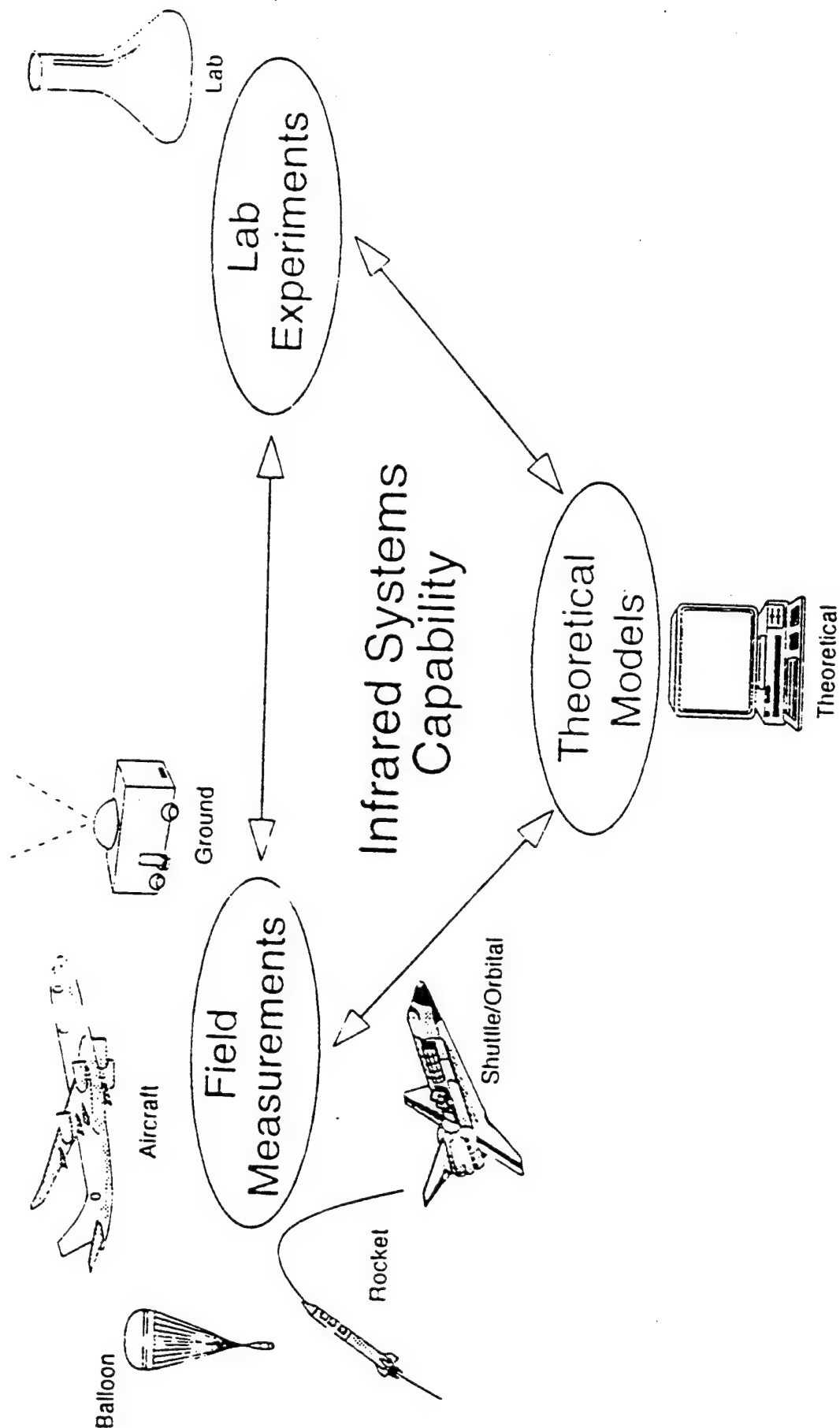
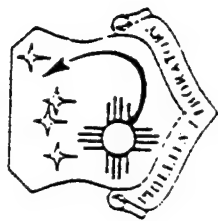
- o Study Battlefield Conditions
- o Develop Models of Dust, Smoke, Chemicals, Propagation,
and Diffusion Effects

NAVY

- o Develop Models for Marine Environment
- o Measure/Model Atmospheric Propagation



OPTICAL ENVIRONMENT DIVISION





CODES



LOWTRAN/MODTRAN: LTE TRANSMISSION AND RADIANCE CODES GENERALLY APPLICABLE BELOW 40km ALTITUDE

ARC (ATMOSPHERIC RADIANCE CODE): A RESEARCH CODE FOR UPPER ATMOSPHERIC RADIANCE

AARC (AURORAL ATMOSPHERIC RADIANCE CODE): EXTENDS ARC TO AURORA

SHARC: AN NLTE CODE, GENERALLY USED ABOVE 50km ALTITUDE
A TRUE USER CODE

FAUST: A DATA BASE TO COMBINE LTE AND NLTE REGIMES

SAMM: SHARC AND MODTRAN MERGED

FASCODE: A LINE-BY-LINE CODE-HIGHLY ACCURATE BUT MUCH SLOWER-REQUIRED FOR LASER PROPAGATION

MOSART: COMBINES MODTRAN WITH APART (A PROPRIETARY CODE) TO PROVIDE AN ATMOSPHERIC CODE WITH GROUND RADIANCE EFFECTS

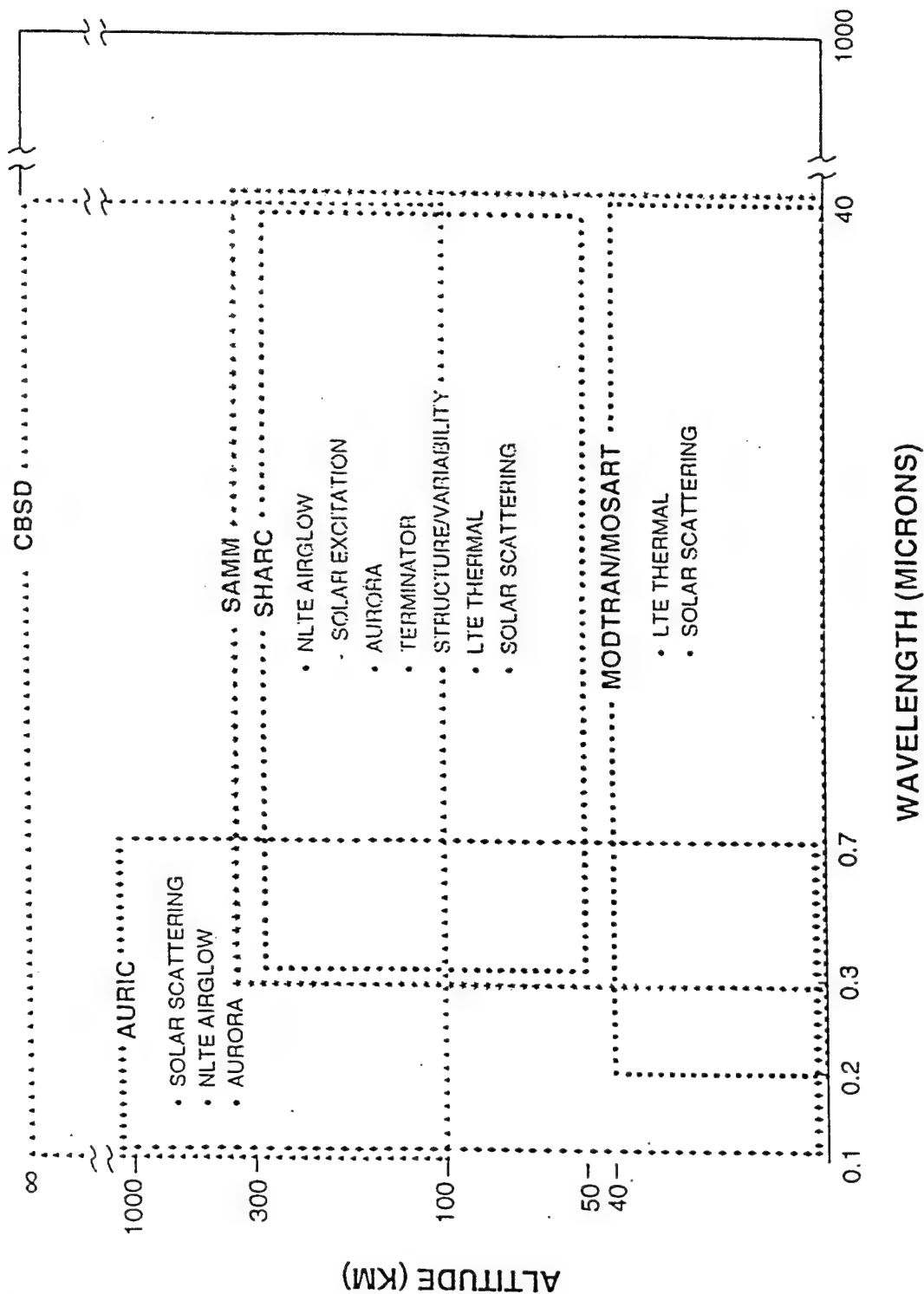
CBSD: CELESTIAL BACKGROUND SCENE DESCRIPTOR - TWO DIMENSIONAL

PLEXUS: (PHILLIPS LABORATORY EXPERT UNIFIED SIMULATOR):

- COMBINES ALL OF THE ABOVE INTO A USER FRIENDLY FORMAT
- PROVIDES ARCHITECTURE FOR 2-D CODES



PL/GP OPTICAL BACKGROUND CODES COVERAGE CAPABILITY



The Problem: *RADIATIVE TRANSFER*

1. The Atmosphere as a contaminant for E/O Systems
2. The Atmosphere as a signature source for natural variability

Solutions: *DEFINITIONS*

1. State variables (T, p, μ_i , Cld, Aer) along line-of-sight
2. Spectral Characteristics of the Path Variables
3. Viewing Geometry
4. E/O System Characteristics (Spectral Range & Resolution, Platform, Objective)

Solutions: *OPTIMIZATION*

1. Efficient Mathematical Algorithms (Line-by-Line)
2. Accurate Band Model Options
3. User Friendly
4. Validation/Documentation

Solutions: *DATA ANALYSIS*

1. Information Theory
2. Inversion Algorithm Development
3. Ground Truth
4. Validation and Error Estimation

DEFINITIONS

κ_i = absorption cross section, related to molecular properties,
pressure (p), temperature (θ)

η_i = column amount of absorbing (i'th) species = $\int n_o ds$

ds = path increment; n_o = volumn density

τ_i = optical depth = $\kappa_i \eta_i$

T_i = transmittance = $\exp (-\tau_i)$

T_{mol} = total molecular transmittance = $\prod T_i = T_1 \cdot T_2 \cdot T_3 \cdot T_4 \dots$

T_T = total transmittance = $T_{\text{mol}} \cdot T_{\text{continua}} \cdot T_{\text{scat}} \cdot T_{\text{aerosol}}$

$B(\theta)$ = Planck Function for temperature θ

$\pi \mathcal{F}$ = Solar (Lunar) Source Function

\mathcal{E} = Non-LTE Source Term

W = Weighting Function = (dT_T/ds)

OPERATIVE EQUATION:

$$\mathfrak{R} = \text{Thermal Radiance} = \int B(\theta) dT_T = \int B(\theta) (dT_T/ds) ds$$

AND FOR A SINGLE LAYER:

$$\mathfrak{R} = \int B(\theta) dT_T = B(\theta) [1-T_T]$$

and, finally, combining thermal, solar, and non-LTE sources with multiple scattering,

one can replace the Planck source function with a more general source function:

$$B(\theta) \Rightarrow J(\tau, \zeta)$$

$J(\tau, \zeta)$ = general source function dependent on optical depth (τ) and viewing geometry (ζ = zenith & azimuth cosines)

$$\begin{aligned} &= (\omega_o/4\pi) \pi \mathcal{F} T(\zeta) \wp && \text{[SOLAR]} \\ &+ [1-\omega_o] B(\theta) && \text{[THERMAL]} \\ &+ \mathcal{E} && \text{[N-LTE]} \\ &+ J_{MS} && \text{[MUL.SCAT.]} \end{aligned}$$

where:

ω_o = single scattering albedo = $\tau_s / (\tau_s + \tau_a)$

$T(\zeta)$ = transmittance from top of atmosphere to layer

\wp = scattering phase function

J_{MS} = m.s. for both solar and thermal terms (complicated)

and other terms are as previously defined!!

ATMOSPHERIC STATE VARIABLES

MOLECULAR, PARTICULATE, THERMAL PROFILES

Some thoughts on the subject:

$$\mathfrak{R} = \text{Thermal Radiance} = \int B(\theta) dT_T$$

1. First Order Impact on Radiance Accuracy:

$\theta(z)$ = temperature profile

$B(\theta)$ = "driving" Planck Function

2. Second Order Impact on Radiance Accuracy:

$\mu(z)$ = mixing ratio profiles

$d(z)$ = atmospheric density profile

$\kappa(z)$ = molecular absorption coef. (θ and p)

$T(z) = \exp(-\Sigma\tau) = \exp(-\Sigma\kappa \mu(z)d(z) \Delta z)$

Given that:

- o the molecular spectroscopy is "in hand", although always requiring "investment" in order to stay state-of-the-art,

And:

- o the **LARGEST** error sources in the forward calculations are the descriptions of the "state variables", e.g. temperature, pressure, mixing ratio, and particulate (aerosol and hydrometeor) profiles,

Then:

- o why work so hard on code accuracy?
- o why continue the "investment" in "state-of-the-art" spectroscopy?
- o what is the end benefit?

ANSWERS (from a neutral observer!)

* *VALIDATION for Signatures*

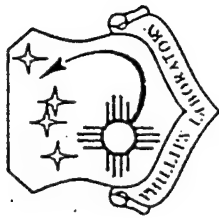
1. *targets/pollutants against backgrounds-
estimate of variability
estimate of go/nogo
estimate of true/false; reduce false ID
incorporate "target signatures"*
2. *atmospheric specification
local and/or global "weather"
atmospheric contaminants become signatures*
3. *higher resolution spectroscopy with high spectral
accuracy may minimize confusion, increasing
signal/noise for both contaminants and state
specification.*

* *REAL-TIME ANALYSIS with speed*

1. *Line-by-line (LBL) codes and their derivatives work -
"exact" physics must remain state-of-the-art;
Because physicists drive technology to higher resolution:
lidar/laser applications
interferometers at $<.01\text{cm}^{-1}$ resolution
remote sensing issues: line coupling, mm-wave
new/old/unsettled issues:
CFC x-sections, H₂O continua, CO₂ χ factor
NLTE issues
However:
"LBL" is slow, slow, slow!!!*
2. *Band Models (pragmatic, expedient parameterizations) trail
"LBL" in "state-of-the-art",
but they are the codes of the NOW and FUTURE for
issues and analyses with compatible spectral resolution!*



DoD Spectral Radiance Transmittance Codes



Phillips Laboratory (GPO) code responsibility

Develop, maintain, continuously improve, and transition atmospheric radiance and transmittance codes

Common elements of LOWTRAN, MODTRAN, and FASCODE

Ultraviolet to microwave ($.2\mu$ to ∞ or 0–50000 cm^{-1})

Default molecular profiles

Default aerosol, cloud, rain, fog descriptions

Solar/lunar source spectra

Single and multiple scattering

Flexible spherical geometry package for arbitrary lines-of-sight

Transmittance, radiance, weighting functions, etc.

Instrumental convolution functions (scanning & filter)



Characteristics of MODTRAN2 and FASCOD3



MODTRAN2:

Embeds LOWTRAN

2 cm⁻¹ resolution

Local Thermodynamic Equilibrium ONLY

Upper Altitude Limit – 60km (LTE)

HITRAN92 compatibility

Applications: Plume, Background, E/O Design
Inversion Algorithm, Data Analysis

FASCODE: (FASCOD3)

"Exact" spectral resolution, dictated by Voigt line shape at highest altitude
Optimized layering and line shape functions

Full CFC cross-section compatibility

HITRAN92 compatibility

Non-LTE capability (in conjunction with SHARC)

No solar capability

Applications: Laser, Lidar, E/O Design, Plume
Inversion Algorithm, Data Analysis

MODTRAN ASSUMPTIONS:

- No overlap between species:

$$\text{e.g.: } T(\text{total}) = T(\text{H}_2\text{O}) \cdot T(\text{CO}_2) \cdot T(\text{O}_3) \cdot T(\text{CH}_4) \cdot \dots$$

- Line strength temperature dependence can be interpolated:

$$\text{e.g.: } S_i(\theta) = \mathcal{F}(\theta_n) \text{ for } n = 200, 225, 250, 275, 300\text{K}$$

- Voigt line shape is appropriate, based on "path weighted" p

$$\text{e.g.: } \mathcal{L}(p, \nu) = \text{line shape function where } \alpha_v(p) = \text{constant}$$

- Line contributions falling outside of bin ($\Delta\nu=1 \text{ cm}^{-1}$) but within $\pm 25 \text{ cm}^{-1}$ can be adequately described:

$$\text{e.g.: "special MODTRAN continua"}$$

- Two band model parameters are sufficient:

$$\text{e.g.: } S/d = \text{average line strength in bin} = (1/\Delta\nu) \sum S_i$$

$$\begin{aligned} n &= \text{ave. \# of lines in bin} \\ &= 1/d = (1/\Delta\nu) (\sum \sqrt{S_i})^2 / \sum (S_i^2) \end{aligned}$$

MODTRAN2 Band Model Equations:

$T(\text{total}) = \text{Total Transmittance}$

$$= \prod_i T_i = T(\text{H}_2\text{O}) \cdot T(\text{CO}_2) \cdot T(\text{O}_3) \cdot T(\text{CH}_4) \cdot \dots$$

and $T_i = \left\{ (2/\Delta\nu) \int_0^{\Delta\nu/2} \exp[-S_\nu \bar{u}_i \mathcal{L}(p, \nu)] d\nu \right\}^n$

where:

$$\Delta\nu = 1 \text{ cm}^{-1} \text{ bin}$$

$$S_\nu = (S/d) / (1/d) = \text{absorption coef./density param.}$$

$$\bar{u}_i = \text{path column am't of } i\text{th species}$$

$$\mathcal{L}(p, \nu) = \text{line shape function where } p = \text{path pressure}$$

$$n = (1/d) \Delta\nu \sim \text{ave. \# of lines in bin}$$

CONTRAST: Line-by-Line vs. Band Model

FASCODE Transmittance: (LBL)

$$\sum k(\ell, \nu, i) n(\ell, i) = \sum \tau(\ell, \nu, i) = \sum \text{optical depth}(i) \text{ in layer } \ell$$

$$T(\nu) = \exp[-\sum \sum k(\ell, \nu, i) n(\ell, i)]$$

or

$$T(\nu) = \prod_{\ell} T_{\ell} = T_1 \cdot T_2 \cdot T_3 \cdot T_{\ell} \cdot \dots$$

and

$$T(\Delta\nu) = \int (T(\nu) d\nu) / \Delta\nu$$

MODTRAN Transmittance: (BM)

$$T_i(\Delta\nu) = \left\{ (2/\Delta\nu) \int_0^{\Delta\nu/2} \exp[-S_{\nu} \bar{u}_i \mathcal{L}(p, \nu)] d\nu \right\}^n$$

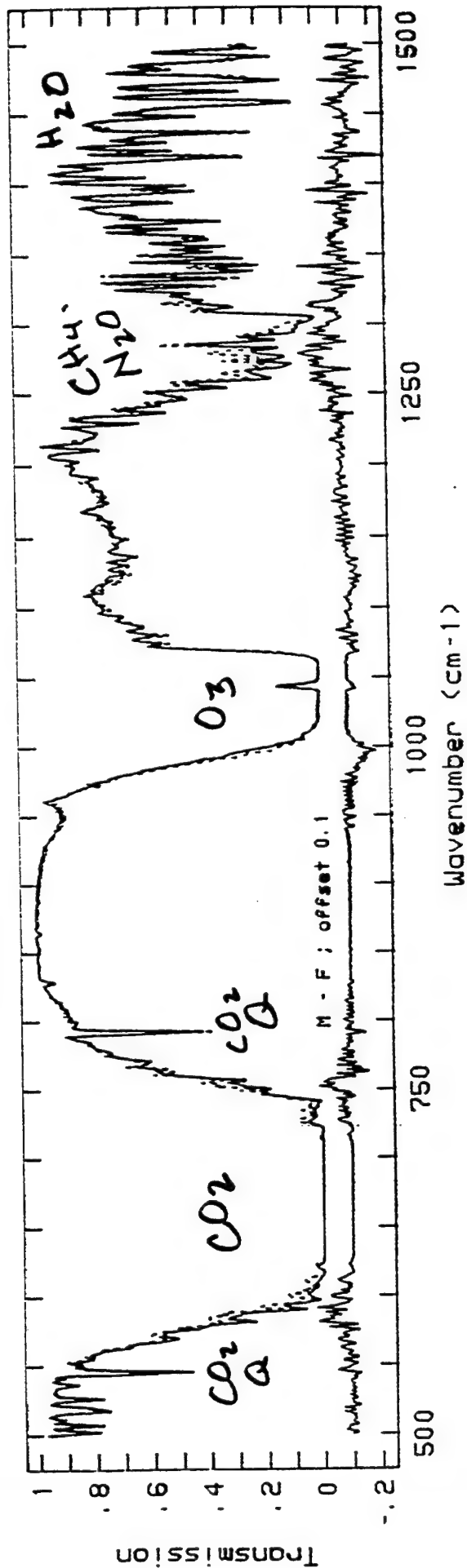
$$T(\Delta\nu) = \prod_i T_i(\Delta\nu) = T(\text{H}_2\text{O}) \cdot T(\text{CO}_2) \cdot T(\text{O}_3) \cdot T(\text{CH}_4) \cdot \dots$$

MODTRAN2

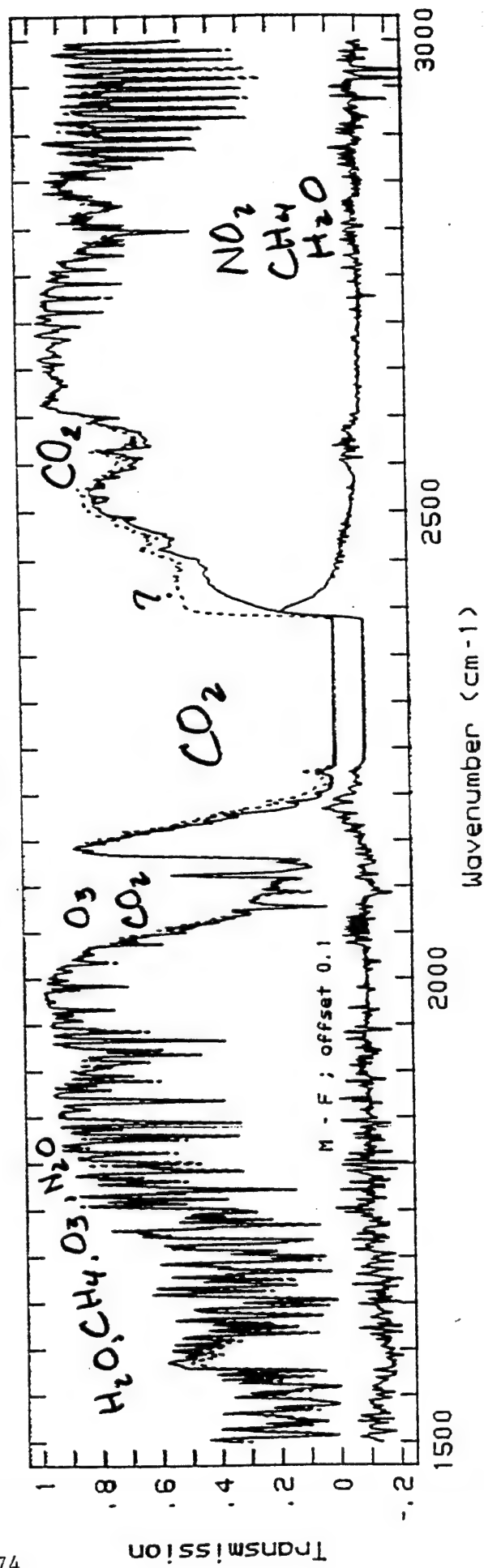
New Features:

1. HITRAN92-Based Band Model
2. New Geometry Package with Consistent Range Determinations
3. New Radiance Algorithm ("Linear in Optical Depth")
4. Spectrally-Dependent Surface Emissivity/Albedo
5. Flux Divergence Capability

FASC003 (solid) and MOOTRANL (dashed)



174



FREQ (cm ⁻¹)	ALT (km)	T (K)	RANGE (km)	MEAN TRANS		DIF	VAR (rms ²)
MOD(86)	FAS(86)						
0- 500	45	200	500000	.61717	.71211	.09494	4.93700E-3
	30	200	5000	.68104	.66882	.01228	5.06760E-4
	30	300	5000	.71678	.71211	.00467	2.69819E-5
	15	275	10	.87833	.87800	.00033	2.61406E-5
	15	225	10	.86676	.86513	.00163	4.90820E-5
	0	300	.005	.44175	.44270	.00095	2.78848E-4
	0	250	.005	.42247	.41378	.00869	3.16083E-4
500- 1000	45	300	500000	.59798	.53966	.05832	3.29788E-3
	30	260	5000	.65704	.61798	.03905	6.05537E-3
	15	260	500	.57125	.56280	.00844	4.04609E-3
	15	260	10	.81105	.80050	.01055	2.67364E-4
	0	300	1	.51721	.51560	.00161	4.55383E-4
	0	260	1	.49087	.48749	.00339	3.36086E-4
1000- 1500	45	300	500000	.68805	.62673	.06132	1.93994E-3
	30	260	10000	.63912	.59061	.04851	2.39270E-3
	15	260	50	.80956	.79412	.01544	1.64402E-3
	0	300	1	.48765	.48703	.00062	2.78078E-5
	0	260	.1	.68762	.68686	.00076	3.01251E-5
1500- 2000	45	260	500000	.75053	.72518	.02534	4.86761E-4
	30	300	10000	.75174	.73917	.01257	2.25932E-4
	30	260	5000	.81098	.79915	.01183	2.04952E-4
	15	260	500	.55166	.55034	.00132	6.32165E-5
	0	300	.0	.33631	.33473	.00158	1.10876E-4
2000- 2500	45	260	5000	.78488	.74690	.03798	1.68926E-3
	30	300	100	.77980	.75394	.02586	1.15226E-3
	30	260	500	.69492	.66327	.03165	1.43556E-3
	15	300	10	.70192	.68788	.01404	6.32160E-4
	15	260	50	.59330	.57749	.01581	5.87976E-4
	0	300	.1	.73014	.72594	.00420	1.76310E-4
	0	260	1	.53847	.52832	.01015	2.40155E-4
2500- 3000	45	300	1000000	.84432	.79373	.05059	4.56036E-3
	30	300	50000	.75861	.71130	.04731	2.79251E-3
	30	260	10000	.87683	.85817	.01866	5.74034E-4
	15	300	1000	.72777	.70690	.02087	8.53069E-4

BETA) and CASE 2B (H1, H2, RANGE).

Table 4 compares the MODTRAN and MODTRAN2 output ranges for various CASE 2C inputs. For small input ranges, MODTRAN output ranges differ greatly from the input values. For input ranges of 2.0, 6.0, and 20.0 km, MODTRAN did not yield any output values. The reason is that, after these CASE 2C inputs were converted to CASE 2D, the computation of ANGLE did not converge.

Table 4. Examples for CASE 2C with H1 = 5 and H2 = 5 km.

<u>INPUT</u>	<u>RANGE (km)</u> <u>MODTRAN</u>	<u>MODTRAN2</u>
2.01	—	2.00
4.7	5.31	4.72
6.0	—	6.01
8.0	7.51	8.01
9.0	7.51	9.01
10.0	9.20	10.02
20.0	—	20.01
50.0	50.51	50.02
100.0	100.52	100.01
200.0	199.96	200.01
300.0	300.13	300.01

NEW RADIANCE ALGORITHM: APPROXIMATIONS FOR OPTICALLY THICK LAYERS

Looking only at a single isolated layer, straightforward application of the simple radiance equation leads to:

$$R = B \, dT \text{ or } R = (1-T) B \quad (5)$$

where: R = Radiance,
 B = Planck Function,
 and $dT = (1-T)$, the change in transmittance, T , across the layer.

The Planck Function is defined for a Curtis-Godson density-weighted temperature for the layer. For an optically thin case, the observed radiance in this simple scenario is independent of viewing direction.

[Note that for typical lines-of-sight across a multilayered atmospheric path, radiance is dependent on viewing direction while total transmittance remains independent of the observer's position.]

However, if this single layer is optically thick and includes a directional temperature gradient, the observed radiance will be either larger (emanating from a warmer thermal region closer to the observer) or smaller (emanating from the closer cooler region).

A simple approximation assumes that the Planck function and optical depth vary linearly between the boundaries of the layer:

$$R = (1-T) \{ B_n + 2(B-B_n) [1/t - T/(1-T)] \} \quad (6)$$

where: n implies the nearest boundary,
 t = layer optical depth between boundaries,
 and T = layer transmittance, again for a single layer.

NEW RADIANCE ALGORITHM: Pg2

For a multi-layer scenario, this local layer radiance becomes the input for its neighbor, and the full path solution is reached through recursive calculations and the layer transmittance then becomes:

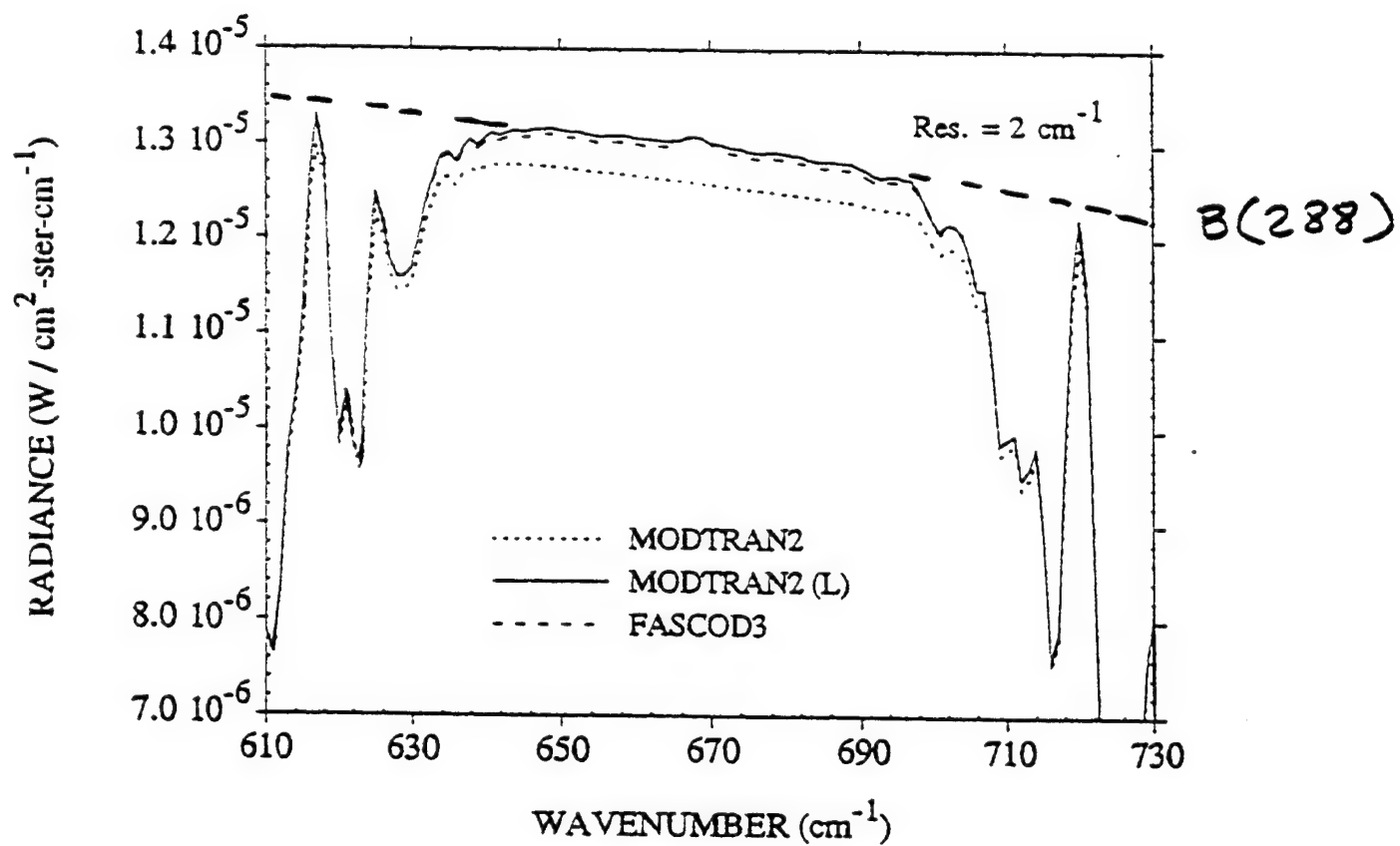
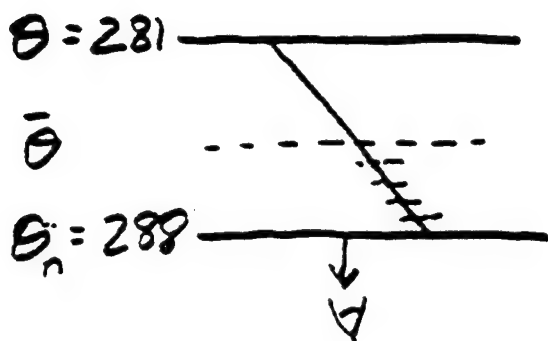
$$T = T(b+1)/T(b)$$

where: $T(b)$ and $T(b+1)$ are the full path transmittances from observer to boundary b and $b+1$, respectively.

Because of the degraded 2 cm^{-1} resolution, the required optical depth term is, in reality, an "effective" optical depth, also derived from the ratios of adjacent full path transmittances at MODTRAN resolution:

$$\tau = -\ln\{T(b+1)/T(b)\}. \quad (7)$$

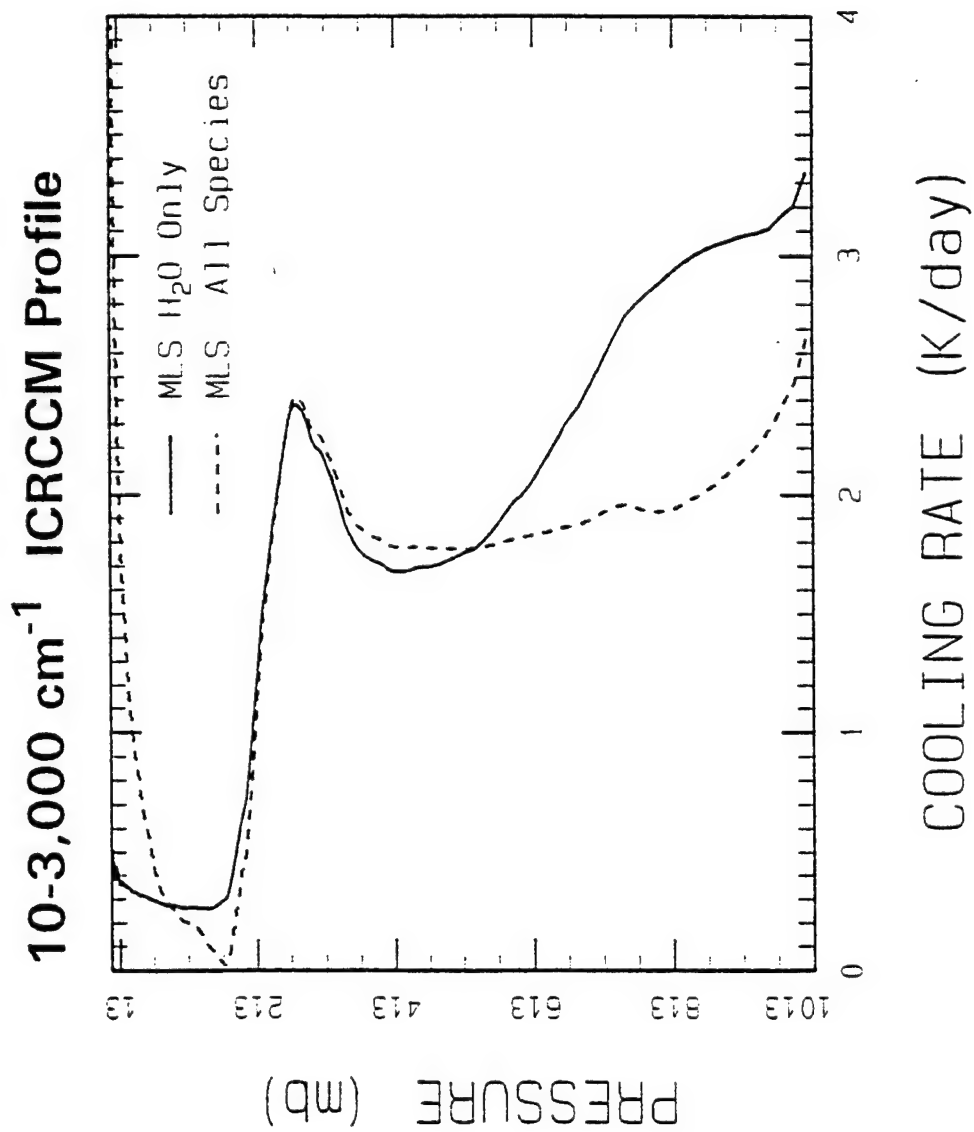
The radiance equation for a single layer (Eq. 6), including the "linear in tau" approximation, appears the same as the simple radiance equation (Eq. 5) if the bracketed quantity $\{\}$ is thought to contain an "equivalent" Planck function, defined by the optical depth weighting.



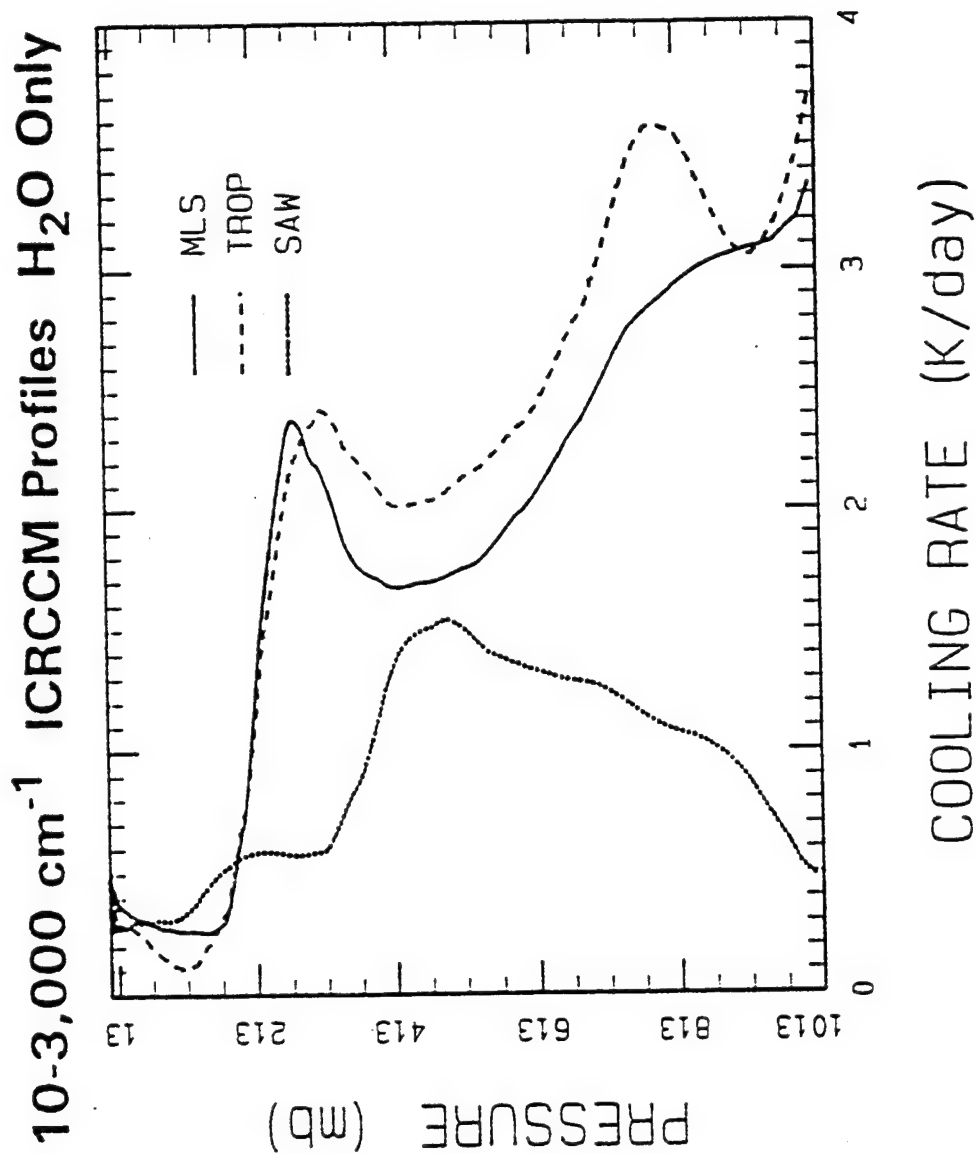
COMPUTATIONAL APPROACH

- COMPUTE LINE-OF-SIGHT(LOS) UPWELLING(F^+) AND DOWNWELLING(F^-) THERMAL FLUXES AT TOP AND BOTTOM OF EACH ATMOSPHERIC LAYER.
- COMPUTE SEVERAL LOS'S AT DIFFERENT ELEVATION ANGLES TO APPROXIMATE THE HEMISPHERICAL FLUX INTEGRATION.
 - 1st MOMENT 2-POINT GAUSSIAN QUADRATURE
- LOCAL COOLING RATES PROPORTIONAL TO PRESSURE DERIVATIVE OF THE LOCAL FLUX DIFFERENCE($F^+ - F^-$).
- TYPICAL CALCULATION REQUIRES 128 SEPARATE MODTRAN RADIANCE CALCULATIONS (32 LAYERS x 2 ANGLES x 2 DIRECTIONS).

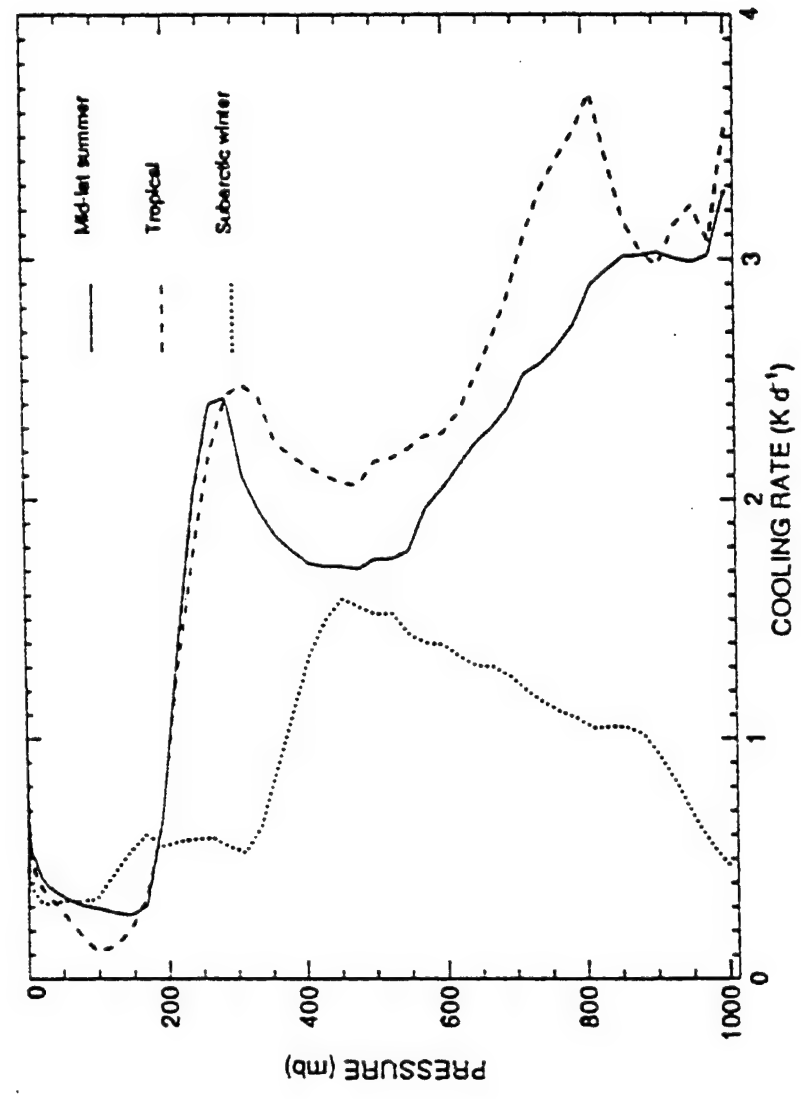
MODTRAN CALCULATIONS



MODTRAN CALCULATIONS



FASCODE CALCULATIONS*



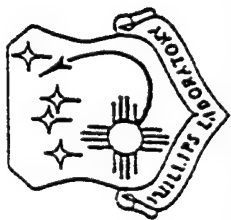
* Clough et. al., JGR, 97, 15761(1992).

MAJOR COMPUTATIONAL DIFFERENCES

- NUMBER OF ATMOSPHERIC LAYERS.
 - FASCODE: 60 LAYERS
 - MODTRAN: 32 LAYERS
- HEMI-SPHERICAL FLUX INTEGRATIONS.
 - FASCODE: 1'st MOMENT 3-POINT QUADRATURE
 - MODTRAN: 1'st MOMENT 2-POINT QUADRATURE
- PLANCK FUNCTION VARIATION THRU LAYERS.
 - FASCODE: ONE TERM PADE APPROX.
 - MODTRAN: LINEAR IN OPTICAL DEPTH APPROX.

SUMMARY OF KEY RESULTS

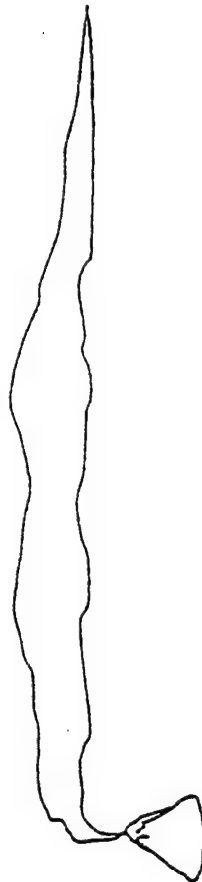
- ACCURACY: INITIAL RESULTS INDICATE POTENTIAL TO REPRODUCE BENCHMARK LINE-BY-LINE CALCULATIONS TO WITHIN THE $\approx \pm 0.05$ K/DAY SPREAD FOUND BETWEEN LBL MODELS.
- SPEED: MUCH FASTER THAN LBL MODELS WITH TYPICAL RUN TIMES FOR A COMPLETE ATMOSPHERIC COOLING PROFILE OF ≈ 4 MIN. ON A FAST WORK STATION (HP 735) AND ≈ 1 HR. ON A PC (486 33 MHZ).



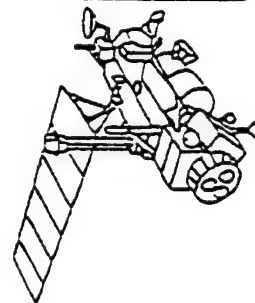
CIRRIS 1A AND MSX DATA IN SUPPORT OF GLOBAL CLIMATE CHANGE INVESTIGATIONS



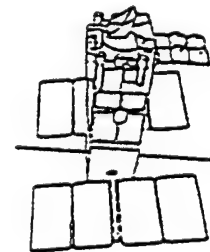
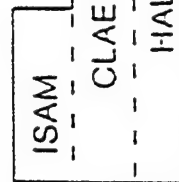
CIRRIS 1A
(APRIL 29-MAY 1)



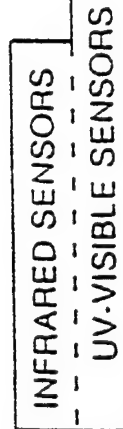
MT PINATUBO
(JUNE 9)



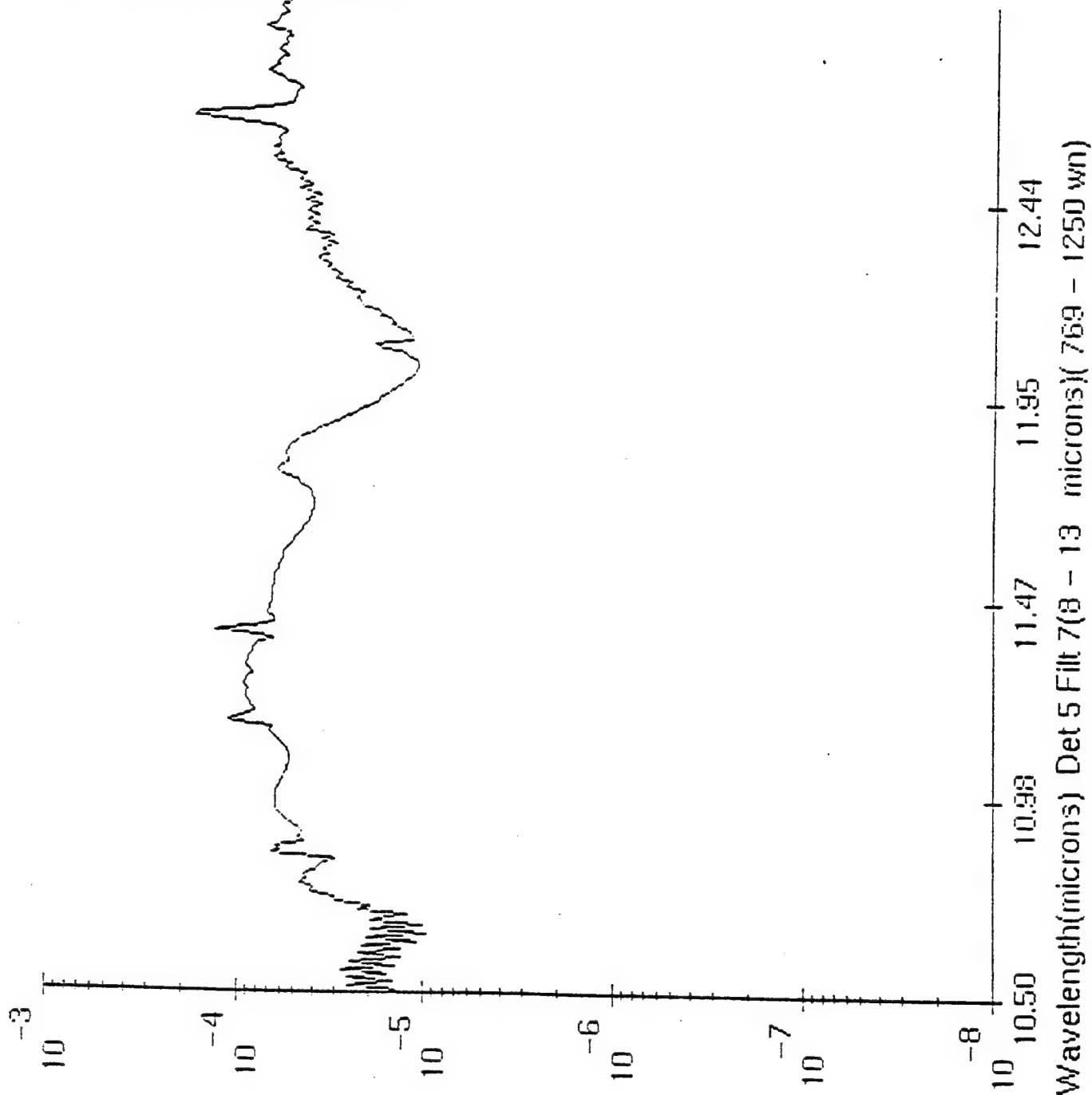
UARS
(SEPT 9)



MSX
(JAN 94)

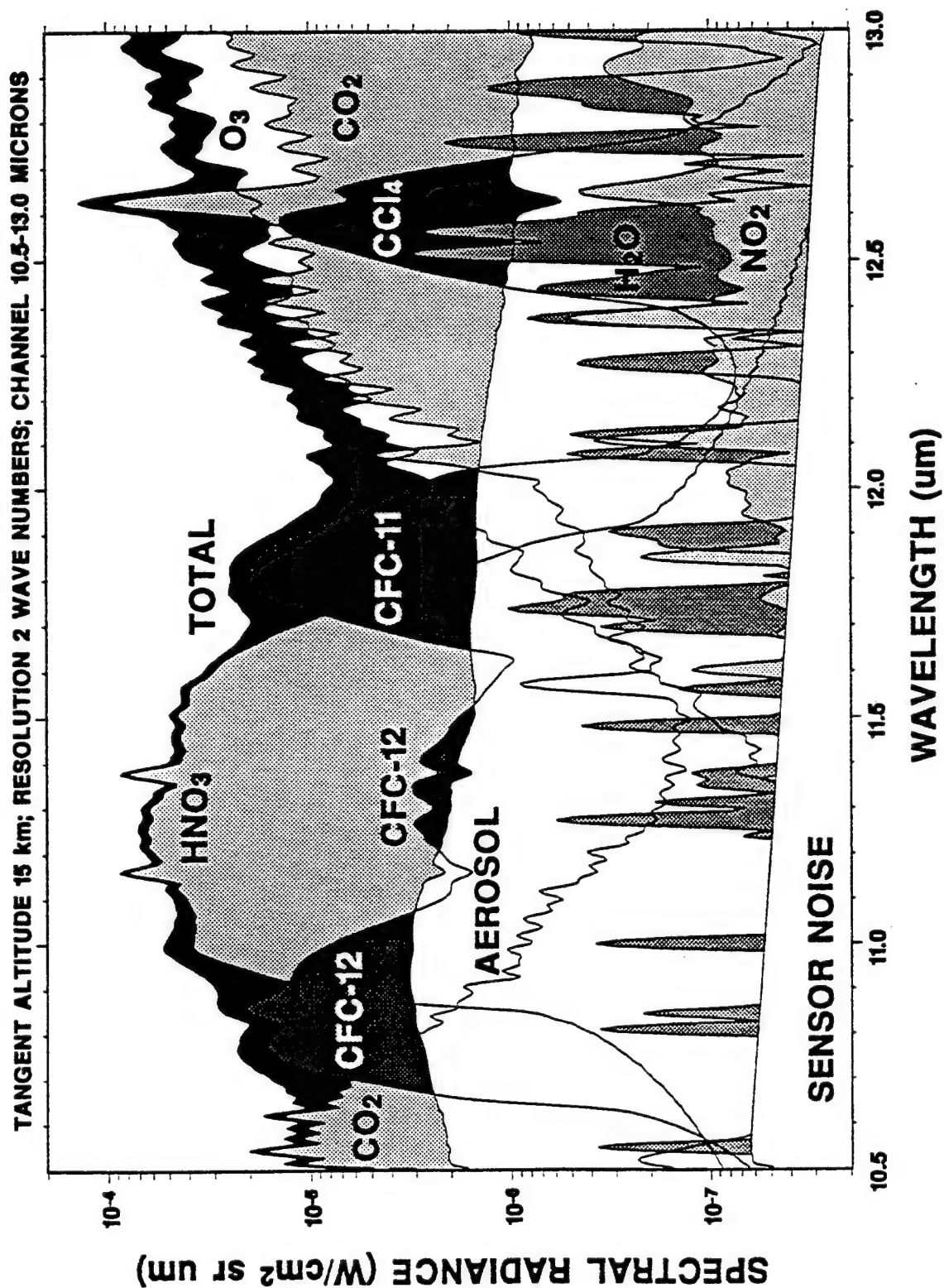


C SPECTRA(PO)-K20
 PC12A_35-2
 01/13-15:38.403
 SCAN 1692 TYPE L
 INH(CAS55MB) 16.31
 FOCAL PLANE POS
 INH(DIF) -2.04
 TH MIN-MX 15.9 16.6
 LATIP 63.83
 LONG TP 179.05
 LOCAL TIME 13.25
 SOLAR ZENITH 51.1
 SUN/SHADE SUN
 PHOT 1/2 10/0
 G/BADR M/N/A
 D NO/5 N/RES 1.04
 BAND_INT 1.20E-04



w a t t / c m 2 / s t r / u m

SIMULATED MEASUREMENT CAPABILITY OF THE SPIRIT III INTERFEROMETER



SAMME will provide a code ready for extensive testing in the CRAY environment.

The analysis activities will include:

1. *vector optimization*
 2. *instantaneous full spectral analysis of heating/cooling rates*
 - a. *incorporation of molecular/thermal climatological variability (using NRL-derived climatologies) and assessment of sensitivities and hemispheric asymmetries*
 - b. *(as above) with multiple scattering*
 - c. *(as above) with simple cloud types and new NRL/DOE-derived climatologies*
 3. *calculations of photo-dissociation rate coefficients with:*
 - a. *molecular/thermal climatologies, diurnal, and solar variability, again with a full accounting of sensitivities and hemispheric asymmetries.*
 - b. *include polar day/night/twilight scenarios in conjunction with NRL/NASA.*
 - c. *(as above) with assessment of uv-A/B at the surface*
 4. *exploration of energy exchange between upper and lower atmospheres as a function of climatological and auroral variability, etc. (NLTE)*
 5. *implement "alternate" inversion algorithm schemes for any SERDP, ARM or other fielded instruments with compatible SAMME spectral resolution; employ compatible simultaneous retrieval algorithms.*
-

SAMME VIRTUES

o accomplish with one radiance/irradiance code:

- complete with solar source function,
- molecular absorption-emission descriptions,
- cloud, aerosol, and molecular default profiles,
- validated NLTE rapid algorithm
- plus the ability to input new data as appropriate

o determination of the suitability of current coarse approximations:

- heating/cooling rate algorithms
- photodissociation rate coefficients
- energy exchange between lower and upper atmosphere

o current climate-related state-of-the- art:

- extensive spectral degradation for efficiency
- UV CFC photodissociation can be in error by 10-15%
by ignoring Schumann-Runge O₂ bands T-dependence
- small, systematic errors a function of season and latitude
- similar approximations in the IR
- no systematic NLTE coupling with lower atmosphere

o exploration of this net impact can be addressed with SAMME

- preliminary assesement this summer: IR WMO/ICRCCM

CONCLUSIONS

The capabilities of the MODTRAN2 code have yet to be fully exploited.

- o Increased accuracy of the new band model, coupled with:
 - the LOWTRAN 7 and FASCOD3 common elements
coarse continua (CO_2 , H_2O , N_2 , O_2 , etc.),
spherical refractive geometry,
default constituent profiles for gases, clouds,
aerosols, fogs, rains, etc.,
molecular and particular multiple scattering,
plus ease of use
- o MODTRAN2 may be effectively employed for:
 - atmospheric remote sensing, radiative transfer
- o MODTRAN2 transmittance calculations are within %'s of FASCOD3:
 - statistically and in spectral detail
 - for simulations at 2 cm^{-1} and greater resolution,
MODTRAN2 may be substituted for FASCOD3
 - layer-specific radiance contributions are excellent, e.g.:
detailed agreement in the Jacobian comparisons
primitive cooling rate calculations excellent
- o MODTRAN2 flux-divergence quantities will be further explored:
 - optimized estimates of up- and down-welling fluxes
 - appropriate heating/cooling rates and photodissociation rates
 - more comparisons with experimental data

However, if, as expected, both the "total path" and "layer" integrity of the MODTRAN2 calculations are maintained, the community-at-large should find this new tool a welcome addition.

Retrieval of Tropospheric Profiles from IR Emission Spectra: Preliminary Results with the DBIS

J.-M. Thériault

DREV-Defence Research Establishment Valcartier
P.O. Box 8800, Québec, Canada, G0A 1R0

G. P. Anderson, J. H. Chetwynd, E. Murphy, V. Turner,
M. Cloutier and A. Smith
Geophysics Directorate / PL, Hanscom AFB, MA 01731 USA

J.-L. Moncet

Atmospheric and Environmental Research, Inc., Cambridge, MA 02139 USA

1. INTRODUCTION

Recently, Smith and collaborators^{1, 2} from University of Wisconsin- Madison have clearly established the possibilities of sounding tropospheric temperature and water vapor profiles with a ground-based uplooking interferometer. With the same perspective but for somewhat different applications, the Defence Research Establishment Valcartier (DREV) has initiated a project with the aim of exploring the many possible avenues of similar approaches. The central objective is the development of methods for the remote sensing of atmospheric profiles, mainly temperature and water vapor, that affect IR propagation and degrade Electro-Optical (EO) system performances. There are several important issues that remain to be addressed prior to the definitive implementation of such a technique into an operational system that responds to our needs. In order to address some of these issues, DREV in collaboration with BOMEM (Québec Canada), has developed an instrument referred to as the Double Beam Interferometer Sounder (DBIS). This sounder has been conceived to match the needs encountered in many remote sensing scenarios: slant path capability, small field of view, very wide spectral coverage and high spectral resolution. Preliminary tests with the DBIS have shown sufficient accuracy for remote sensing applications³. In a series of field measurements, jointly organized by the Geophysics Directorate / PL, Hanscom AFB, and DREV, the instrument has been run in a wide variety of sky conditions. Several atmospheric emission spectra recorded with the sounder have been compared to calculations^{4, 5} with FASCODE and MODTRAN models. The quality of measurement- model comparisons has prompted the development of an inversion algorithm based on these codes. The purpose of this paper is to report the recent progress achieved in this research. First, the design and operation of the instrument are reviewed. Second, recent field measurements of atmospheric emission spectra are analyzed and compared to models predictions. Finally, the simultaneous retrieval approach selected for the inversion of DBIS spectra to obtain temperature and water vapor profiles is described and preliminary results are presented.

2. INSTRUMENT DESCRIPTION

Essentially the DBIS is made of one or optionally two 10-in. diameter Cassegrain telescopes, optically coupled to a double-input port Fourier transform spectrometer and two detection units (output optics 1 and 2). Figure 1 summarizes the design of the instrument. This configuration allows measurements of calibrated spectra according to the following specifications: any selectable zenith angle, scene field of view of 5 mrad, spectral coverage from 3 to 20 μm and a spectral resolution of 1 cm^{-1} or greater. As a part of the input modules, a large flat plate scene mirror placed in front of each telescope can be either rotated to the selected scene or oriented in a position for the acquisition of calibrated reference spectra. The pointing capability of this scene mirror allows slant path measurements from 0 to 360 degrees with a tilt adjustment of ± 10 degrees in azimuth and an accuracy of 0.1 degree. The coarse adjustment in azimuth is simply achieved by rotating the whole assembly mounted on a tripod. After reflection on the scene mirror, the beam is then successively focussed by the Cassegrain telescope and reflected by an off-axis parabolic mirror (PM) to produce a collimated beam of proper diameter at the entrance of the spectrometer. The two output modules are identical, except that channel-1 includes a MCT detector optimized for the 5-20 μm spectral region while channel-2 includes an InSb detector optimized for the 2-5 μm region. Note that the InSb module is not explicitly shown in Fig. 1. These modules contain parabolic and condensing mirrors that focus the beam coming from the interferometer onto a detector (MCT or InSb) of 1 mm diameter. An aperture wheel (AW) mounted with stops of different diameters permits the adjustment of the field of view of the instrument (5 mrad or smaller). A CCD camera integrated into the telescope module can be used to aim and visualize the scene under consideration.

DOUBLE BEAM INTERFEROMETER SOUNDER (DBIS)

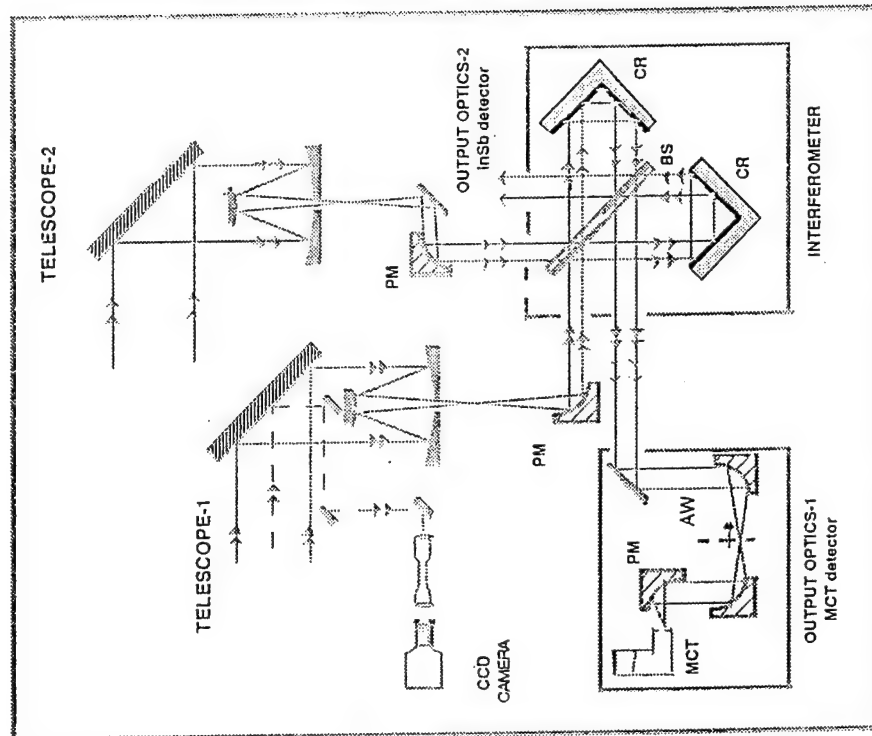


Figure 1: DBIS Optical Train.

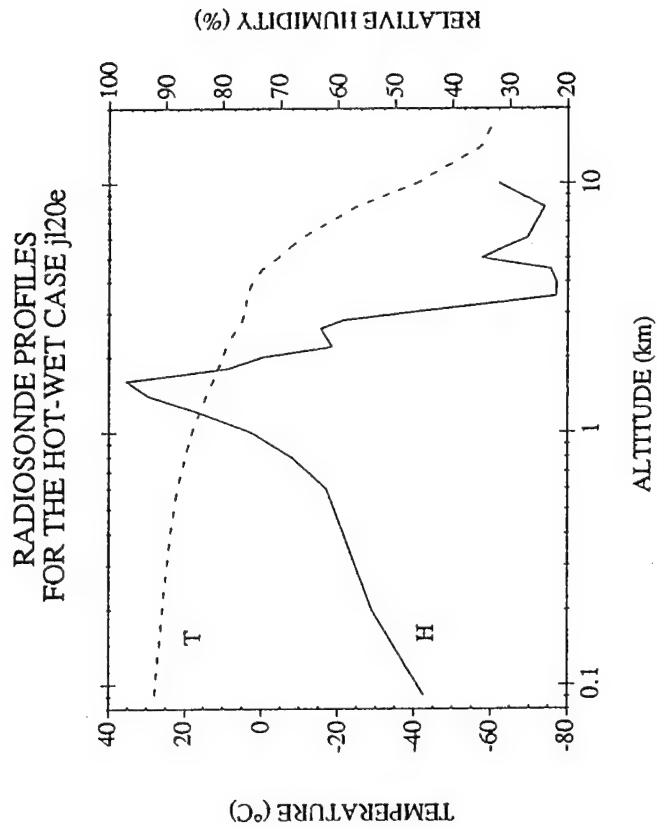


Figure 2: Vertical Profiles of T and RH.

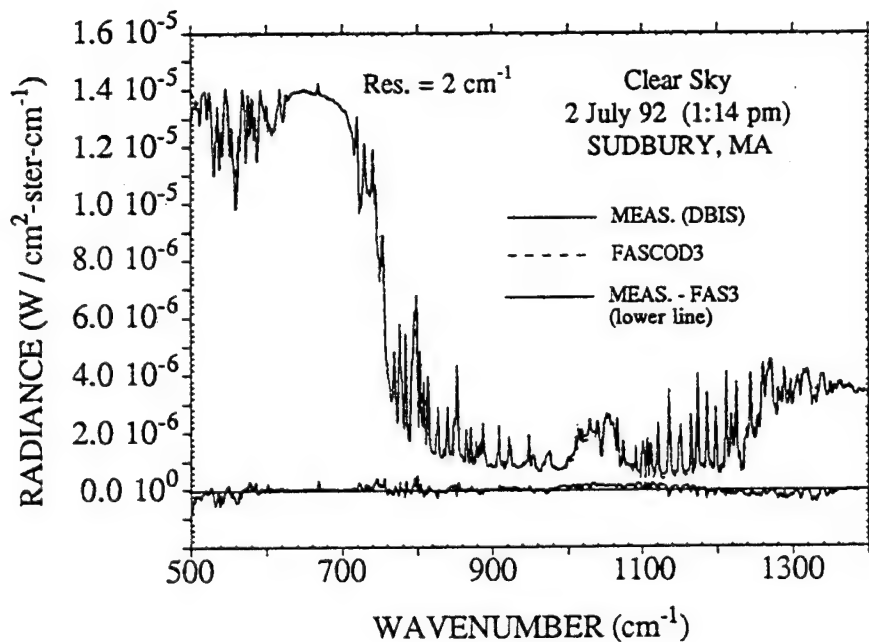


Figure 3. Atmospheric uplooking emission spectra as measured by the DBIS system and calculated by FASCOD3.

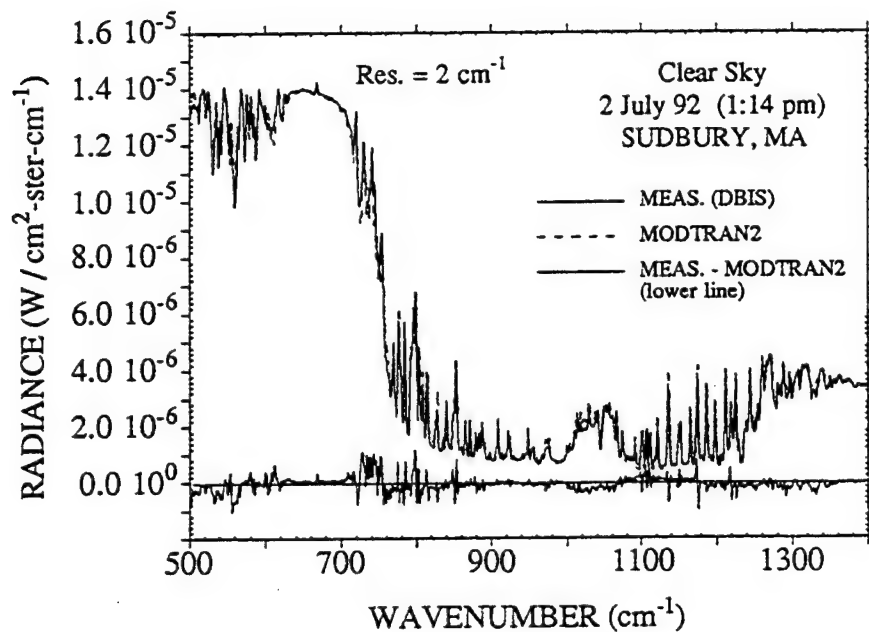


Figure 4. Atmospheric uplooking emission spectra as measured by the DBIS system and calculated by MODTRAN2.

INVERSION ALGEBRA:

Theriault and Moncet (TM) have established the development of a successful simultaneous (temperature and water vapor profile) retrieval algorithm, based primarily on FASCOD3 forward calculations, with accompanying derivative matrices.

Traditionally the derivative matrices required for the least square residual technique embody time-consuming forward runs of full-path FASCODE radiance predictions, each run differing from its predecessor by a single small perturbation,

$$x = x_0 + x',$$

where: $x = T(K)$ or $H_2O(g/m^3)$, for each layer, l .

The Jacobian matrix is then defined as the set of differences in total radiance:

$$\frac{dR(x,l)}{dx} = \frac{R(x,l) - R_0}{x'} \quad (8)$$

where: R_0 is the unperturbed total radiance
and $R(x,l)$ is the total radiance with a single perturbation
($x = x_0 + x'$ and $x' = T'$ or H_2O') at layer l

The size of the original matrix is: $j \times k$

where: j is the number of spectral channels,
often dependent on spectral resolution,
and k is (at minimum) the number of atmospheric layers
or boundaries times the number of constituents
undergoing perturbation in the simultaneous retrieval.

MODTRAN2 vs. FASCOD3 JACOBIANS

Moncet and colleagues³³ have recently devised a scheme to greatly optimize calculations of the Jacobian elements, based on FASCODE.

However, even with these modifications, the task still consumes a formidable amount of computer time.

MODTRAN2 Jacobian calculations: each full path radiance calculation has been done with and without the perturbation at each layer over the spectral range of the DBIS instrument.

The subsequent derivative matrix elements have then been compared to the equivalent FASCODE elements.

The RMS differences in the Jacobian radiances (Eq. 8 with the denominator set to unity) are of the order of $1.e-8$ to $1.e-10$ compared to an average radiance of $3.e-6$ W/(cm²-ster-cm-1), smaller than 3 parts in 1000.

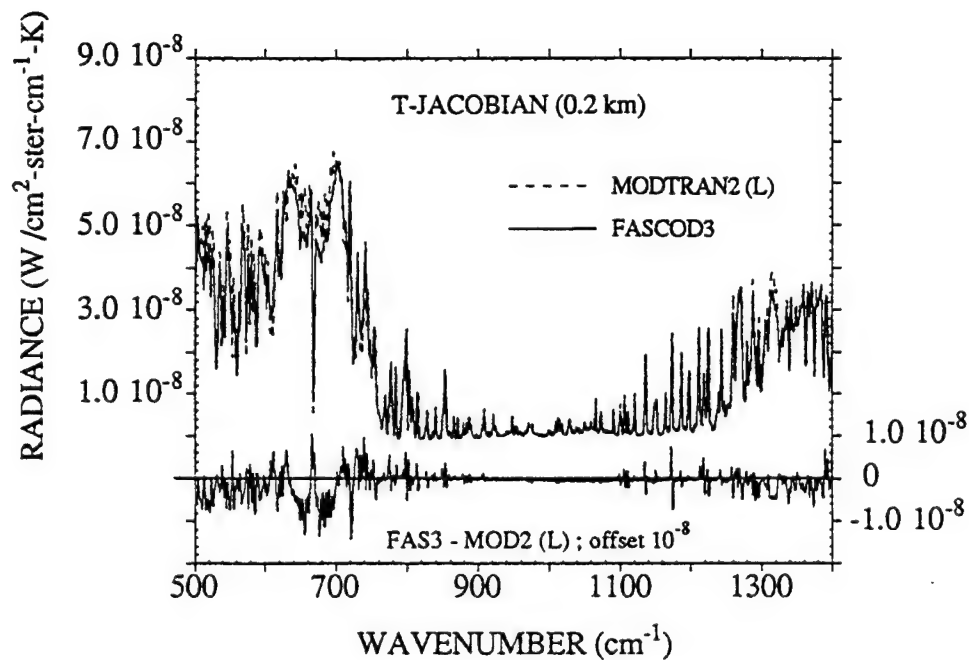


Figure 5. Temperature Jacobians for a 2 K temperature perturbation at an altitude of 0.2 km and where the original temperature and water vapor profiles correspond to supporting radiosonde data appearing in Fig. 2 (jl02).

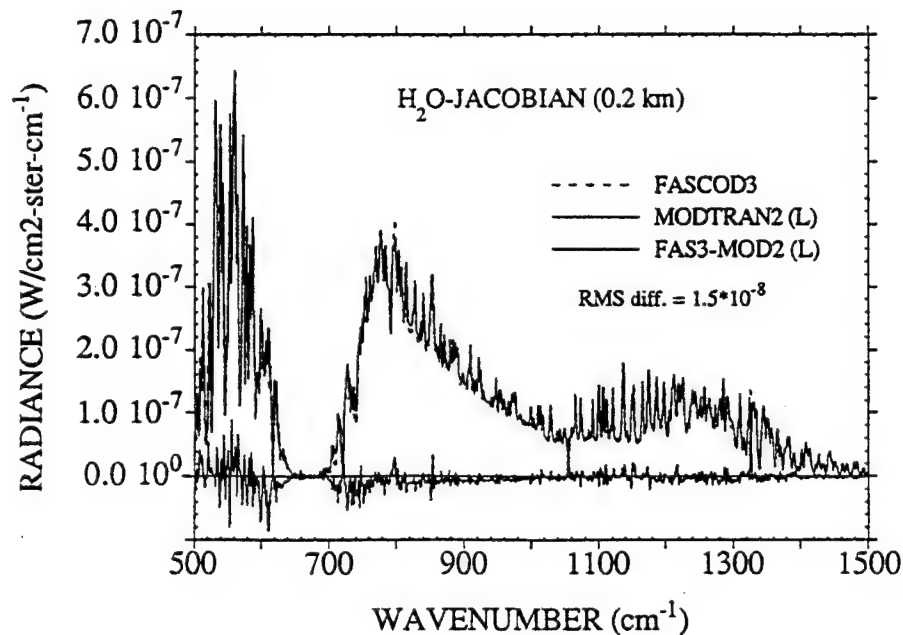


Figure 6. Water vapor Jacobians for a 0.1 g/m^3 perturbation at 0.2 km for the same conditions as Fig. 5.

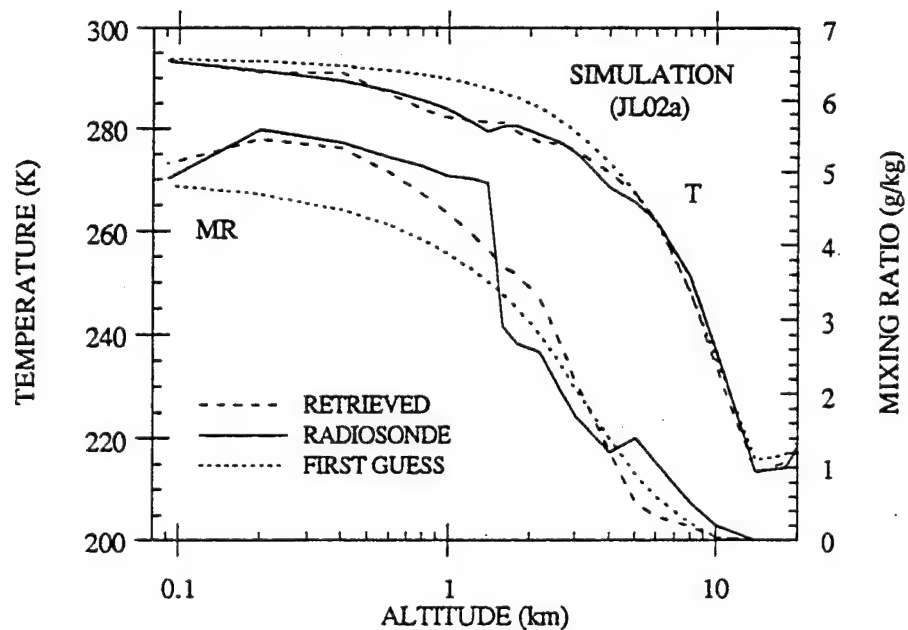


Figure 7. Simultaneous retrieval of T and H₂O profiles for the hot-dry case : Inversion from SIMULATED spectrum.

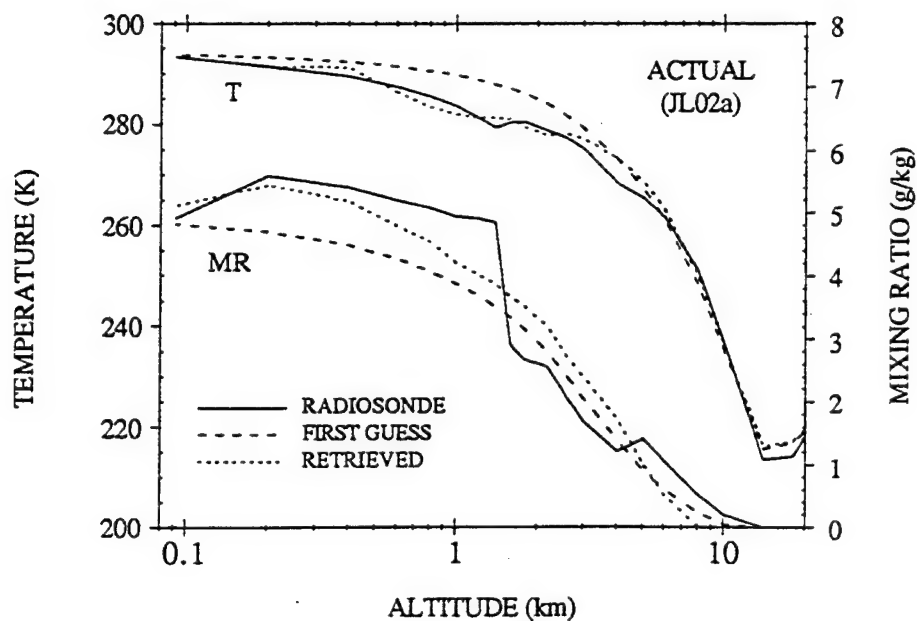


Figure 8. Simultaneous retrieval of T and H₂O profiles for the hot-dry case : Inversion from MEASURED spectrum.

PCModTRAN 2:
ONTAR'S PC COMPATIBLE MODTRAN 2 SOFTWARE

**L.W. Abreu, J. Schroeder, A. McCann,
J. Kristl, S. Harvey and M. Voltaire**

ONTAR Corp.
129 University Road
Brookline, MA 02146

PCModTRAN 2 is an implementation of the Phillips Laboratory/Geophysics Directorate's MODTRAN 2 model and contains user-friendly software for manipulation of the input and output of the calculations. This package is compatible with IBM and all other personal computers. The software package has an input generation shell, on-line help capability, an ASCII text file viewer for all output files, screen graphics and hard copy graphics. A Cooperative Research and Development Agreement for MODTRAN 2 is awaiting final approval by Phillips Laboratory.

PCModTRAN 2:
ONTAR's PC COMPATIBLE
MODTRAN 2 SOFTWARE

L.W. Abreu, J. Schroeder, A. McCann,
J. Kristl, S. Harvey and M. Voltaire

ONTAR Corporation,
9 Village Way, North Andover, MA 01845

Presented at
Annual Review Conference on Atmospheric Models
8-9 June 1993
Geophysics Directorate/Phillips Laboratory
Hanscom AFB, MA 01731

ONTAR
CORPORATION

PC VERSION OF LOWTRAN 7

PCTRAN 7

* COOPERATIVE RESEARCH AND DEVELOPMENT AGREEMENT
GEOPHYSICS DIRECTORATE/PHILLIPS LABORATORY

AND

ONTAR CORPORATION

* PCTRAN 7 has been validated by Phillips Laboratory

PCTRAN 7

Personal Computer Version of the LOWTRAN 7 Atmospheric Model

Version 2

June 1990



ONTAR Corporation
129 University Road
Brookline, MA 02146
(617)-739-6607



Air Force Geophysics Laboratory
Hanscom AFB, MA 01731

PC VERSION OF MODTRAN 2

PCModTRAN 2

*** COOPERATIVE RESEARCH AND DEVELOPMENT AGREEMENT
GEOPHYSICS DIRECTORATE/PHILLIPS LABORATORY**

AND

ONTAR CORPORATION

*** Awaiting Approval by AFMC
and
Validation by Phillips Laboratory**



Hardware and Software Requirements

Personal Computer - XT, AT, 80386, 80486 (Compatible, Clone)

1.2 Mbyte Diskette Drive, Hard Disk

640 Kbytes of Memory

CGA, EGA, or VGA Graphics Board and Monitor - for Screen Plots

Printer - for Hard Copy

Numeric Co-processor Highly Recommended



ONCORE Suite of Atmospheric Modeling Tools
 MODTRAN2/LOWTRAN7/SENTRAN7 Models
 Ontar Corporation

```

< ONIN > A View and edit model inputs
< MODTRAN > B Run the model
< ONPLT > C Plot model outputs
< PRTPLT > D Plot hardcopy
< ONMPIN > E Multiple plots
< ONFILIN > K Filter function inputs
< ONFIL > L Run filter function
View FILEOUT> M View filter output
View FILE9> P View scan output
< Exit ONCORE > X Return to DOS
<Debug DOS Shell>
  
```

Misc functions
 < Help > I
 <Configure paths> J

CASEM1	CASEM10	CASEM11	CASEM12	CASEM13	CASEM2	CASEM3	CASEM4
CASEM5	CASEM6	CASEM7	CASEM8	CASEM9	CASEM10	CASEM11	CASEM12

F10=Keys

Select DataBase File

A10MOZ	ACZ20V	ACZDENMS	ACZMS	ACZMS20	ACZMSUN	ACZND20	ACZNDEN
ACZOCT	ACZRUR	ACZSS	ALANG	ALANGMD	AMATER	ANDYMR	APIRT
APLTST	APTSTMD	BALL40T	BALLANGL	BETABALL	BETLOR	BETLOWT	BETSENT
BOWER	BOWER2	BOWERST	CASE1	CASE10	CASE11	CASE12	CASE13
CASE2	CASE3	CASE4	CASE5	CASE6	CASE7	CASE8	CASE9
CASEM1	CASEM10	CASEM11	CASEM12	CASEM13	CASEM2	CASEM3	CASEM4
CASEM5	CASEM6	CASEM7	CASEM8	CASEM9	CCASE2	CCASE3	CLOSE
CLOSLIN	CSEM1A	CSEM1SS	CSEM1T	CZTDEC	DC1000	DC250	DC2520
DCSTSPC	DUANE	DUANE100	DUANE1M	DUANE3KM	DUANE7	GEOERR	HIGGF8
INDYM3	KEIL229	KEILFTL	KEILNMS	MCASF2	MCASF3	MORTN	NEW
OPM-A	OPM-B	OPMVER	POROLIN	POROS	SCHHEEL	SEN1	SEN2
SINGAP	SOIRAD	SWIRATH	T1ONCH42	T1ONCH45	T1ONCO	T1ONCO22	T1ONCO23
T1ONCO25	T1ONH205	T1ONH213	T1ONH202	T1ONHNO3	T1ONN202	T1ONO32	T1ONO33
T1ONO35	T15NCH45	T2ONCH45	T2ONCO2	T2ONCO25	T2ONH20	T2ONN205	T2ONN23
T2ON0358	T2ONOHNO	T2ONW58	T3ONCH42	T3ONCH45	T3ONCO	T3ONCO22	T3ONCO25
T3ONH202	T3ONH205	T3ONN202	T3ONN205	T3ONN032	T3ONN035	T4ONCH45	T4ONCO25
T4ONH205	T4ONHNO3	T4ONN205	T4ON033	T4ON035	T4ONOCO2	T4ONOH20	T4ONOHNO
T4ON003	T5M7TOT	T5NH2013	T5NO3L7	T5O3ONTY	T5TOT17	TAN201R	TAN20RSC
TAN20T58	TAN30T25	TAN30T58	TAN4013	TAN40CO2	TAN40H20	TAN4003	TAN40T13
TAN40T58	TEST	TN10NN20	TN10R13	TN10R25	TN10R5R	TN15NH20	TN15NN20
TN15NO35	TN15R58	TN3NN20	TN3RD58	TN5NCH45	TN5NH205	TN5NN20	TN5NO35
TN5RD13	TN5RD58	TN8NN20	TN8R58	TSTFTL	TZ	URAT	URATO
URAIAL1	ZZ	ZZZ	NEW FILE				

Select DataBase File

F10=Keys

Atmospheric Model to Use Model Atmosphere	MODTRAN Tropical Model
Type of Atmospheric Path	Horizontal Path
Mode of Execution	Transmittance
Executed With Multiple Scattering	No
Temperature & Pressure Altitude Profile	Tropical Model
Water Vapor Altitude Profile	Tropical Model
Ozone Altitude Profile	Tropical Model
Methane Altitude Profile	Tropical Model
Nitrous Oxide Altitude Profile	Tropical Model
Carbon Monoxide Altitude Profile	Tropical Model
Other Gases Altitude Profile	Tropical Model
Radlosonde Data are to be Input	No
Output File Options	Include ATM Profiles
Temperature at Path Start (K)	.0000
Surface Albedo (reflectivity)	.0000
Run # 1 of 1	MODTRAN
	Card 1
	<Next> <Plot> <Exit> <F10 = Keys>

Aerosol Model Used

Seasonal Modifications to Aerosols

Upper Atmosphere Aerosols (30-100 km)

Air Mass Character for Navy Maritime Aerosols

Use Cloud/Rain Aerosol Extensions

Use of Army (VSA) for Aerosol Extension

Surface Range for Boundary Layer

Wind Speed-Navy Maritime Aerosols(m/s)

24-Hr Ave Wind Speed-Navy Maritime(m/s)

Rain Rate (mm/hr)

Ground Altitude above Sea Level (km)

Navy Maritime

Determined by Model

Background Stratospheric

0

No Clouds or Rain

No

.000

.000

.000

.000

.000

Run # 1 of 1

MODTRAN

Card 2

<Prev>

<Next>

<Home>

<Exit>

<F10 = Keys>

Initial Altitude (km)		.000	
Final Altitude/Tangent Height (km)		.000	
Initial Zenith Angle (degrees)		.000	
Path Length (km)		10.000	
Earth Center Angle (degrees)		.000	
Radius of Earth (km) [.000 - default]		.000	
Type of Path	Short		
Initial Frequency	900.000 cm ⁻¹	Wavelength	8.696 μ m
Final Frequency	1150.000 cm ⁻¹	Wavelength	11.111 μ m
Frequency Increment (wavenumber)			1.000
FWHM of Triangular Slit (wavenumber)			2
Run # 1 of 1	LOWTRAN	CARDS 3 & 4	F10 = Keys

Plot Type
 Type of X Axis
 Type of Y Axis
 Number of Decimal Digits for Y Axis
 Length of X Axis (in inches)
 Beginning Wavenumber/Wavelength
 Ending Wavenumber/Wavelength
 X Axis Annotation Interval
 X - Number of Minor Ticks / Division
 Length of Y Axis (in inches)
 Autoscale Y Axis
 Minimum Transmittance/Radiance
 Maximum Transmittance/Radiance
 Y Axis Annotation Interval
 Y - Number of Minor Ticks / Division
 Plot Grids (Graph Paper)

Transmittance in cm-1
 Linear
 Linear
 1
 7.0000
 900.0000 cm-1
 1150.0000 cm-1
 50.0000 cm-1
 5
 6.0000
 No
 0.00E+00
 1.00E+00
 2.00E-01
 4
 No Grids

Run # 1 of 1

ONPLT Scaling

Plot # 1

F10=Keys

Plot Title:

CASE #7

Line Type (-99 no line)

Total Transmittance
Water Vapor Band Transmittance
Uniformly mixed Gases Transmittance
Ozone Transmittance
Trace Gases Transmittance
Nitrogen Continuum Transmittance
Water Vapor Continuum Transmittance
Molecular Scattering Transmittance
Aer-Hyd Transmittance
Nitric Acid Transmittance
Aer-Hyd Absorptance
CO Transmittance
CH4 Transmittance
N2O Transmittance
O2 Transmittance
NH3 Transmittance
NO Transmittance
NO2 Transmittance
SO2 Transmittance
CO2 Transmittance

Run # 1 of 1

ONPLOT Lines

Plot #1

F10 = Keys

Run # 2 of 4 LOWTRAN7 Cards 3 & 4

CONTINUED

PC-TRAN7 Batch Mode Manager.

ESC - Quit LOWIN (write LOWIN and LOWPLT.DAT)
F2 - Edit current run.
F3 - Edit next run.
F4 - Edit previous run.
F5 - Add new run (to end) and go to that run
F6 - Delete current run.
F7 - Go to run.

Database name MCASE3

Number of runs in this database 4 Current run 3

LOWTRAN7 Card 5

CONTINUED

SAMM: SHARC AND MODTRAN MERGED

**A. Berk,¹ D.C. Robertson,¹ L.S. Bernstein,¹
R.L. Sundberg,¹ R.D. Sharma,² G.P. Anderson,²
J.H. Chetwynd,² M.L. Hoke,² and R.J. Healey³**

¹Spectral Sciences, Inc.
99 South Bedford Street, #7
Burlington, MA 01803-5169

²Phillips Laboratory/GPOS
29 Randolph Road
Hanscom AFB, MA 01731-3010

³Yap Analytics
594 Merrett Road
Lexington, MA 02173

Radiation transport calculations of ambient IR radiation can be roughly divided into two categories, the lower altitude regions below about 30 km which are in local thermodynamic equilibrium and the non-LTE contributions at higher altitudes. MODTRAN is a low altitude radiance code which models aerosol and molecular scattering and absorptions, refractive path geometry, and multiple scattering. SHARC models high altitude line-of-sight radiances by solving the pertinent chemical kinetic equations and performing equivalent width line-by-line (LBL) calculations. We discuss the development of a merged model which has been dubbed SAMM, SHARC And MODTRAN Merged. SAMM includes a fast expanded LBL approach which is applicable to both altitude regimes, and contains all MODTRAN and SHARC model features. We will demonstrate that SAMM predictions vary smoothly as LOS tangent heights are increased from low to high altitude.

SAMM: SHARC AND MODTRAN MERGED

WORK SUPPORTED BY SDIO, PMA-1105

A. BERK, P. K. ACHARYA, J. GRUNINGER,
M. W. MATTHEW & D. C. ROBERTSON
SPECTRAL SCIENCES, INC., BURLINGTON, MA 01803

R. D. SHARMA, G. P. ANDERSON,
J. H. CHETWYND & J. H. BROWN
AF PHILLIPS LABORATORY, HANSCOM AFB, MA 01731

R. J. HEALEY & J. J. VAIL
YAP ANALYTICS, INC., LEXINGTON, MA 02173

ANNUAL REVIEW CONFERENCE ON
ATMOSPHERIC TRANSMISSION MODELS

8 JUNE 1993



MOTIVATION

- SYSTEM STUDIES AND DATA ANALYSIS FROM MEASUREMENT PROGRAMS OFTEN REQUIRE SIMULTANEOUS EXAMINATION OF LOW (LTE) AND HIGH (NON-LTE) ALTITUDE REGIONS
- SHARC PREDICTS HIGH ALTITUDE LOS RADIANCES, WHILE MODTRAN PREDICTS LOW ALTITUDE LOS RADIANCES
- RADIANCE PROFILES PRODUCED BY MERGING PREDICTIONS FROM THE TWO CODES OFTEN YIELD A DISCONTINUITY ARISING FROM
 - ATMOSPHERIC PROFILE DISCREPANCIES
 - NON-LTE EFFECTS
 - SCATTERING
 - RADIANCE ALGORITHM DIFFERENCES
- SAMM IS THE SOLUTION, A SINGLE CORRELATED LOS RADIANCE MODEL



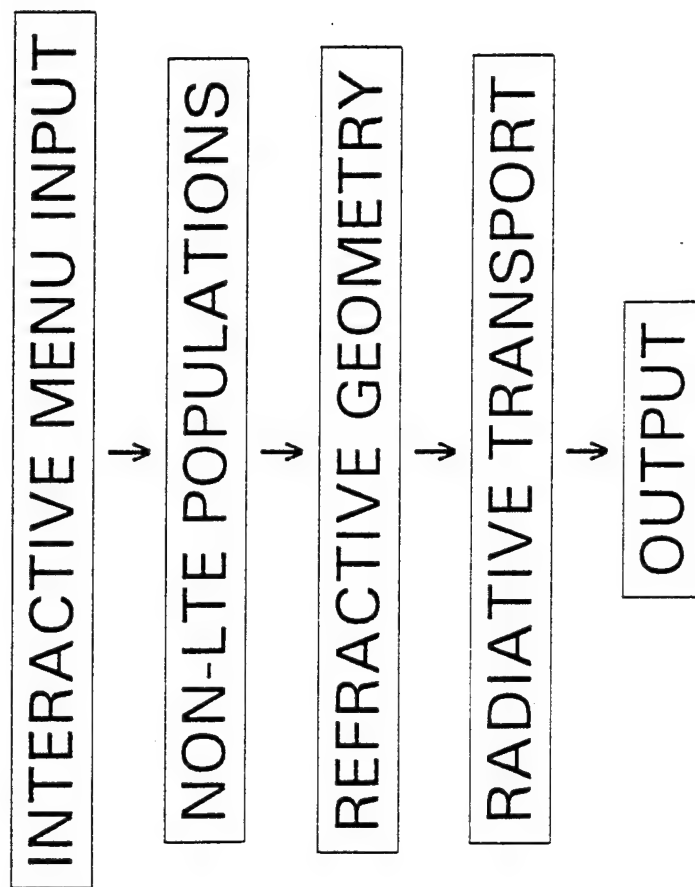
SAMM OVERVIEW

SAMM IS A MODEL FOR ATMOSPHERIC RADIANCE AND TRANSMITTANCE CREATED BY INTEGRATING SHARC AND MODTRAN

- SEAMLESS ATMOSPHERE AND CORRELATED RADIATIVE TRANSPORT ALGORITHM
- ARBITRARY LOS FROM GROUND THROUGH THERMOSPHERE (300 KM)
- 2 TO 40 μm SPECTRAL RANGE, 1 CM^{-1} BINS
- AUROREAL AND TERMINATOR CHEMISTRY
- AEROSOLS, CLOUD & RAIN MODELS
- SINGLE AND MULTIPLE SCATTERING
- REPEAT RUN OPTIONS



CALCULATIONAL SEQUENCE





INPUT MODULE (SAMPLE MENU)

SHARC-3 AND MODTRAN-2 MERGED, SAMM

REVIEW OR MODIFY INPUT PARAMETERS

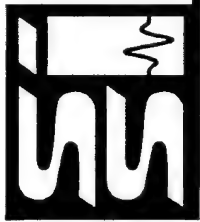
- 1) TITLE FOR CALCULATION
 - 2) REGION DEFINITION
 - 3) LOS GEOMETRY
 - 4) SPECTRAL INTERVAL, RESOLUTION AND SPECIES
 - 5) OUTPUT DATA
 - 6) STANDARD SET-UP FOR FILE NAMES
 - 7) INSTALLATION SETUP
 - 8) UPDATE DEFAULT FILE AND EXIT FOR BATCH EXECUTION
 - 9) UPDATE DEFAULT FILE AND EXIT
 - 10) EXIT WITH NO UPDATE OF DEFAULT FILE
 - 11) MODTRAN PARAMETERS
- ENTER # OF ITEM TO BE CHANGED OR
999 TO CONTINUE SAMM EXECUTION



NON-LTE POPULATIONS MODULE

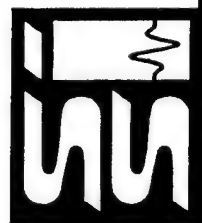
SAMM CALCULATES AN ALTITUDE
PROFILE OF VIBRATIONAL POPULATIONS
FOR EACH NON-LOCAL THERMODYNAMIC
EQUILIBRIUM (NON-LTE) MOLECULE

- CALCULATES SOLAR EXCITATION AND
EARTHSHINE PUMPING RATES
- SOLVES INPUT AMBIENT & AURORAL
CHEMICAL KINETIC EQUATIONS
- DETERMINES ENHANCEMENTS FROM
LAYER - TO - LAYER PUMPING



REFRACTIVE GEOMETRY MODULE

- TRACKS ALTITUDE, LATITUDE AND LONGITUDE ALONG LOS AND SOLAR PATHS
- MODELS REFRACTION BELOW 30 KM
- ALLOWS MULTIPLE REGIONS ABOVE 30 KM
- DETERMINES OPTICAL AND SOLAR PATH COLUMN DENSITIES



RADIATION TRANSPORT MODULE

EMISSION

- LINE-BY-LINE AT ALL ALTITUDES FOR MOLECULES
NON-LTE AT HIGH ALTITUDES
(H₂O, CO₂, O₃, CO, CH₄, NO, OH & NO⁺)
- BAND MODELS FOR OTHER RADIATORS
(NO₂, O₂, SO₂, NO₂, NH₃, HNO₃, AEROSOLS & CONTINUA)
- WEIGHTED AVERAGE USED TO COMBINE LTE
BLACKBODY AND NON-LTE SOURCE TERMS

SCATTERING

- SINGLE SCATTER SOLAR WITH PRE-STORED
MIE, HENY-GREENSTEIN OR USER-DEFINED
PHASE FUNCTIONS
- 2-FLUX MULTIPLE SCATTERING CALCULATION

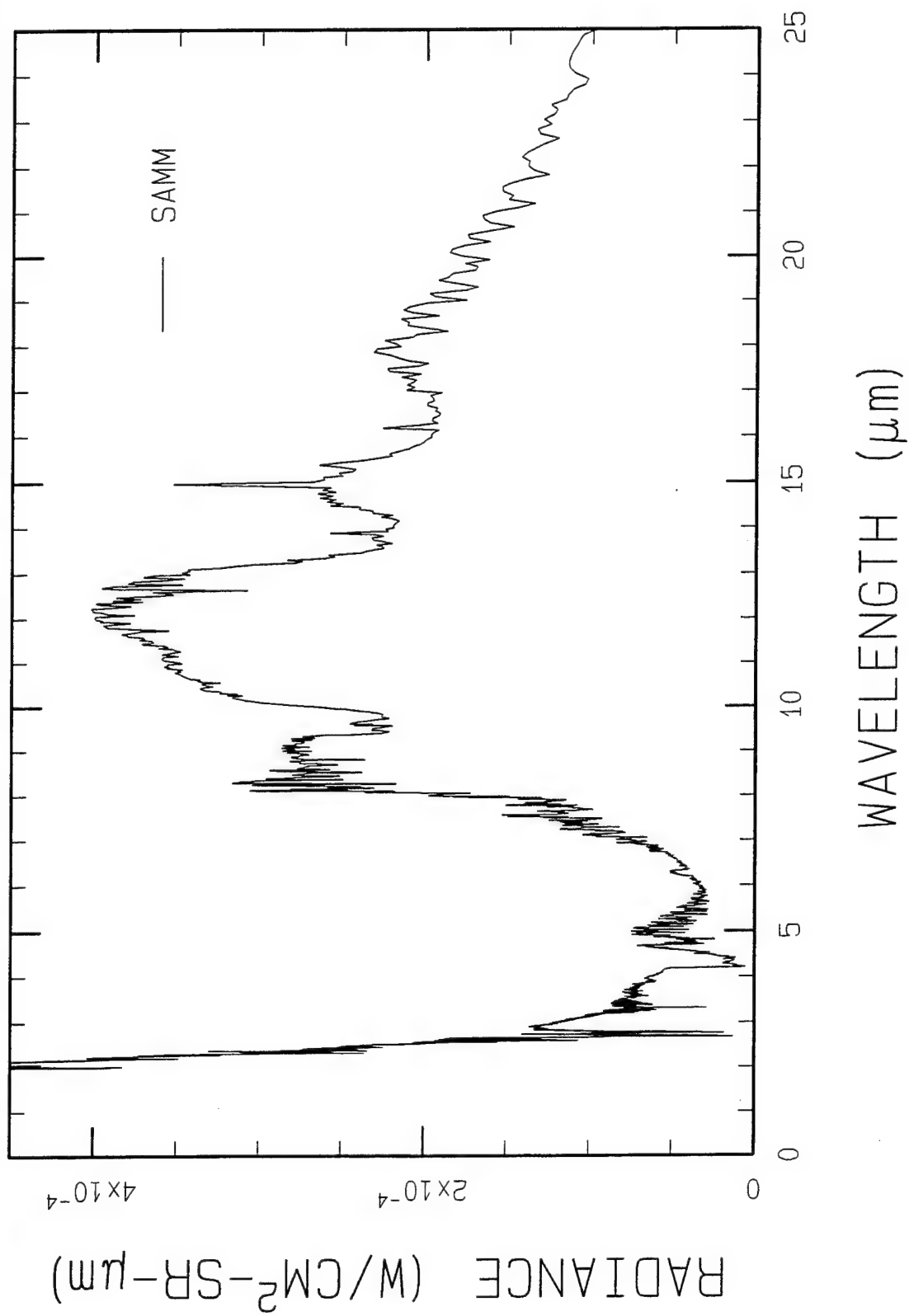


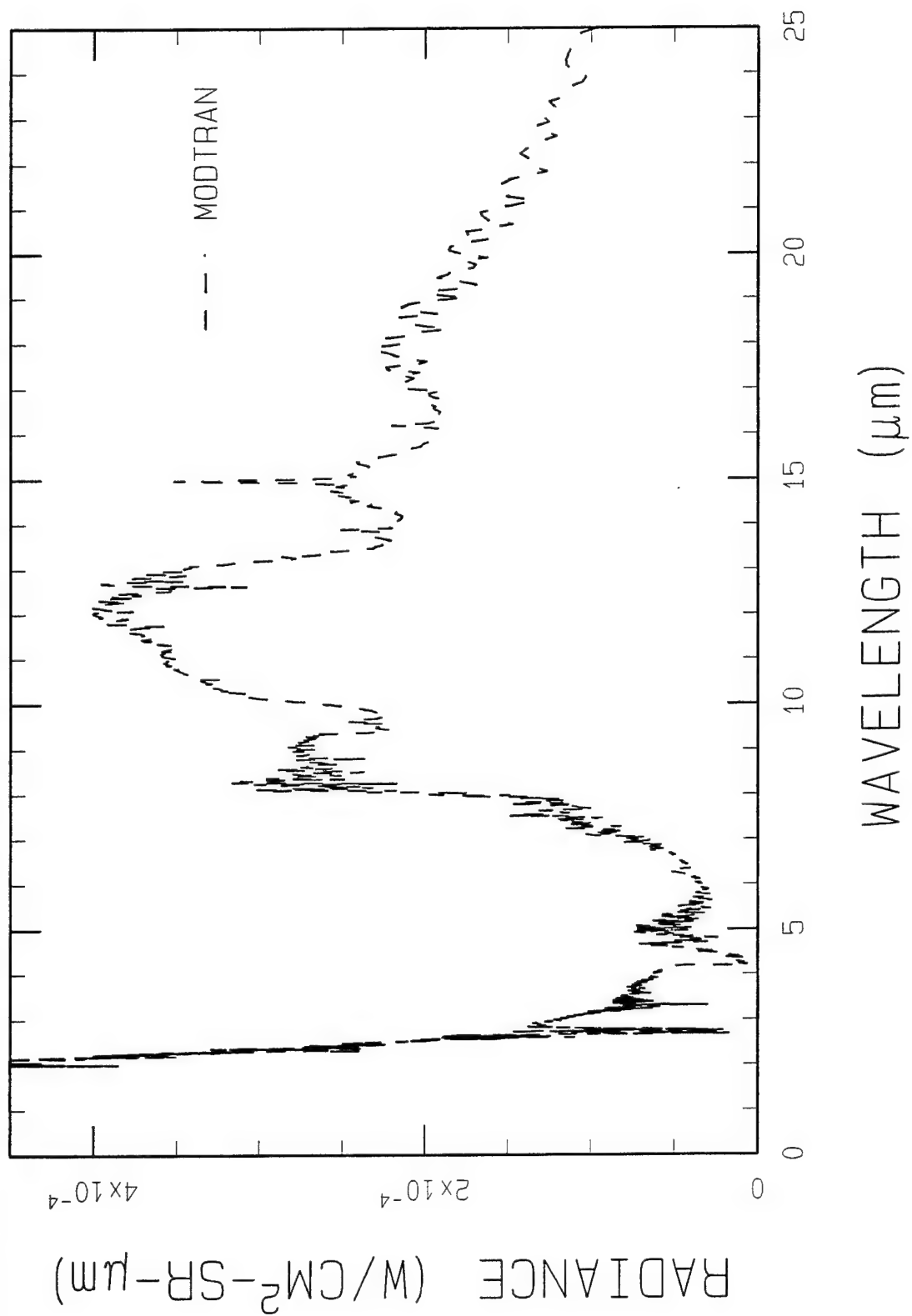
INITIAL VALIDATION

- SAMM HAS BEEN COMPILED AND RUN SUCCESSFULLY ON 4 DIFFERENT SYSTEMS, AND A PC VERSION IS PRESENTLY BEING TESTED.
- INITIAL VALIDATION OF SAMM IS BASED ON COMPARISONS TO SHARC AND MODTRAN.
- MODTRAN AND SHARC HAVE BOTH BEEN EXTENSIVELY VALIDATED AGAINST DATA.
 - SHARC FOR LOS ABOVE 50 KM
 - MODTRAN FOR LOS BELOW 50 KM
- SOME ILLUSTRATIVE VALIDATION CASES ARE PRESENTED.



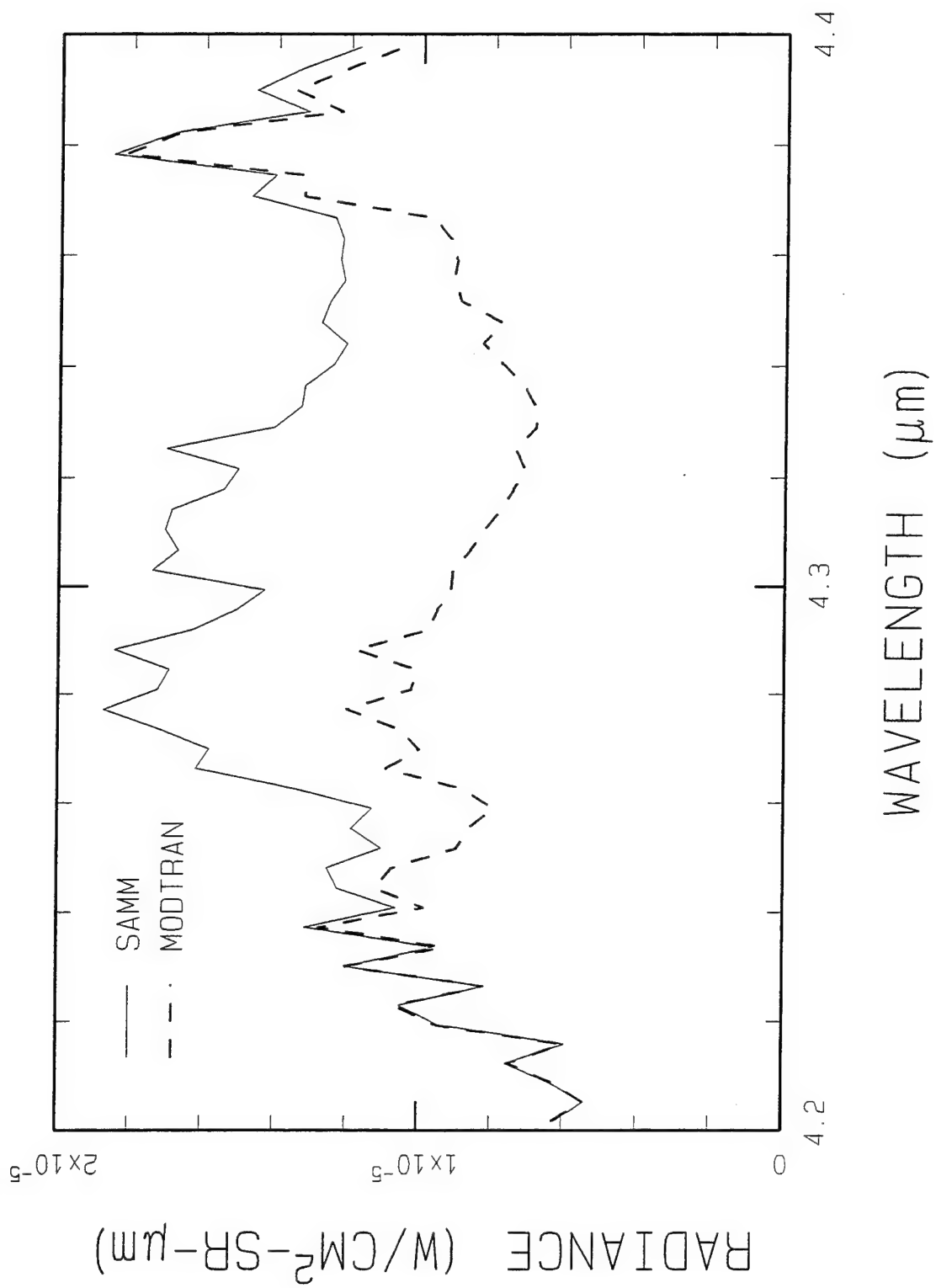
MIDDAY LIMB, TANGENT TO GROUND





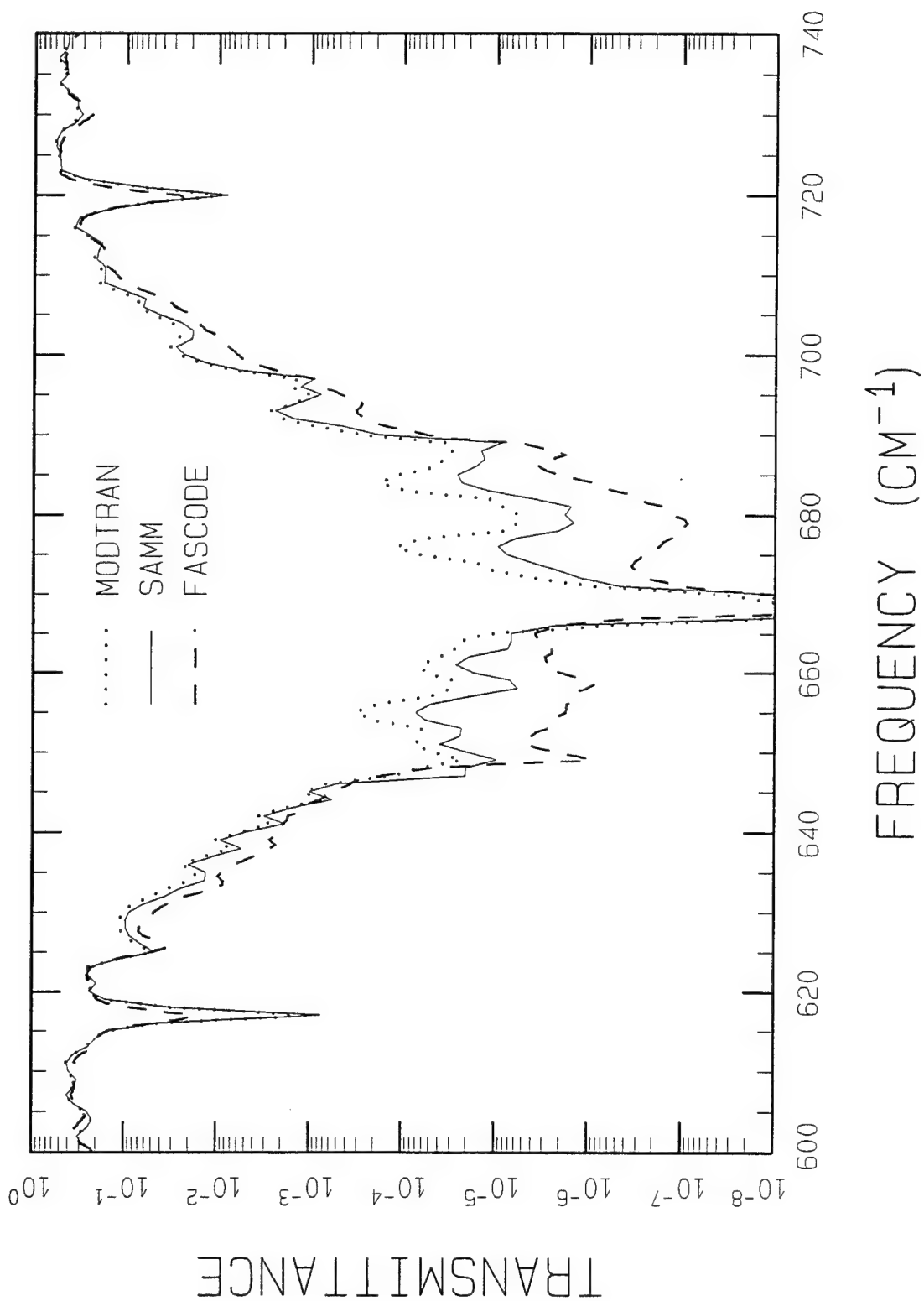


MIDDAY LIMB, TANGENT TO GROUND



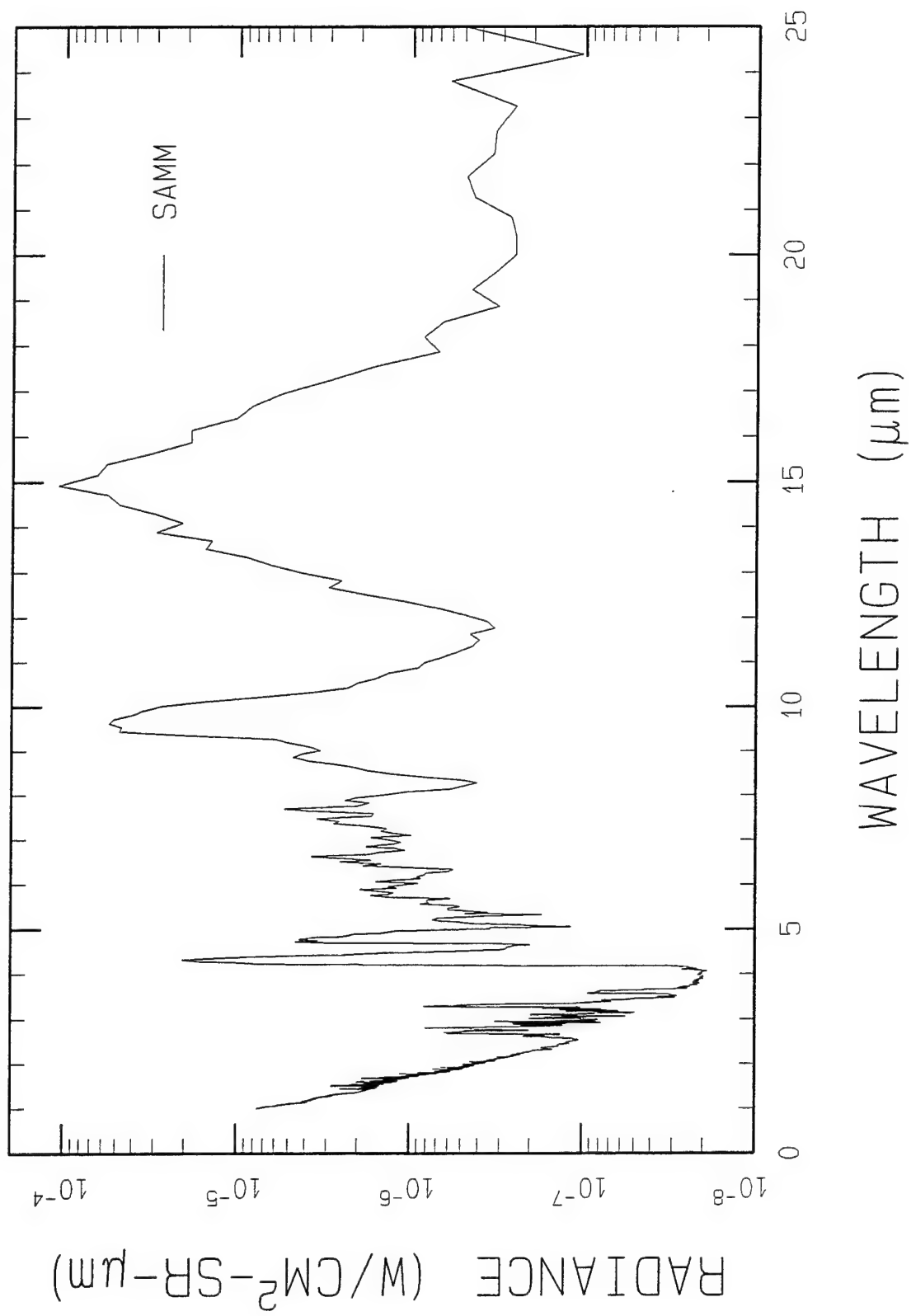


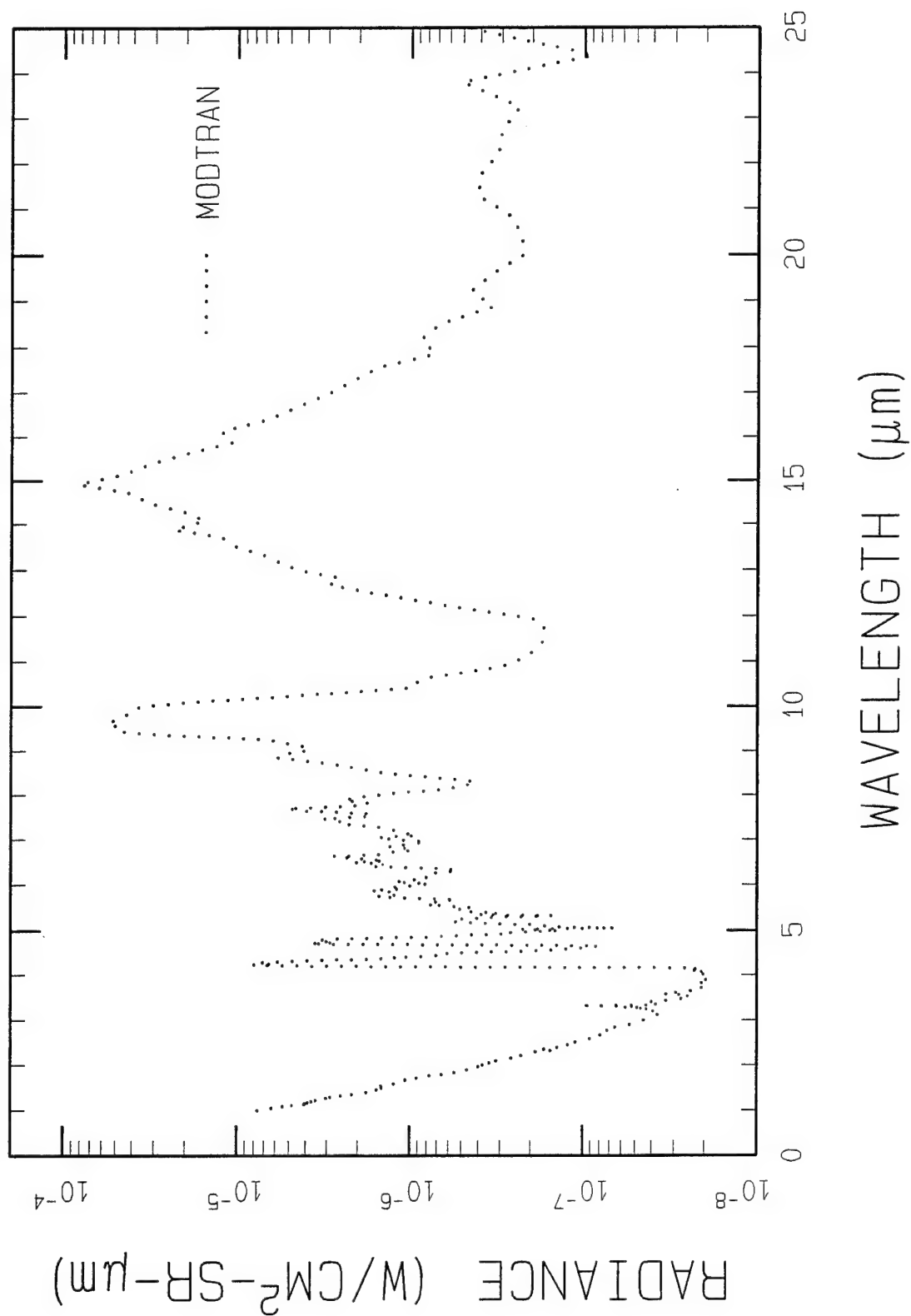
VERTICAL LOS FROM 0 TO 1 KM

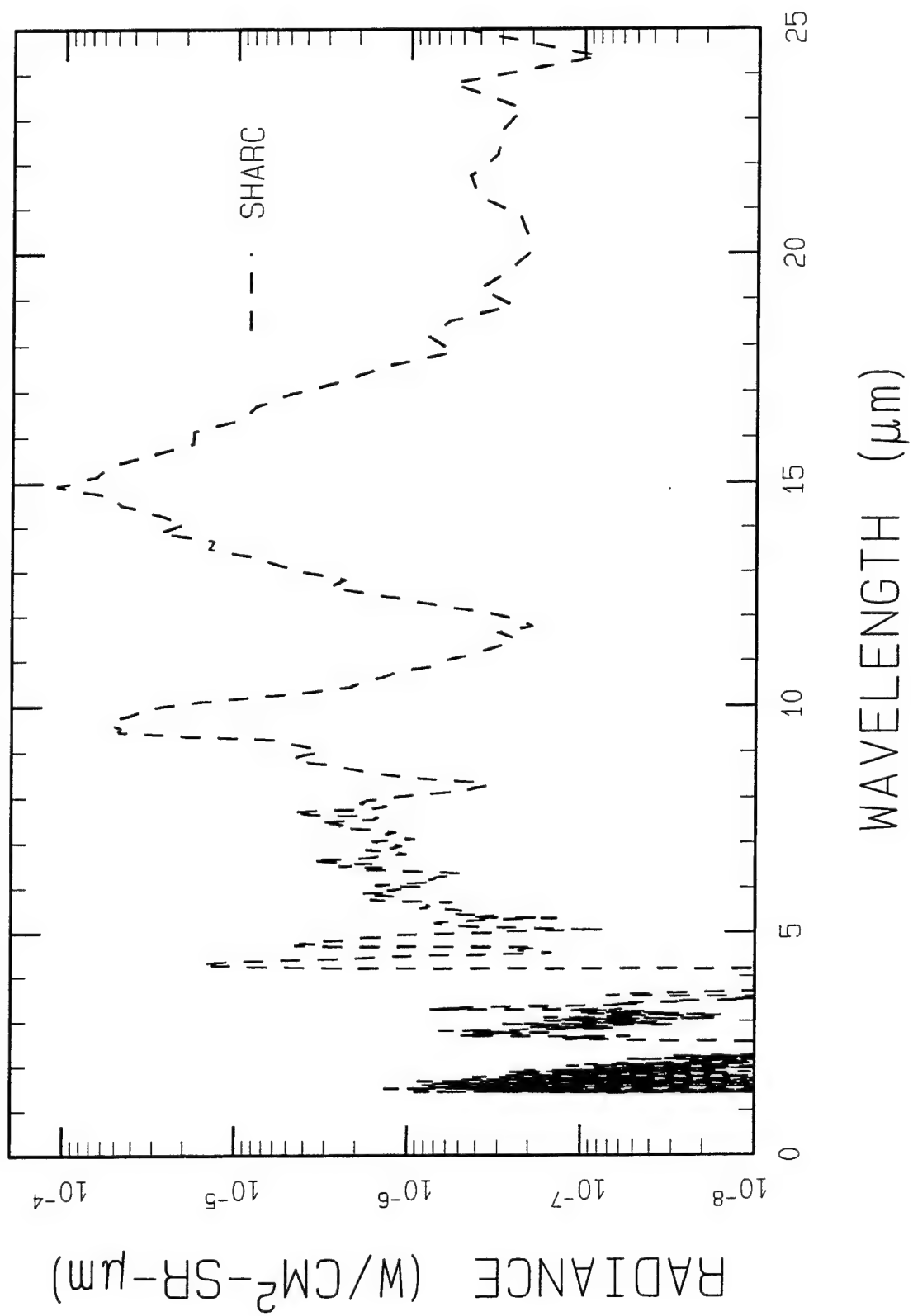




MIDDAY LIMB, TANGENT TO 50 KM

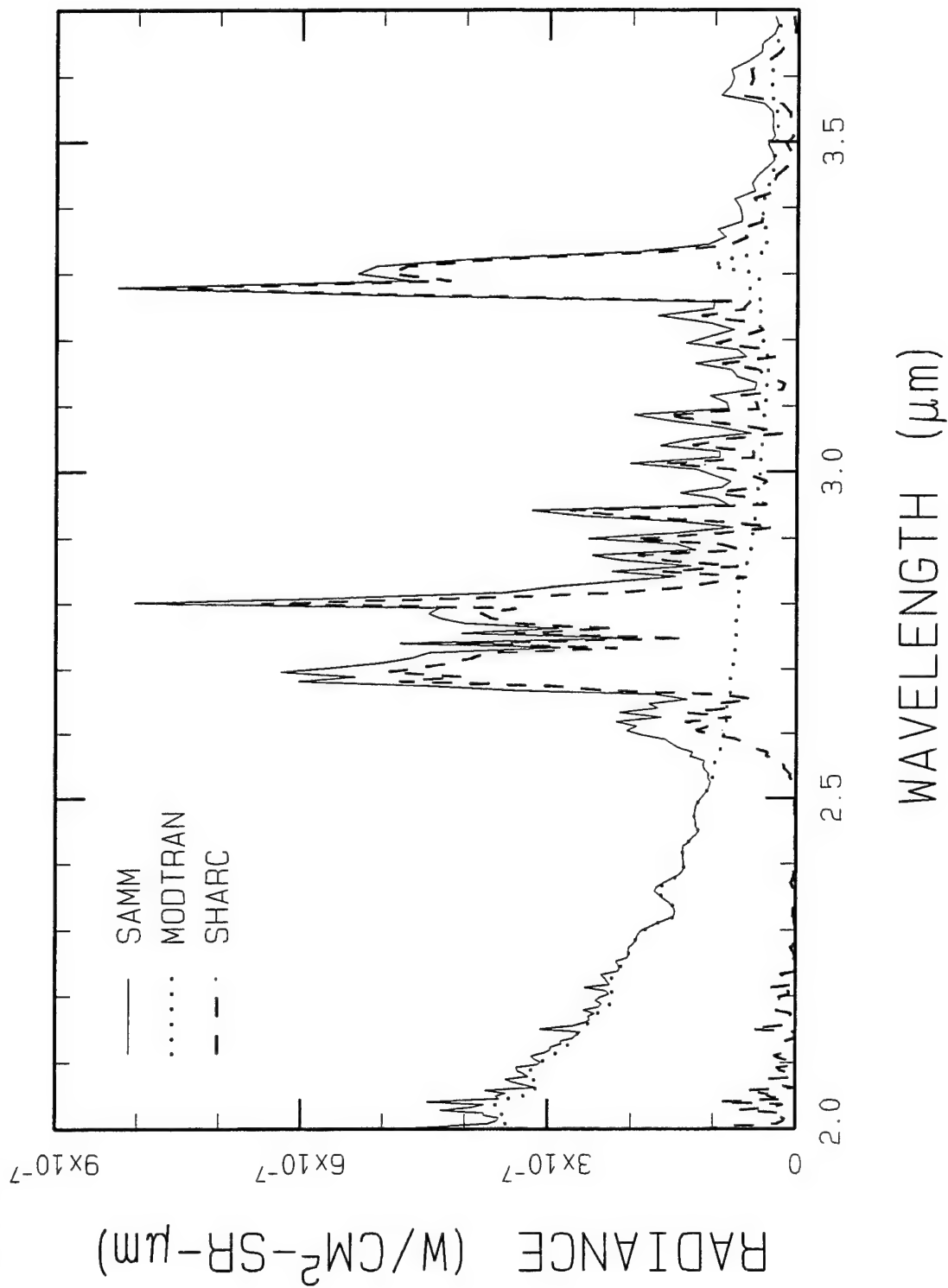








MIDDAY LIMB, TANGENT TO 50 KM





FUTURE PLANS

SAMM

- SAMM IS PRESENTLY UNDERGOING ADDITIONAL VALIDATION IN PREPARATION FOR A FALL '93 DISTRIBUTION.

SAMM2

- SAMM WILL BE MERGED WITH MOSART TO UPGRADE SURFACE EMISSION / REFLECTION PREDICTIONS.
- SHARC-4 WILL BE INTEGRATED INTO SAMM TO PERMIT MODELING OF ATMOSPHERIC STRUCTURE



SUMMARY

- SHARC-3 AND MODTRAN-2 HAVE BEEN SUCCESSFULLY MERGED INTO A SINGLE CODE.
- FOR LOS OR PROFILE STUDIES INVOLVING BOTH THE LOW (<50 KM) AND HIGH (>50 KM) ALTITUDE REGIMES, SAMM IS PREFERRED OVER USE OF SHARC-3 AND MODTRAN-2 INDIVIDUALLY.
- NON-LTE EFFECTS ARE IMPORTANT FOR SOME BANDPASSES EVEN WHEN THE LOS PASSES THROUGH LOWER ALTITUDES.
- SCATTERING CAN DOMINATE HIGH ALTITUDE LOS RADIANCES BELOW 4 μm .

**THE MODERATE SPECTRAL ATMOSPHERIC RADIANCE
AND TRANSMITTANCE (MOSART) PROGRAM**

W.M. Cornette

D.C. Robertson

Photon Research Assoc., Inc.
10350 N. Torrey Pines Road
Suite 300
La Jolla, CA 92037-1020

Spectral Sciences, Inc.
99 South Bedford Street, #7
Burlington, MA 01803-5169

The MOSART program, a new computer program for predicting and evaluating the radiative environment, incorporates features from the MODTRAN 2 and APART (Version 7.00) programs, plus adding some additional new features. The MODTRAN 2 1 cm^{-1} and LOWTRAN 7 20 CM^{-1} band parameters and geometry specifications are combined with the APART global climatology data bases, global terrain background data bases, and ray tracing algorithm to produce a combined atmosphere and background program for supporting target and background scene modelling, in particular the Strategic Scene Generation Model. The program can interpolate primary atmospheric parameters over multiple model atmospheres as well as use a single model atmosphere. Heat transfer calculations for the terrain materials are included, and terrain clutter parameters (i.e., mean, standard deviation, PSD) are output. Utilities for creating input files, spectral tables, spectral plots, luminance, and statistical two-dimensional backgrounds are included.

THE MODERATE SPECTRAL ATMOSPHERIC RADIANCE AND TRANSMITTANCE (MOSART) PROGRAM

Presented at the
Annual Review Conference on Atmospheric Models
Hanscom AFB, Massachusetts
8-9 June 1993

Presented By:
Dr. William M. Cornette
Photon Research Associates, Inc.
La Jolla, California

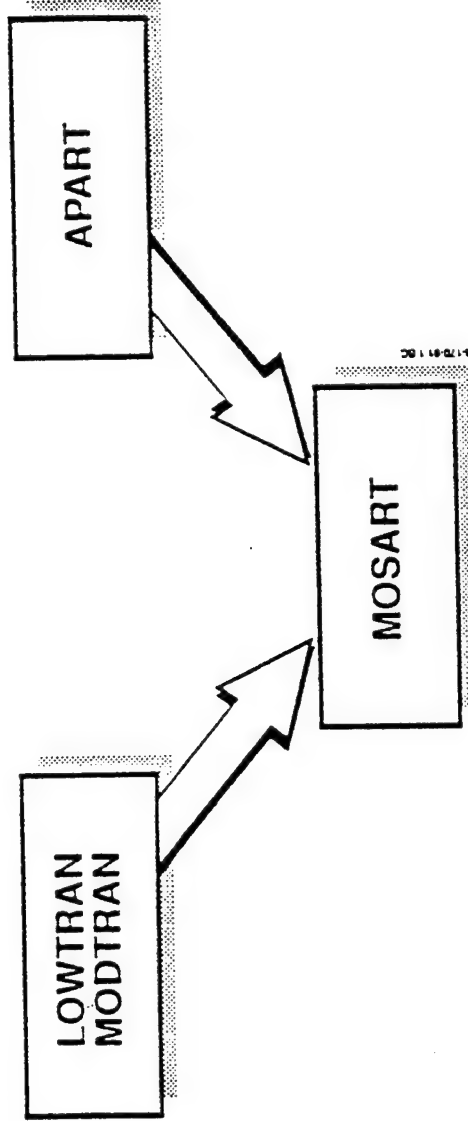
and
Dr. David C. Robertson
Spectral Sciences, Inc.
Burlington, Massachusetts

MOSART

The MOderate Spectral Atmospheric Radiance and Transmittance (MOSART) program has been developed in response to needs and requirements stipulated by the Strategic Scene Generation Model (SSGM) for a seamless approach to modelling atmospheric effects in the lower part of the earth's atmosphere. MOSART represents a merging of the government-standard LOWTRAN and MODTRAN codes and the APART code, developed by Photon Research Associates, Inc. (PRA) in support of a number of target and background simulations.

MOSART

- Moderate Spectral Atmospheric Radiance and Transmittance



- Strategic Scene Generation Model Requirements

SSGM Requirements for MOSART

The development of the MOSART program is driven in part by the requirements stipulated in "SSGM Development Requirements," PRA Report R-102-91 (Revision 1), dated December 1991. The MOSART code must provide line-of-sight (LOS) attenuation and radiance parameters and the earth limb, currently provided by MODTRAN in conjunction with SHARC. In addition, the MOSART code must provide the necessary interfaces with the heat transfer code DYNTP, the terrain scene code GENESIS, the cloud scene code CLDSIM, and the low altitude horizon scenes, all currently supplied by APART. To generate the necessary bidirectional reflectance functions (BDRF) for the CLDSIM code, the MOSART code must interface with the MSRAT code.

Potential growth in the SSGM may require additional support from the MOSART program. The first area is with respect to target signatures, both hard body (e.g., the VISIG code) and plumes (e.g., SIRRM). N.B.: The SIRRM code contains an early version of the APART code, and SIRRM can be interfaced with the MOSART code with only minimal changes to SIRRM. SSGM may also add the requirement to be able to include structured statistical terrain scenes for full global coverage, together with the various effects associated with atmospheric turbulence. Finally, the coupling of the local thermal equilibrium (LTE) MOSART code and the non-LTE (NLTE) SHARC code may be desirable in the near future.

SSGM REQUIREMENTS FOR MOSART

- Present:
 - LOS Attenuation and Radiance
 - Horizon and Limb Scenes
 - Terrain Scenes (GENESSIS)
 - Cloud Scenes (CLDSIM)
 - BRDF Data Base Generation (MSRAT)
- Future:
 - Target Signatures (VISIG and SIRRIM)
 - Structured Statistical Terrain Scenes
 - Turbulence
 - LTE/NLTE Coupled Code

Radiative Transfer

The radiative transfer calculations combine the best elements of the LOWTRAN, MODTRAN, and APART codes. For example, the molecular absorption parameters are taken from both LOWTRAN and MODTRAN. The multiple scattering uses the LOWTRAN and APART decomposition of the curves of growth into sums of exponentials, and the Cornette-Shanks phase function from APART is used to determine the forward scattering component. The ability to take line correlation along bent lines-of-sight, an improved solution to the equation of transfer assuming variations across layers, the calculation of in-scattered transmittance, and turbulence calculations have been extracted from APART. The concept of using a slit function for a user-defined resolution has been taken from MODTRAN. However, this approach has corrected for the problem in MODTRAN of convolving the transmittance with slit function before calculating the path radiance. The broad band thermal and solar loading calculations have been taken from the APART code.

RADIATIVE TRANSFER

- Molecular Parameters (13):
 - LOWTRAN 7: 20 cm^{-1}
 - MODTRAN 2: 1 cm^{-1}
- Multiple Scattering:
 - LOWTRAN: 3 Terms
 - MODTRAN: 2 - 15 Terms (Malkmus Curve-of-Growth)
 - Cornette-Shanks Phase Function
 - N-Stream Model
- Correlation Along "Bent" Lines-of-Sight
- Continuous Atmosphere Solution to Equation of Transfer
- In-Scattered Transmittance Calculated
- Turbulence Calculations:
 - Scintillation
 - Emitted and Scattered Path Radiance Variations
- Resolution (Corrected from MODTRAN):
 - Triangular Slit Function
 - Square Slit Function
 - User-Designed Slit Function
- Broad-Band Thermal and Solar Loading

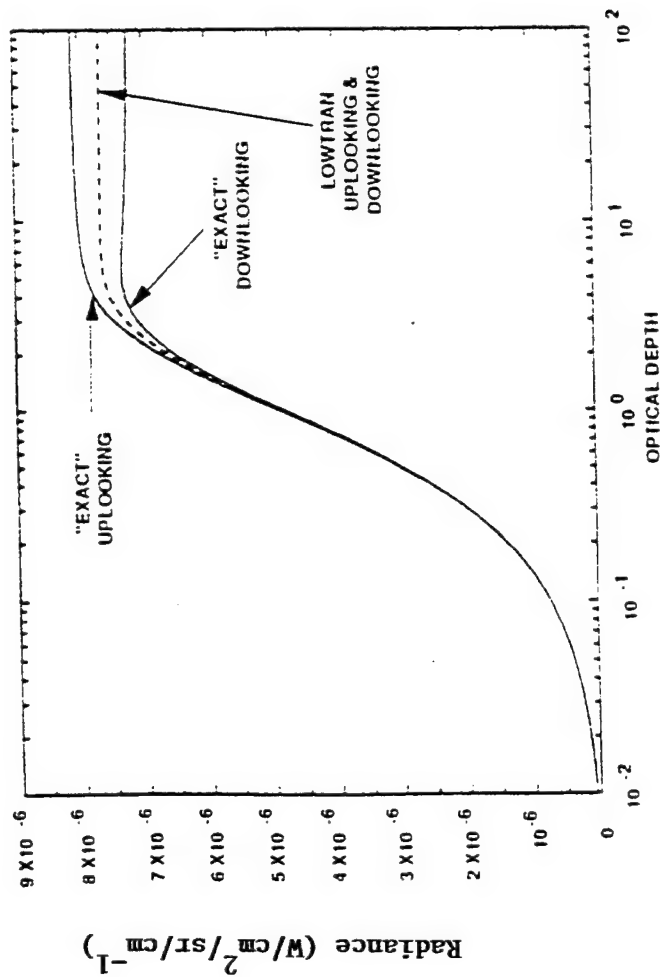
Thermal Path Radiance

For a single layer in the single scattering mode, LOWTRAN and MODTRAN use an average layer temperature to determine the thermal radiance from that layer. In the view graph, for a wavelength of 10 μm and a single layer temperature with a 6.5 K temperature gradient, the up-looking (hot-to-cold) and down-looking (cold-to-hot) thermal path radiances are shown for both the LOWTRAN/MODTRAN and MOSART implementations. The LOWTRAN/MODTRAN path radiances are identical for the up-looking and down-looking cases. The "exact" solutions were obtained by dividing the layer into 100 sub-layers and integrating the equations of transfer numerically. The relative errors for the LOWTRAN/MODTRAN solution were 5.5-5.9% maximum and 5.2-5.6% rms.

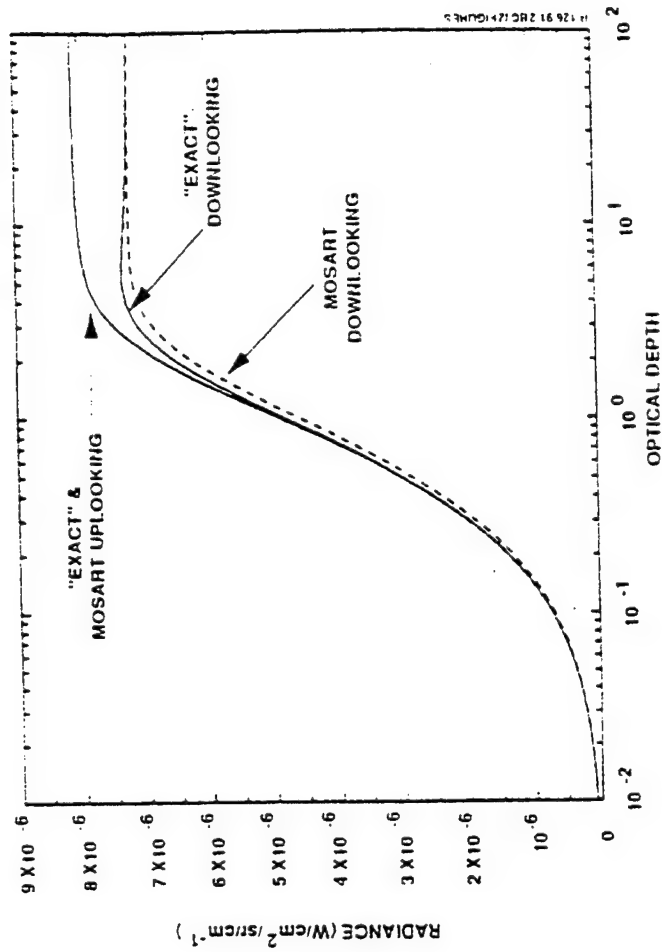
The MOSART implementation is also presented. The "exact and MOSART" up-looking curves are essentially coincident with a maximum error of 0.043% and an rms error of 0.012%. For the down-looking case, the agreement is not quite as good, with a maximum error of 5.7% and an rms error of 0.99%.

THERMAL PATH RADIANCE

MODTRAN



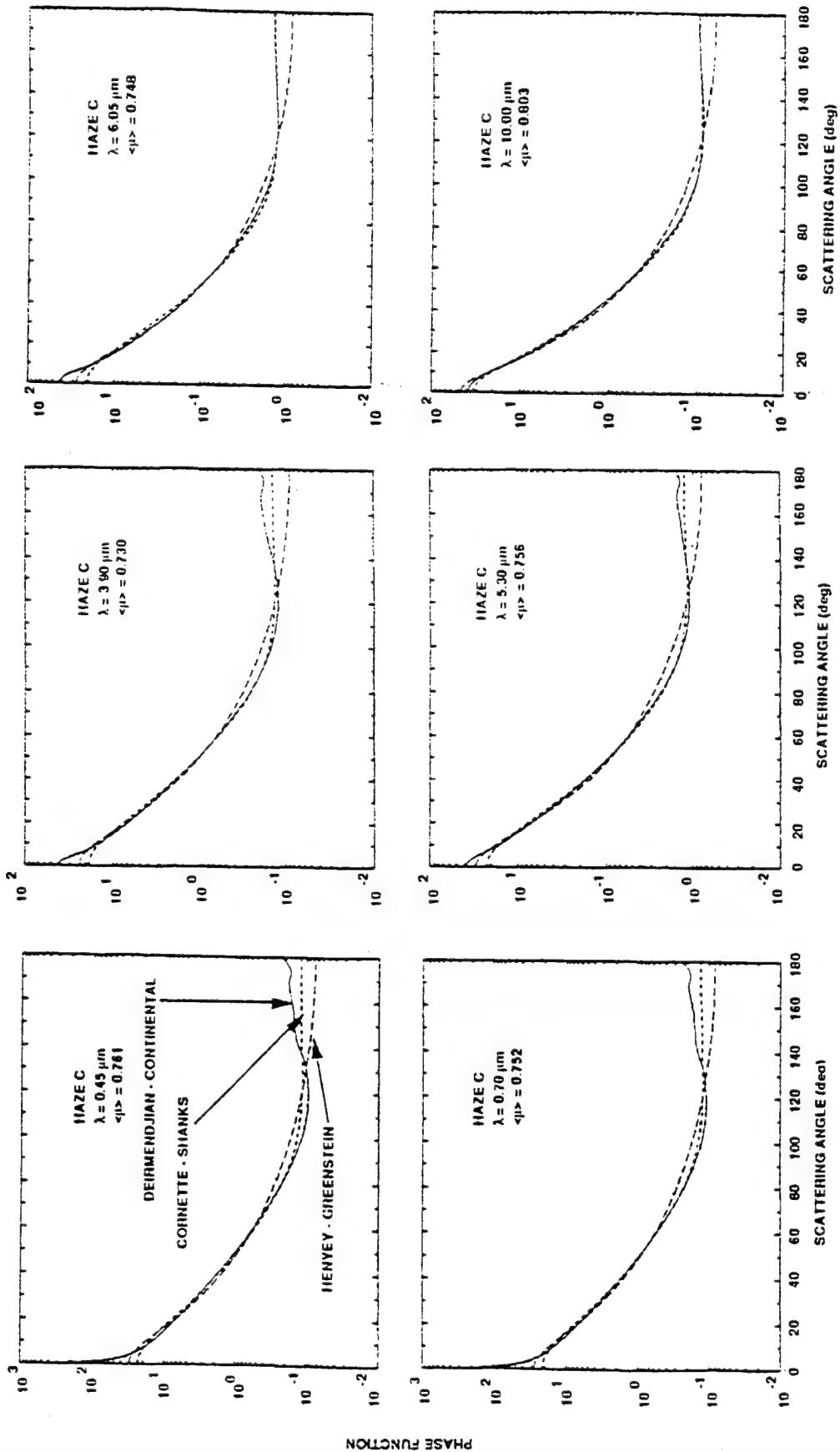
MOSART



New Phase Function

Cornette and Shanks (Applied Optics 1992) have developed an analytic phase function to replace the Henyey-Greenstein phase function in both single and multiple scattering applications. The new phase function provides a significantly better approximation to phase functions associated with naturally occurring aerosols (e.g., the Deirmendjian Continental aerosol model), particularly at the smaller values of the size parameter (i.e., at longer wavelengths). It should be noted that the Cornette-Shanks phase function is essentially coincident with the Deirmendjian Continental phase function for wavelengths more than 6 μm , except near the forward scattering peak.

NEW PHASE FUNCTION



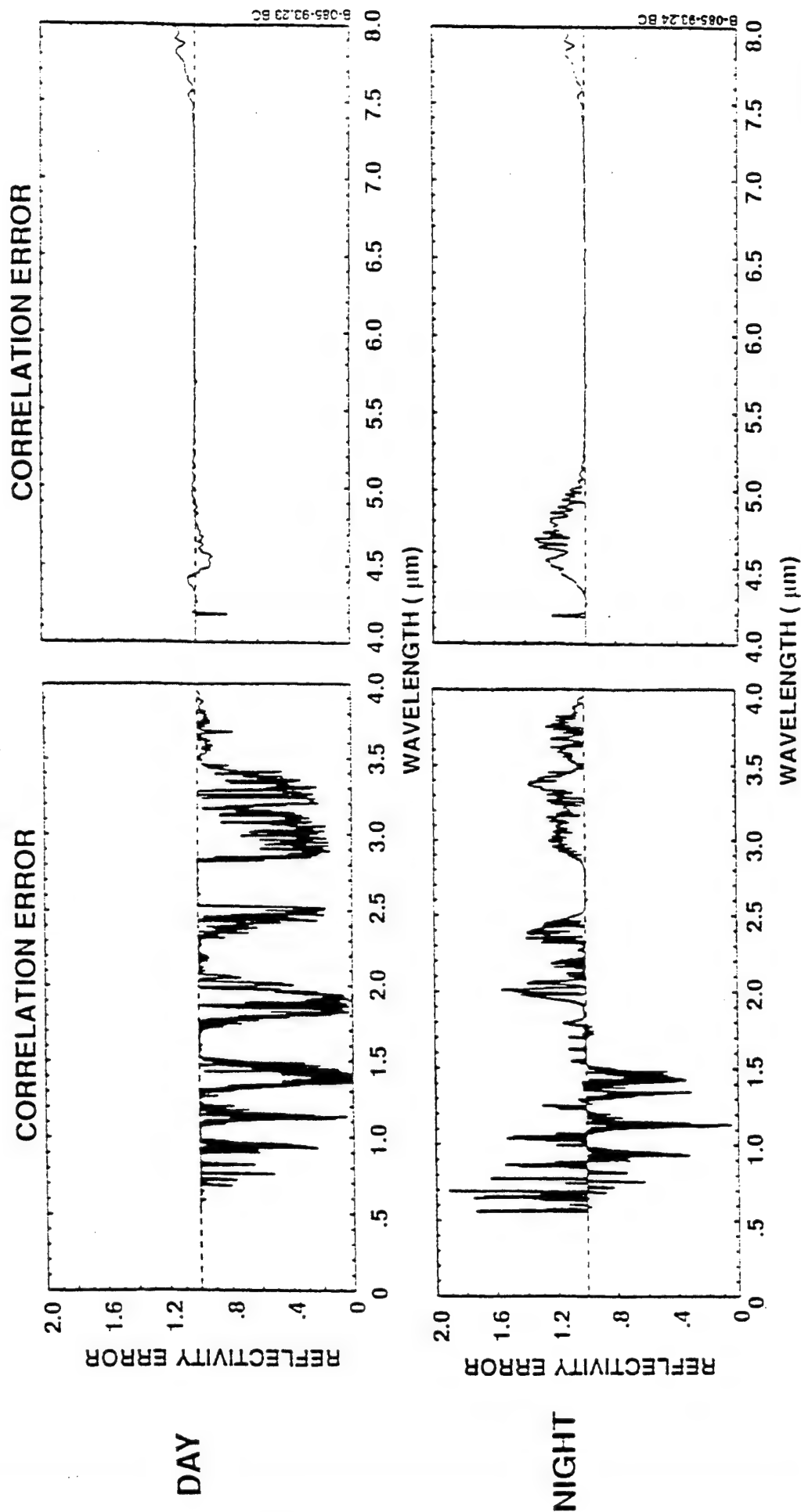
13-00000-01-01C-0001

Line Correlation Effects

The incorporation of line correlation in modelling the reflected radiance from a terrain material can be significant, particularly for wavelengths below 4 μm . These figures show the error in the reflected component for a diffuse reflector with reflectivity of unity for a Midlatitude day and night.

LINE CORRELATION EFFECTS

- Midlatitude
- Diffuse $\rho = 1.0$



Sky Noise

The MOSART code uses the thermal sky noise algorithm in APART and extends the algorithm to include both Rayleigh and aerosol scattering. The only significant assumption is that the aerosol number density fluctuations are driven by the air density fluctuations.

SKY NOISE

- Thermal Emission:
 - Convert C_n^2 to C_T^2 to C_{Jam}^2
- Rayleigh Scattering:

$$K_S = \frac{24\pi^3}{N} \left(\frac{n^2 - 1}{n^2 + 2} \right) \left(\frac{6 + 3\sigma}{6 - 7\sigma} \right) v^4$$
 - So Convert C_n^2 to C_{ks}^2 to $C_{Jsc(mol)}^2$
- Aerosol Scattering:
 - Assume Aerosol Number Density Fluctuates with Fluctuations in Air Density
 - So Convert C_n^2 to C_p^2 to C_{ND}^2 to $C_{Jsc(aer)}^2$

Atmospheric Characterization

The characterization of the atmosphere (e.g., pressure, temperature, molecular concentrations, hydrometeors) is extracted from LOWTRAN and MODTRAN with a few extensions available from APART. In addition to the six (6) model atmospheres from LOWTRAN, seventeen (17) model atmospheres from APART are included, together with the LOWTRAN user-defined atmosphere. MOSART has been upgraded so that a global atmosphere is available by interpolating in latitude from the available model atmospheres. The basic atmospheric properties are interpolated for each line-of-sight, so that the emitted path radiance looking north will be different from the line-of-sight looking south.

The aerosols from LOWTRAN have been supplemented by a temperature-dependent background stratospheric aerosol model. The LOWTRAN haze profiles can have either the LOWTRAN break points of 10 km and 35 km or the tropopause and stratopause defined by the model atmosphere.

The LOWTRAN hydrometeor (i.e., water clouds, cirrus clouds, rain) models have been increased to four (4) fog models, eleven (11) non-precipitating clouds, five (5) precipitating clouds, five (5) rain models, and six (6) snow models. A user-defined profile is also available. The two (2) LOWTRAN cirrus cloud models are included, together with the temperature-dependent Heymsfield cirrus model.

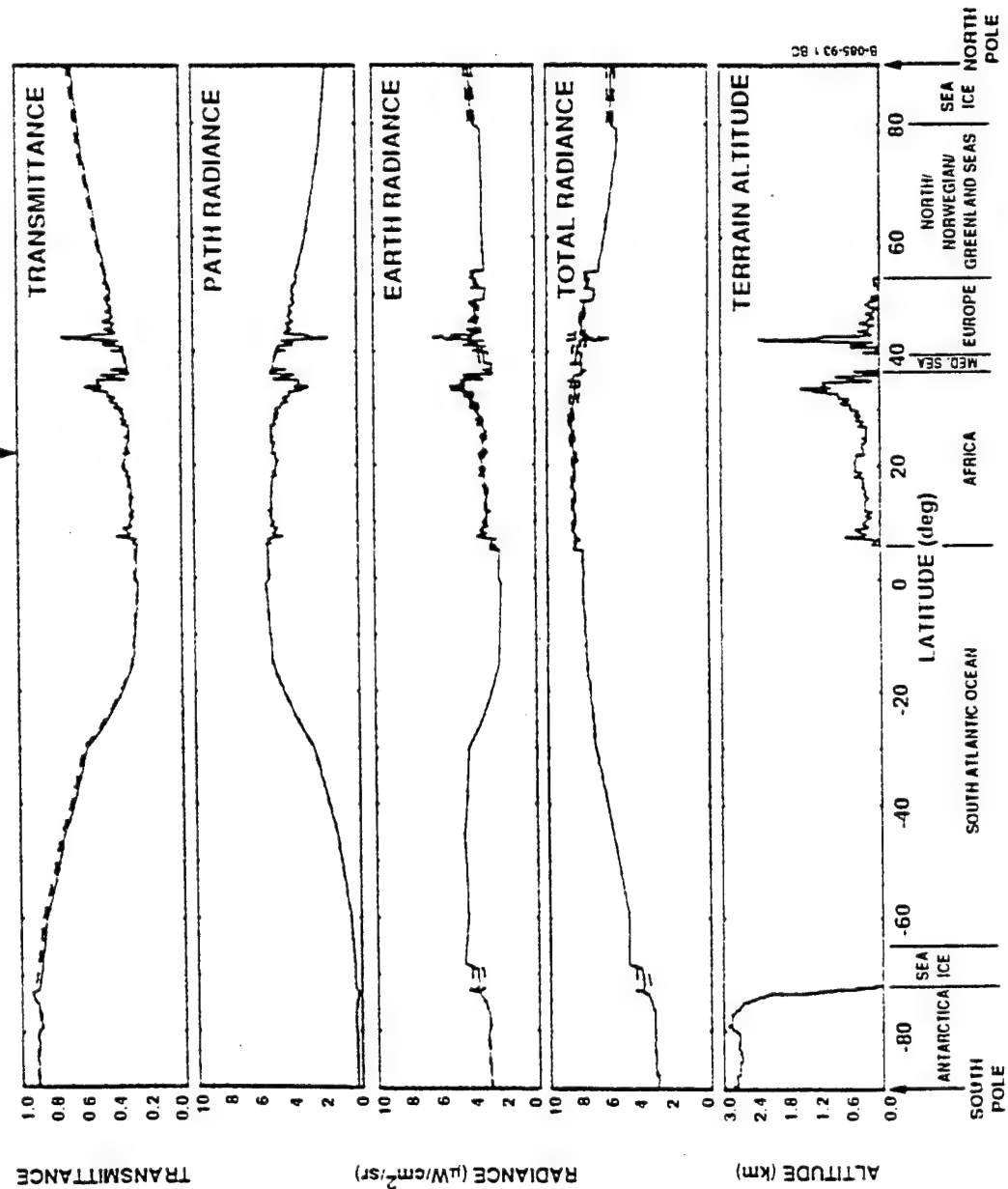
ATMOSPHERIC CHARACTERIZATION

- Atmospheres:
 - 23 Model Atmospheres
 - Global Atmosphere
 - User-Defined Atmospheres
- Aerosol Types and Haze Profiles:
 - MODTRAN Aerosols Plus Temperature Dependent Background Stratospheric
 - Fixed Plus Atmosphere Dependent Haze Profiles
- Hydrometeors:
 - Four Fog Models
 - Eleven Non-Precipitating Clouds
 - Five Precipitating Clouds
 - Five Rain Models
 - Six Snow Models
 - User Defined Profile
- Cirrus Clouds:
 - Standard (64 μm + Extinction)
 - Subvisual (4 μm + Extinction)
 - Heymsfield (Temperature Dependent)

Global Climatology Profile: 11 um; Nadir View

Using the global atmosphere option in MOSART, the transmittance, the path radiance, and the earth radiance (including the transmittance) are shown for a longitude of 0 degrees (i.e., Greenwich meridian) from the South pole to the North pole. The total radiance (i.e., path plus earth) is also presented for a narrow spectral band centered around 11 um on 21 June 1993 at 12:00 GMT. The altitudes of the terrain, together with basic geographic features, are shown. A list of the terrain scene types encountered are also listed.

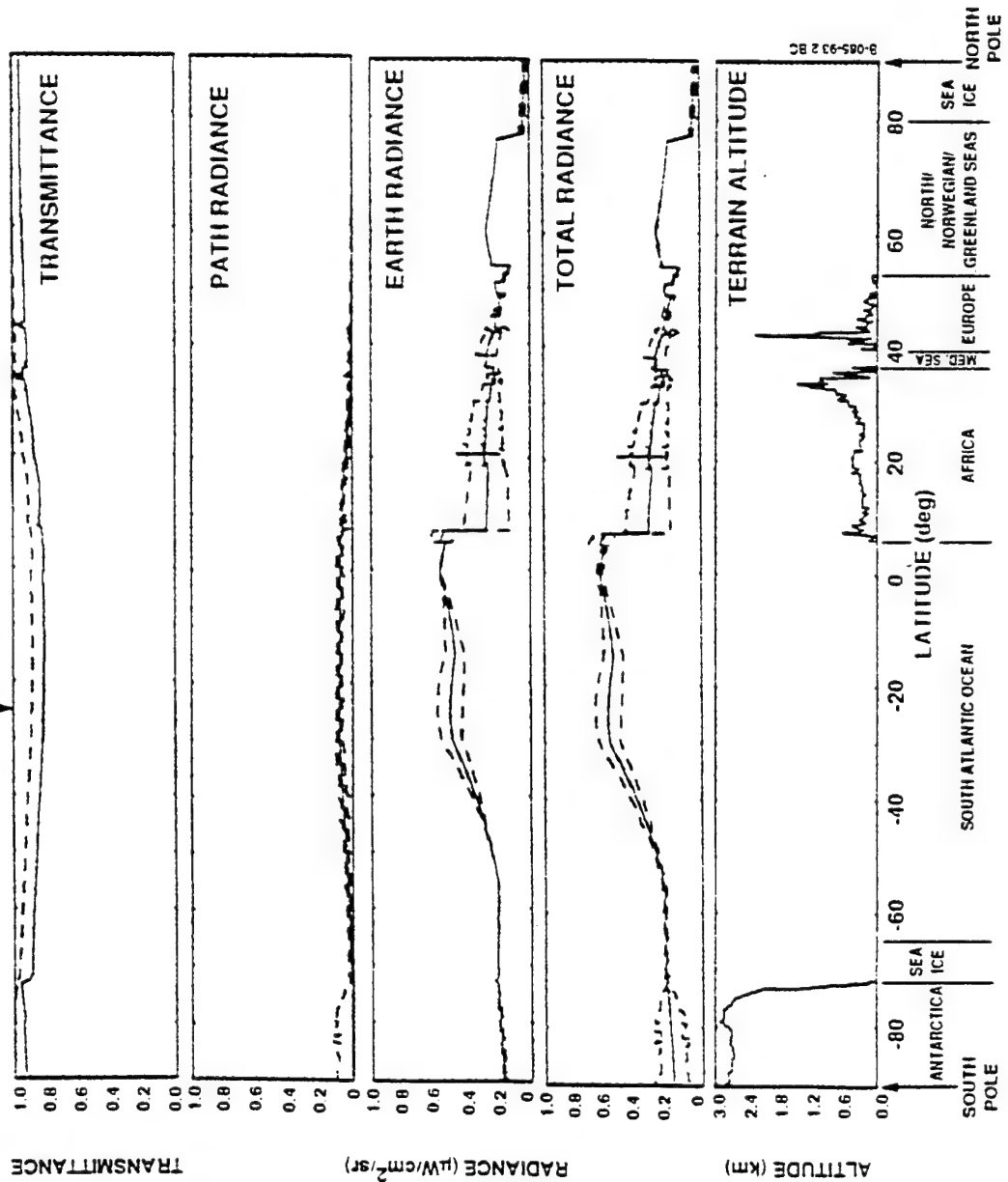
GLOBAL CLIMATOLOGY PROFILE: 11 μm ; NADIR VIEW; 0° LONGITUDE; 21 JUNE 1993, 12:00



Global Climatology Profile: 4 um; Nadir View

Using the global atmosphere option in MOSART, the transmittance, the path radiance, and the earth radiance (including the transmittance) are shown for a longitude of 0 degrees (i.e., Greenwich meridian) from the South pole to the North pole. The total radiance (i.e., path plus earth) is also presented for a narrow spectral band centered around 4 um on 21 December 1993 at 12:00 GMT. The altitude of the terrain, together with basic geographic features. Are shown. A list of the terrain scene types encountered are also listed.

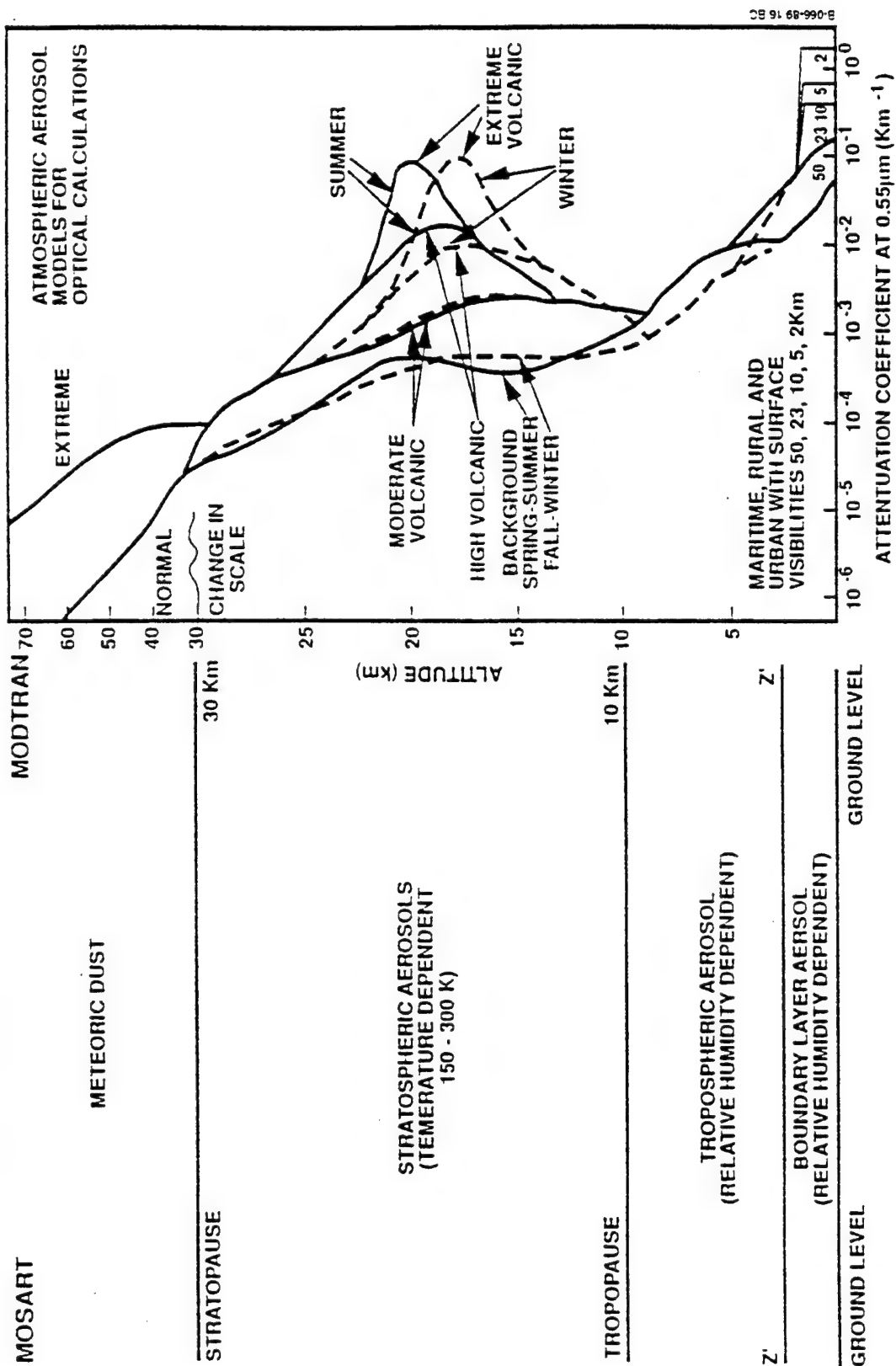
GLOBAL CLIMATOLOGY PROFILE: 4 μm ; NADIR VIEW; 0° LONGITUDE; 21 DECEMBER 1993, 12:00



Aerosol Types and Haze Profiles

The aerosols from LOWTRAN have been supplemented by a temperature-dependent background stratospheric aerosol model. The LOWTRAN haze profiles can have either the LOWTRAN break points of 10 km and 35 km or the tropopause and stratopause defined by the model atmosphere.

AEROSOL TYPES AND HAZE PROFILES



Background Representation

The earth and space backgrounds have been taken directly from the APART code. The various aspects of this part of the MOSART code are discussed in greater detail later in the presentation.

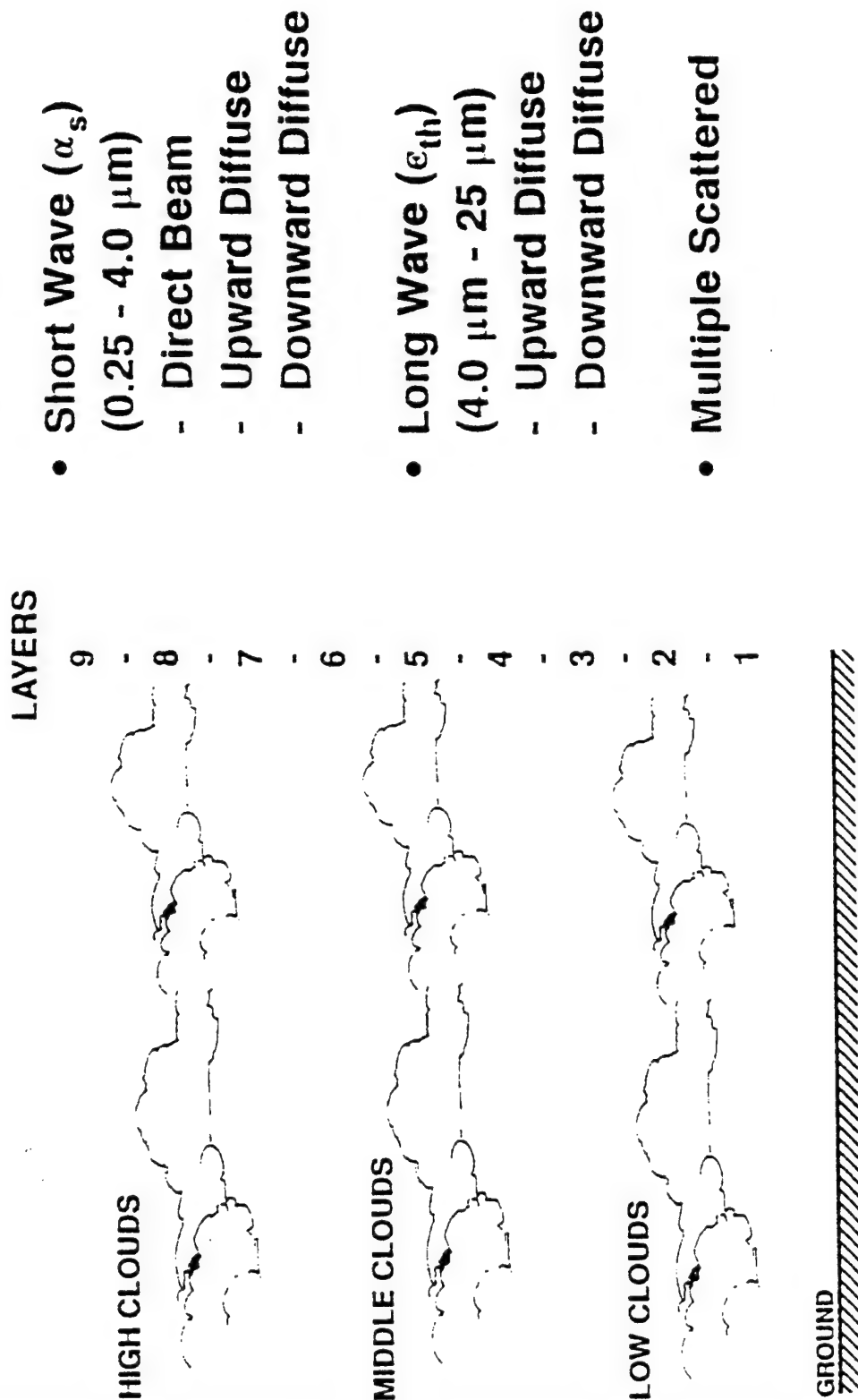
BACKGROUND REPRESENTATION

- Composite Terrain Scenes:
 - Global Seasonal Coverage (1° Resolution)
 - 35 Scenes
 - Monthly Snow Cover (4.5° Resolution)
- Terrain Altitude (10 Minute Resolution)
- Terrain Materials:
 - 28 Types
 - Optical Properties
 - Thermal Properties
- Broad Band Heat Transfer:
 - Solar Loading
 - Thermal Loading
 - Diurnal Temperature Cycle
- Space:
 - Zodiacal Light
 - Mean Star Radiance
 - Galactic and Extra-Galactic Radiances

Heat Transfer

The MOSART code contains a broad-band heat transfer model that uses a three-stage cloud structure with multiple scattering to determine the solar and thermal loading as a function of altitude and time of day. These parameters are used to determine the earth material temperatures. The loading is also available by way of a binary output file for use by other codes.

HEAT TRANSFER

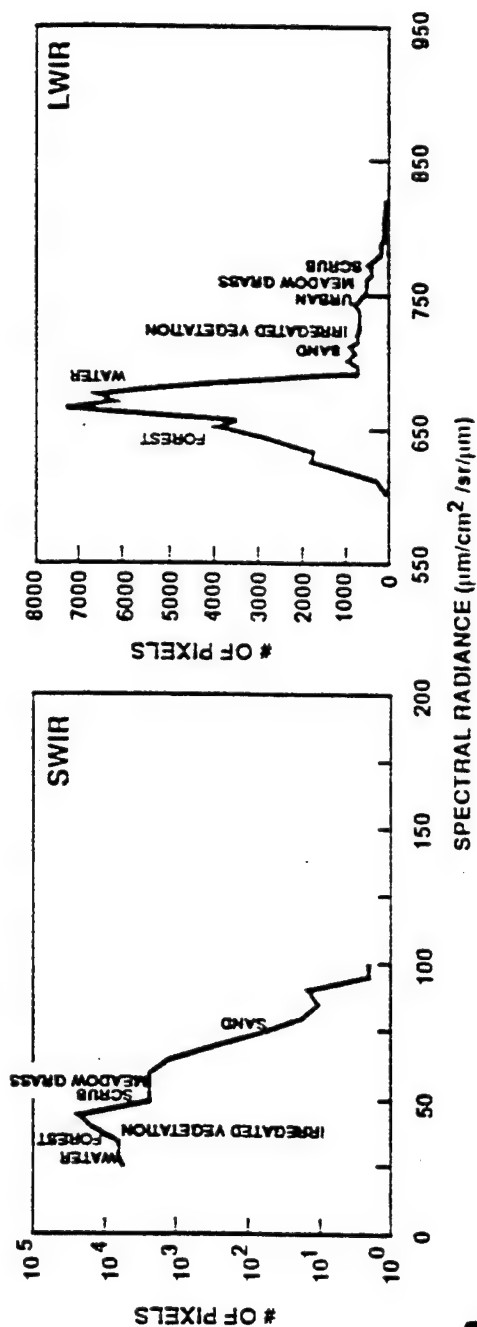


Santa Cruz, California, Scene

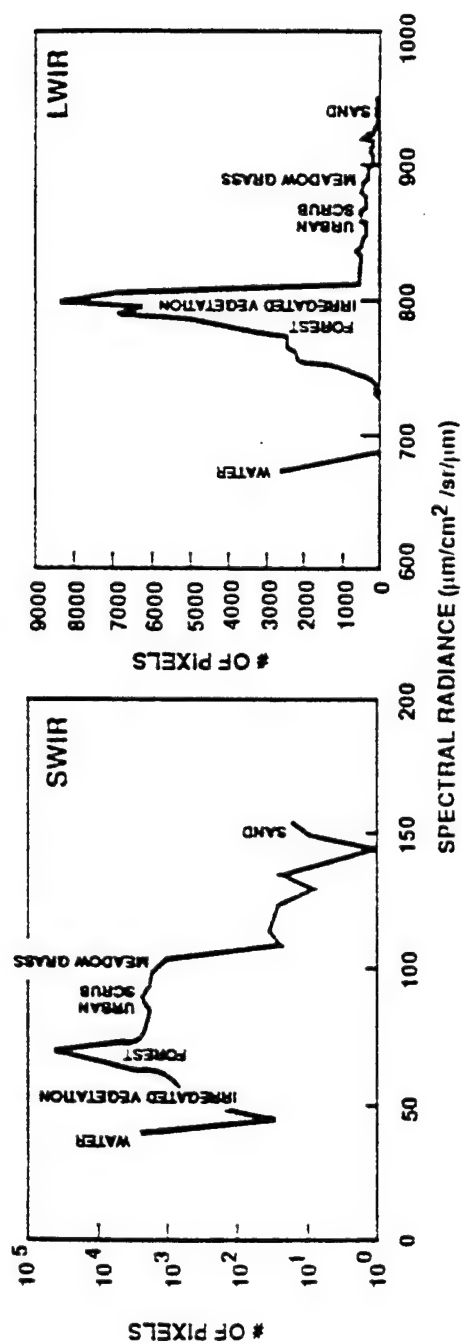
The ability to decompose a deterministic scene, such as this one of Santa Cruz, California, until the appropriate terrain materials, allows the MOSART code to contain a statistical representation of the deterministic scene.

SANTA CRUZ, CALIFORNIA, SCENE

• Dawn Plus One Hour



• Noon

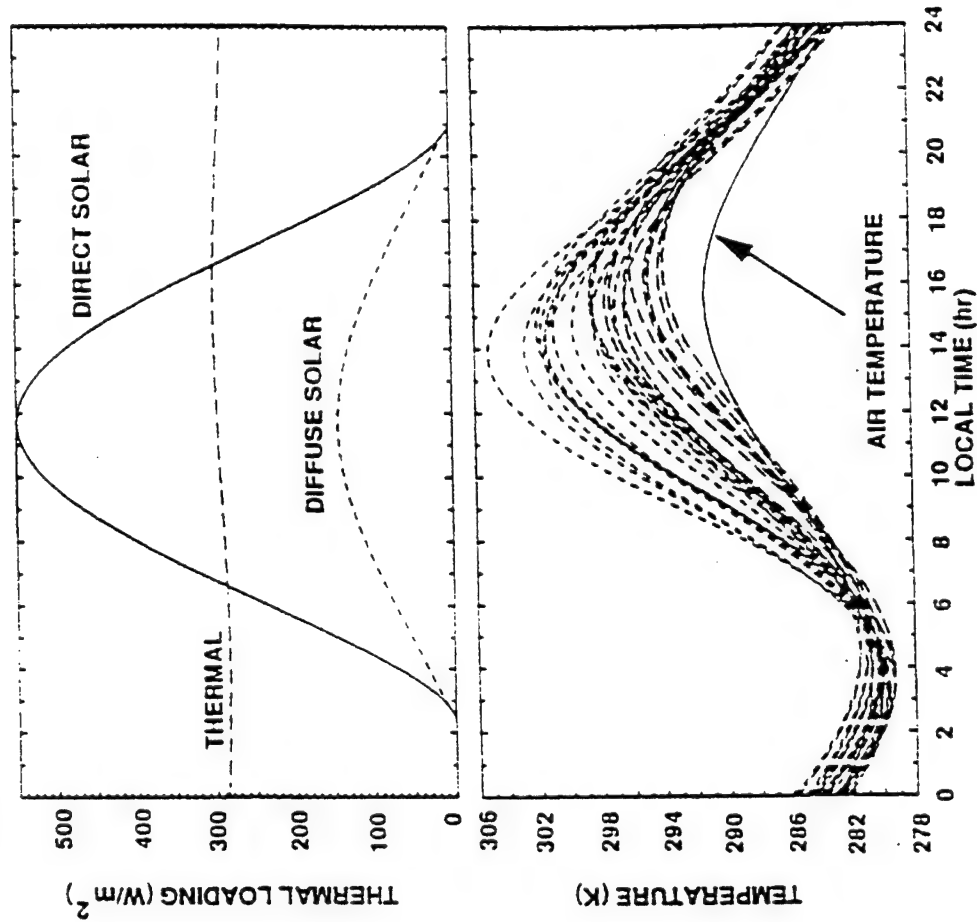


Subarctic Summer Atmosphere

Using the broad-band heat transfer and the various terrain materials in a scene, it is possible to determine the solar and thermal loading on the terrain and the temperatures of the materials as a function of time of day. The curves shown here are for a Subarctic Summer atmosphere, where the terrain temperatures are driven by the local air temperature.

SUBARCTIC SUMMER ATMOSPHERE

- Driven by Local Air Temperature
- Cooling Observed at Night Below Local Air Temperature
- Large Day-Night Air Temperature Variations

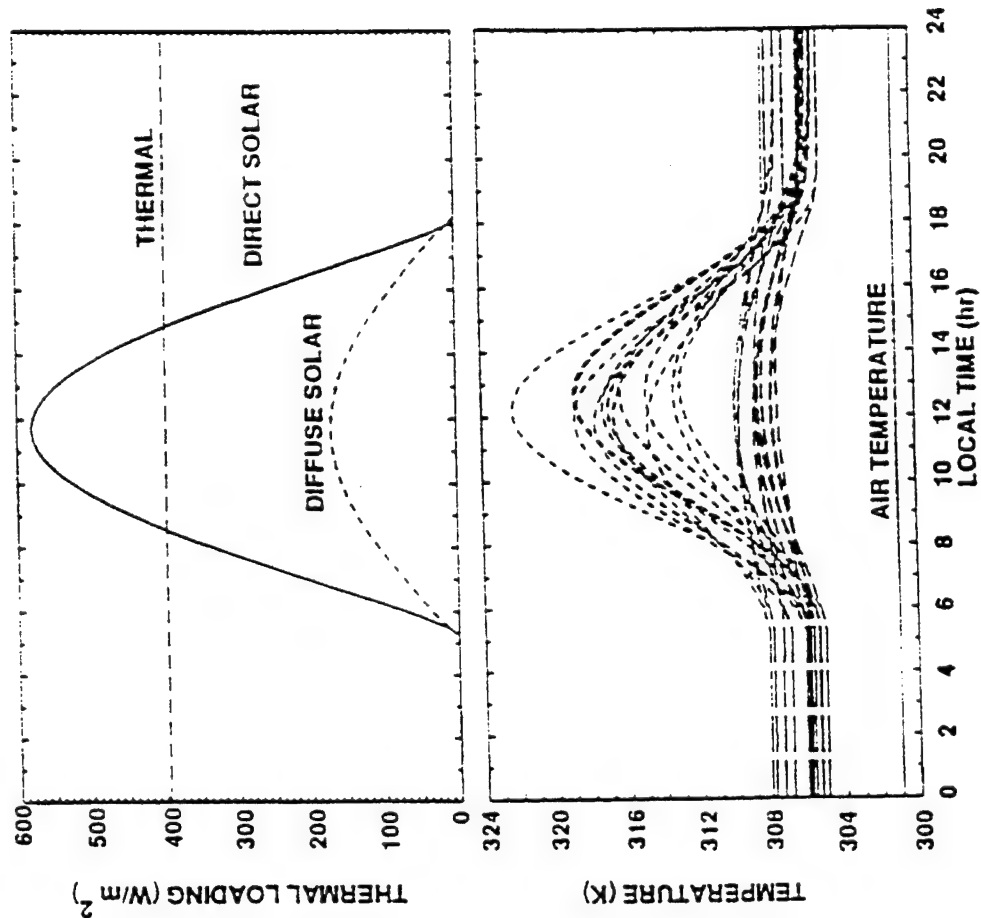


Tropical Atmosphere

Using the broad-band heat transfer and the various terrain materials in a scene, it is possible to determine the solar and thermal loading on the terrain and the temperatures of the materials as a function of time of day. The curves shown here are for a Tropical atmosphere, where the terrain temperatures are dominated by thermal loading at night and solar loading during the day.

TROPICAL ATMOSPHERE

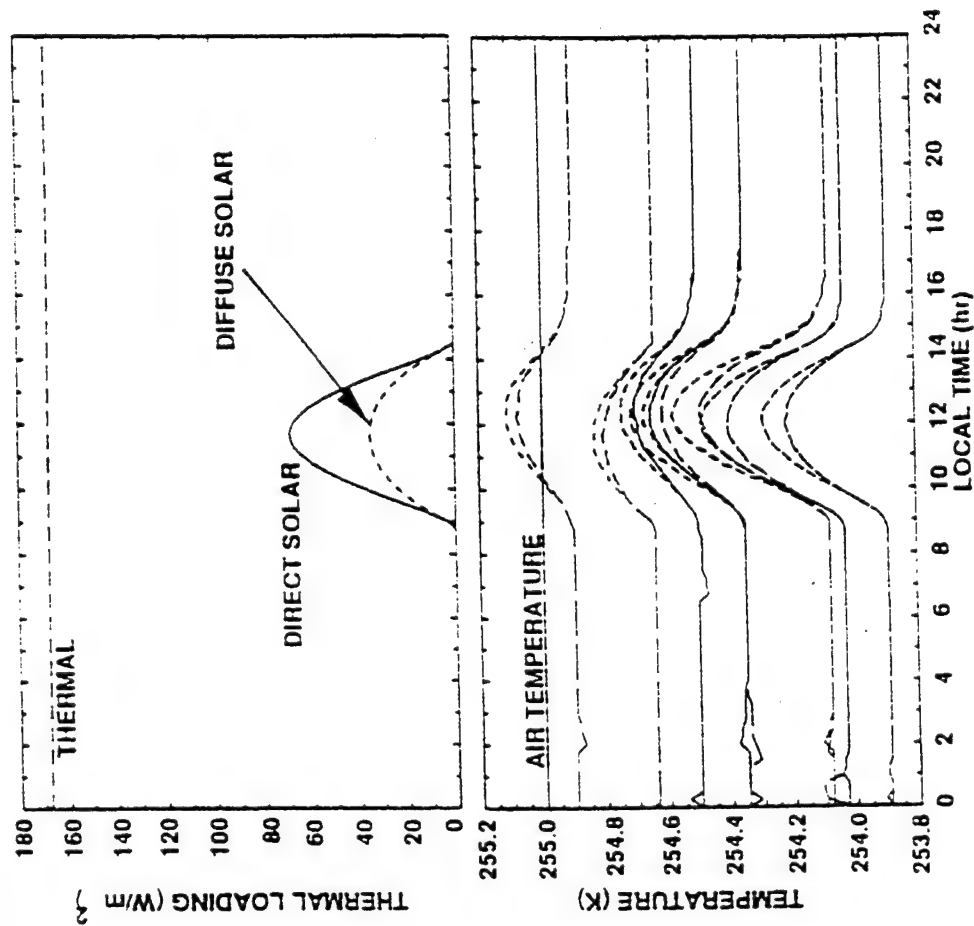
- Thermal Loading by Atmosphere Dominates at Night
- Heavy Cloud Cover Prevents Cooling at Night
- No Day-Night Air Temperature Variations



Subarctic Winter Atmosphere

Using the broad-band heat transfer and the various terrain materials in a scene, it is possible to determine the solar and thermal loading on the terrain and the temperatures of the materials as a function of time of day. The curves shown here are for a Subarctic Winter atmosphere, where the terrain temperature variations are quite small. In fact, some of the variations at night are essentially computational "noise" that are indicative of the stability of the algorithm (i.e., approximately 0.05 K).

SUBARCTIC WINTER ATMOSPHERE



- Small Thermal and Solar Effects
- No Day-Night Air Temperature Variations
- Numerical "Noise" of Algorithm Seen in Temperature Curves

Miscellaneous Features

This view graph lists some miscellaneous features of the MOSART code.

MISCELLANEOUS FEATURES

- Automatic Atmosphere Profiling:
 - In-Band and Spectral
 - Atmospheric Analyses
 - Terrain Altitude Effects
- Ephemeris:
 - Solar and Lunar
 - Year-to-Year Variations
- Relative Humidity (Goff-Gratch)
- Additional Molecules in Ultraviolet:
 - O₂
 - O₃
 - H₂O
 - SO₂
 - N₂O
 - NO₂
 - N₂O₂
- Spectral Calculations:
 - Variable Spectral Sampling
 - Wavelength vs. Wavenumber Resolution and Sampling
- Ray Tracing:
 - Refractivity
 - Anomalous Propagation

Utilities

A number of utility programs are delivered with the MOSART to assist in installation (i.e., FPTEST and INSTDB), to manipulate and create files (i.e., ASCBIN and CRFILE), to process the output (i.e., ASCBIN, BBTEMP, VISUAL, and PLTGEN), and to create statistical terrain scenes (i.e., SCNGEN).

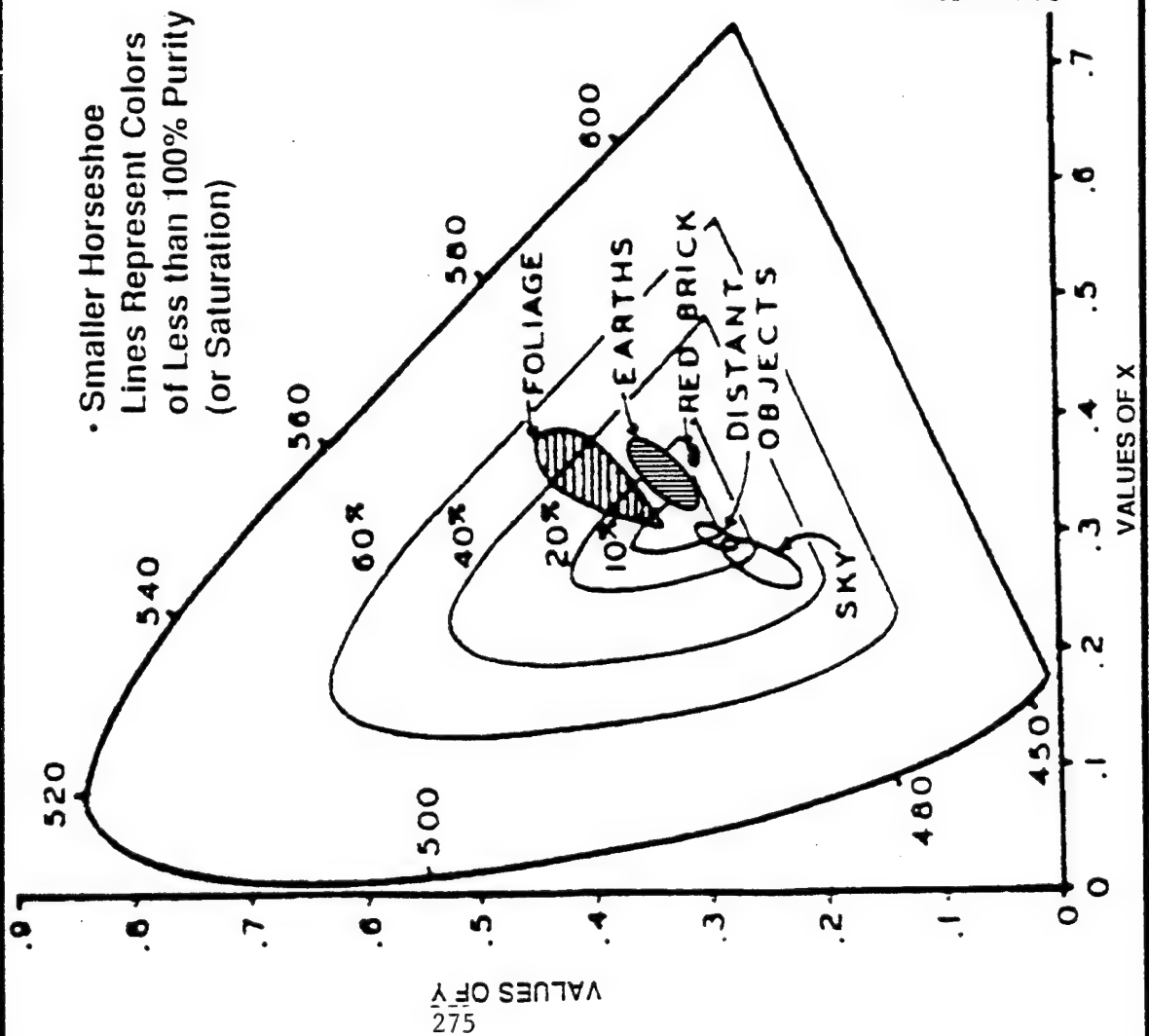
UTILITIES

- **FPTEST:** Tests Machine-Dependent Features
- **INSTDB:** Installs Binary Data Bases
- **ASCBIN:** ASCII/Binary Conversion and Creates Spectral Tables
- **CRFILE:** Creates Input Files Interactively
- **BBTEMP:** Converts Radiance to Equivalent Blackbody Temperature
- **VISUAL:** Converts Radiance to Luminance and CIE Color Coordinates
- **PLTGEN:** Produces Spectral Plots (NCAR or DISSPLA)
- **SCNGEN:** Create Deterministic/Statistical Terrain Scenes

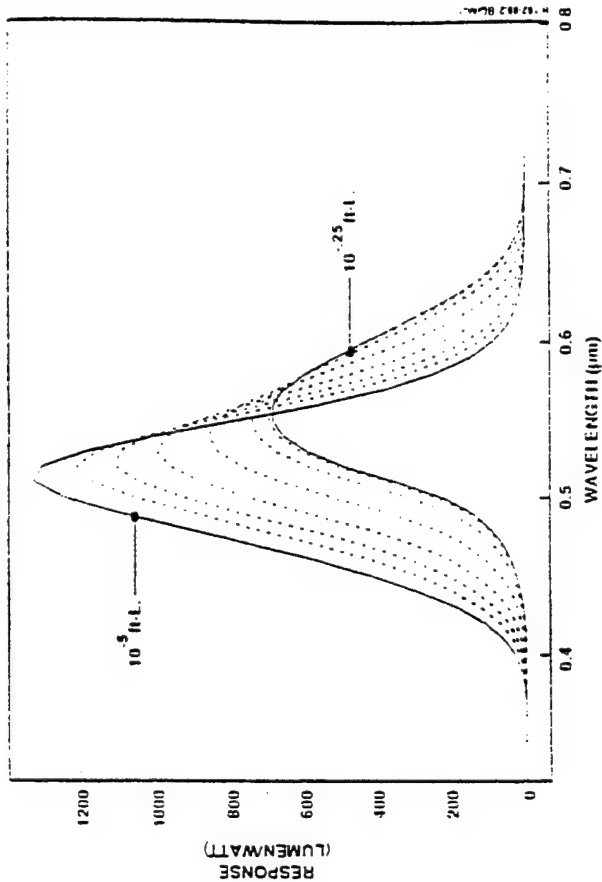
VISUAL Utility Code

The VISUAL utility code converts the transmittance, radiance, and irradiance values calculated by the MOSART code and converts them into transmittance, luminance, and illuminance values as perceived by the human eye. The eye response is modelled as a spectrally adaptive filter, varying from scotopic to photopic, depending upon the background luminance level. The color of each luminance and illuminance value is given in terms of the CIE (x,y) coordinates.

VISUAL CODE



HUMAN EYE RESPONSE



B-010-90C.12BC/Mac

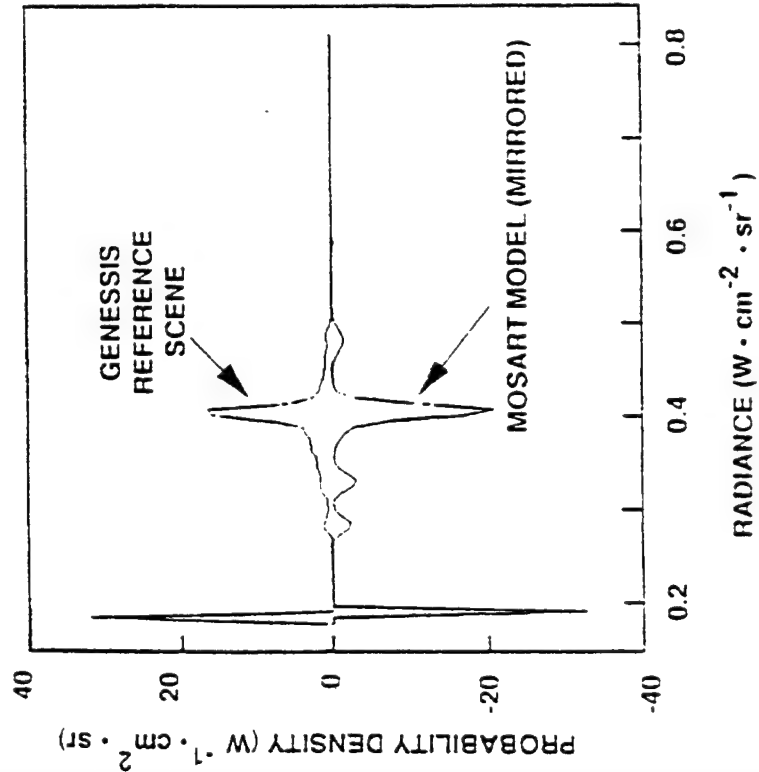
San Diego, California, Scene

Using the statistical representation of the San Diego, California, scene, the MOSART code can approximate the probability density function and the power spectral density for the deterministic scene.

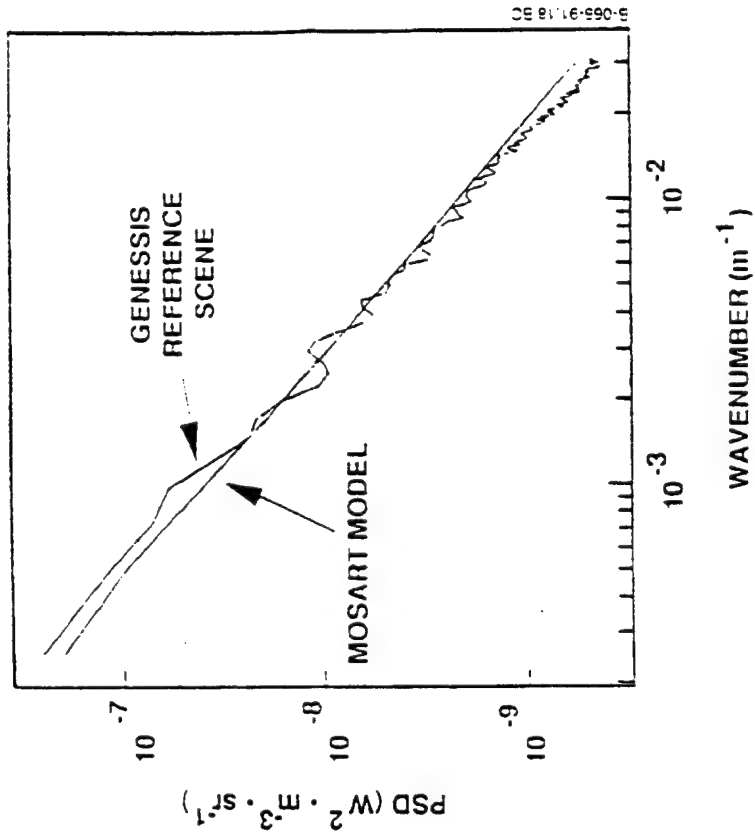
SAN DIEGO, CALIFORNIA, SCENE

- Noon
- 3.7 - 4.1 μm

Probability Density Function

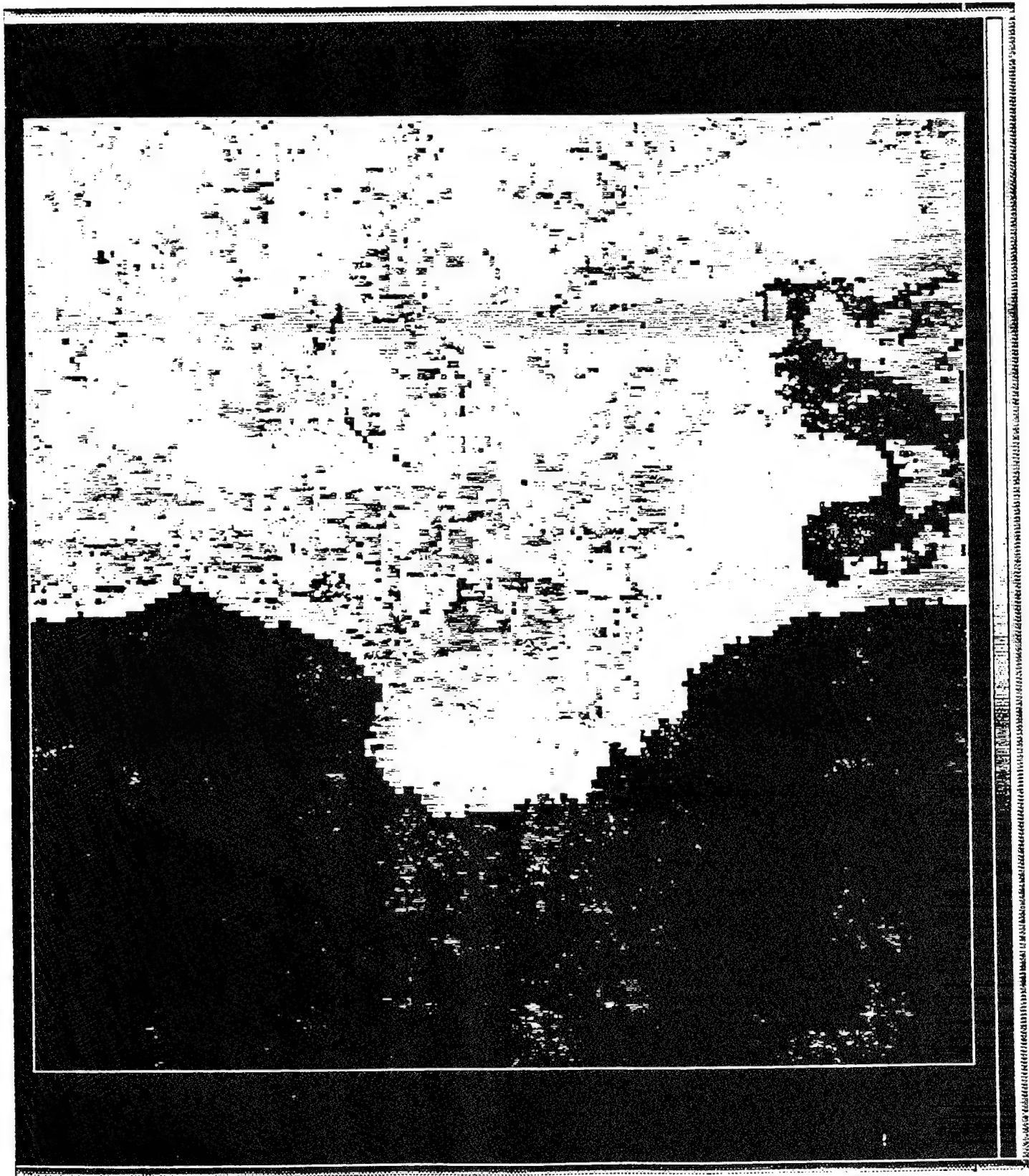


Power Spectral Density



Statistical San Diego, California, Scene

The scene shown in the view graph was created by the SCNGEN code using the statistical terrain parameters generated by the MOSART code (i.e., material radiances - mean and standard deviation, material spatial structure - power spectral density slope and correlation length, and scene composition). To insure that the scene would look somewhat like San Diego, California, a template of land and sea was input to the code at 100 meter resolution. The SCNGEN code used fractals to increase the resolution to the 25 meters shown. Amount of sun and shade for each material was determined using a fractally generated cloud cover map. (N.B.: Clouds are not included in the SCNGEN at the present time, only shade due to clouds.)



Code Documentation

Internal code documentation will be provided in compliance with the PRA Software Standard. Such documentation includes routine prologues that discuss the purpose of the routine, full descriptions of all arguments, and liberally scattered comments throughout the code.

External documentation includes a full set of manuals covering installation, day-to-day usage of the code, technical descriptions of the algorithms and data bases, and the structure of the software and variable definitions.

CODE DOCUMENTATION

- Internal Documentation:
 - Routine Prologues
 - Comments
- External Documentation:
 - Installation Reference Manual
 - User Reference Manual
 - Technical Reference Manual
 - Software Reference Manual

Sample Input File

The view graph presents a sample MOSART input file. The four (4) sections shown are those required for all runs of the code:

- User-supplied Parameters
- Position Parameters
- Geometry Parameters
- Spectral Parameters

Other optional sections (e.g., solar definition, atmosphere definition, terrain definition, hydrometeor definition) can be added when required.

SAMPLE INPUT FILE

Moderate Spectral Atmospheric Radiance and Transmittance (MOSART) (Ver. 1.00)

User-specified Parameters -----

Header Sample Input File
 Printout Switch (S/M/L) Large
 Temperature Calculations (Y/N) No
 Multiple Scattering (Y/N) No
 Solar/Lunar Ephemeris (Y/S/L/N) No

Position Parameters -----

Latitude (deg) (+ North, - South) 50.
 Longitude (deg) (+ East, - West) -100.
 Day of the month (integer) 21
 Month of the year (integer) June
 Year (integer) 1991
 Time of day (24-hr HH.MMSS) 12.00
 Time index (LST/GMT) LST
 Coordinate Reference (Obsv/Source) Source

Geometry Parameters -----

Observer Azimuths (deg) (<=8) 0. 90. 180. 270.
 Azimuth Reference (Relative/True) True

SAMPLE INPUT FILE

No.	Index	Obsv. Alt. (Km)	Src. (Km)	Alt. (Km)	Sl. Rng. (Km)	Earth Ang. (deg)	Obsv. Angle (deg.)	Src. Angle (deg.)	Length Switch
1	Se	100.0	1.0	1.0	1.0	1.0	1.0	1.0	0
2	Be	100.0	1.0	1.0	1.0	1.0	1.0	1.0	0
3	Ce	100.0	1.0	1.0	1.0	1.0	1.0	1.0	0
4	Ce	100.0	1.0	1.0	1.0	1.0	1.0	1.0	0
5	Cz	100.0	1.0	1.0	1.0	1.0	1.0	1.0	0
6	Cl	100.0	1.0	1.0	1.0	1.0	1.0	1.0	0
7	Ae	1.0	1.0	1.0	1.0	1.0	1.0	1.0	0
8	He	1.0	1.0	1.0	1.0	1.0	1.0	1.0	0
9	Le	400.0	1.0	1.0	1.0	1.0	1.0	1.0	0
10	Le	100.0	1.0	1.0	1.0	1.0	1.0	1.0	0
11	Le	400.0	1.0	1.0	1.0	1.0	1.0	1.0	0
12	Le	400.0	1.0	1.0	1.0	1.0	1.0	1.0	0

End of Geometry Data/

Spectral Parameters -----

Spectral Calculations (MO/LO/MM) MO

Wavenumber or Wavelength (WN/WL) WN

Initial wavenumber (cm**-1/um) 3000.

Final wavenumber (cm**-1/um) 3000.

Calculation Width (cm**-1/um/GHz) ... 5.

Resolution (cm**-1/um/GHz) 20.

Execution Time

To compare the execution time for MODTRAN and MOSART, both codes were executed under nearly identical conditions. (i.e., same compiler options, approximately same load factor) on a Silicon Graphics Personal IRIS Workstation 4D/35, operating at 36 MHz. A single line-of-sight passing through 33 atmospheric layers (space-to-ground for MODTRAN) was used for calculations for the 2000-3500 wavenumber spectral region. The execution times were separated into an initialization time and the time for each spectral calculation. It should be noted that there is a fair amount of variability in the execution time from run to run, so these execution times should be considered approximate.

The MOSART code does take somewhat longer to initialize. If terrain temperatures are to be calculated, the initialization time is fairly large; however, this calculation is a user option, and results from previous calculation can be used to by-pass this calculation. For a single line-of-sight, the overhead associated with each spectral calculation is significantly greater for MOSART than for MODTRAN. However, if multiple lines-of-sight are desired, the time difference is not significant.

Work is continuing on improving the execution speed of the MOSART code.

EXECUTION TIMES

- Silicon Graphics Personal IRIS 4D/35 (36 MHz)
- Slant Path, 33 Layers, 2000 - 3000 cm^{-1}

	Initialization Calculations (sec)	Spectral Calculations (sec/spectral point)
MODTRAN	2.59 - 3.46/LOS	0.111 - 0.239/LOS
MOSART		
Arbitrary Sun Position	1.43 - 2.03 +	0.260 - 0.647 +
High Sun Approximation	0.95 - 0.99/LOS 1.37 - 2.07 +	0.223 - 0.242/LOS 0.270 - 0.721 +
	0.34/LOS	0.022 - 0.026/LOS

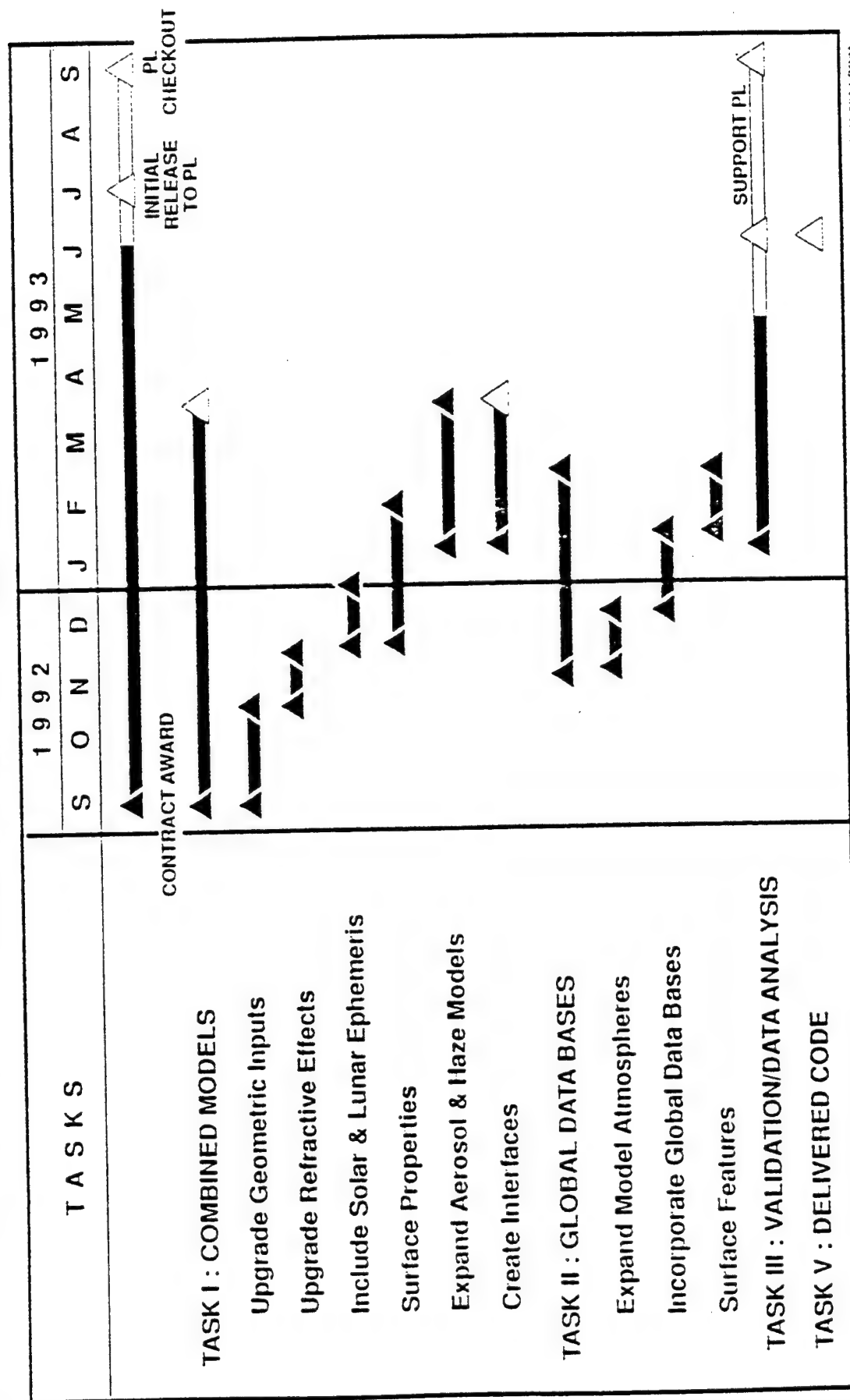
- Terrain Material Calculations ~ 95 Seconds
- Global Atmosphere Calculations * 3 (Approximately)
- Time Ranges for No Multiple Scattering and Multiple Scattering

Schedule

The schedule for this phase of the development effort is shown. All elements of the work are either ahead of schedule or on schedule except for the creation of the necessary interfaces. The ability to create a file analogous to TAPE7 from MODTRAN and LOWTRAN is still being worked on. Testing is continuing, with the initial code delivery planned in July 1993.

PHASE II SCHEDULE

• Contract Start Date: 16 Sep 1992



8101 027.1 BC/Mac

B 085 03.14

MOSART Code Upgrades

The current phase of the MOSART code development was concerned primarily with merging the existing capabilities of the LOWTRAN, MODTRAN, and APART codes. Although a few new capabilities were added (e.g., global backgrounds, ocean temperatures), a number of capabilities have been deferred until the next phase of code development. For example, the U.S. Air Force Phillips Laboratory is currently developing new multiple scattering algorithms for inclusion in a future release of MODTRAN. If appropriate, these new algorithms will be incorporated into MOSART.

The terrain structure statistics and the turbulence-induced sky noise models currently in MOSART require significant refinement and validation. Similarly, the ability to model polarization of atmospheric and terrain radiation may be desirable in the future.

Since one of the major reasons behind the development of the MOSART program is to provide the SSGM with a "seamless" approach to modelling atmospheric effects in the lower atmosphere, an anticipated area of future growth will be to couple the non-local thermal equilibrium (NLTE) calculations of SHARC and the LTE calculations of MOSART.

MOSART CODE UPGRADES

- Incorporate New Multiple Scattering Algorithms
- Upgrade Background Structure Statistics
- Validate/Improve Turbulence/Scintillation/Sky Noise
- LTE/NLTE Coupling (SAMM)
- Polarization

INCLUSION OF ACCURATE MULTIPLE SCATTERING IN MODTRAN

K. Stamnes and S. Tsay

M. Yeh

Geophysical Institute
Univ. of Alaska
Fairbanks, AK 99775-0800

Caelum Research Corp.
Silver Spring, MD 20901-4554

Our work on the MODTRAN computational code aimed at improving the computation of multiple scattering not only in the infrared part of the spectrum, but also in the solar part where scattering effects are important under both cloudy and clear sky conditions. This task is concerned with the inclusion of the general-purpose multiple scattering algorithm DISTORT (Discrete Ordinate Radiative Transfer code as summarized by Stamnes et al., 1988) into MODTRAN, including proper interfaces to allow for accurate computation of multiple scattering effects. In the solar part of the spectrum this is important for clear sky conditions (Rayleigh scatter) as well as cloudy and hazy situations. In the terrestrial infrared part of the spectrum (beyond 4 microns) molecular (Raleigh) scattering is negligible, but scattering from clouds and aerosols can not be ignored. Results were compared between the two versions and their differences and improvements will be discussed.

Inclusion of Accurate Multiple Scattering in MODTRAN

**K. Stamnes and S. Tsay
Geophysical Institute
University of Alaska Fairbanks
Fairbanks, AK 99775-0800**

**M. Yeh
Caelum Research Corporation
11229 Lockwood Drive
Silver Spring, MD 20901**

Motivation

- * **Multiple scattering** in MODTRAN is based on a 2-stream code (BMFLUX) with an isothermal layer approximation from which upward and downward fluxes are obtained.
- * These fluxes are then converted into hemispherical intensities by assuming that the intensity is uniform in each hemisphere so that the hemispherical intensity is obtained from the flux by dividing it by π .
- * **Single scattering** is already computed accurately in MODTRAN including curvature and refraction effects.
- * This approach is justifiable if the single scattering contribution dominates as may frequently be the case for clear sky conditions. However,

In the presence of clouds and aerosols the multiple scattering contribution to the radiance may dominate!

Therefore, a better multiple scattering scheme is expected to improve

- * accuracy of calculations of atmospheric transmission and reflection;
- * accuracy of retrievals of remotely-sensed atmospheric properties that rely on the interpretation of measured radiances (ground-based or from space).

HOW do we Improve Multiple Scattering (MS) Treatment?

Simple answer: Replace existing scheme (based on BMFLUX) with a more accurate one based on a multi-stream approach (DISORT) to compute multiple scattering.

DISORT computes complete radiance, but MODTRAN needs only Multiple Scattering component of the source function. Therefore

More complete answer: To minimize changes in MODTRAN we have extended DISORT to compute only the MS component of the source function for use in MODTRAN.

IMPORTANT: Both MODTRAN and DISORT are very complex codes. Therefore

- * interfacing of DISORT with MODTRAN must be done very carefully;
- * extensive testing is required and must be carefully executed. This is a time-consuming undertaking.

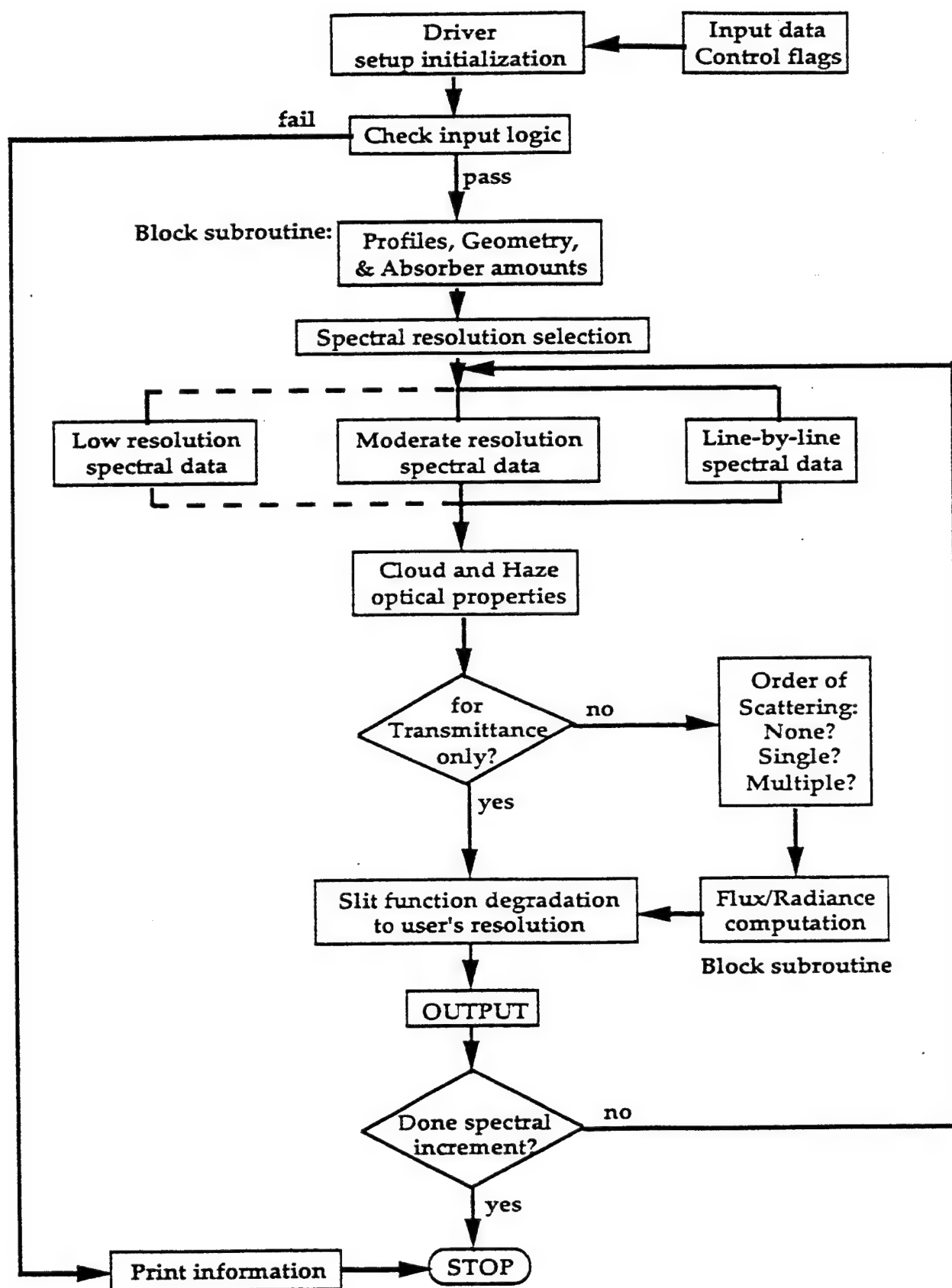


Figure 1. Flowchart.

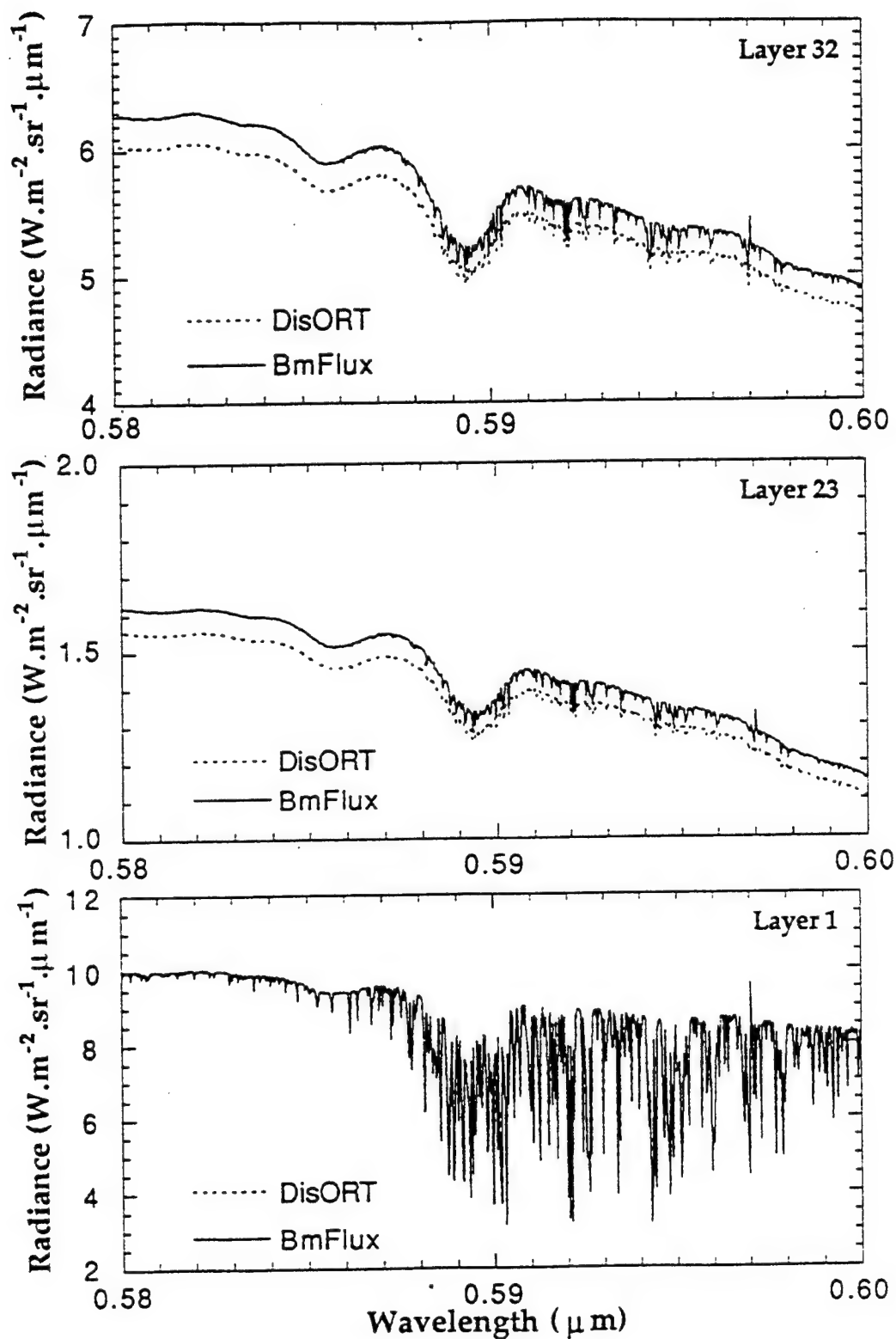


Figure 2. Comparison of solar multiple scattering source function for a clear sky sub-arctic winter McClatchey atmosphere, layer 1 for the lowest atmospheric layer and layer 32 for the highest layer.

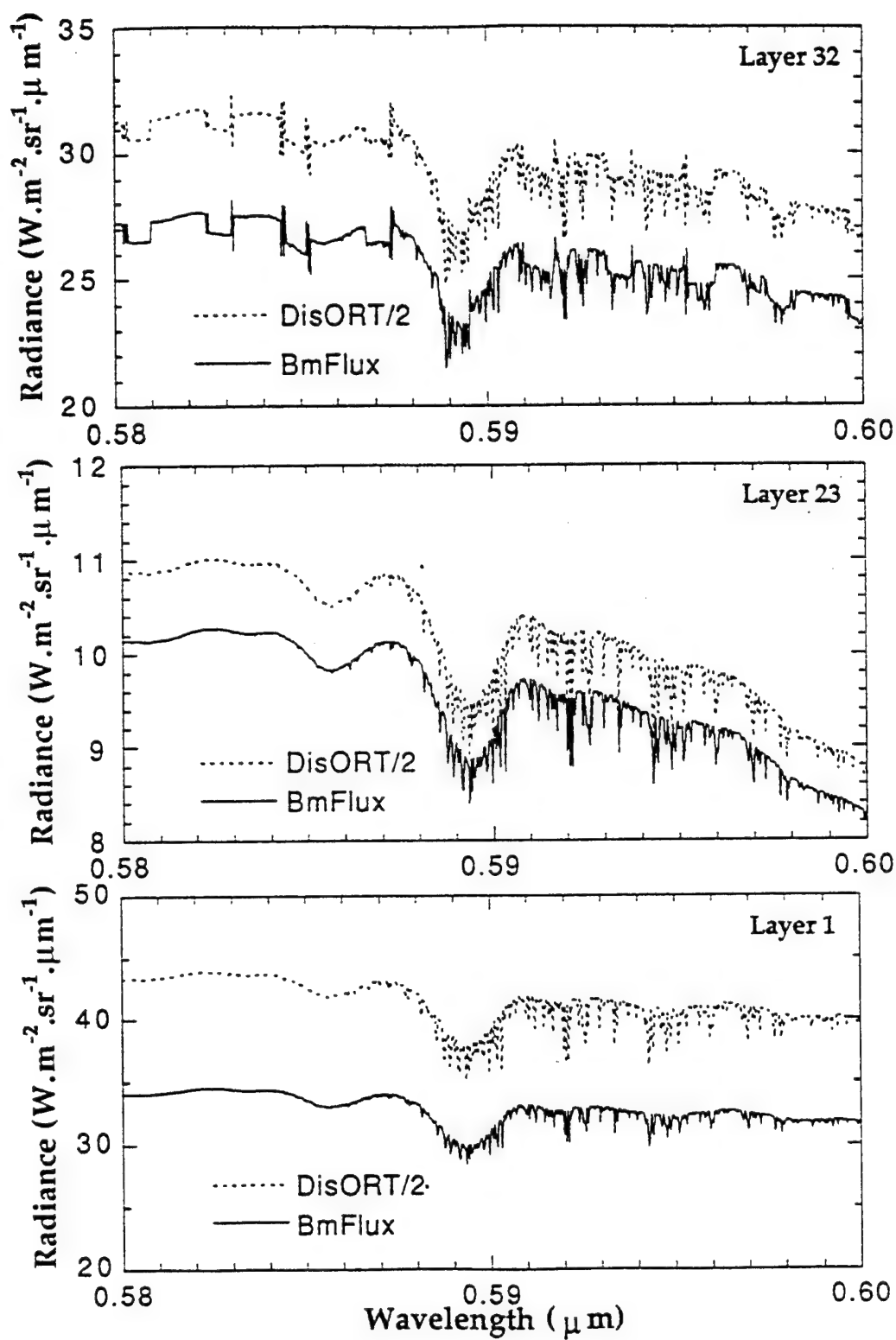


Figure 3. Same as in Figure 2, but for hazy sky condition (IHAZE=2).

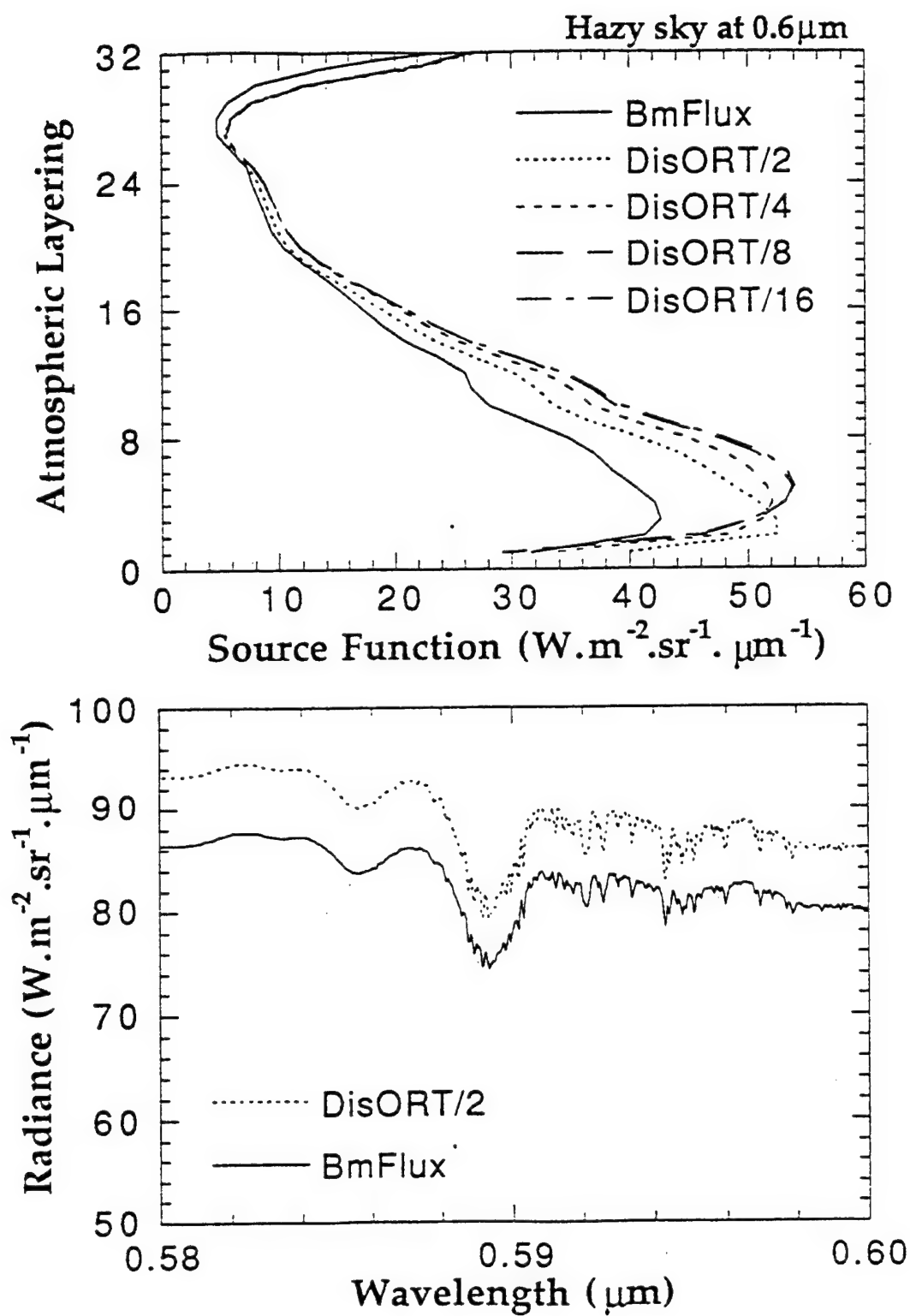


Figure 4. Same as in Figure 3, but for vertical profiles of source functions at 0.6 μm and spectral total radiance at top for an observer looking straight down.

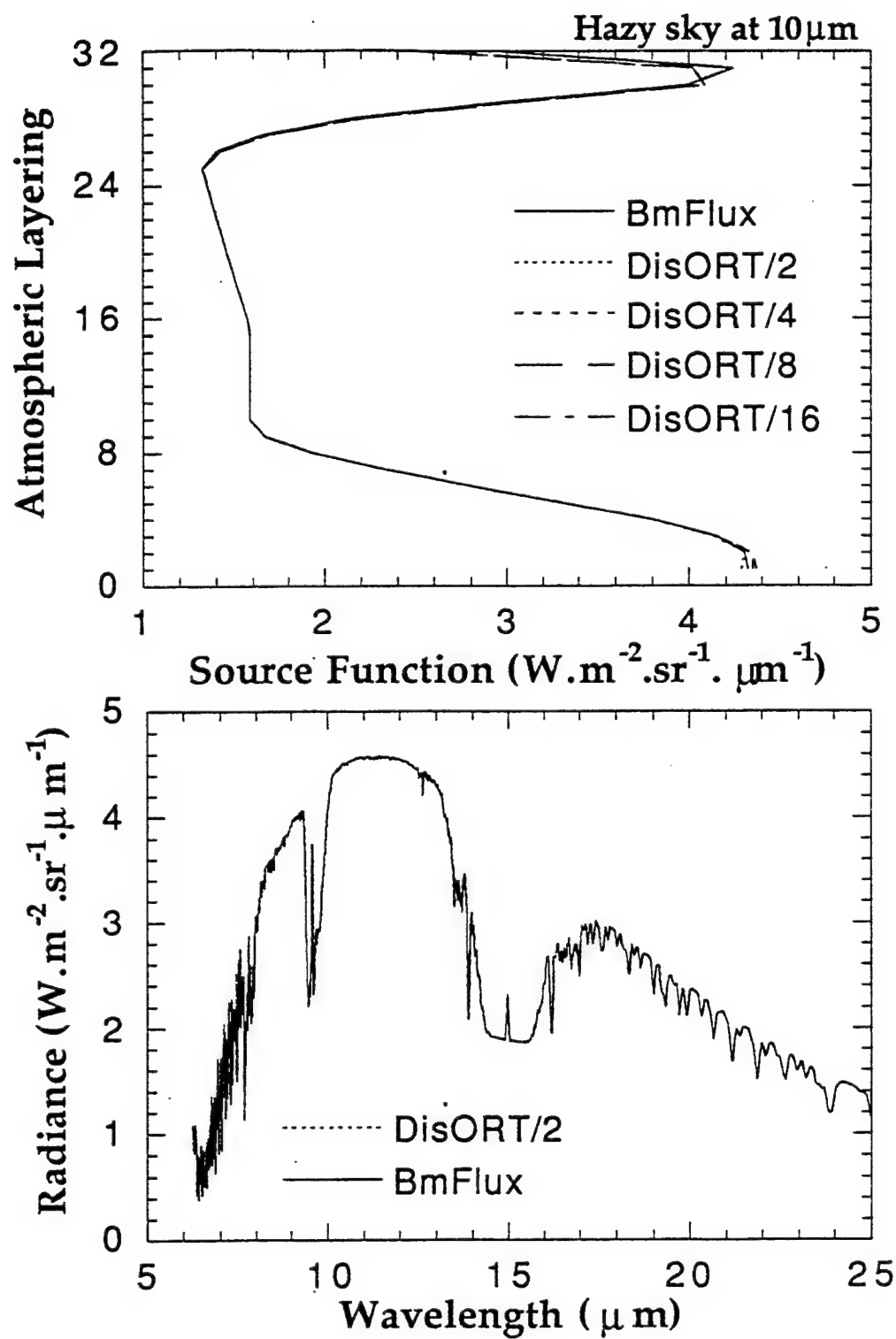


Figure 5. Same as in Figure 4, but for hazy sky thermal condition.

POSSIBLE AND DESIRABLE EXTENSIONS

A. Multiple Scattering in Plane Geometry

Present inclusion of multiple scattering (as the one based on BMFLUX) deals exclusively with the azimuthally-averaged component of the radiance.

This represents no limitation in the infrared where the source function is azimuth-independent.

In the solar, however, the existing azimuth-dependence of the MS source function is ignored, although the single scattering contribution is computed correctly including azimuth-dependence. Therefore, the following questions arise:

How large an error do we make by ignoring the azimuth-dependence of the multiple scattering term?

How can we correct the error made by this approach?

POSSIBLE APPROACHES

First approach: Incorporate full azimuth-dependence of the intensity, by using DISORT. But implementation in present version of MODTRAN is difficult and may require substantial restructuring of MODTRAN in order to accomodate the interface with DISORT.

Second approach: Use MODTRAN to compute optical properties and let DISORT handle the complete radiative transfer computation. In fact, the new version of DISORT (to be released soon) will have fast computation of multiple scattering and 'exact' computation of the single scattering component of the radiance.

Thlrd (hybrld) approach: If scattering is isotropic, then only the azimuthally-averaged component contributes and present approach is sufficient. Therefore, an approximate hybrid approach may consist of

- (i) scaling the anisotropic scattering so that the problem is reduced to one with isotropic scattering (similarity transformation);
- (ii) solving for the multiple scattering component based on the 'scaled' (isotropically scattering) problem for which only the azimuthally-averaged component contributes;
- (iii) combining this approximate multiple scattering solution with the 'exact' single scattering solution based on the complete phase function.

The third approach is attractive because it is expected to be very efficient. Therefore it would be of great interest to find out under what conditions it is valid.

B. Multiple Scattering in Spherical Geometry

Possible approach:

- (i) Use plane geometry to approximate derivative term, but compute Chapman function correctly using spherical geometry.
- (ii) Compute 'exact' single scattering solution as follows: Use iteration to incorporate the missing derivative terms due to plane geometry in the single scattering approximation. Thus, start with solving problem (i) above (ignoring multiple scattering) and use this solution to compute the missing terms. Add these contributions to the source term and solve problem (i) again with the additional source. Repeat this procedure, which should converge if the additional derivative terms due to spherical geometry are small enough. This should yield an 'exact' solution in the single scattering approximation.
- (iii) Solve for the multiple scattering component based on the 'scaled' (isotropically scattering) problem for which only the azimuthally-averaged component contributes.
- (iv) Combine this approximate multiple scattering solution with the 'exact' single scattering solution based on the complete phase function obtained as outlined in (ii) above.

This approach is expected to be quite efficient and may be accurate enough for many purposes.

Note:

1. For nadir and zenith directions there is by definition no azimuth-dependence. Therefore this procedure will give the complete solution.
2. For isotropic scattering there is nothing 'driving' azimuth-dependence. So solution will be azimuth-independent in this case.

C. Multiple Viewing Directions

MODTRAN presently computes for a single viewing direction and starts from 'scratch' when a new direction is desired. In contrast

DISORT can return *an arbitrary number of desired output directions* at insignificant additional computational cost.

Thus, if multiple viewing directions are desired it would be most efficient to:

- (i) use MODTRAN to compute optical properties,
- (ii) use MODTRAN's geometry package including curvature and refraction effects to compute the single scattering source term, and finally
- (ii) use new version of DISORT to do the complete radiance computation.

Accurate Computation of Heating/Cooling Rates and Photolysis Rates

MDTRAN has sufficient resolution to make it ideal for the computation of accurate heating/cooling rates and photolysis rates.

We envision that it could be used to establish an affordable 'benchmark' against which simpler more efficient schemes for use in large-scale models could be tested.

It should also be very useful for comparing detailed spectral measurements of radiative fluxes.

RAYLEIGH AND AEROSOL SCATTERING IN THE TROPOSPHERE AND STRATOSPHERE IN THE SPECTRAL RANGE 175-850nm: AN INTERACTIVE MODEL

D.E. Anderson

R. De Majistre and S. Evans

The Johns Hopkins Univ.
Applied Physics Lab
Laurel, MD 20723

Computational Physics, Inc.
Fairfax, VA 22231

We have developed an interactive version of the radiation field model described by Anderson and Lloyd (1990), Anderson and DeMajistre (1992) and DeMajistre, Zasadil and Anderson (1992). The model provides solution for the diffuse radiation field including ground albedo, aerosols and absorption by molecular oxygen and ozone. The integral equation solution has been coded for representation of the radiation field and accurate ($\sim 10 \rightarrow 20\%$) approximations to anisotropic scattering are included. LOWTRAN model atmospheres and Rayleigh, aerosol and ozone optical parameters have been utilized in the model. A spherical shell model for initial energy deposition is employed.

Rayleigh and Aerosol Scattering in the Troposphere and Stratosphere in the Spectral Range 175-850 nm

D. E. Anderson
Robert DeMajistre
Scott Evans

June 8, 1993

/homes/spike/pubs/models93/modelpres.doc

Overview

We have developed a radiation field model for the wavelength range 175-850 nm. This model has the following properties

- Calculates the source function (normalized monochromatic flux) for user specified altitude, solar zenith angle and wavelength grid.
- Includes the effects of O₂, O₃ absorption, rayleigh and aerosol scattering and spherical/refractive geometry.
- Model atmospheres and aerosol properties have taken from MODTRAN.
- Implements a rapid and reasonably accurate multiple scattering algorithm.
- Implements a preliminary version of a new refraction algorithm.
- Can be used with a prototype interactive IDL interface
- Modular design for use with different applications

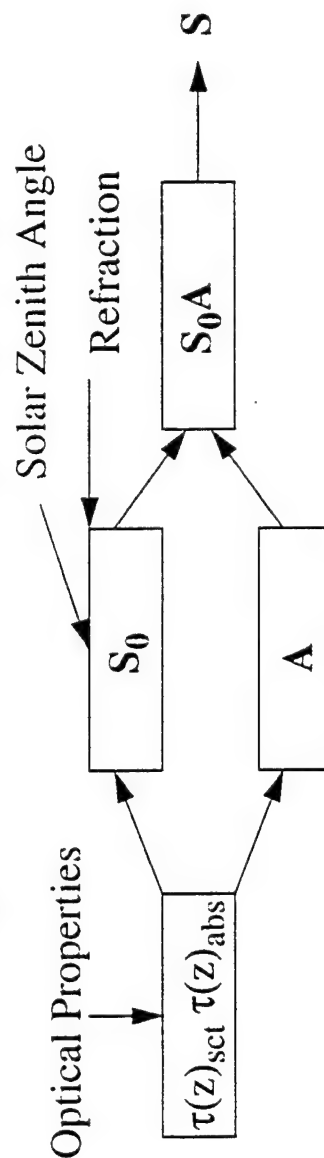
Algorithm

The basic equation used in the model is

$$S(\lambda, \theta) = S_0(\lambda, \theta) A(\lambda)$$

Where S is the vector of source functions, S_0 is the vector of single scattered source functions and A is a matrix derived from the properties of the model atmosphere.

The S_0 term is simply the attenuated solar beam flux plus a term from lower boundary reflection ($S_0 = e^{-\tau} + S_{0\text{alb}}$). Spherical and refractive geometry is used to calculate S_0 . A is the inverse of a matrix whose elements are functions of the absorption and scattering optical depths at the various altitudes. Note that this matrix need only be calculated once for each wavelength; it is independent of solar zenith angle.



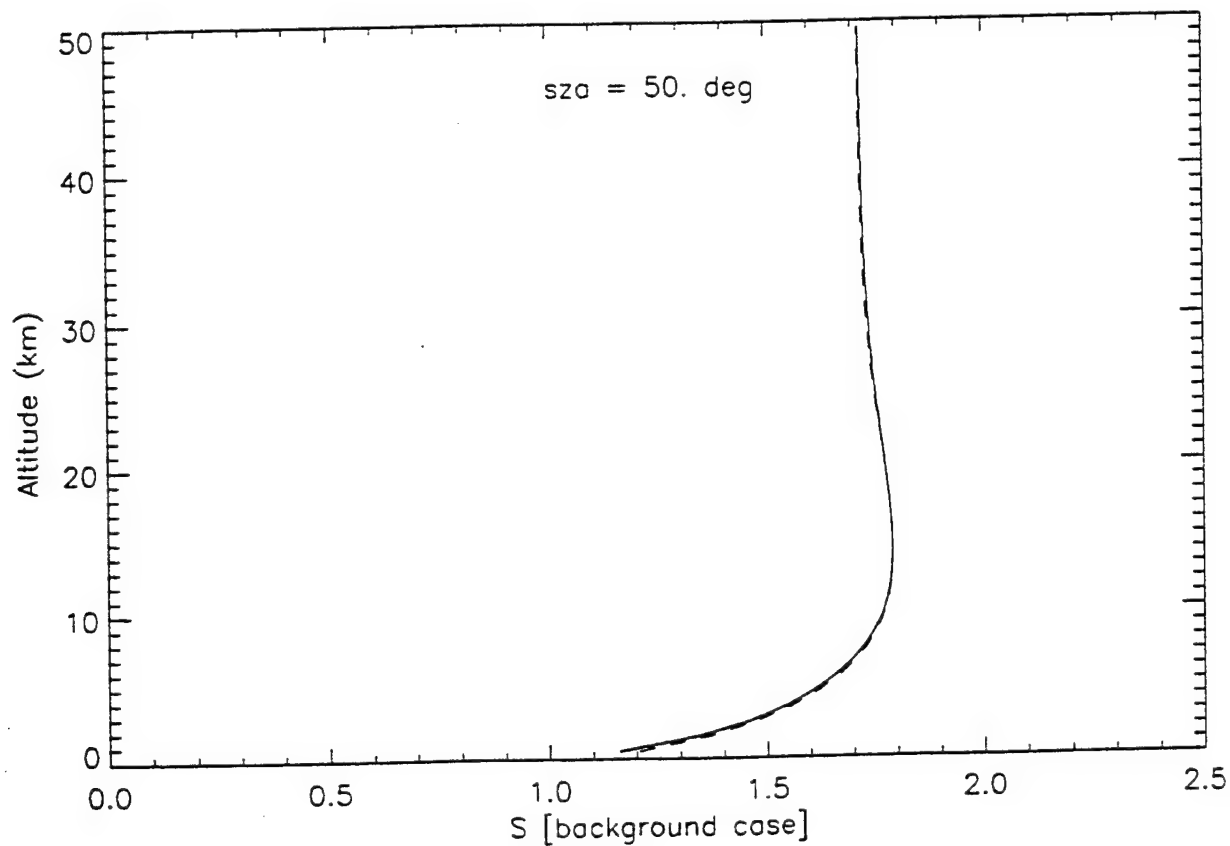
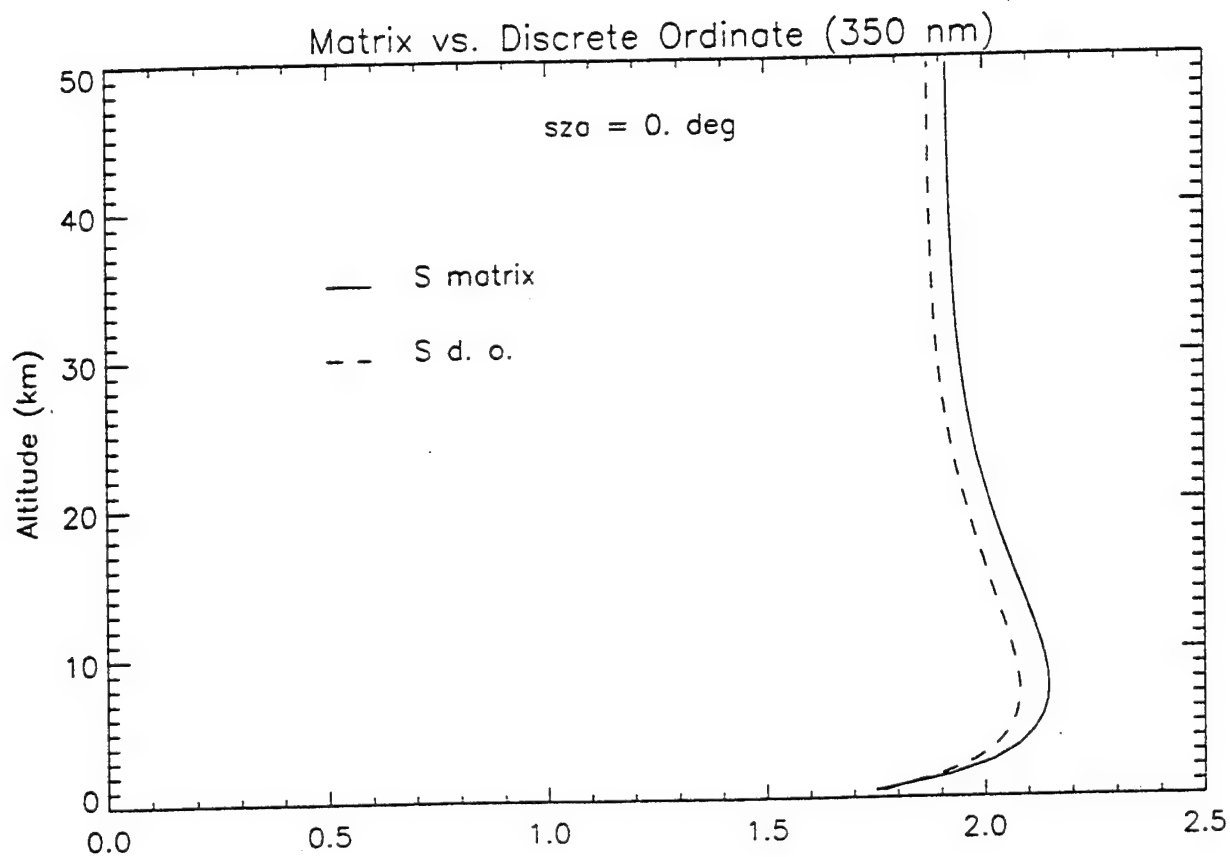
Optical Properties Database

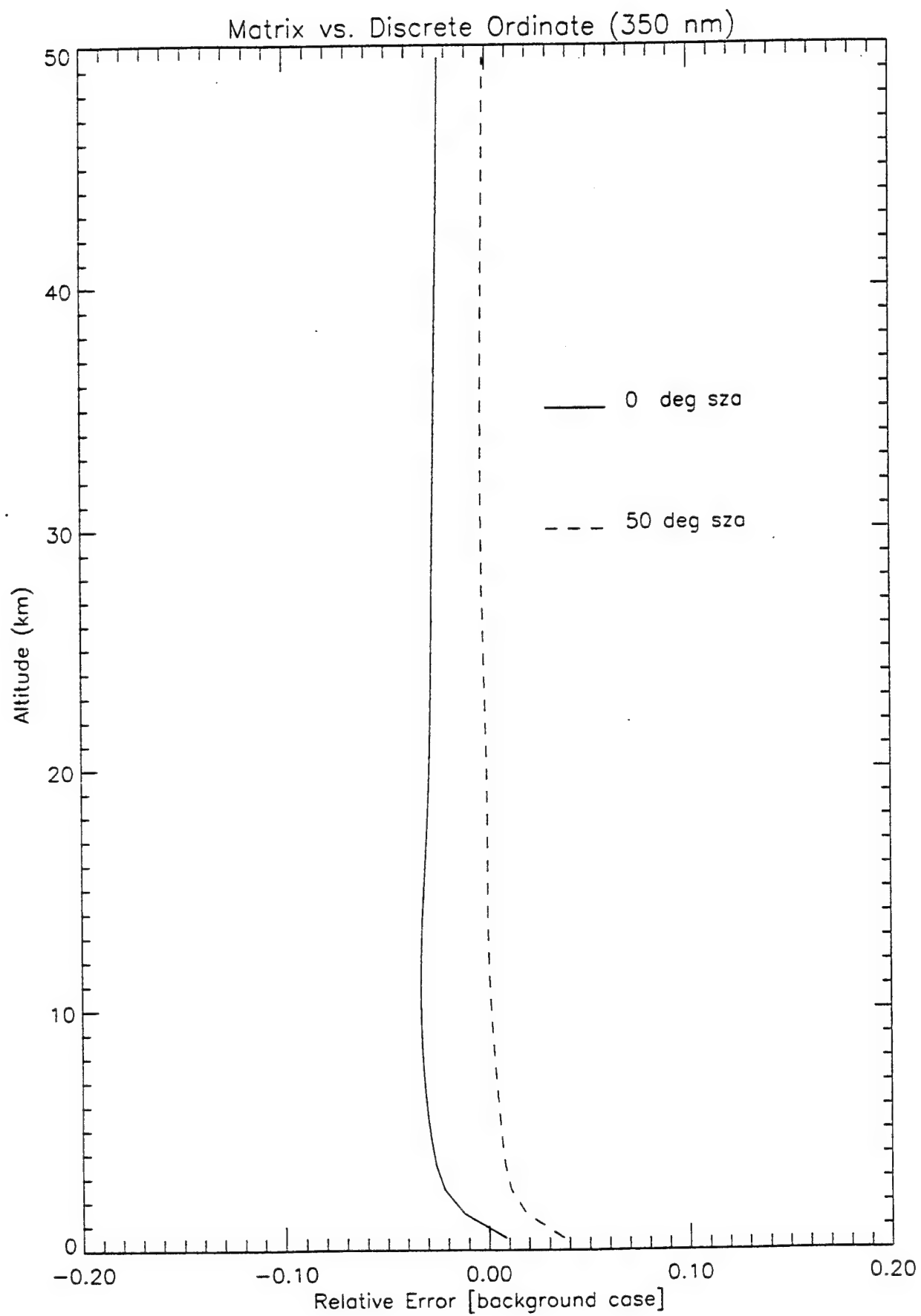
All the model atmospheres in MODTRAN are also available in our model. The aerosol models are also included (with the exception of clouds and fog). The aerosol phase functions are not used, but the asymmetry parameters in the database are used to calculate reduced cross sections. These reduced cross sections are used to correct for forward scattering in our isotropic approach. We also consider the absorption by aerosols parameterized in the database.

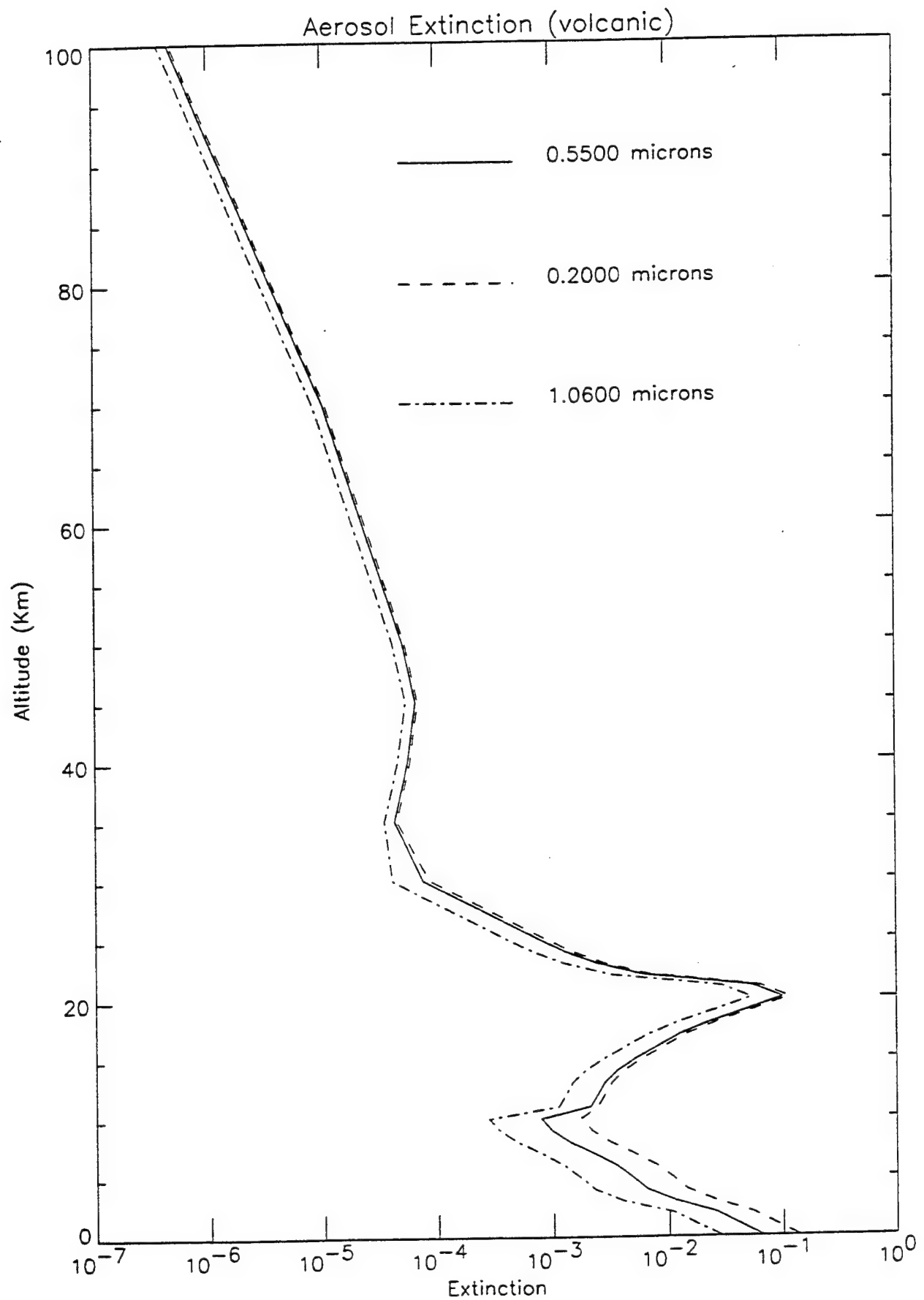
Temperature dependent ozone cross sections are taken from Molina and Molina and WMO 1985. O₂ Schumann-Runga cross sections are taken from Allen and Fredrick, and Herzberg continuum parameterization from Yoshino *et al.*

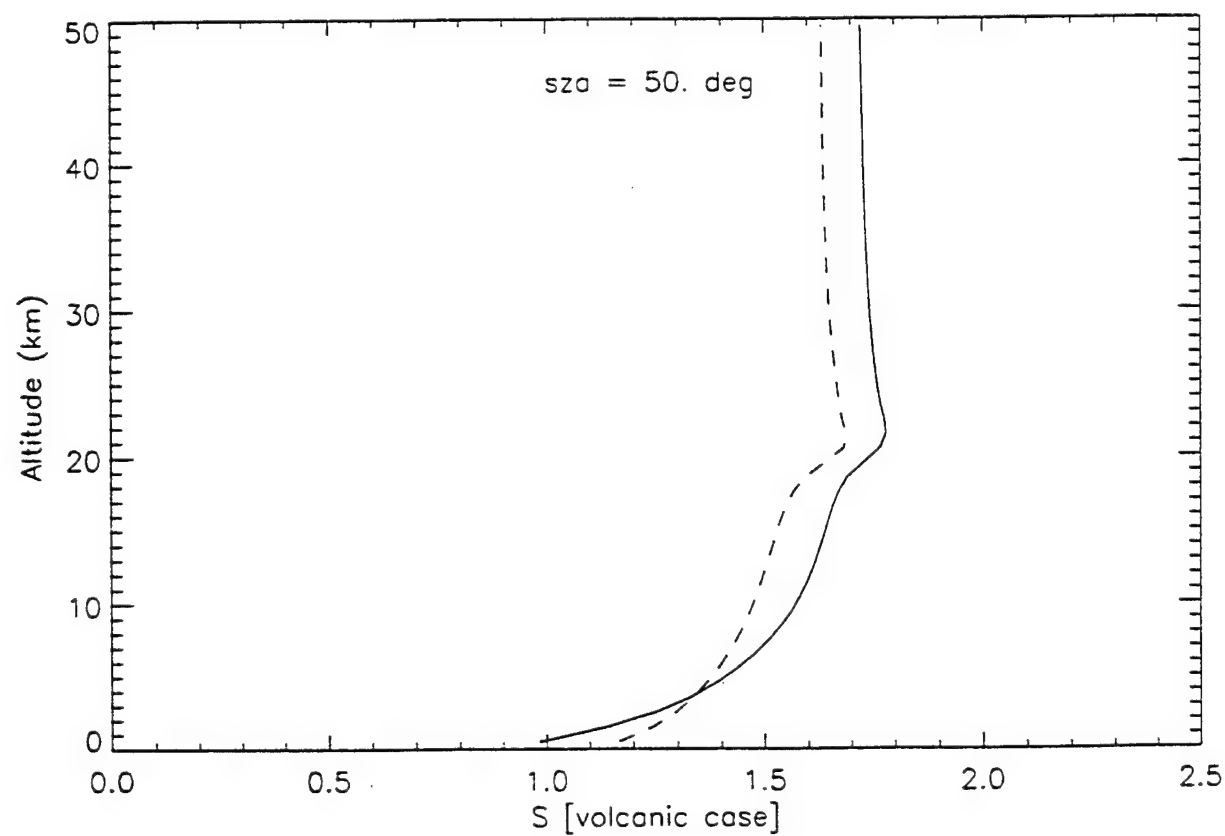
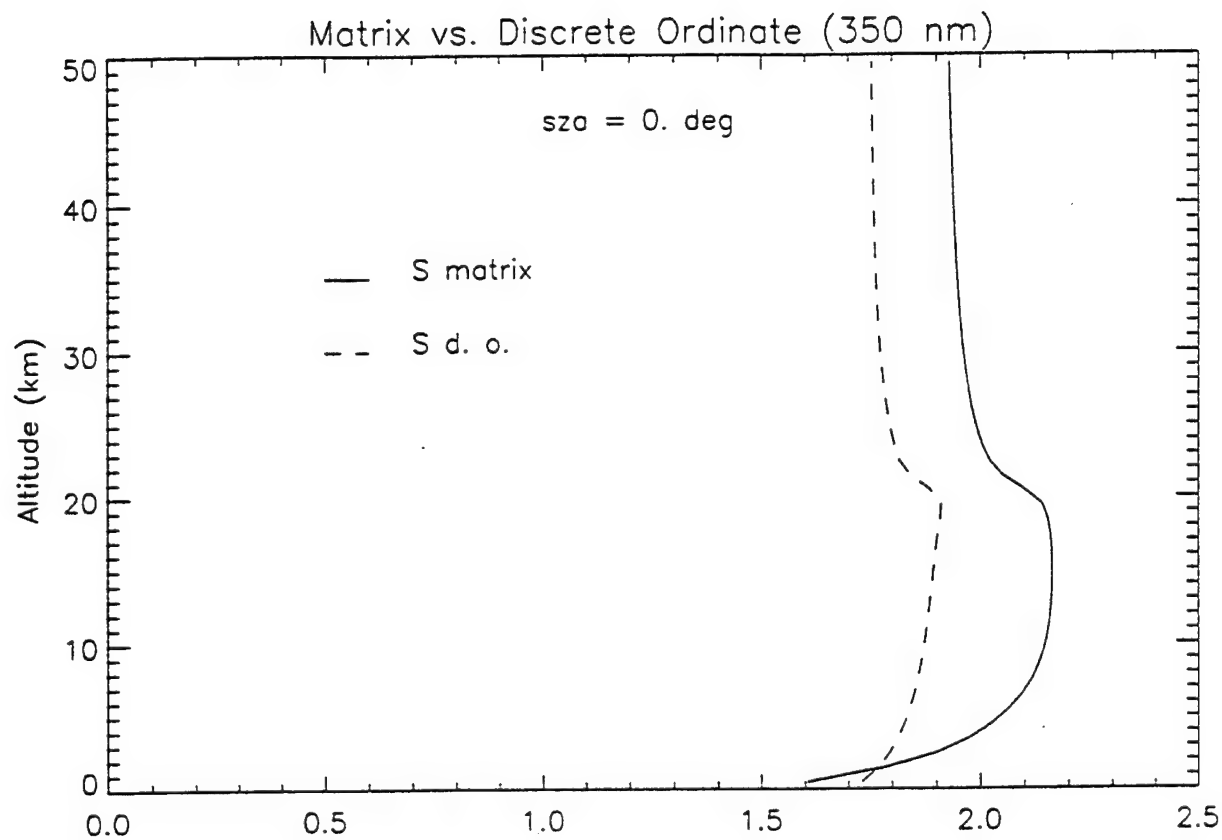
Model Accuracy

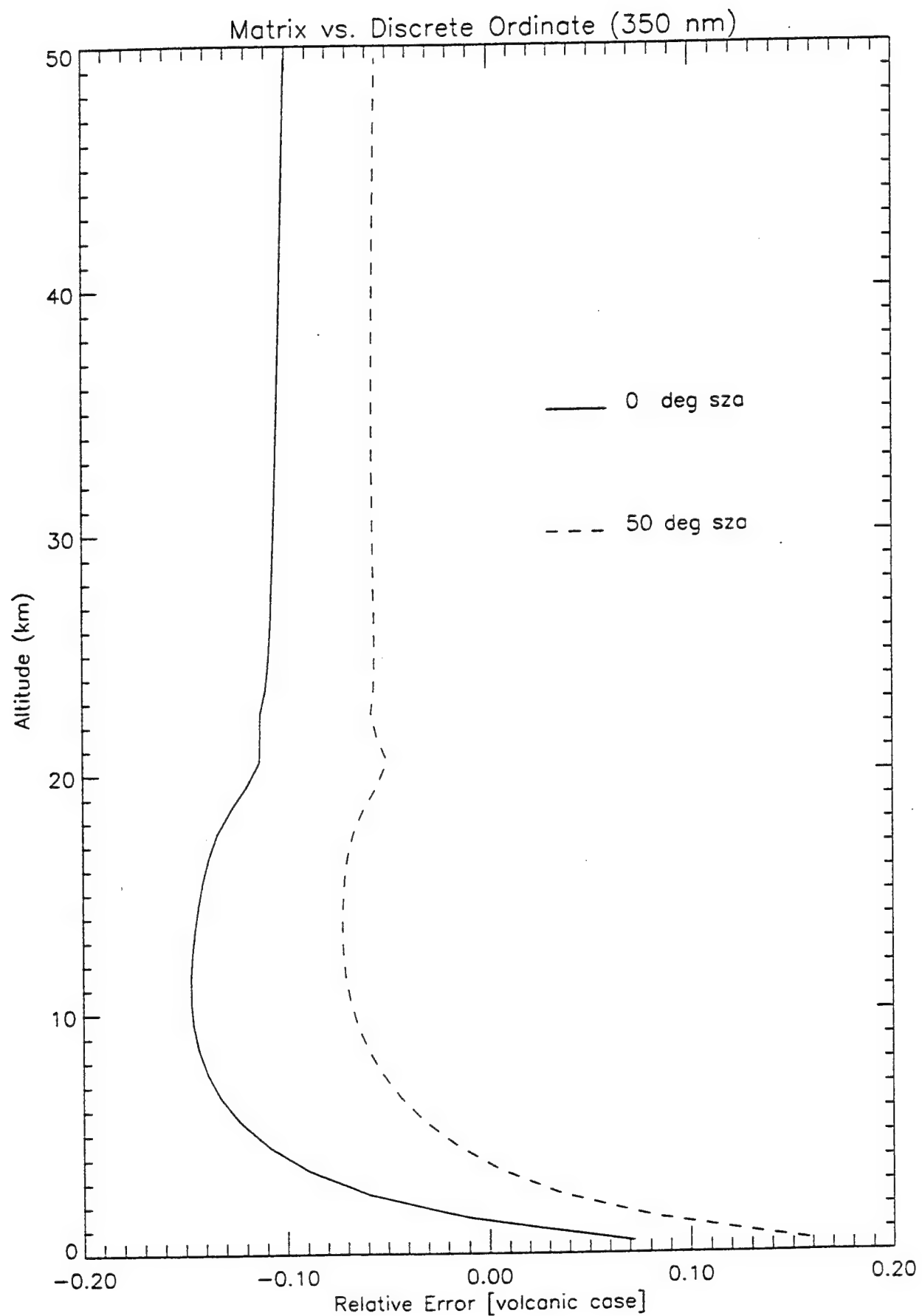
Comparisons have been made with DISORT (Stamnes *et al.*) for various conditions. Using a background aerosol, our method is within 5% of the discrete ordinate method. With an extreme volcanic aerosol, agreement is within 15%.











Main Menu

Files

Altitude Grid:

min: 0 max: 80 (km) 0: 25

Ground Albedo: 0.0000 0.5000 0.5 Scale: 1.00000

SSA: 30.0000 00.0000 10.0000 00.0000

LOWTRAN aerosol model ☒ YES ☐ NO

Atmosphere:

Tropical
Midlatitude Summer
Midlatitude Winter
Subarctic Summer
Subarctic Winter
1976 U.S. Standard

Create Rayleigh Scattering input file

Start Run

Lowtran Aerosol Model

Use (1-g) correction to aerosol optical depth

Boundary Layer (0-2 km)

Visibility:

00 km
25 km
10 km
5 km
1 km

size distribution:

RURAL
URBAN
DESERT

Stratospheric (2-10 km)

Visibility

25 km
50 km

Stratospheric - Mesospheric (10-90 km)

Altitude Profile

Background
Moderate Volcanic
High Volcanic
Extreme Volcanic

Size Distribution

Background
Aged Volcanic
Fresh Volcanic

Season

Spring/Summer Fall/Winter

Done

315

Plot



Altitude	SEA	Wavelength
1.00000	30.0000	1762.15
3.00000	60.0000	1777.81
5.00000	70.0000	1793.76
7.00000	80.0000	1809.99
9.00000		1826.52

Applications

We have used the model to calculate

- Photodissociation frequencies
- Local fluxes (ground level and stratospheric)
- Effective albedo of the atmosphere
- Limb profiles (Rayleigh scattered component)
- The effects of various cross section values

The model is particularly well suited to exploring the effects of ozone and aerosol variations.

The speed and method of the multiple scattering calculation make this model ideal for use in photochemical models and other applications which depend on fluxes or averaged intensities.

EXPERT SYSTEM IN PLEXUS

P.C.F. Ip, S.B. Downer, M. Noah,
K. Radermacher, J.P. Kennealy

F.O. Clark

Mission Research Corp.
One Tara Blvd., Suite 302
Nashua, NH 03062

Geophysics Directorate,
Phillips Laboratory
Hanscom AFB, MA 01731-3010

This talk will review the principles behind building the PLEXUS expert system. The use of an expert system in the PLEXUS interface will intelligently assist users in solving atmospheric background problems by directing them to the appropriate atmospheric codes(s) and only querying them for parameters important to their application. Building the PLEXUS expert system is a long and detailed process involving several iterative phases. The knowledge base is acquired by researching existing code documentation, consulting experts in the field, and establishing trends from running the atmospheric codes. As the knowledge base is developed, it is organized into meaningful subtopics and then translated into rules used by the expert system shell. Examples of each of these phases will be given, with main emphasis placed on the results obtained from a systematic study of MODTRAN input parameters. This study has yielded some results of interest to a large number of MODTRAN users.

EXPERT SYSTEM in PLEXUS



*P.C.F. Ip, S.B. Downer, M. Noah,
K.J. Radermacher, and J.P. Kennealy
Mission Research Corporation
Nashua, NH*

*F.O. Clark
Geophysics Directorate, Phillips Laboratory
Hanscom AFB, MA*

MRC

PLEXUS Expert System Goals

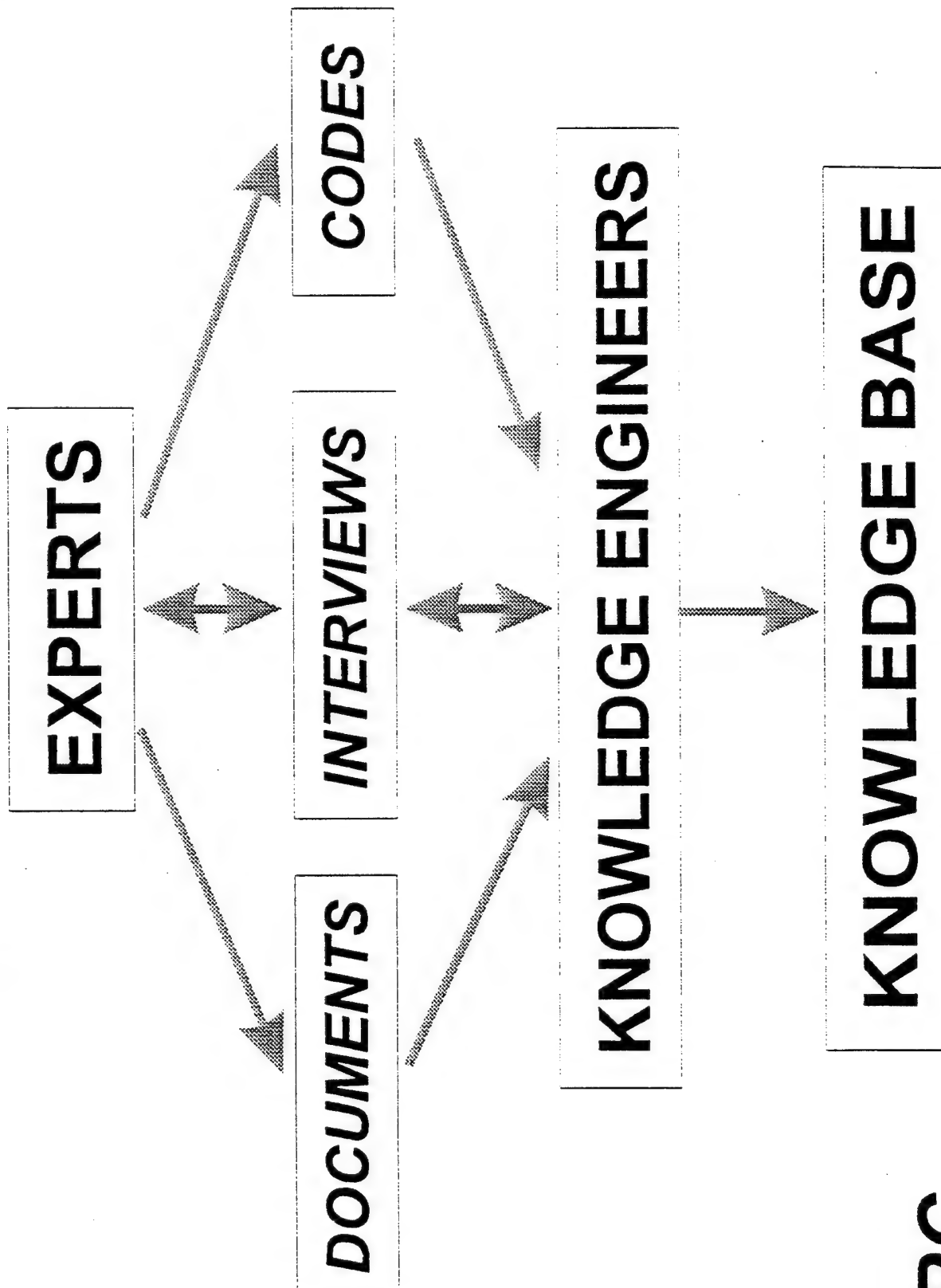


- Focus on Issues Important to User
- Minimize User Specifications
- Verify Parameters Dynamically
- Offer Appropriate Pre-Calculated Results

MRC



Knowledge Acquisition Process



MRC

MODTRAN Parametric Studies



* Clouds

Rain

Aerosols

Ground Altitude

Boundary Temperature

Surface Albedo

Multiple Scattering

Model Atmosphere

Vertical Structure Algorithm

MRC



MODTRAN Cloud Studies

SUN

LINE-OF-SIGHT

CUMULUS CLOUD

3.0 KM

EARTH SURFACE

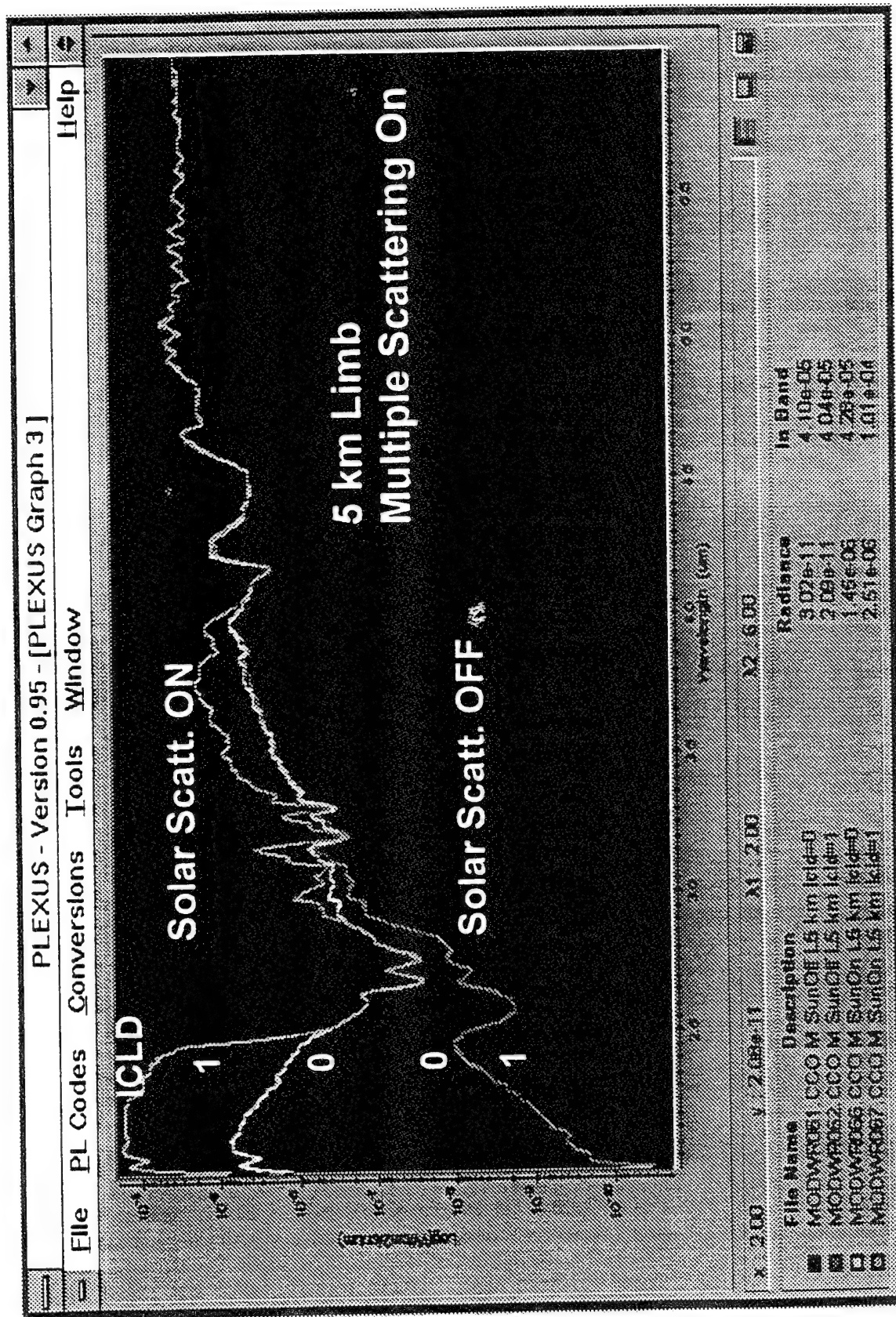
0.66 KM

Solar Scattering
Scattering Angles
Multiple Scattering
Short and Long Paths
Surface Albedo

MRC

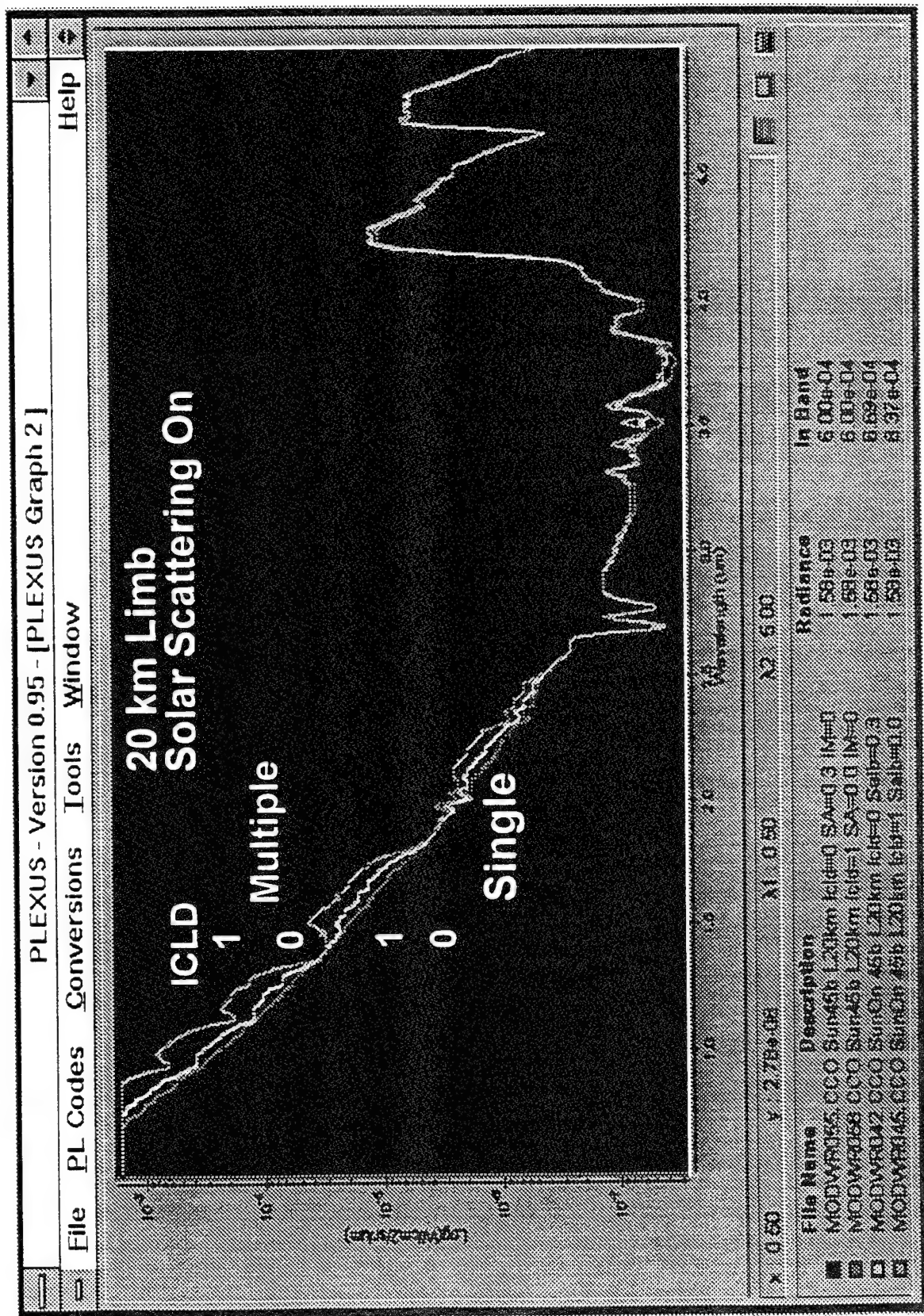


Effect of Cloud with Solar Scattering Off and On





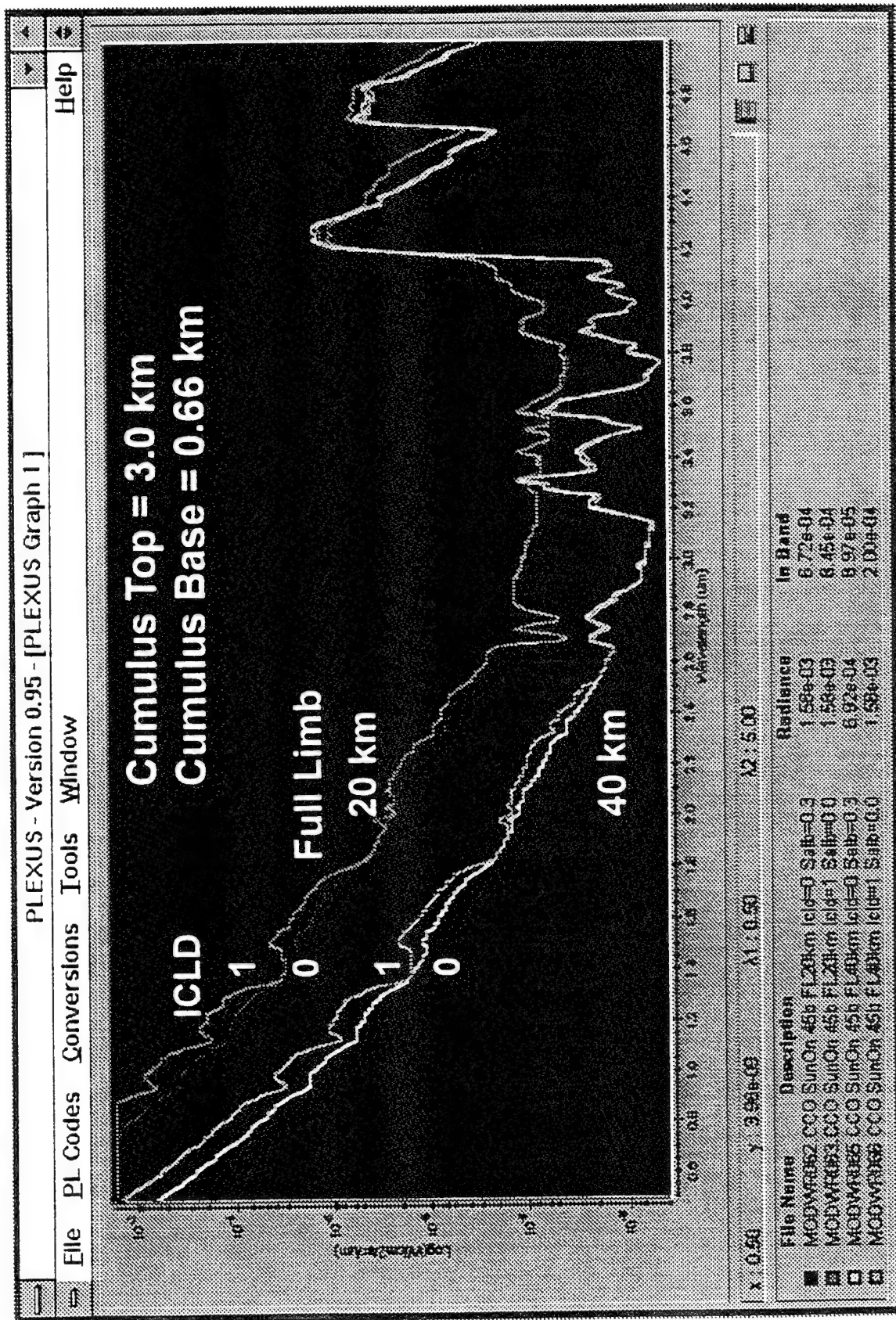
Effect of Cloud for Single and Multiple Scattering



MRC

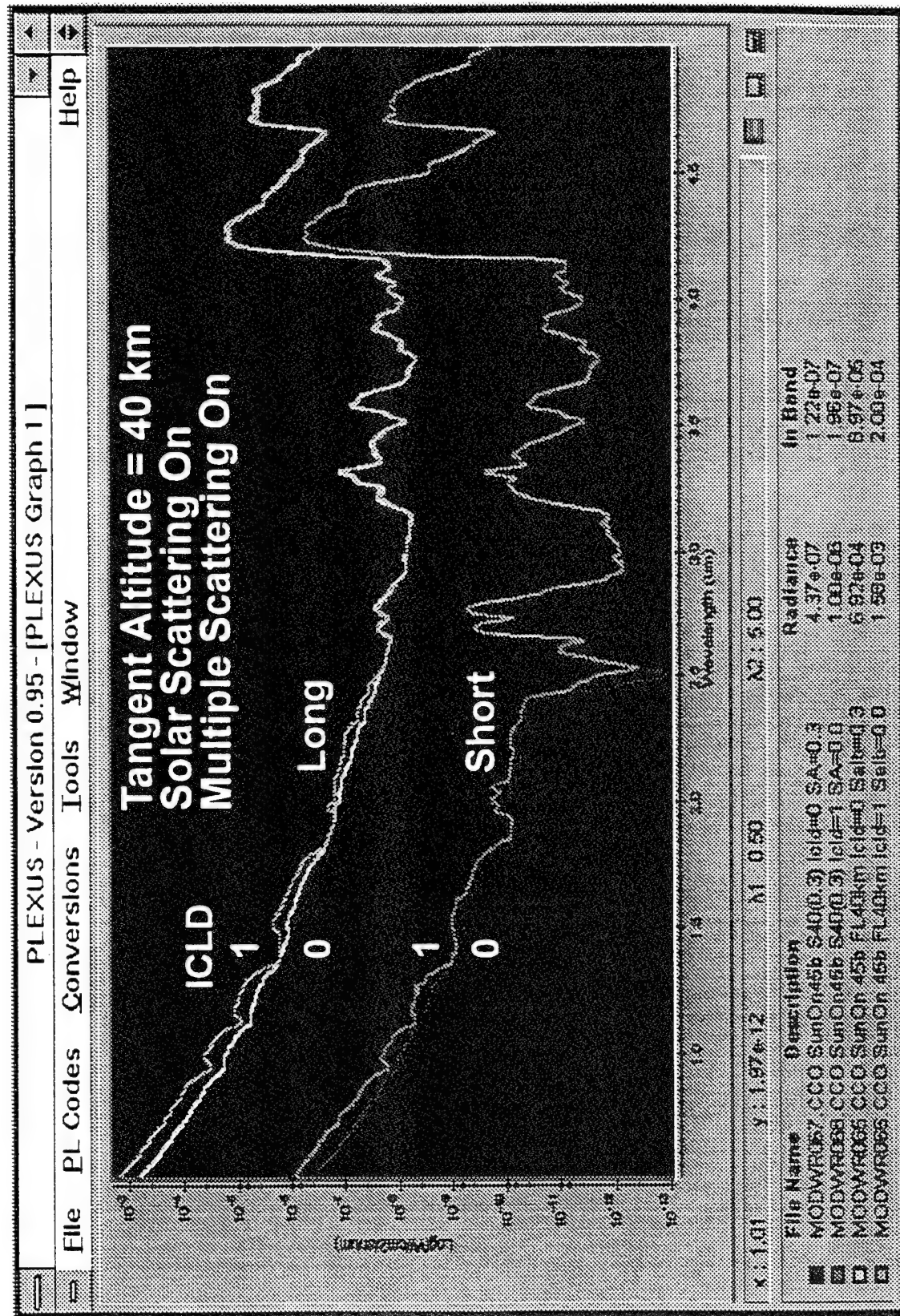


Effect of Cloud under Multiple Solar Scattering





Effect of Cloud for Short and Long Paths



MRC

PLEXUS Expert System Dialog



Static Facts

Max. Cloud Ht. = 20 km
Solar Scatt. < 5 micron

Dynamic Facts

Line-of-Sight,
Date, Time,
Output Mode,
Spectral Range, etc.

Rules

Rule 15
if (LOS, Date, Time known) then
calculate Sun Visibility to LOS

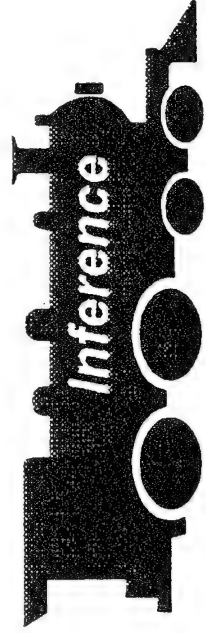
Rule 30
if (Tangent Alt. \leq 20 km) then
ask for CLOUD information

Rule 36
if (Tangent Alt. > 20 km)
if (Mode is Radiance)
if (Solar Multiple Scattering is On) then
ask for CLOUD information

knowledge base

Agenda

Rule 45, Rule 35



shell

MRC

PLEXUS Expert System Plans



- Append Knowledge Base
- Offer Explanation Facility
- Give Solution Confidence Factor

MRC

PHILLIPS LABORATORY'S EXPERT-ASSISTED USER SOFTWARE
(PLEXUS)

**S.B. Downer, J.P. Kennealy, P.C.F. Ip,
M. Noah, K.J. Radermacher, D. Einstein**

F.O. Clark

Mission Research Corp.
One Tara Blvd., Suite 302
Nashua, NH 03062

Geophysics Directorate,
Phillips Laboratory
Hanscom AFB, MA 01731-3010

PLEXUS Version 1.0 is now available for general release. This version supports the DoD Atmospheric codes LOWTRAN, MODTRAN, SHARC, the CBSD Celestial Codes and the FAUST Method. The FAUST Method is designed to help fulfill current DoD requirements for downward-looking background radiance and transmittance descriptors. By combining the results from the equilibrium lower atmospheric model (MODTRAN) and non-equilibrium upper atmospheric model (SHARC), a unified seamless single answer is generated. The FAUST user interface, coupled to an intelligent knowledge-based, assists users of all abilities in correctly setting up and running calculations of this nature.

PLEXUS provides a number of data visualization tools as well as importing, exporting, and printing functions. Two such tools, integrated band intensities and filter convolutions allow users to explore sensor operability ranges. Present and future capabilities are presented with a demonstration of the first general release, PLEXUS Version 1.0.

PLEXUS

Phillips Laboratory Expert-assisted User Software

*S.B. Downer J.P. Kennealy, P.C.F. Ip, M. Noah,
K.J. Radermacher, and D. Einstein
Mission Research Corporation
Nashua, NH*

*F.O. Clark
Geophysics Directorate, Phillips Laboratory
Hanscom AFB, MA*





PLEXUS Objectives

DOD/SDIO-Standard Phenomenologies

- Single User Interface
- Support a Diverse User Base
- Generate "Unified" Solutions
- Pre-Calculated LOS Library
- Extensive Data Analysis Tools
- Multi-Spectral Data Fusion



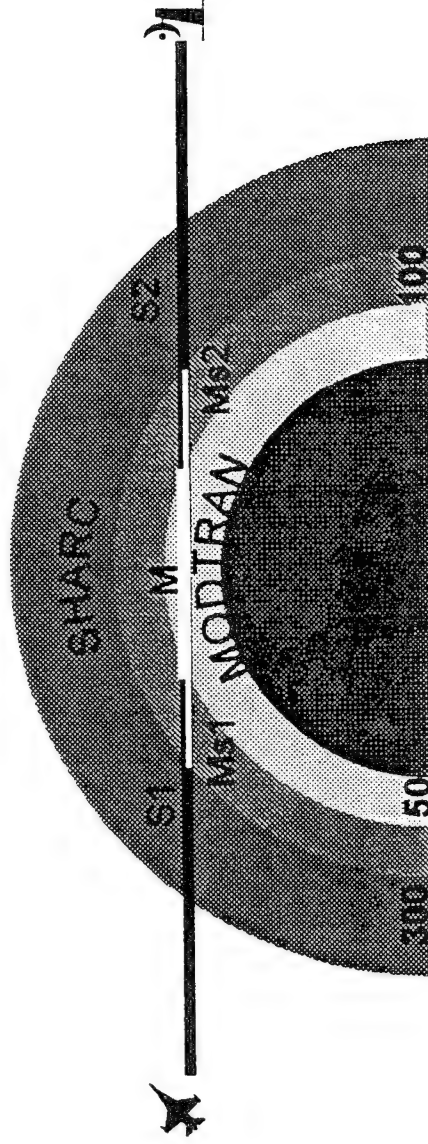
PLEXUS Current Status

- MS Windows 3.1
- Beta Testing Winter 1993
- General Release Summer 1993
- Supports
 - MODTRAN/LOWTRAN7
 - SHARC
 - CBSD
 - Rapid Response Data Base
 - FAUST Method

MRC



FAUST Method



$$\text{Radiance} = (R_{S1} + R_{Ms1}) * T_M * T_{S2} + R_M * T_{S2} + R_{S2} + R_{Ms2}$$

$$\text{Transmittance} = T_{S1} * T_M * T_{S2}$$

MRC

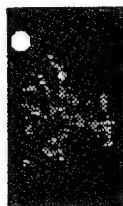


FAUST Method Interface

- Multiple Expertise Levels
- Automatic Unit Conversions
- Express Key Input
- Arbitrary LOS
- Graphical Geometry
- Knowledge Base Driven
- Sets Up and Runs Multiple Codes
- Correct Code Selection

MRC

Enter The Time of Observation



Spring

☒ Day ☐ Night

Express Keys
Click/Drag Earth on Orbit

Click/Drag Earth on Orbit

FALL

SUMMER

WINTER

SMITHS

[March]		1993				
S	M	T	W	T	F	S
	1	2	3	4	5	6
7	8	9	10	11	12	13
14	15	16	17	18	19	20
21	22	23	24	25	26	27
28	29	30	31			

Greenwich 0.0

Hours

12

Minutes

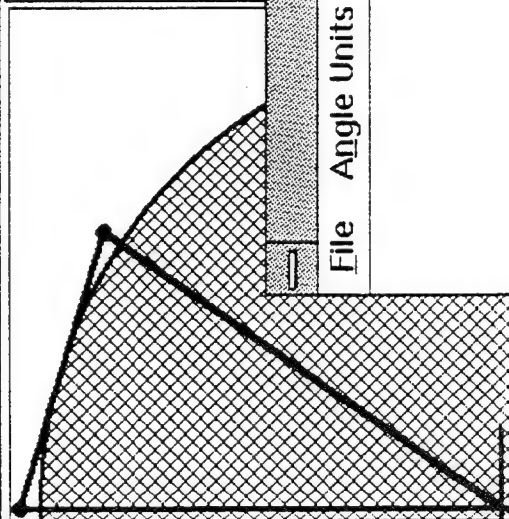
Seconds

Go Back

Continue

Time and Date set the Solar Position.

Form 3 of 7



Line-Of-Sight Specification

File Angle Units Lat Units Lon Units Altitude Units Help

Path Description

Slant Path

Initial (Observer) Location

Altitude	KM
300.00	

Latitude Deg 42.76

Longitude Deg+E
-71.38

Sensor Geometry

Azimuth Angle	Deg
0.000000	0.000000

Zenith Angle	Deg
107.219216	

Range to Path End KM ☐ Infinity

Express Keys

Initial Point Location

426

USA

Nashua NH

Initial Point Altitude

Save 300.00

Calculator...

Go Back

Continue

Earth's air and water. The mean water temperature is 10.7°C. The mean air temperature is 10.0°C.

1940



PLEXUS Upgrades

- User Defined Atmospheric Profiles
- Expanded Printing
- Spectral Filter Functions
- SAMM
- UNIX, X-Windows
- Altitude Profiles
- Cross Plots
- SAG
- CD ROM Distribution

MRC



PLEXUS Future Support

- FASCODE
- AURIC
- Additional PL Codes
- SAMM Generated Result Data Base
- Graphical Geometry Descriptor
- Batch Processing

MRC

EARTHLIMB BACKGROUNDS IN THE STRATEGIC SCENE GENERATOR MODEL

Susan McKenzie

Mission Research Corporation
One Tara Blvd., Suite 302
Nashua, NH 03062

The Strategic Scene Generator Model (SSGM) is a computerized methodology which generates viewer-perspective radiance maps of quiescent and enhanced natural backgrounds and perturbed backgrounds with embedded targets and target induced/related events. The Earthlimb Backgrounds represents an on-line phenomenology capability for the SSGM Baseline design. The components for this phenomenology have been provided by Phillips Laboratory codes. RAD_E v4.4 is the computer model that generates structured Earthlimb 2D radiance maps in the SSGM. The 1D radiance profiles are computed by one of two options: on-line calculations by PL radiance codes or extractions from the FASTLIMB database. FASTLIMB is a 1% resolution database generated off-line using PL radiance codes and is supplied for rapid-running profile generation. Both options store in-band 1D radiance profiles and structure information for generating 2D image output. 2D structured images can be generated by RAD_E directly. This structure contains stochastic, non-homogeneous, non-stationary spatial structure. A correlated multi-frame option is included in this process for frame-to-frame continuity. RAD_E radiance and structured image output generated using these methodologies will be presented.



EARTHLIMB BACKGROUNDS

IN THE

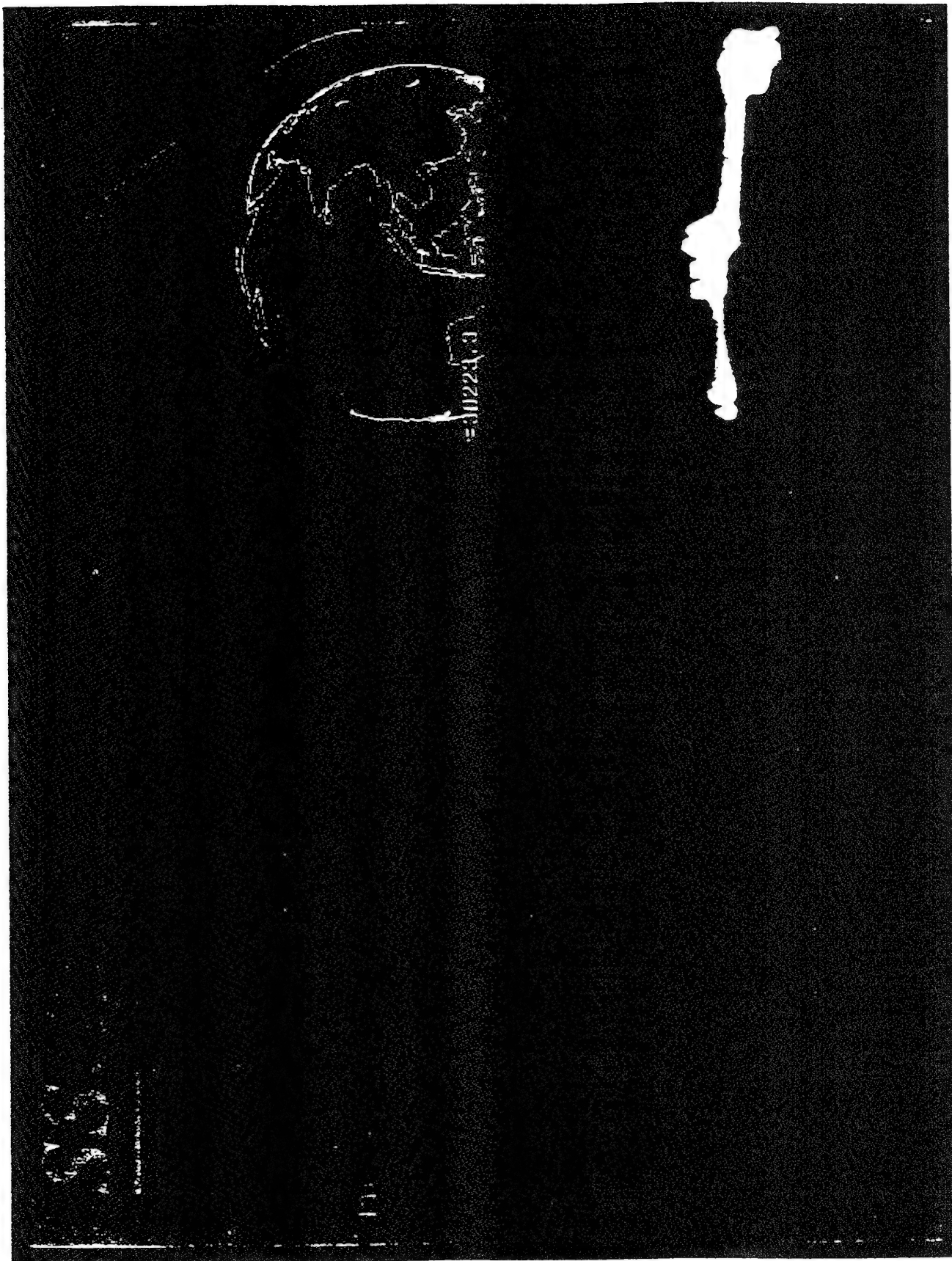
STRATEGIC SCENE GENERATOR MODEL

Susan M. McKenzie
Russell A. Armstrong
Sean P. McGowan

Mission Research Corporation
1 Tara Blvd. Suite 302
Nashua, New Hampshire 03062

June 8 - 9, 1993

 *Mission Research Corporation*





STRATEGIC SCENE GENERATOR MODEL TECHNICAL DESCRIPTION

SSGM DEFINITION

A computerized methodology by which viewer-perspective radiance maps are derived from an ensemble of standard models and authenticated data bases via an interactive software system which executes the pertinent codes and selects the required data bases from which the scenes are generated using resampling, interpolation, and image composition techniques.

SSGM PHENOMENOLOGY

Quiescent and enhanced natural backgrounds and perturbed backgrounds with embedded targets and target induced/related events.

- | | |
|-------------------------------------|---------------------------|
| Earth Terrain and Ocean | Celestial Backgrounds |
| Opaque and Semi-transparent Clouds | Missile Bodies and Plumes |
| Quiescent Atmosphere with Airglow | Fuel Vents and Debris |
| Enhanced Atmosphere with Aurora | PBV's and RV's |
| Nuclear Perturbations to Atmosphere | Decoys and Satellites |

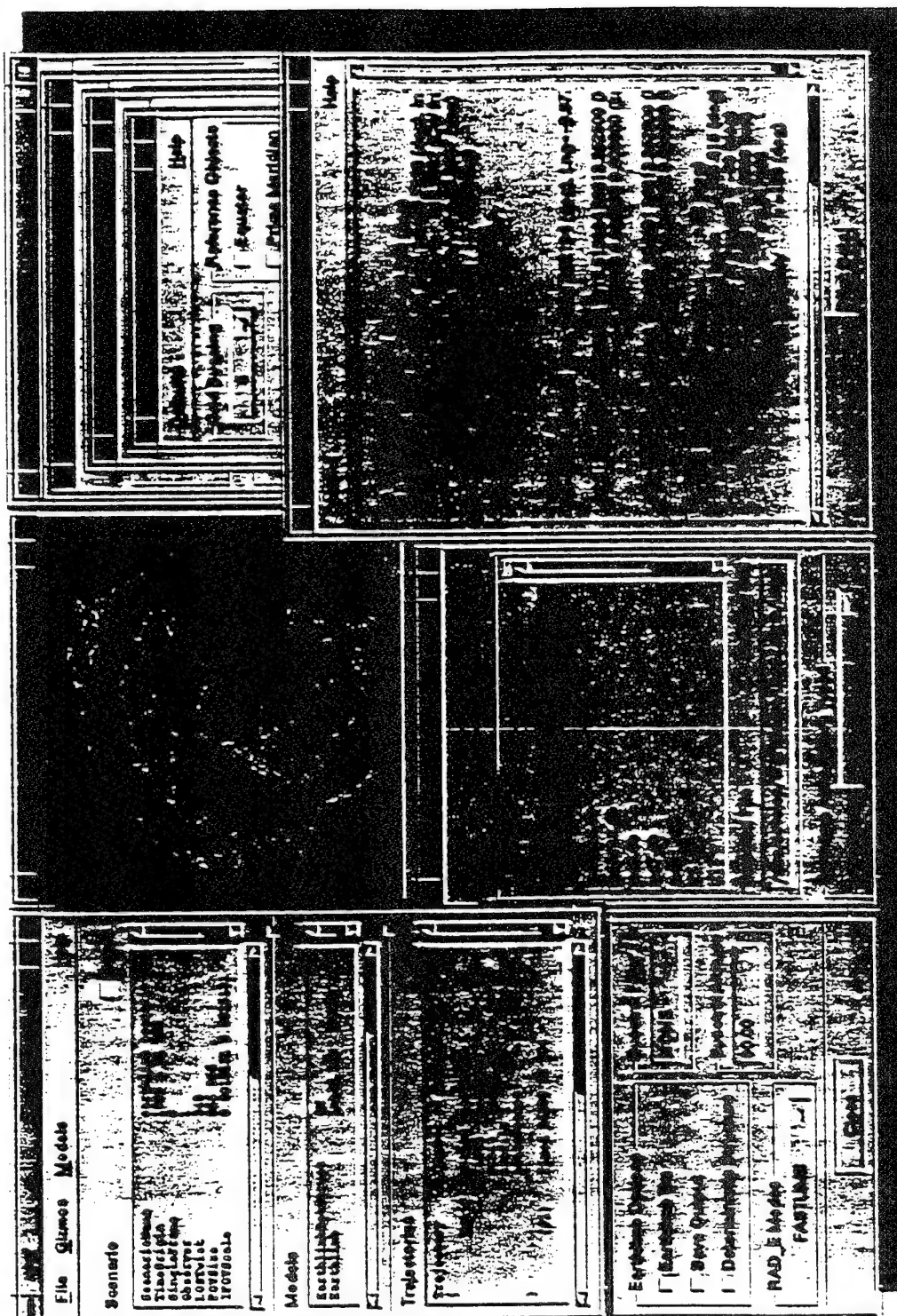


Mission Research Corporation



STRATEGIC SCENE GENERATOR MODEL

SCENARIO CONSTRUCTION TOOL: EARTH/LAMB COMPONENT



Mission Research Corporation



EARTHLIMB

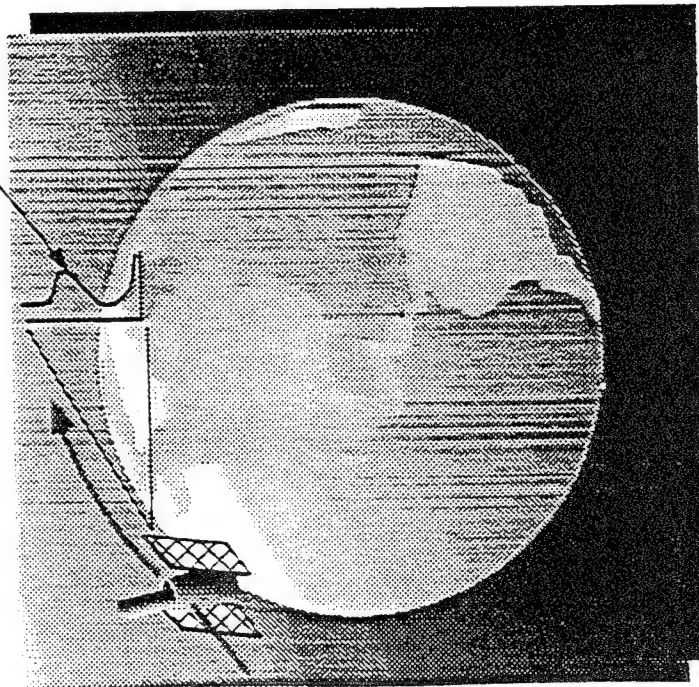
- Two Operational Modes:

- 1D Profile
- 2D Image

- 1D Profile Mode:

- User-Specified Observer Location, LOS Boresight, Date, Time
- LOS Radiance is Computed by RAD_E from -512 to 715 km Tangent Height by One of Two Options:
 - FASTLIMB
 - MODTRAN/SHARC
- Negative Tangent Height Radiance Provides Earth Atmosphere Radiance Below-the-Horizon
- 1D Profile is Mapped to Two-Dimensional Image by MAKEFRAME and Stochastic Structure is Added as an Option

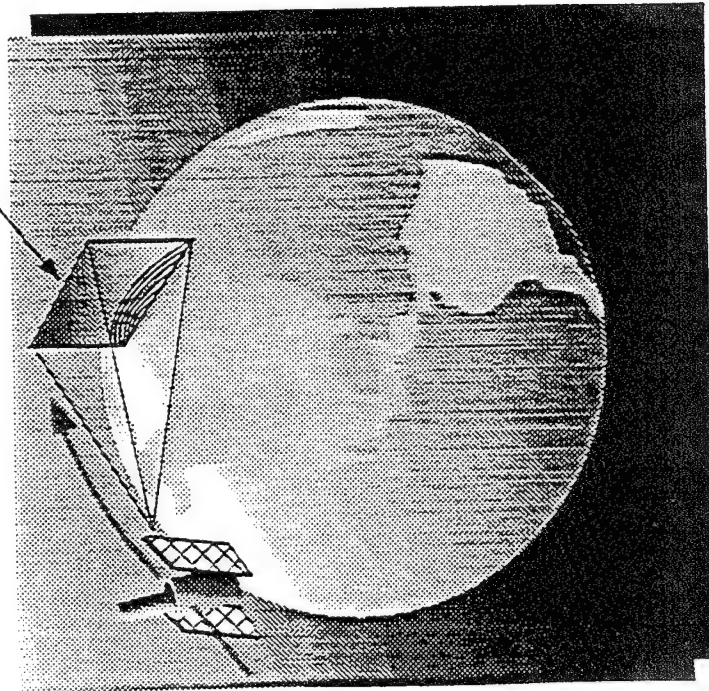
1D LOS RADIANCE
PROFILE





EARTHLIMB 2D IMAGE

SCENARIO - SPECIFIC
2D IMAGES



B 030 92 14

- User-Specified Observer Location and LOS Boresight for Each Frame
- User-Specified IFOV, # Rows, # Columns
- 1D Profiles are Computed for Each Frame Using Either FASTLIMB or MODTRAN/SHARC Option
- Two-Dimensional Images are Computed for Each Frame by CLUTTER Code for User-Specified IFOV and FOV Array
- CLUTTER Computes Local Values of LOS Radiance (from 1D Profile), PSD Component for Each Scale Height, Sub-Scenes with Invariant Structure Statistics, and Composite Scenes by Overlapping Sub-Scenes
- 2D Scenes are Not Processed Further by MAKEFRAME

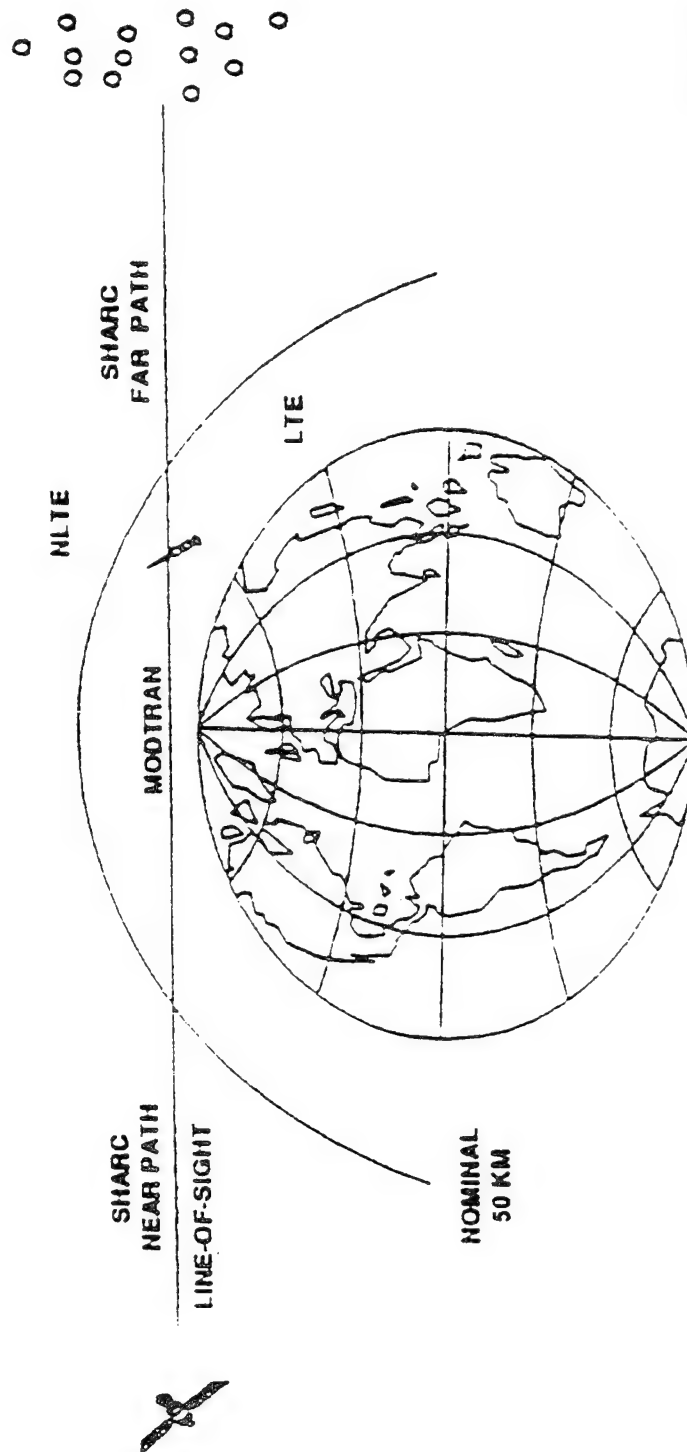


MODTRAN/SHARC

- MODTRAN/SHARC Invokes the MODTRAN 92 Code (LTE) for Tangent Heights from 0 to 50 km (Every 1 km) and the SHARC (V2.0) Code (NLTE) from 50 to 295 km (Every 5 km). Database Extrapolated to 715 km.
- LOS Radiance for Paths Intercepting Both LTE and NLTE Atmospheres are Computed with Coupled Treatment
- Output Resolution is 2 cm^{-1} for Both Codes Which is Spectrally Integrated to Yield In-Band Radiance
- Two Model Atmospheres are Supported: U.S. Standard 1976 and Subarctic Summer
- MODTRAN Represents 12 Atmospheric Molecules and Multiple Scattering from Aerosols
- SHARC Represents NO, CO, N₂O, O₃, NO⁺, and Three Isotopes of CO₂



EARTHLIMB MODELING



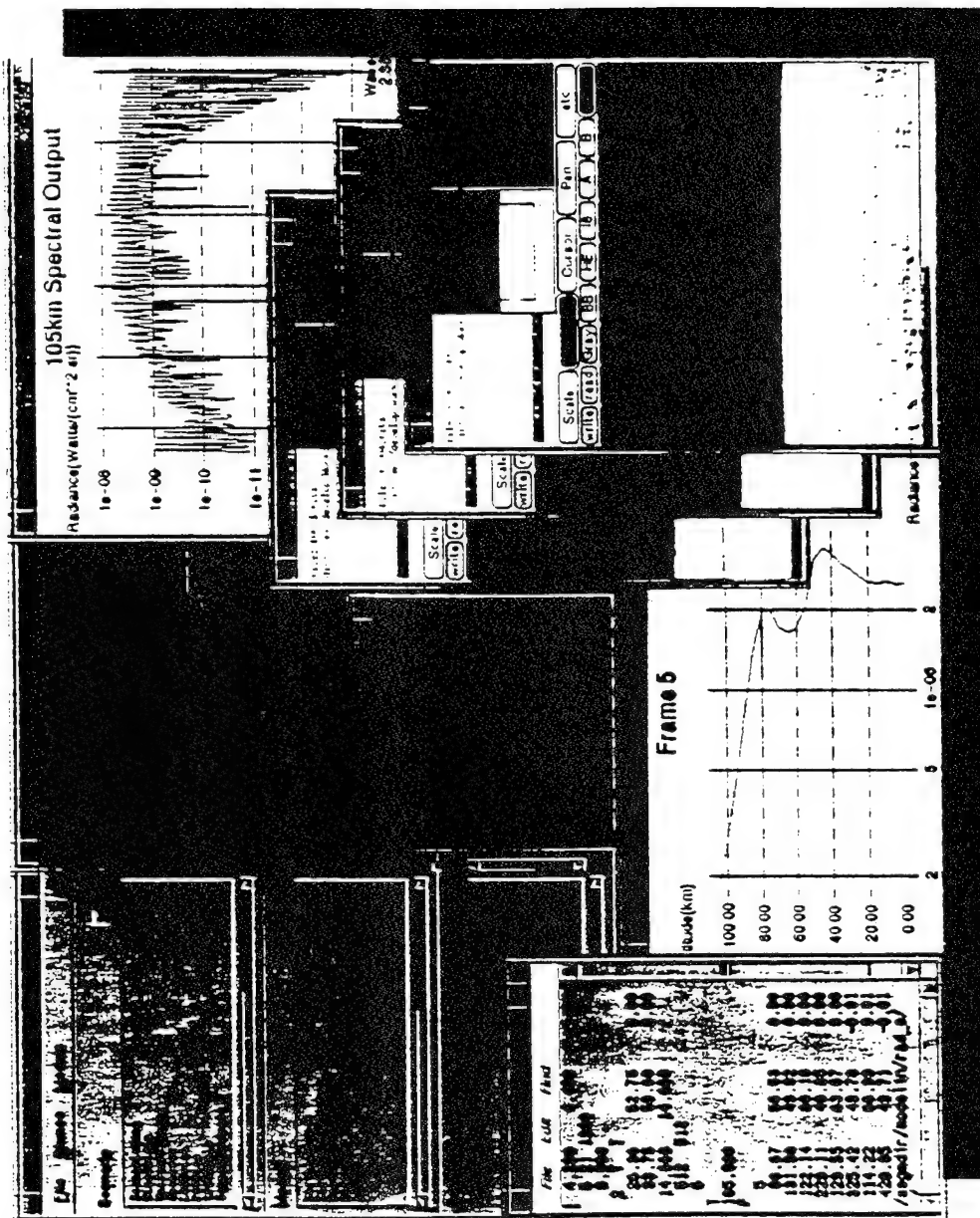
8 030 05 17 04



Mission Research Corporation



STRATEGIC SCENE GENERATOR MODEL REPRESENTATIVE EARTHLEMB IMAGE AND ASCII OUTPUT



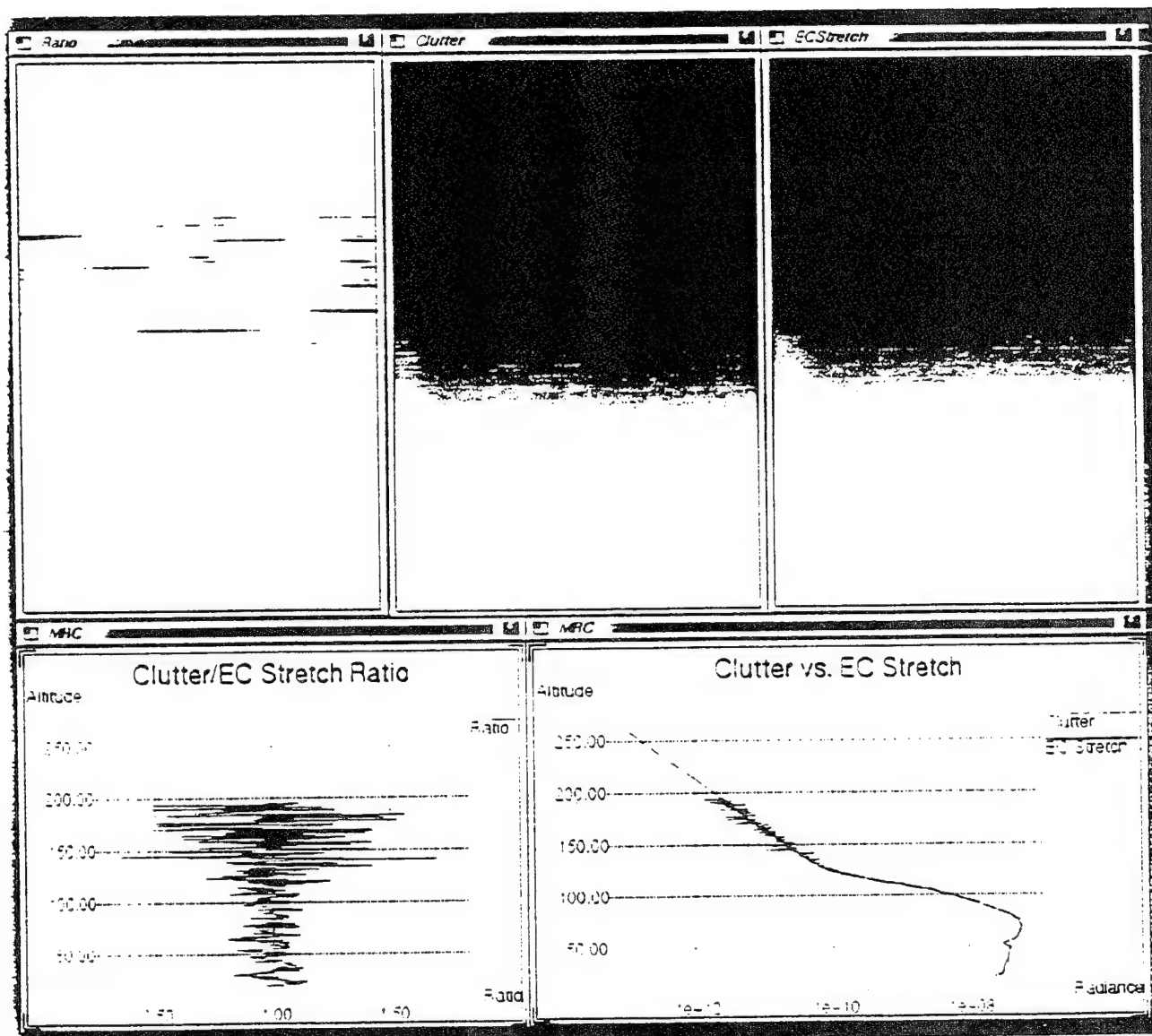
Mission Research Corporation





STRATEGIC SCENE GENERATOR MODEL

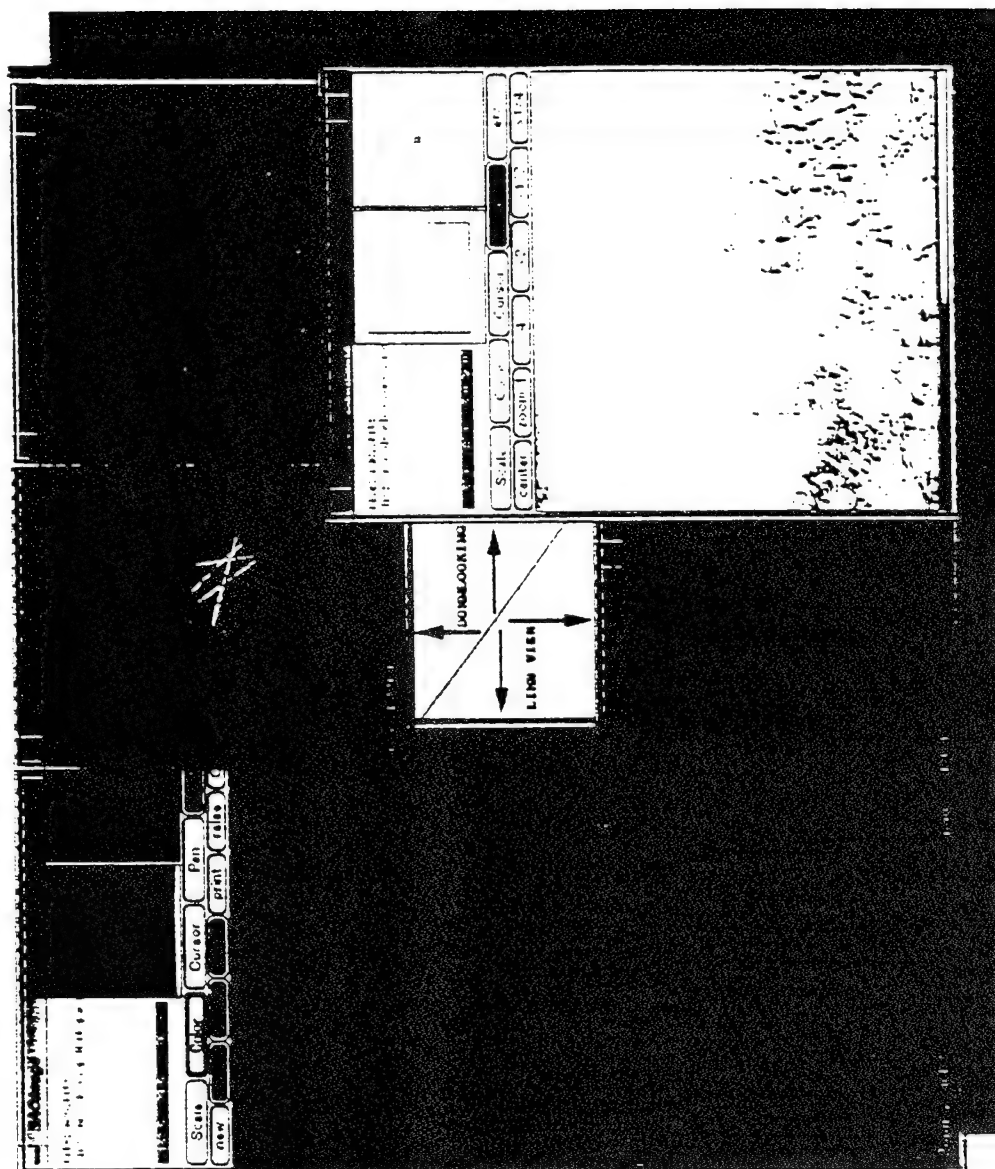
REPRESENTATIVE STRUCTURED EARTHLIMB IMAGE OUTPUT





STRATEGIC SCENE GENERATOR MODEL

AIR-TO-AIR AND AIR-TO-GROUND IR SCENES



 **Mission Research Corporation**



EARTHLIMB MODELING OPERATIONAL SSGM



GLOBAL ATMOSPHERIC STATES

Expand current configuration (Modtran/Share), including MSIS applications and coupling to the nuclear heave.

LIMB TERMINATOR TREATMENT

Limb terminator treatment via database approach and on-line algorithms.

RADIATION TRANSPORT ALGORITHMS

M/S LOS Transmission via on-line and database approach.
Implement SAM Single LTE/NLTE Model when available.

ATMOSPHERIC PERTURBATIONS

Man-made dynamics, Deterministic Gravity Waves and Stochastic Turbulant Variability Updates

EXTEND WAVELENGTH COVERAGE TO THE UV

Extend wavelength coverage via database approach and on-line capabilities.



ATMOSPHERIC EXTINCTION ANALYSIS FOR THE AIR FORCE AIRBORNE LASER PROGRAM

Larrene K. Harada and Daniel H. Leslie

W.J. Schafer Associates
Arlington, VA

The Air Force is developing an airborne laser system capable of engaging targets at ranges of at least several hundred km, at elevation angles from 1 to 4 degrees. We will present our wavelength-trade analysis comparing the capability of several candidate laser systems. The impact of molecular and aerosol scattering and absorption has been assessed using FASCOD2 and the HITRAN92 database, and these results will be presented. We are using the NASA SAGE satellite data base to provide recent stratospheric extinction data, and comparisons with standard LOWTRAN models will be described.

Wednesday 9 June 1993 a.m.

SESSION C: SPECTROSCOPY APPLICATIONS

Chair: Laila Jeong, PL/GPOS

A FAST SCHEME FOR A LINE-BY-LINE FORWARD MODEL

S. Kadokura, A. Shimota

A fast scheme for a line-by-line forward model has been developed. The keypoint of the scheme is a hybrid of analytical and numerical integration, and it reduces the calculation time approximately by an order of magnitude as compared with that of the classical scheme. The scheme is summarized as follows: (a) divide the whole range of the wave number, ν , into many intervals with various widths, so that a quadric is obtained as an approximation of the cross section for each interval (making a data base of the cross section); the transmittance for a wave number interval, T , is the integral of the exponential function of the optical depth, τ , where τ is expressed approximately with a quadric by that approximation, i.e. (b) if $a > 0$, calculate the exponential or error function to obtain the integral; (c) if $a < 0$, divide the interval into sub-intervals where the terms of ν^2 can be neglected, so that the transmittance for the sub-interval, T_s , is expressed with the exponential function; calculate the weighted mean of T_s to obtain T .

VIEWGRAPHS UNAVAILABLE

APPLICATION OF FASCODE PROGRAM TO A HIGH TEMPERATURE GAS MONITORING

N. Takeuchi

Remote Sensing & Image Res. Center
Chiba University
1-33, Yayoi-cho, Inage-ku, Chiba-shi
Chiba 263 Japan

FASCODE program was used to investigate the interference absorption by CO₂, which affects the monitoring of CO concentration at a high temperature state. A tunable lead salt diode laser was used in 4.5 micron region and it was found that the hot band gas absorption is not satisfactorily explained by the program.

Application of FASCODE Program to a High Temperature Gas Monitoring

— Interference Absorption
by High Temperature CO₂ Gas. —

Nobuo TAKEUCHI
RSIRC, CHIBA UNIVERSITY.

Monitor of CO in an exhaust flue.
Interference by High temperature CO₂ gas.
Comparison with FASCODE calculation.

in cooperation with
W. Ihashi, S. Yajima (IHI Lab.)

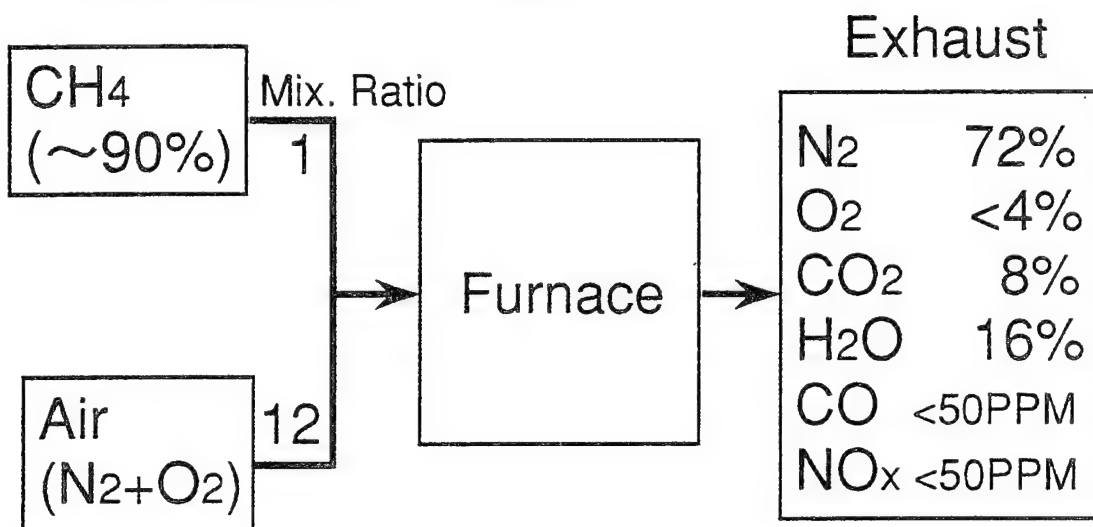
Spectroscopy of Combustion.

- Flame
- Engine
- Exhaust Flue

Physical Quantities to be measured:

- Velocity
- Temperature
- Pressure
- Density
- Concentration of Chemical Species
- Particles
- Size Distribution of Fuel Particles

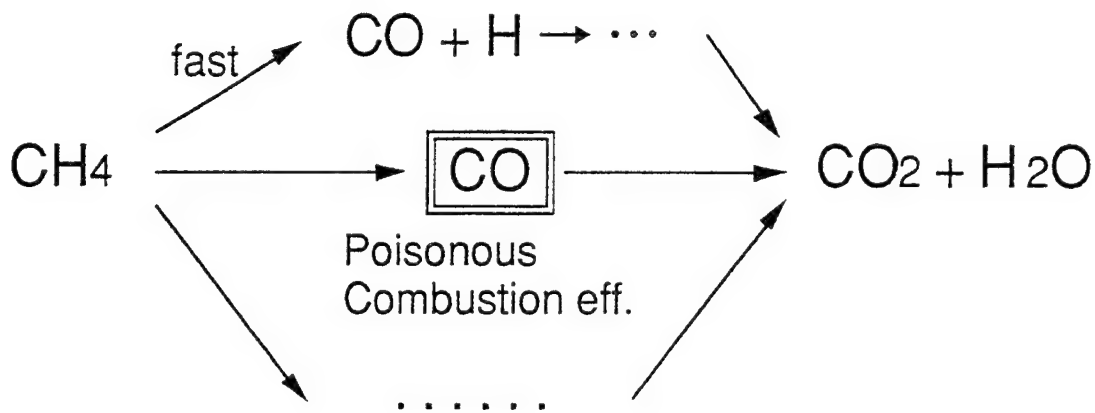
Combustion of LNG



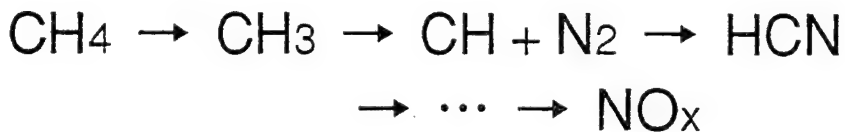
* Air : 20% excess for complete combustion.

Current Topics of Combustion.

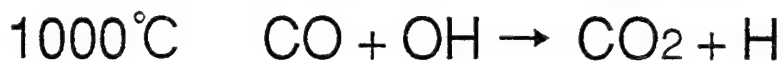
Intermediate Product



Flame Temp.	High	Low
Lower	CO	NO _x
Higher	NO _x	CO

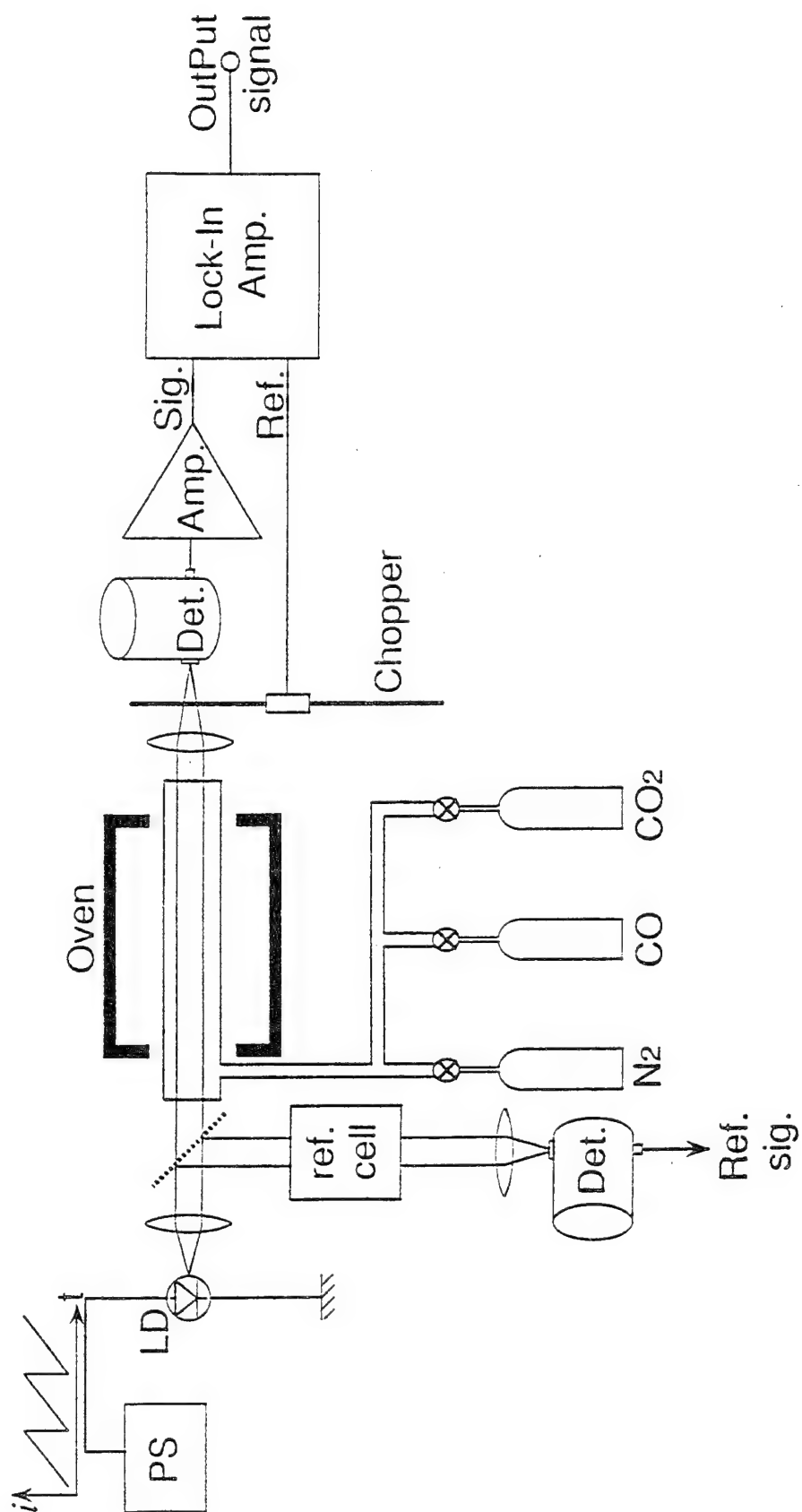


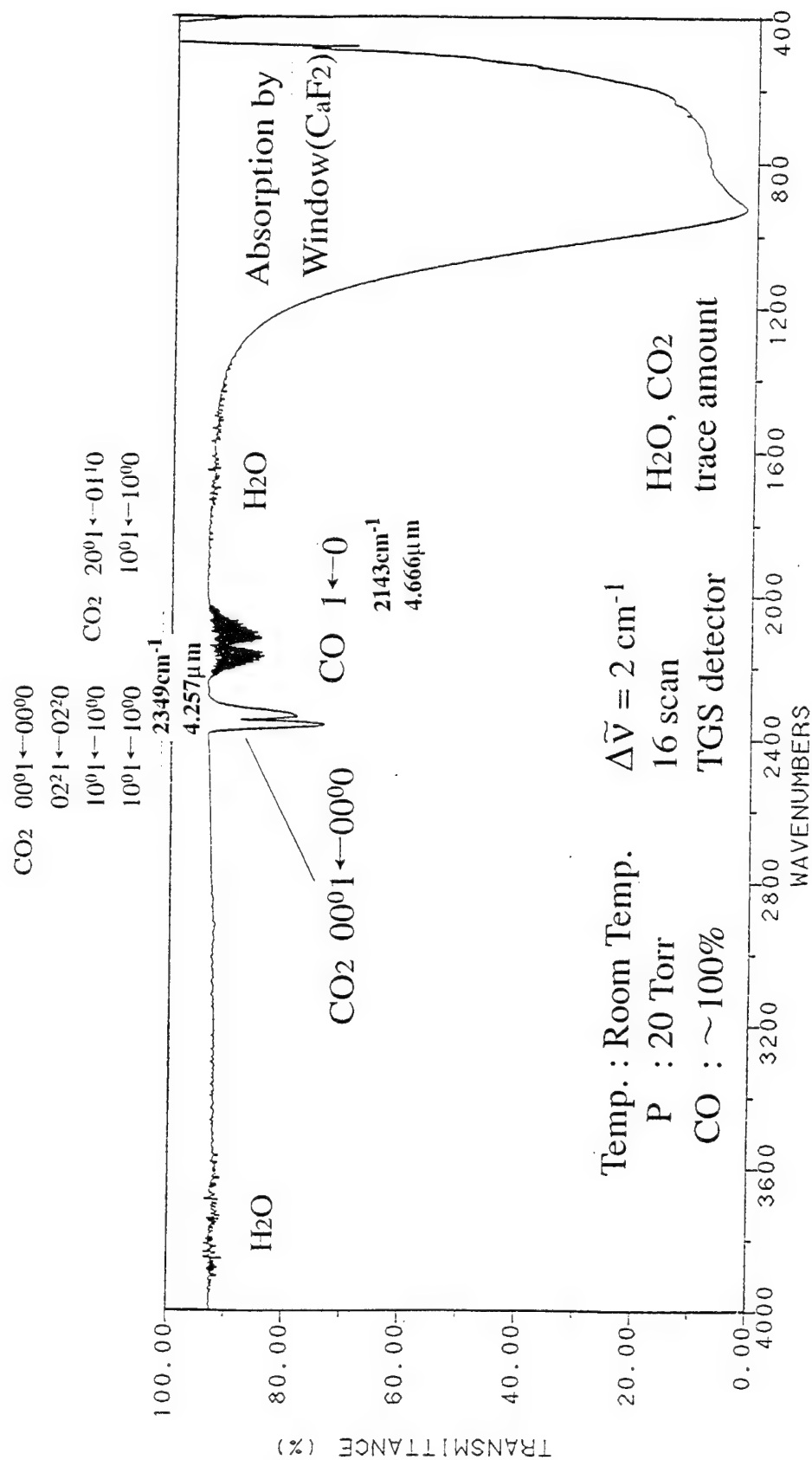
400°C No growth of reaction



preferable spatially homogeneous temperature distribution to burn at higher temperature.

Schematic Diagram of Laboratory Experiment. for Absorption Measurement by High Temperature Gases.





FT-IR Spectrum by CO Absorption.

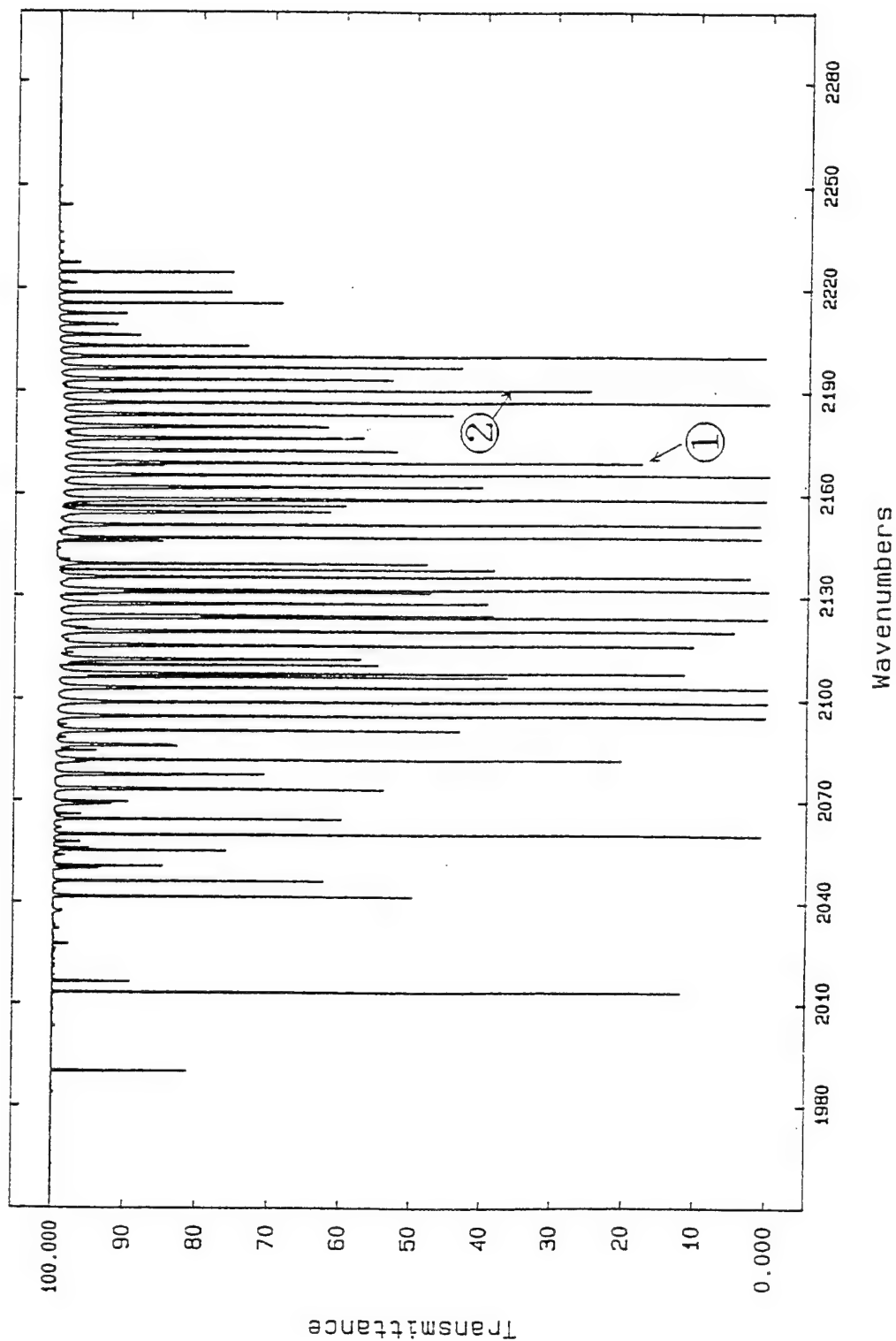
HITRAN Data for CO and CO₂

CO

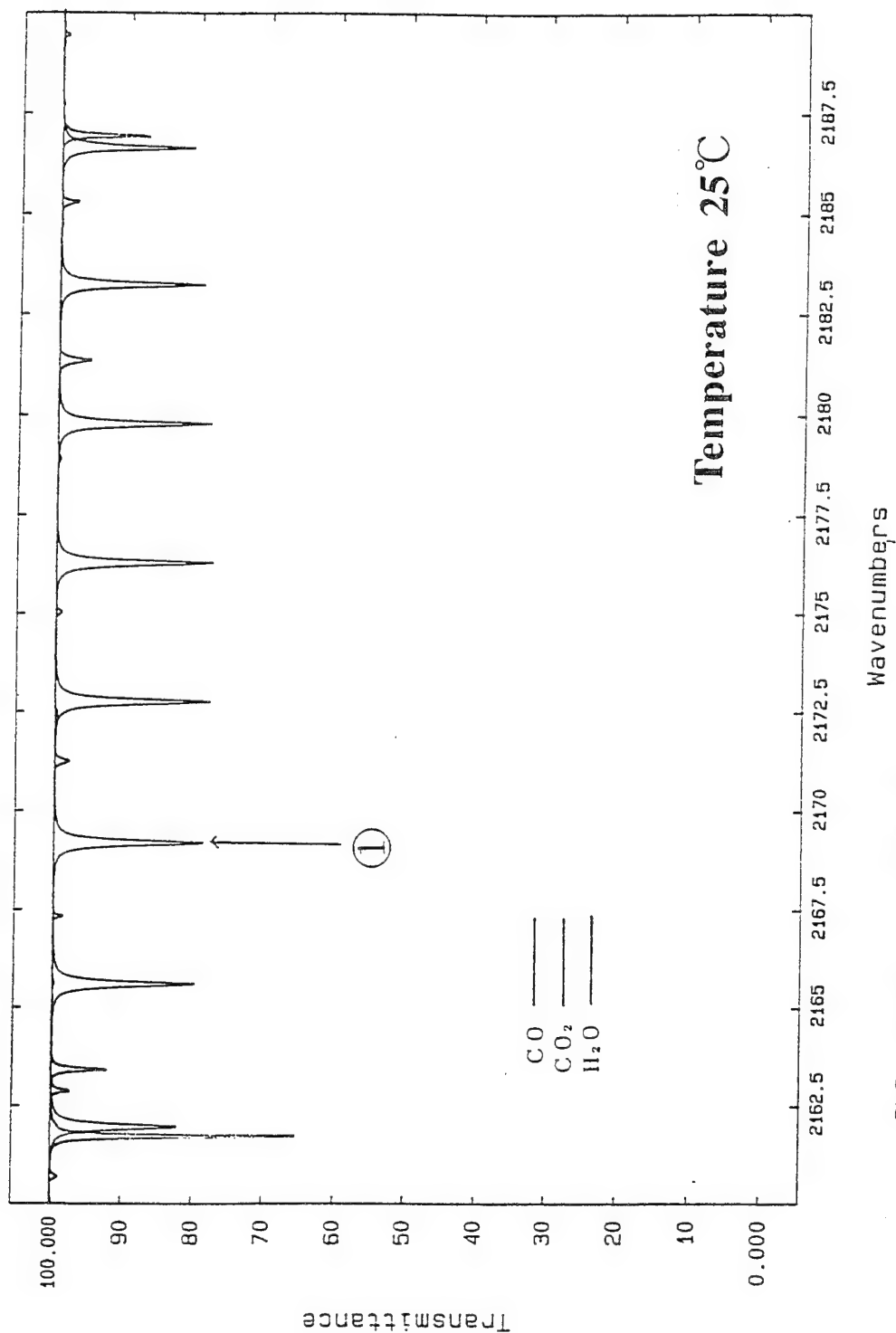
$v'-v''$	$v_0(\text{cm}^{-1})$	$v_{\min}-v_{\max}$	ΣS	S_{\max}
1-0	2143.27	1911-2288	1.036E-17	4.636E-19
2-0	4260.06	3985-4361	7.692E-20	3.532E-21
3-0	6350.44	6032-6418	4.909E-22	2.338E-23
4-0	8414.47	8053-8465	1.531E-24	8.159E-26

CO₂

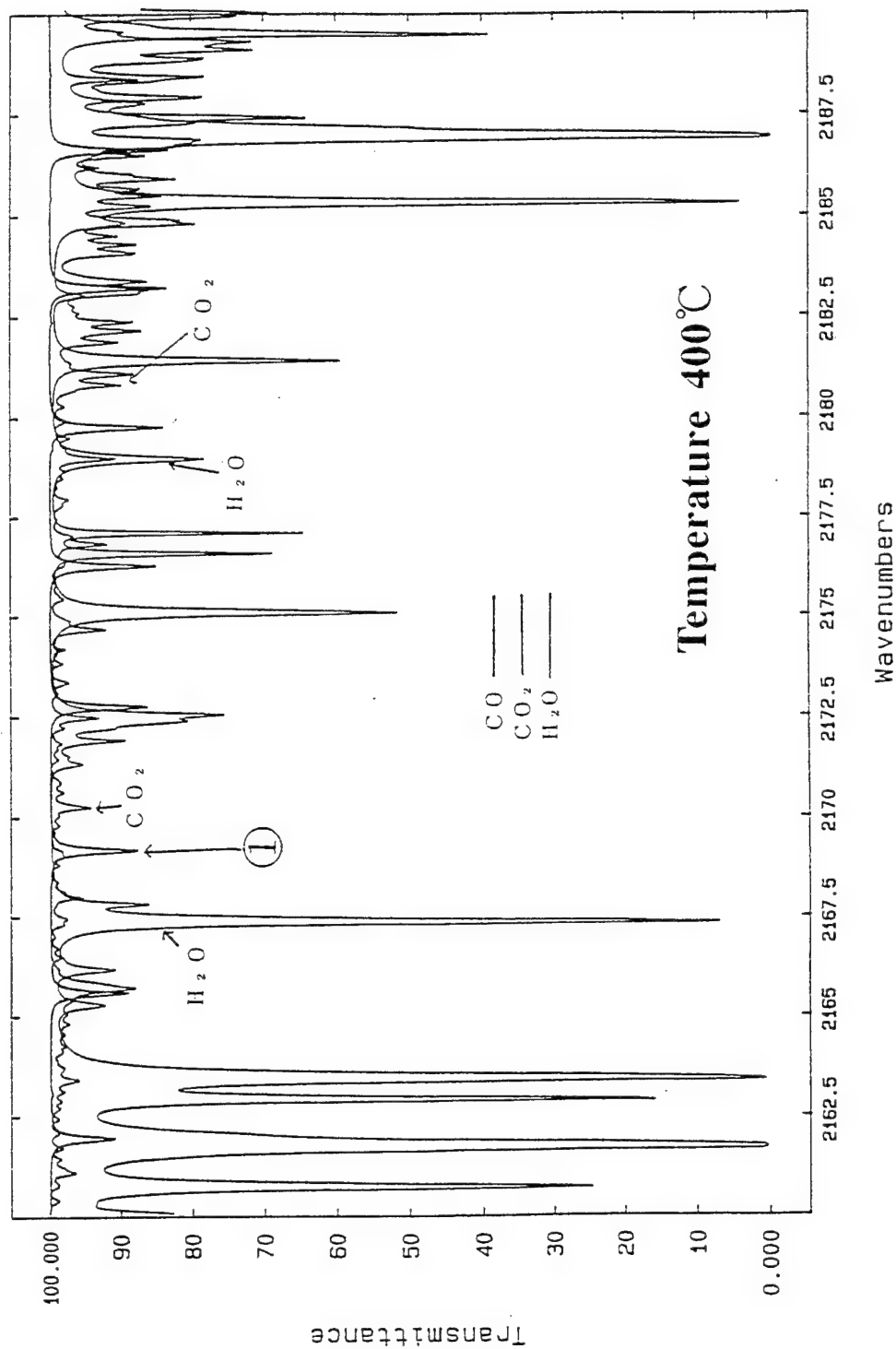
$v'-v''$	$v_0(\text{cm}^{-1})$	$v_{\min}-v_{\max}$	ΣS	S_{\max}
$10^0 02-01^1 01$	618.03	546-687	1.46E-19	5.459E-21
$01^1 01-00^0 01$	667.34	593-752	8.02E-18	2.982E-19
$02^2 01-01^1 01$	667.75	600-750	6.09E-19	1.122E-20
$10^0 01-01^1 01$	720.80	649-791	1.564E-19	5.850E-21
$02^2 11-02^2 01$	2324.14	2227-2371	2.601E-19	4.985E-21
$10^0 11-10^0 01$	2326.60	2231-2372	1.021E-19	3.929E-21
$10^0 12-10^0 02$	2327.43	2231-2374	1.716E-19	6.621E-21
$01^1 11-01^1 01$	2336.63	2227-2384	7.011E-18	1.344E-19
$00^0 11-00^0 01$	2349.14	2230-2397	9.157E-17	3.526E-18
$10^0 12-00^0 01$	3612.84	3509-3661	1.003E-18	3.855E-20
$10^0 11-00^0 01$	3714.78	3610-3763	1.504E-18	5.846E-20



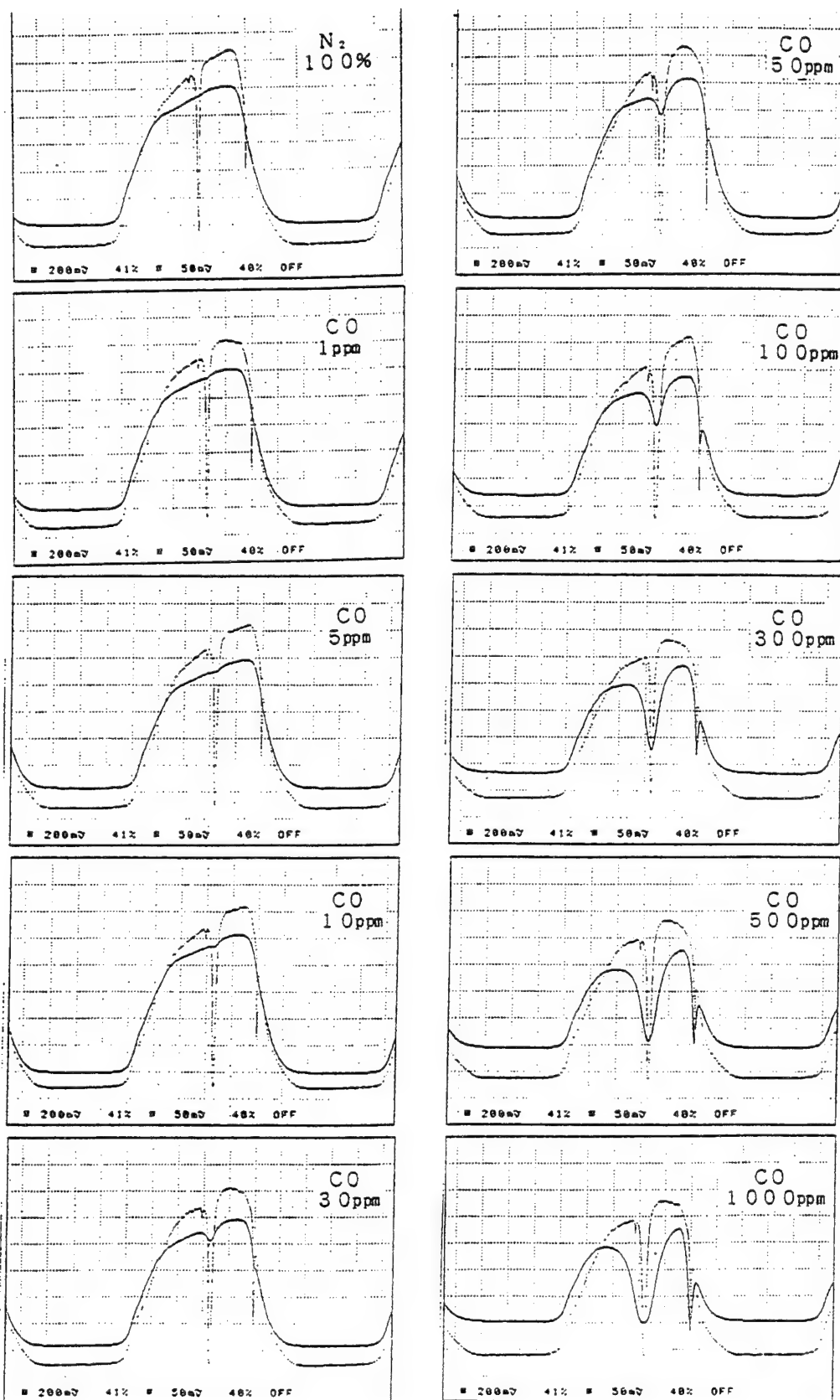
FASCODE calculation of the 1-0 CO absorption band
 (Room Temp., 20torr, 100%)



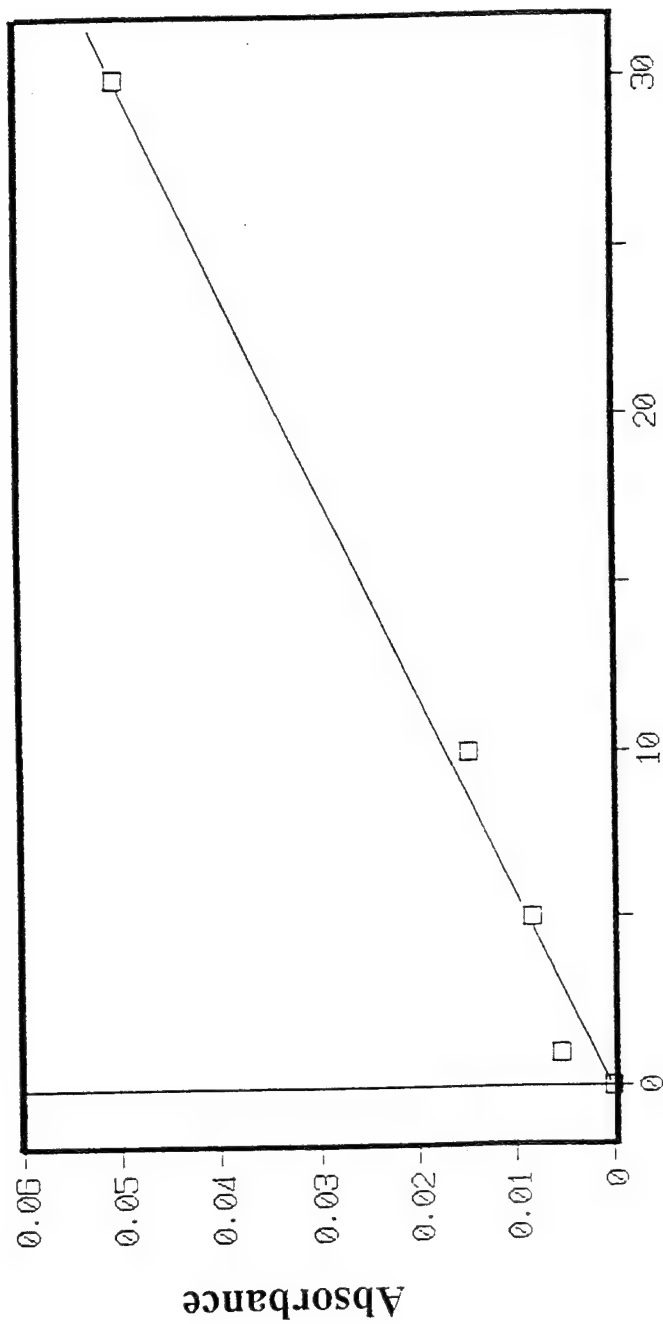
**CO, CO₂, and H₂O Absorption Spectrum Calculated
with FASCODE. (CO 50ppm, CO₂ 15%, H₂O 20%)**



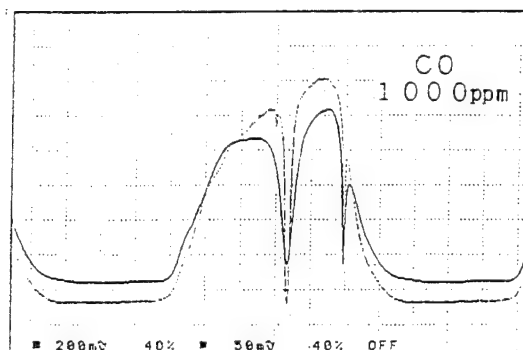
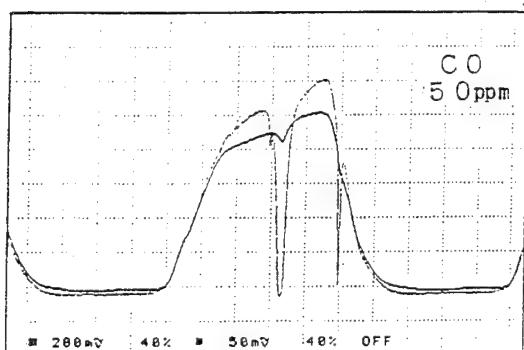
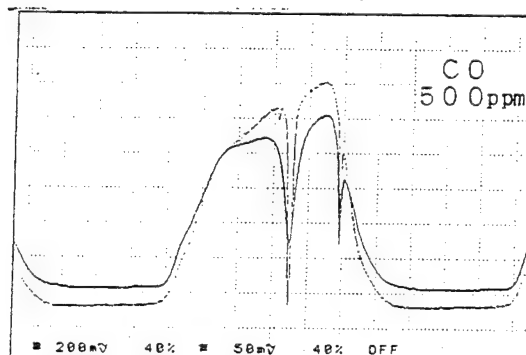
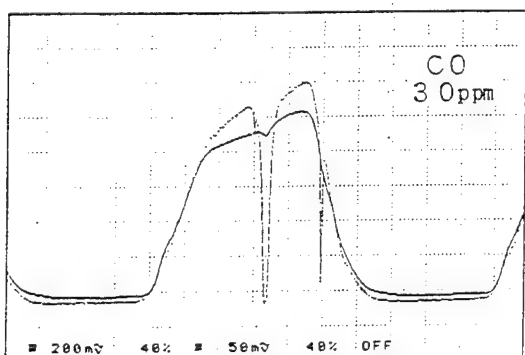
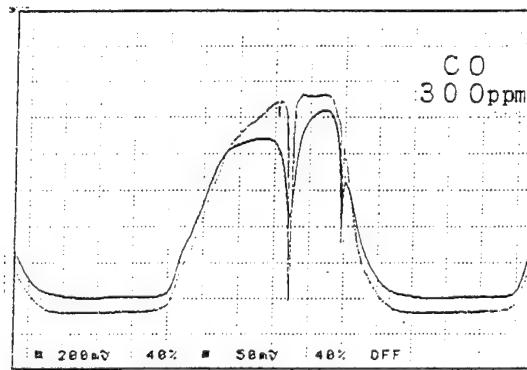
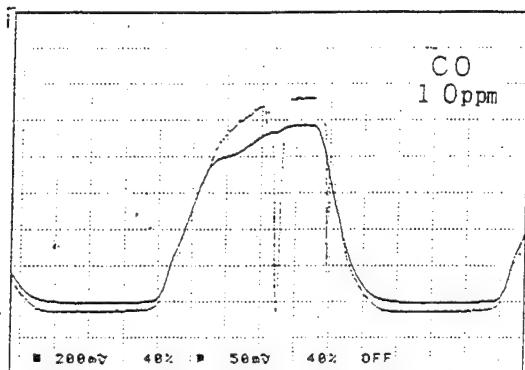
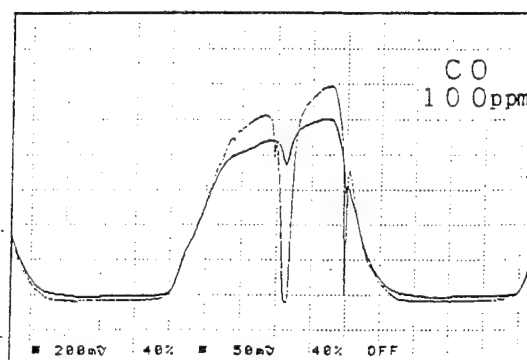
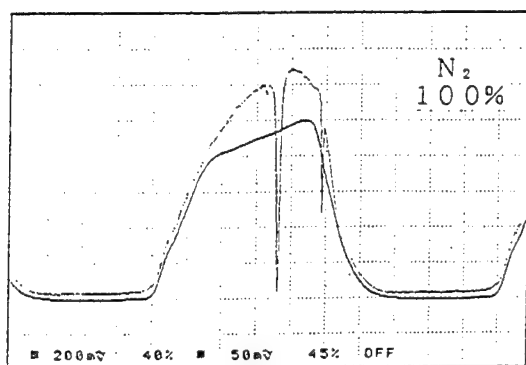
CO, CO₂, and H₂O Absorption Spectrum at 400°C
Calculated with FASCODE.
(CO 50ppm, CO₂ 15%, H₂O 20%)



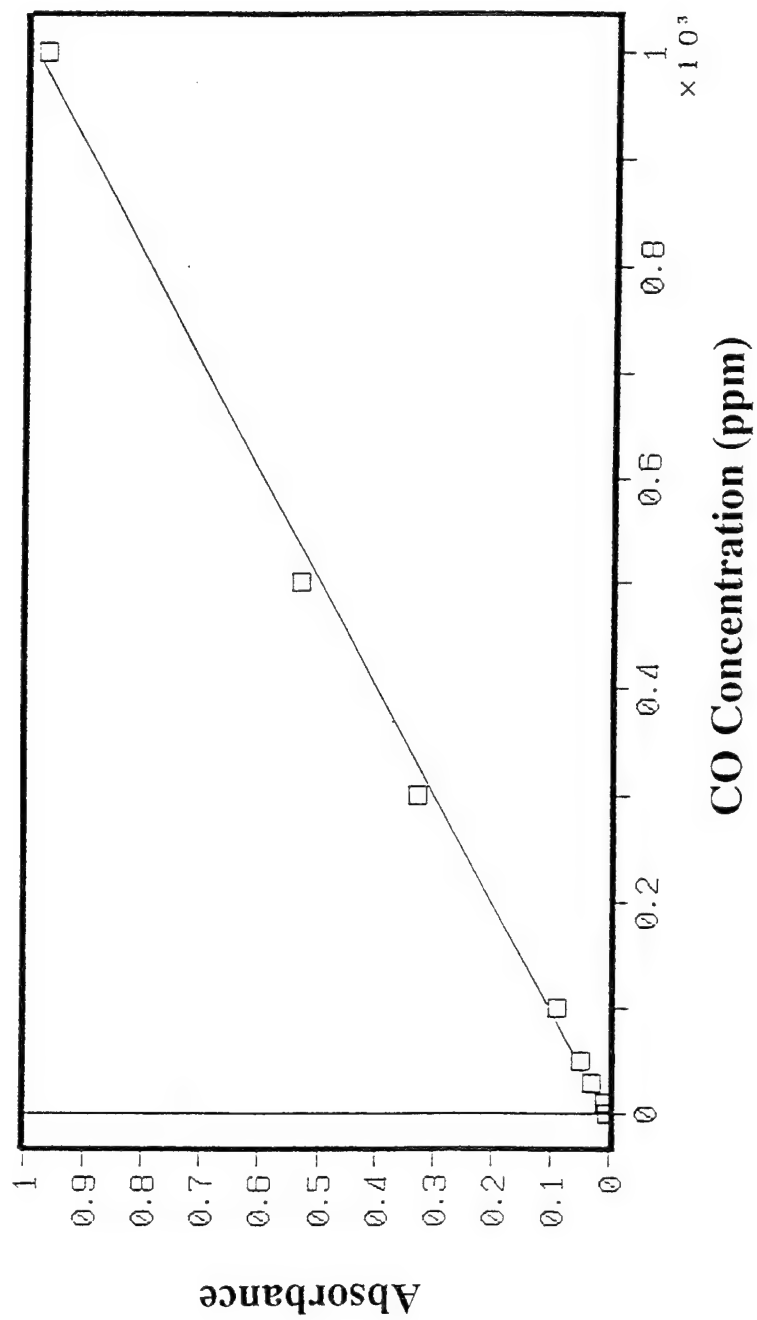
Absorption at 2169.1984cm⁻¹ (Room Temperature)



Absorbance at 2169.1984cm^{-1} vs. CO Concentration.
4.610 μm (Room Temperature)



Spectrum at 2169.1984cm^{-1} vs. CO Concentration.
($T=400^{\circ}\text{C}$)



Absorbance at 2169.1984cm^{-1} vs. CO Concentration.
 $4.6100\mu\text{m}$
($T=400^\circ\text{C}$)

Line Strength S(T)

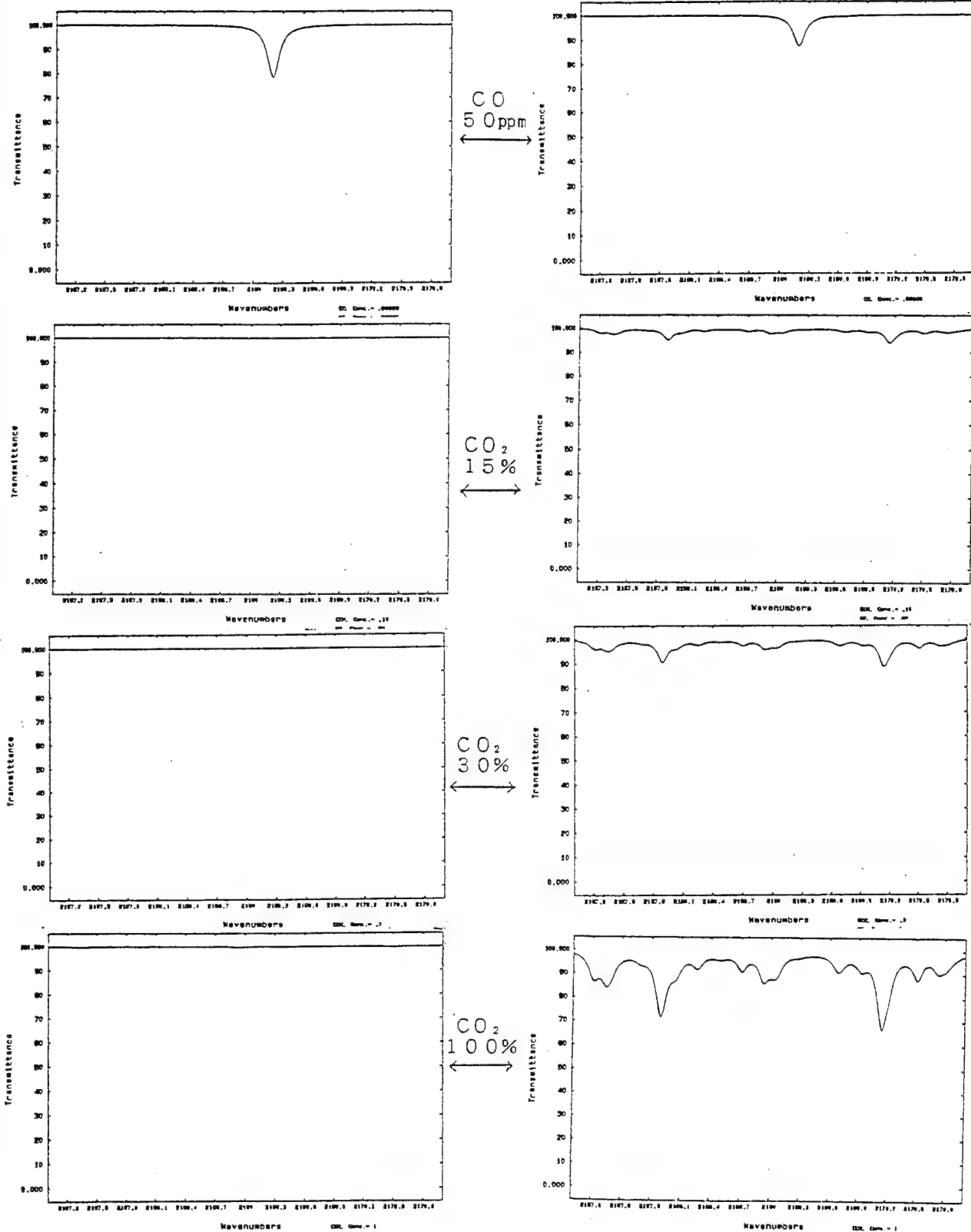
$$S(T) = \frac{8\pi^3}{3hc} \frac{S_L A_i}{Q(T)} \nu_0 R_0 \times 10^{-36} \exp\left(-\frac{hcE_L}{k_B T}\right) \times \left[1 - \exp\left(-\frac{hc\nu_0}{k_B T}\right)\right]$$

Optical Depth τ

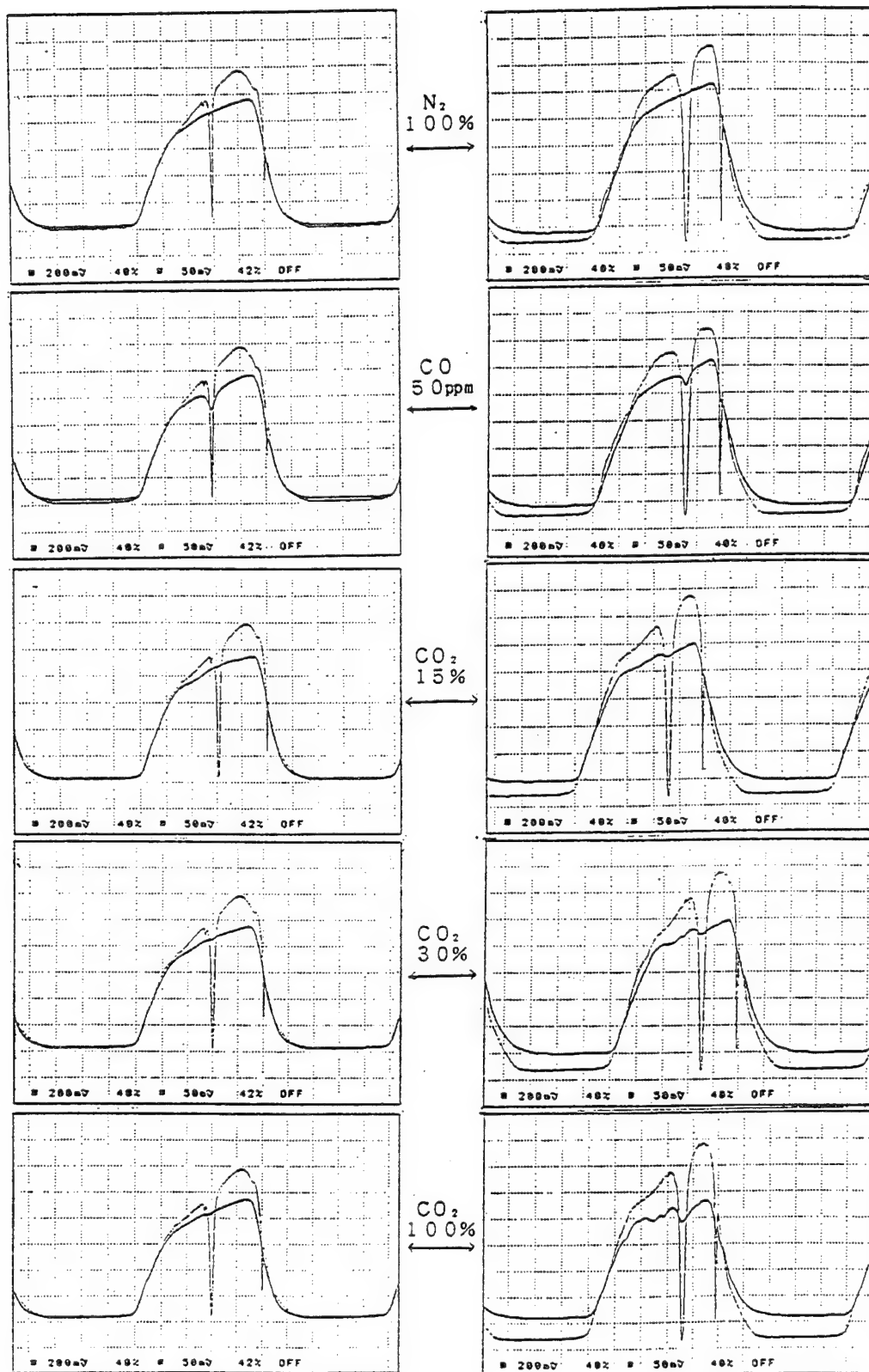
$$\tau = \int_{z_1}^{z_2} k(\nu, z) \, d\rho_a(z) \, dz$$

$$k(\nu) = S \, g(\nu)$$

$$\int g(\nu) \, d\nu = 1$$



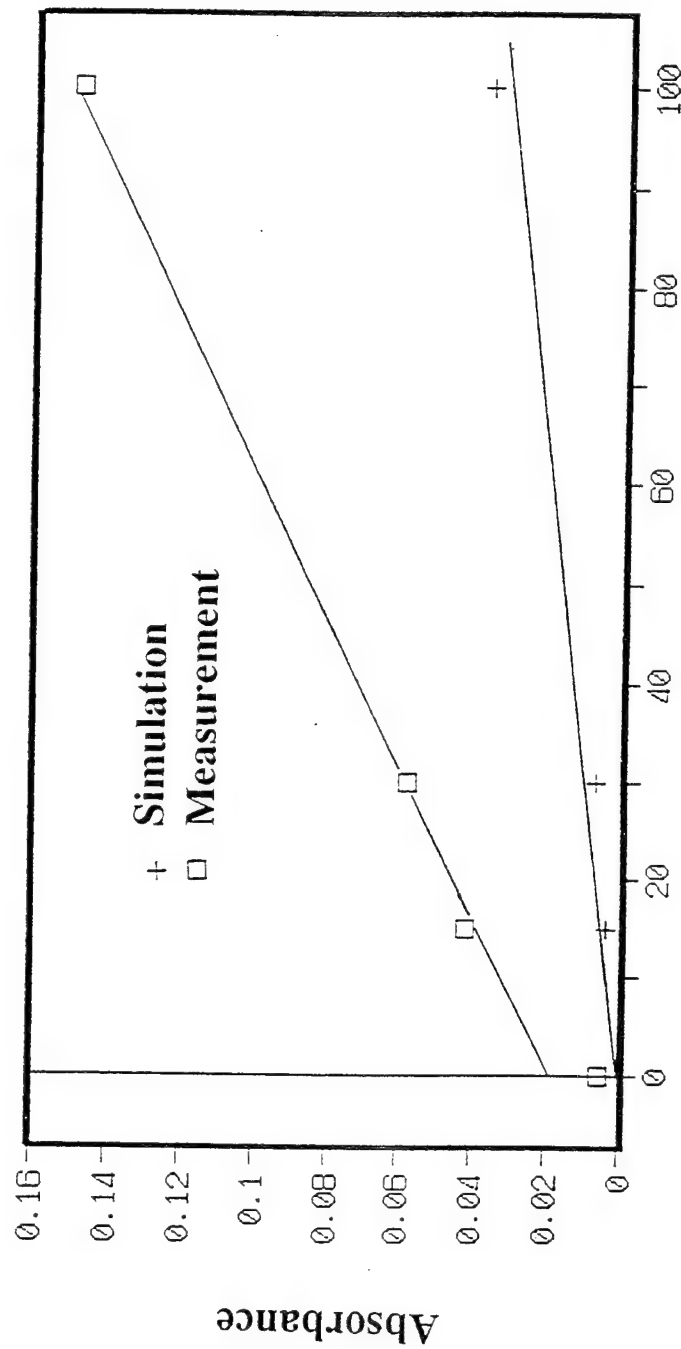
Room Temperature
400°C
Calculated Spectrum at 2169.2cm⁻¹ with FASCODE



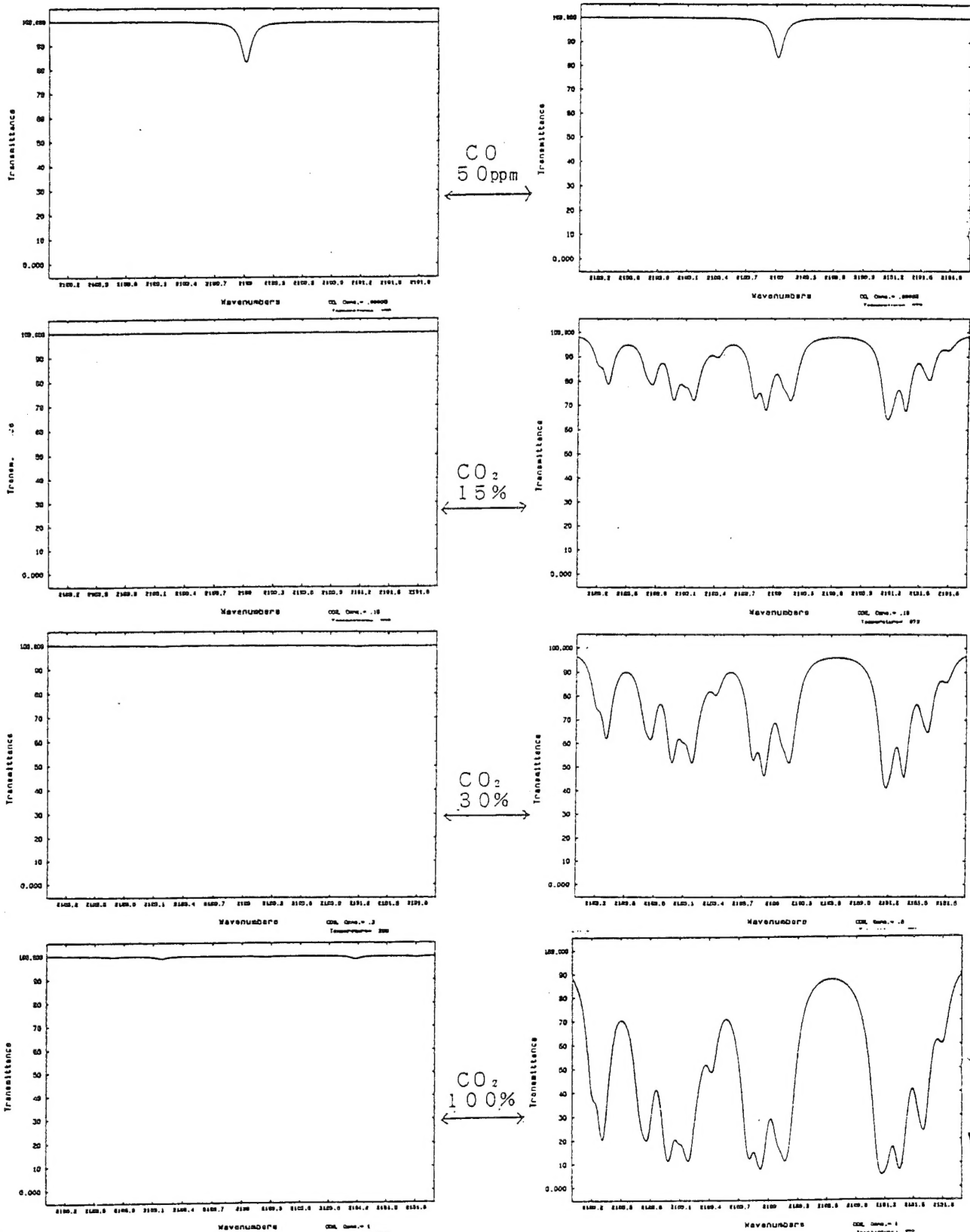
Room Temperature

400°C

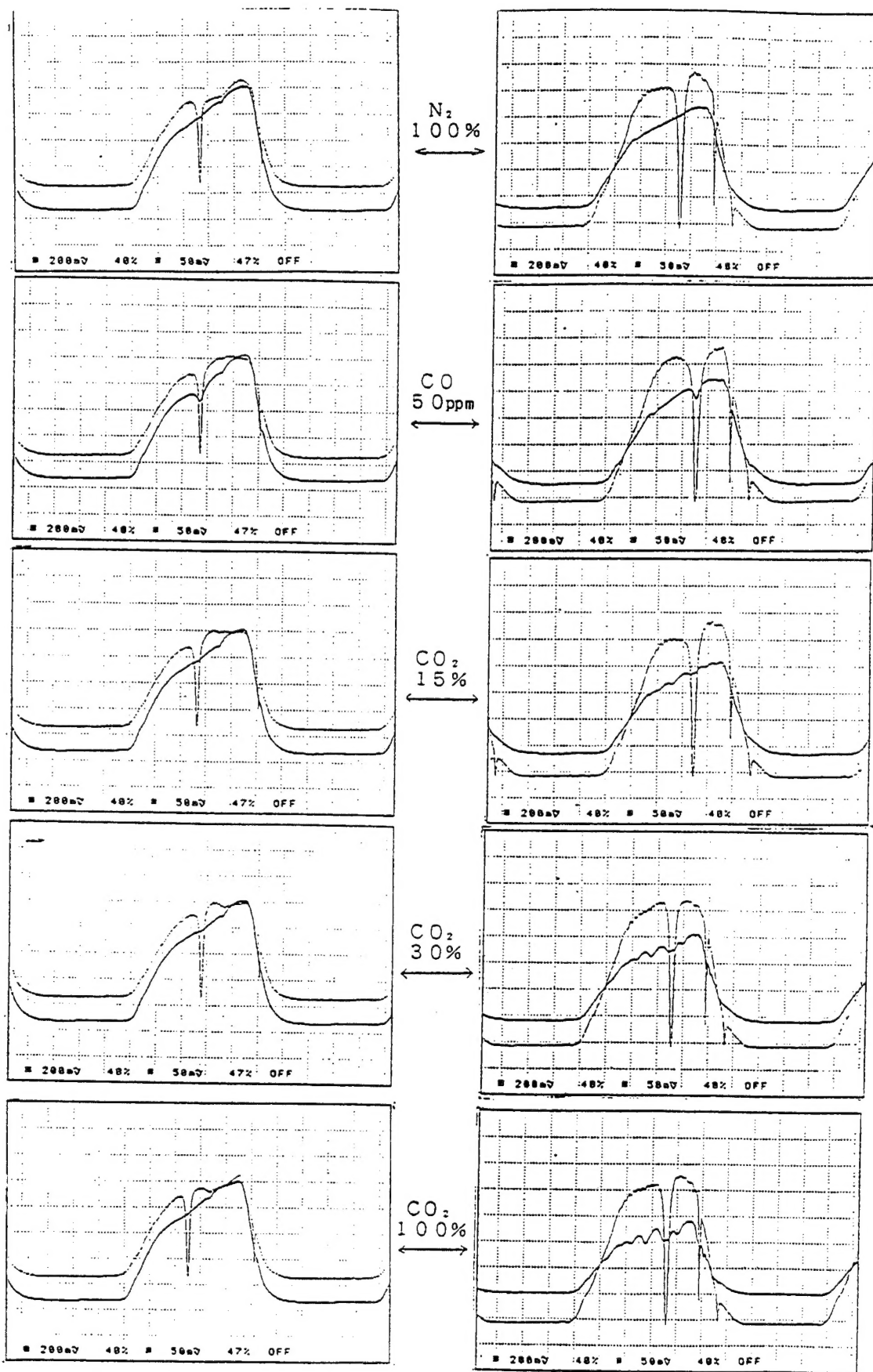
Observed Spectrum at 2169.2cm⁻¹



CO₂ Concentration (%)
Absorbance at 2169.1984cm⁻¹ vs. CO₂ Concentration in N₂.
4.6100μm
(T=400°C)



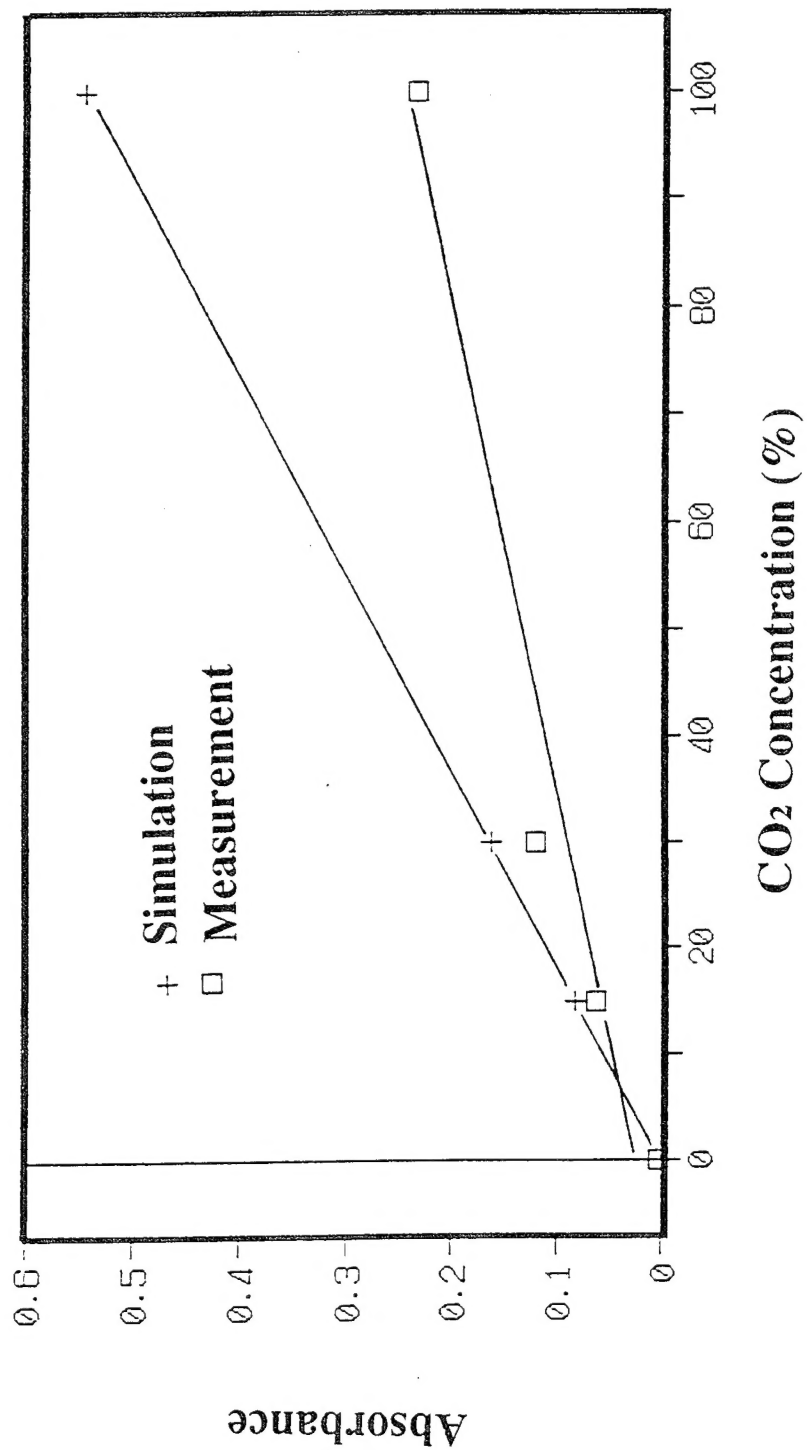
Room Temperature
 400°C
 Calculated Spectrum at 2190.0cm⁻¹ with FASCODE



Room Temperature

400°C

Observed Spectrum at 2190.0cm⁻¹



Absorbance at 2190.0180cm^{-1} vs. CO₂ Concentration in N₂.
4.566 μm (Room Temperature)

Summary

An application of FASCODE to a high temperature gas monitoring was presented.

Some Discrepancy between the
measurement and an estimation
using FASCODE
for CO₂ absorption at 400°C

Reason : line parameter error
poor algorithm
line-coupling
or
experimental error ?